

**Liquid Chromatography/  
Mass Spectrometry for the Analysis of  
Non-Polar Compounds**

**Heiko Hayen**

Members of the committee:

Chairman/secretary:	Prof. Dr. Ir. A. Bliet	Univ. Twente
Promotor:	Prof. Dr. U. Karst	Univ. Twente
Members:	Prof. Dr. Ir. A. van den Berg	Univ. Twente
	Prof. Dr. R. Bischoff	RU Groningen
	Prof. Dr. J.F.J. Engbersen	Univ. Twente
	Prof. Dr. J.-M. Kauffmann	Univ. Libre de Bruxelles
	Dr. H. Luftmann	Univ. Münster
	Prof. Dr. Ir. J.W.M. Noordermeer	Univ. Twente



Twente University **Press**

Publisher: Twente University Press,

P.O. Box 217, 7500 AE Enschede, The Netherlands,

[www.tup.utwente.nl](http://www.tup.utwente.nl)

Print: Océ Facility Services, Enschede, The Netherlands

© H. Hayen, Enschede, 2003.

No part of this work may be reproduced by print, photocopy, or other means without the permission in writing from the publisher.

ISBN 90-365-1965-9

**LIQUID CHROMATOGRAPHY/  
MASS SPECTROMETRY FOR THE ANALYSIS OF  
NON-POLAR COMPOUNDS**

**DISSERTATION**

to obtain

the doctor's degree at the University of Twente,

on the authority of the rector magnificus,

prof. dr. F.A. van Vught,

on account of the decision of the graduation committee,

to be publicly defended

on Friday October 3rd, 2003 at 13:15

by

Heiko Hayen

born on September 13th, 1973

in Wittmund, Germany

The dissertation has been approved by the promotor:

Prof. Dr. Uwe Karst

*Für meine Eltern*



# Acknowledgements

Almost at the end of the promotion time in the group of Chemical Analysis which has been passing by that rapidly, the end is now getting closer and closer. Parts of this work were carried out at the University of Münster, Germany from October 2000 until September 2001. The main part of my Ph.D. research has been done from October 2001 to October 2003 at the University of Twente in Enschede, The Netherlands. During this time, many persons from various countries gave me helpful advice and valuable support. I would not have managed to complete my work without their contributions. Therefore, I want to start this book acknowledging all of them.

Mein besonderer Dank gilt Herrn Prof. Dr. Uwe Karst für die interessante Themenstellung, die Möglichkeit, an internationalen Konferenzen teilzunehmen und die freundschaftliche Unterstützung bei dieser Arbeit besonders in den Momenten mit viel Arbeit und wenig Zeit.

Nicole Jachmann und Martin Vogel möchte ich besonderen Dank aussprechen. Beide habe ich während des gesamten Studiums in Münster nicht nur als hilfsbereite Kollegen, sondern auch als gute Freunde kennen und schätzen gelernt, deren Freundschaft ich mir auch über die Promotionszeit hinaus sicher bin.

Mein besonderer Dank gilt auch den anderen Laborkollegen in Münster: Georg Diehl, der mich in die Arbeit mit der LC/MS nebst Computern eingeführt hat, Jörg

Meyer, mit dem man so gesellig die langen Laborabende von Martin begleiten konnte, Rasmus Schulte-Ladbeck, der auch zu exotischen Themen immer eine Antwort parat hatte, Tanja Steinkamp, die mit Rasmus und mir den Umzug nach Gronau gewagt hat und den "Neudoktoranden" Sebastian Götz, André Liesener, Hartmut Henneken, Tobias Revermann und Bettina Seiwert und vor allem Christel Hempen, die ich als stets liebenswerte und hilfsbereite Kollegin kennenlernen durfte und die mir auch in meiner Doktorprüfung zur Seite stehen wird.

Desweiteren möchte ich mich für das gute und angenehme Arbeitsklima in Münster auch bei allen Mitgliedern des Arbeitskreises Andersson bedanken

De wisseling naar de Universiteit Twente in Enschede is mij erg aangenaam gemaakt door de hartelijke opname door onze Nederlandse collega's. In het bijzonder onze secretaresse Saskia Tekkelenburg-Rompelman, die mij ook bij organisatorische problemen bij de verhuizing naar Nederland altijd graag behulpzaam was, evenals haar behulpzame collega Carla Weber (vakgroep Supramoleculaire Chemie en Technologie) en sinds kort onze nieuwe secretaresse Susanne van Rijn. Annemarie Montanaro-Christenhusz, Martijn Heuven en in het begin Jan Toersche stonden me in het lab altijd met raad en daad terzijde. Sjoerd Veldhuis en Andràs Perl, bedankt voor jullie medewerking in de vakgroep Chemische Analyse. Nancy Heijnekamp-Snellens en Marcel de Bruine, bedankt voor het bestellen van de chemicaliën, kantoorartikelen en velerlei (!) reserveonderdelen en voor al die andere dingen die jullie hebben gedaan.



Een belangrijke bijdrage aan dit werk is geleverd door 'mijn' afstudeerster Suze van Leeuwen. Zij heeft een prachtig stuk werk geleverd, wat beschreven is in hoofdstuk 4., en de samenvatting vertaald naar het Nederlands. Het was heel leuk en leerzaam om met haar samen te werken en ik ben blij dat ze ook AIO in onze groep gaat worden en dat ze mijn paranimpf wil zijn.

Apart from the people from our group, I would not have completed my work without the contributions and help from other groups within the University of Twente. I would like to thank Audrey Dechamps (Department of Polymer Chemistry and Biomaterials) for giving me insights into the 'polymer world', Montse Álvarez-Grima and Subhas Debnath (Department of Rubber Technology) for an introduction into the 'rubber world' and Dr Roel Fokkens (Department of Supramolecular Chemistry and Technology and MESA<sup>+</sup> Research Institute) for his advice concerning mass spectrometric questions. Furthermore, I would like to thank Henrik Hillborg (Department of Materials Science and Technology of Polymers) for the amusing coffee breaks.

Weiterhin danke ich Dr. Heinrich Luftmann (Institut für Organische Chemie, Universität Münster) für lehrreiche Diskussionen über massenspektrometrische Fragestellungen und für Tandem-MS-Messungen.

Der Stiftung Stipendienfonds im Verband der Chemischen Industrie (Frankfurt am Main, Deutschland) danke ich für die finanzielle Förderung in Form eines Promotionsstipendiums.

Meiner Familie und vor allem meinen Eltern bin ich auf vielfältigere Weise dankbar als ich in Worte fassen kann.

Ganz besonders möchte ich hier auch Isabell für ihre moralische Unterstützung und Motivation in den letzten Monaten danken.

*Heiko*





# Contents

<b>1.</b>	<b>Introduction and Scope</b>	<b>1</b>
1.1	General Remarks	1
1.2	Scope of the Thesis	2
1.3	References	4
<b>2.</b>	<b>Strategies for the LC/MS Analysis of Non-Polar Compounds</b>	<b>5</b>
2.1	Abstract	5
2.2	Introduction	6
2.3	Coupling Electrochemistry to API-MS	9
2.3.1	<i>General Aspects of Electrochemistry/MS</i>	9
2.3.2	<i>The Electrospray Interface as Electrochemical Reactor</i>	9
2.3.3	<i>Derivatization for Electrochemistry/MS</i>	11
2.3.4	<i>The Use of External Electrochemical Cells</i>	12
2.3.5	<i>Combining Electrochemistry with LC and MS</i>	16
2.4	Atmospheric Pressure Photoionization (APPI)	20
2.5	LC/Atmospheric Pressure Electron Capture Negative Ion-MS	26
2.6	Coordination Ionspray-MS (CIS-MS)	33
2.7	Conclusions	38
2.8	References	39

<b>3.</b>	<b>Analysis of Phenothiazine and its Derivatives using LC/ Electrochemistry/MS and LC/Electrochemistry/Fluorescence</b>	<b>47</b>
3.1	Abstract	47
3.2	Introduction	48
3.3	Experimental	51
3.4	Results and Discussion	54
3.4	Conclusions	74
3.5	References	75
<b>4.</b>	<b>Liquid Chromatography/Electrochemistry/Mass Spectrometry of Polycyclic Aromatic Hydrocarbons</b>	<b>79</b>
4.1	Abstract	79
4.2	Introduction	80
4.3	Experimental	83
4.4	Results and Discussion	88
4.5	Conclusions	109
4.6	References	111
<b>5.</b>	<b>LC/Electron Capture APCI-MS for the Determination of Nitroaromatic Compounds</b>	<b>113</b>
5.1	Introduction	114
5.2	First Observations of Electron Capture Phenomena in Conjunction with HPLC/APCI(-)-MS	117

5.2.1	<i>Abstract</i>	117
5.2.2	<i>Experimental</i>	118
5.2.3	<i>Results and Discussion</i>	121
5.2.4	<i>Conclusions</i>	131
5.3	Investigations on the Electron Capture Effects during LC/APCI(-)-MS Determination of Nitrobenzoxadiazole Derivatives	132
5.3.1	<i>Abstract</i>	132
5.3.2	<i>Experimental</i>	133
5.3.3	<i>Results and Discussion</i>	136
5.3.4	<i>Conclusions</i>	155
5.4	<i>References</i>	158
<b>6.</b>	<b>Liquid Chromatography/Coordination Ion-spray-Mass Spectrometry for the Analysis of Rubber Vulcanization Products</b>	<b>159</b>
6.1	Abstract	159
6.2	Introduction	160
6.3	Experimental	162
6.4	Results and Discussion	165
6.5	Conclusions	174
6.6	References	175

<b>7. LC/MS Studies on the <i>In Vitro</i> Degradation of Poly(ether ester)</b>	
<b>Block Copolymers</b>	<b>177</b>
7.1 Abstract	177
7.2 Introduction	178
7.3 Experimental	181
7.4 Results and Discussion	184
7.5 Conclusions	198
7.6 References	199
<b>8. Concluding Remarks and Future Perspectives</b>	<b>201</b>
<b>Abbreviations</b>	<b>205</b>
<b>Summary</b>	<b>209</b>
<b>Samenvatting</b>	<b>213</b>
<b>Curriculum Vitae</b>	<b>217</b>
<b>List of Publications</b>	<b>219</b>



# Chapter 1

## Introduction and Scope

### 1.1 General Remarks

The coupling of liquid chromatography with mass spectrometry (LC/MS) has been established as one of the most powerful tools in analytical chemistry over the last decade and has turned out to be a versatile tool for the analysis of environmental and biological samples [1-5]. The most commonly used interfaces in LC/MS are electrospray ionization (ESI) and atmospheric pressure chemical ionization (APCI). As ionization of analyte molecules with these atmospheric pressure ionization (API) techniques typically occurs on the basis of protonation (in the positive ion mode) or deprotonation (in the negative ion mode), ESI and APCI are restricted to the determination of polar or even ionic compounds. Thus, new ionization principles being independent of acid/base reactions occurring in the interfaces would be able to significantly enlarge the number of analytes which could be determined by means of LC/MS.

## **1.2 Scope of the Thesis**

In the last few years, several interesting approaches to expand the applicability of LC/MS to rather non-polar compounds have been suggested. On-line electrochemical conversion of the analytes to more polar reaction products, atmospheric pressure photoionization (APPI), electron capture negative ion APCI-MS and coordination ionspray-MS are the techniques mainly applied for this purpose.

These techniques are presented in detail, compared and discussed critically with respect to their current status and future perspectives in **chapter 2**. Particular focus is directed from a chemical point of view on the substance groups which are accessible by each of the new approaches. Although none of these approaches will achieve the status of a “universal” ionization technique for non-polar compounds, all show good potential for use in particular applications.

Therefore, the objective of the research described in this thesis is to explore the potential of the coupling of electrochemistry to MS, to investigate electron capture effects in APCI-MS and to show the application of coordination ionspray-MS. As APPI sources are already commercially available from nearly all manufactures of atmospheric pressure mass spectrometers, this ionization technique will not be covered in this thesis.

The hyphenation of liquid chromatography, electrochemistry and mass spectrometry is presented in chapter 3 and 4.

The study of on-line electrochemical conversion of phenothiazine and its derivatives after liquid chromatographic separation by mass spectrometry and fluorescence spectroscopy is described in **chapter 3**. The presented method allows rapid investigations on the electrochemical oxidation pathways, as demonstrated for phenothiazine itself. The phenothiazine derivatives are transferred into their strongly fluorescent sulfoxides. Based on this reaction, an LC/electrochemistry/ fluorescence method was developed.

An efficient way for the fast elucidation of electrochemical reactions of polycyclic aromatic hydrocarbons (PAHs) by LC/electrochemistry/MS is described in **chapter 4**. The non-polar PAHs are converted into the respective radical cations. This and the further reaction with constituents of the mobile phase and in additional electrochemical oxidation steps are studied mass spectrometrically.

The LC/MS determination of selected nitroaromatic compounds by means of electron capture ionization using a commercial APCI interface in the negative ion mode is described in **chapter 5**. The electron capture effect is observed for nitroaromatics which do not easily undergo deprotonation under these conditions. The parameters favoring electron capture mechanisms have been thoroughly investigated under consideration of the competing mechanism of deprotonation to allow a better understanding of the electron capture process and to improve selectivity of the analysis.

The application of LC/coordination ionspray-MS for the identification of reaction products in a model rubber vulcanization process is demonstrated in **chapter 6**.

Besides the vulcanization accelerators, various reaction products, including sulfur-chain bridged alkenes were identified.

A detailed study on the *in vitro* degradation of a poly(ether ester) block copolymer based on poly(ethylene glycol) and poly(butylene terephthalate) is presented in **chapter 7**. All major degradation products and several side-products were identified using electrospray-MS. The addition of ammonium and sodium ions was used to provided important complementary information on the number of monomer units.

General conclusions and some remarks concerning the advantages and drawbacks as well as future perspective of the presented approaches for the analysis of rather non-polar compounds are presented in **chapter 8** which concludes the thesis.

### **1.3 References**

- [1] E. Gelpí, J. Chromatogr. A 703 (1995) 59.
- [2] W. M. A. Niessen, J. Chromatogr. A 1000 (2003) 413.
- [3] T. Reemtsma, J. Chromatogr. A 1000 (2003) 477.
- [4] M. Kohler, N. V. Heeb, Anal. Chem. 75 (2003) 3115.
- [5] L. Bonnington, E. Eljarrat, M. Guillamón, P. Eichhorn, A. Taberner, D. Barceló, Anal. Chem. 75 (2003) 3128.

# Chapter 2

## Strategies for the LC/MS Analysis of Non-Polar Compounds\*

### 2.1 Abstract

Electrospray ionization (ESI) and atmospheric pressure chemical ionization (APCI) have recently evolved as very useful tools for the liquid chromatographic/mass spectrometric (LC/MS) analysis of polar substances. Non-polar compounds, however, are difficult to analyze with these atmospheric pressure ionization (API) techniques due to their soft ionization mechanism. Recently, some new approaches have been introduced which are likely to overcome - at least partly - this obstacle. On-line electrochemical conversion of the analytes to more polar reaction products, atmospheric pressure photoionization (APPI), electron capture negative ion APCI-MS and coordination ionspray-MS are four techniques which are presented in detail, compared and discussed critically with respect to their current status and future perspectives. Particular focus is directed from a chemical point of view on the substance groups which are accessible by each of the new approaches.

\*H. Hayen, U. Karst, *J. Chromatogr. A* 1000 (2003) 549.

## 2.2 Introduction

In the last fifteen years, the coupling of liquid chromatography and mass spectrometry (LC/MS) has evolved to an extremely powerful analytical technique. The use of atmospheric pressure ionization (API) techniques, mainly comprising electrospray ionization (ESI) [1,2] with different variations [3,4] and atmospheric pressure chemical ionization (APCI) [5,6], allows both the transfer of the LC effluent into the gas phase and the ionization of the analytes. With protonation (in the positive ion mode) and deprotonation (in the negative ion mode), acid-base reactions are the most frequently observed ionization mechanisms. These reactions will, of course, be observed mainly by strongly polar analytes. Addition of alkali ions as  $\text{Na}^+$  or of other ions as  $\text{NH}_4^+$  in the positive ion mode or of  $\text{Cl}^-$ , formate or acetate in the negative ion mode favors the ionization of rather polar compounds. Therefore, many pharmaceuticals, peptides and proteins are today easily accessible by LC/MS using the API interfaces. Owing to the significance of these techniques, a large number of reviews covers the use of LC/API-MS for the analysis of polar or charged compounds. These include reviews on technological aspects as well as on application in particular fields of research, which are listed in the following.

Niessen has summarized the state of the art in LC/MS with special focus on ionization techniques and mass analyzers [7]. Gelpí has presented the latest developments in the interfacing of liquid-phase separations and mass spectrometry [8]. The technical aspects of the combination of LC and MS will therefore not be covered in this chapter.

The typical ionization mechanisms of ESI and APCI indicate that it will be difficult to analyze non-polar compounds with ESI- or APCI-MS. Substances, which are not prone to undergo acid-base reactions will be detected by ESI-MS only in exceptional cases, e.g., when adducts with polar ions are formed. This, however, is not likely as well for non-polar compounds. This is supported by experimental data, where these substances are determined only with poor limits of detection or not at all. Some expansion of the applicability range of APCI to less polar compounds can be achieved by removing ammonium acetate or formate from the mobile phase. Using normal-phase LC in combination with APCI-MS would be another promising strategy. However, the use of normal-phase LC is associated with a large number of problems, including limited compatibility with water in the samples, which results in limited reproducibility. In most cases, the use of normal-phase LC will therefore not be an option. One could now argue that the determination of low-polarity analytes could generally be carried out better by gas chromatography (GC) with mass spectrometric detection using electron ionization (EI). There are, nevertheless, at least two major reasons that shall explain why it is useful to expand the applicability of LC/MS to less polar analytes:

Not all non-polar substances are accessible by GC/MS with electron ionization. There are limitations caused by the low volatility of the analytes, by their thermolability and by the size of the molecules. ESI and APCI mostly result in mass spectra with the pseudomolecular ion as base peak and little or even no fragmentation. In combination with a tandem mass analyzer (e.g., triple quadrupole or ion trap), additional structural information may be gathered, although the possibilities for library searching are limited in comparison with GC/EI-MS. Tandem

mass spectrometry will also increase the selectivity of the analysis, being advantageous for the determination of trace concentrations in very complex matrices. The capabilities of different mass analyzers have been described in detail in [9] and will therefore not be covered in this chapter.

It is therefore desirable to expand the applicability of LC/MS with API techniques to the determination of rather non-polar compounds. In the last few years, several interesting approaches for this purpose have been suggested. A selection of these is summarized within this section. In the following, background and applications of four different techniques, comprising

- the combination of on-line electrochemical conversions with mass spectrometry,
- atmospheric pressure photoionization (APPI),
- electron capture negative ion APCI-MS and
- coordination ionspray-MS (CIS-MS)

will be presented and critically discussed.



## **2.3 Coupling Electrochemistry to API-MS**

### **2.3.1 General Aspects of Electrochemistry/MS**

With respect to the LC/MS analysis of non-polar compounds, the electrochemical conversion of the analytes to more polar or even charged analytes, which are then easily accessible by ESI- or APCI-MS is the primary goal. Additionally, this technique allows the on-line observation of electrochemical reactions by mass spectrometry, being advantageous compared to the previous off-line techniques. Here, the major issue will be the on-line approach, and particular focus will be directed to those applications where coupling to liquid-phase separation techniques has either been carried out or is in principle possible. However, those key articles which introduced relevant techniques in conjunction with other LC/MS interfaces are summarized as well.

The first publication at all on the on-line coupling of electrochemistry and MS goes back until the early 1970s, where the combination of a porous electrode with the gas inlet system of a mass spectrometer was reported by Bruckenstein and Gadde [10]. Similar techniques were frequently being used for the analysis of volatile species in the following years. These have been reviewed exhaustively by Chang et al. [11], Vielstich et al. [12] and Brajter-Toth et al. [13].

### **2.3.2 The Electrospray Interface as Electrochemical Reactor**

The on-line coupling of electrochemistry with mass spectrometry for the determination of non-volatile compounds in solution was first described by Hambitzer and Heitbaum in 1986 [14], who coupled a three-electrode electrochemical flow cell to a thermospray mass spectrometer. Five years later, it was recognized that the

high potential at the capillary tip of an electrospray needle itself induces redox reactions. Since then, the electrospray interface has been used intentionally as “electrochemical reactor” [15,16]. Many important contributions to this field have been made by Van Berkel and co-workers. To exclude possible interferences from the spraying process, they directly connected an ESI source with the detection cell of a diodearray spectrometer, leaving the oxidized species in solution until their detection [17].

Solvent effects have, of course, to be considered as well. Besides its properties to dissolve the analytes and to stabilize the spray, the formed initial oxidation products, e.g., radical cations, have to be stabilized and to be protected from further reactions [18]. Using the electrospray source as controlled-current electrolytical flow cell, Van Berkel et al. were able to detect metal porphyrins, polycyclic aromatic hydrocarbons (PAHs), phenothiazine and other compounds as their radical cations [19].

Not surprisingly, those compounds that are known to be easily oxidized by means of classical electrochemical conversions are as well likely to undergo electrochemical oxidation in the electrospray interface. These are mainly compounds with low redox potentials and reversible redox kinetics. Cole et al. presented the oxidation of metallocenes and their derivatives in the electrospray emitter [20], while McCarley and co-workers found doubly charged biferrocenes and oligoferrocenyilsilanes with up to four charges per molecule [21]. The separation and identification of higher fullerenes from carbon soot as their respective anions was achieved by Jinno et al. in the negative ion mode, proving that reduction processes may be observed as well

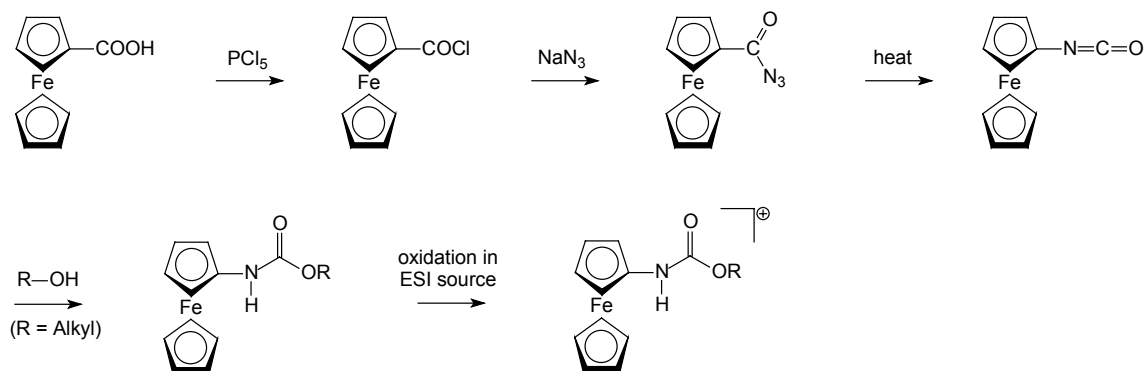
[22]. Other fullerenes and their derivatives have been investigated by ESI-MS in the negative ion mode by Peel et al. [23,24], Gross et al [25] and Drewello et al. [26].

### **2.3.3 Derivatization for Electrochemistry/MS**

Derivatization techniques are of high importance in trace analysis using chromatographic techniques, because they allow the introduction of a functional group which can well be detected with the selected system. Furthermore, chemical and physical properties of the analytes may be changed as desired, e.g., with respect to volatility for GC analysis or to adsorption phenomena in reversed-phase LC. On the other hand, derivatization reactions are typically not the first choice, because they are laborous and they may be a potential source of additional problems. It is frequently observed that the yield of derivatization is far away from quantitative, which will lead to difficult quantification of the analytes. However, in those cases where a direct analysis is either problematic or not possible at all, derivatization is an interesting option. In case of the derivatizing agents mentioned below, the yield of derivatization is high, and strong improvements with respect to selectivity and sensitivity are observed.

The above mentioned findings about the electrospray interface as electrochemical reactor have led to the development of dedicated ferrocene-based derivatizing agents for the ESI-MS analysis of alcohols by Van Berkel et al. [27]. Fruit extracts [27] and plant oils [28] were investigated using this technique, and the tandem MS capabilities of the ferrocene derivatives were investigated more closely [29]. Ferrocenecarboxylic acid azide is used as derivatizing agent, and it is thermally converted into ferrocenyl isocyanate, which then reacts with alcohols under

formation of the respective urethanes. Ionization occurs in the ESI source without the use of an additional electrochemical cell. The respective reaction scheme is presented in Figure 2.1.



**Figure 2.1:** Reaction scheme for the synthesis and the derivatization of alcohols with ferrocenecarboxylic acid azide as well as the in-source oxidation of the formed urethanes [27,28].

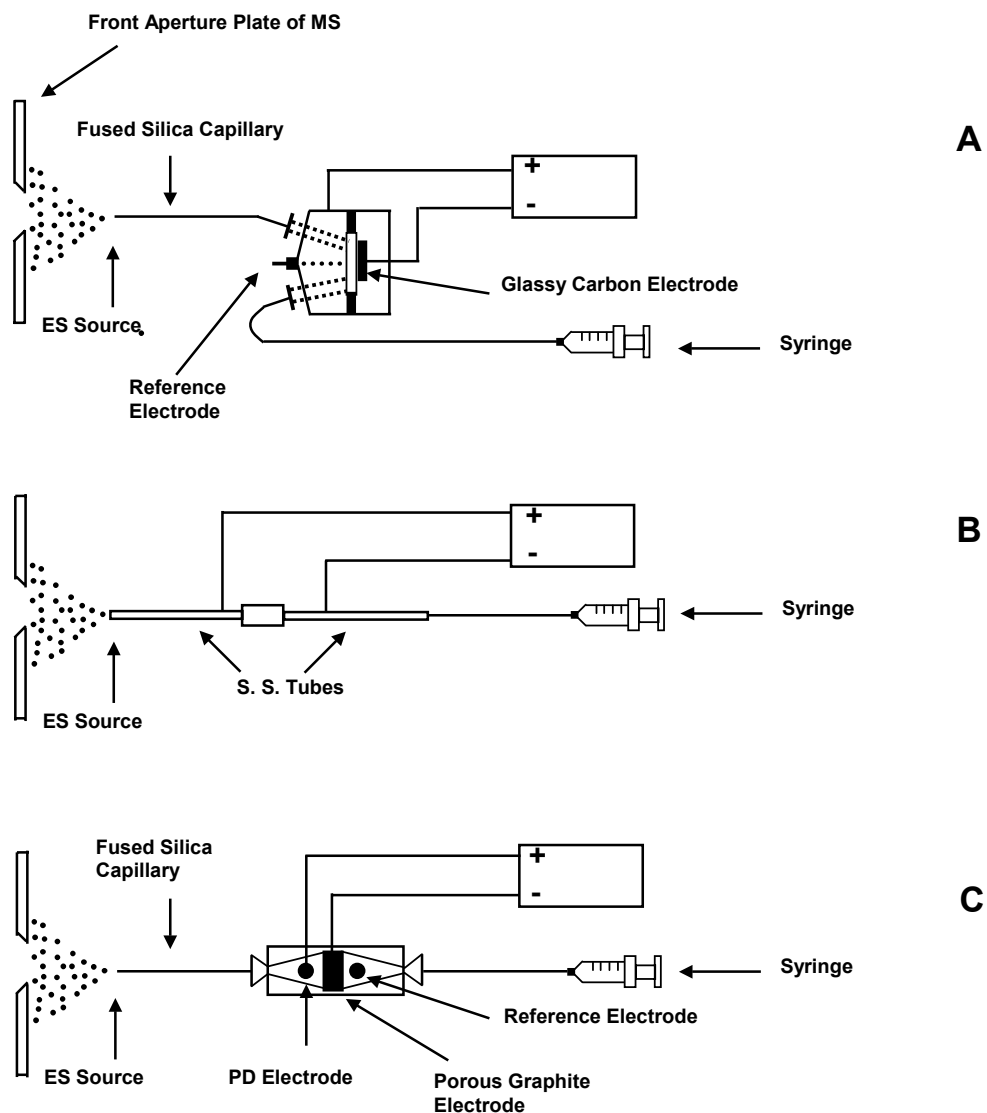
Ferrocene boronic acid may be used to derivatize alkenes after their oxidation to diols [30] and for the analysis of several neutral mono- and disaccharides [31]. A similar approach was used by Williams et al. for the determination of derivatized estrogens [32].

### 2.3.4 The Use of External Electrochemical Cells

All of the authors of the publications summarized in chapter 2.3 were using the electrospray interface without connection to a separation technique, although this is in principle possible. The major advantage of these methods is the easy set-up, as there is no need for any additional equipment. Disadvantages include possible problems to control the conditions for the electrochemical conversions, because it is

extremely difficult to precisely adjust the redox potential for the electrochemical conversions independently from the spray conditions. Additionally, an (almost) quantitative electrochemical conversion, which would lead to higher signals and would be helpful for easy interpretation of the mass spectra in complex samples, may theoretically be achieved only under extremely low flow rates. These are hardly compatible with fast separations in reversed-phase LC.

The use of external electrochemical cells is an easy possibility to overcome these obstacles, although modifications of the equipment have to be carried out. Hambitzer and Heitbaum were the first to couple a three-electrode electrochemical arrangement with thermospray-MS [14]. This approach was expanded to other analytes by Brajter-Toth and Yost, who furthermore applied a commercial “coulometric” cell, which has received this name from its manufacturer, because it may provide for quantitative conversions of the analytes under optimized conditions. This way, uric acid [33,34] and 6-thioxanthine [33] were studied. Regino and Brajter-Toth also used a thin-layer electrochemical cell, which allows easier access to the electrode surface, but which is characterized by a non-quantitative conversion rate [35]. Zhou and Van Berkel [36] connected different electrochemical cells to an electrospray mass spectrometer. The respective experimental arrangements are presented in Figure 2.2.



**Figure 2.2:** Scheme of electrochemical flow cells used on-line with ESI-MS: (A): thin-layer electrode cell, (B): tubular electrode cell, (C): porous graphite electrode cell [36].

A self-assembled tubular electrode cell was used in addition to a commercially available thin-layer cell and a porous glassy carbon electrode. To couple these cells on-line with the electrospray emitter, they must either be used in the “floated mode”, with the potential of the electrospray capillary applied to the cell, or completely decoupled from the high potential of the electrospray needle. To minimize the time

between electrochemical oxidation and mass spectrometric detection of the analytes, Cole et al. constructed a low-volume three-electrode cell within the electrospray probe [37,38]. This arrangement allowed the detection of polycyclic aromatic hydrocarbons as their radical cations. Other redox reactions, including the anodic oxidation of diphenyl sulfide, the reduction of nitrobenzene and the nucleophilic addition of pyridine to the electrogenerated 9,10-diphenylanthracene radical cation were observed using the same set-up [39]. The oligomerization of aniline by using on-line electrochemistry/MS was studied by Deng and Van Berkel et al. [40]. In a thin-layer cell, which was operated at a potential of 1.0V vs. Ag/AgCl, protonated oligomers consisting of up to ten monomer molecules were generated. Kertesz and Van Berkel used the same arrangement to study the electropolymerization of methylene blue [41]. With the oxidation of dopamine in an aqueous/organic phase, Deng and Van Berkel expanded the range of applications to the bioanalytical field [42]. Metabolic oxidation reactions of a dopamine antagonist were mimicked by Bruins et al. in an electrochemistry/MS system [43].

The use of electrochemical cells provides for more defined conditions than the approaches for direct oxidation in the ESI interface. However, it has to be considered that the conversion rate in the electrochemical cell will depend on the type of the cell and the flow rates used. This is one of the most crucial factors when coupling electrochemical conversions on-line with MS. Two different approaches are attractive for the combination of LC, electrochemistry and MS: To identify very complex product mixtures generated in the electrochemical cell, the sequence of electrochemistry with subsequent LC/MS is advantageous. In this case, follow-up reactions may occur due to the long transfer time before detection of the products.

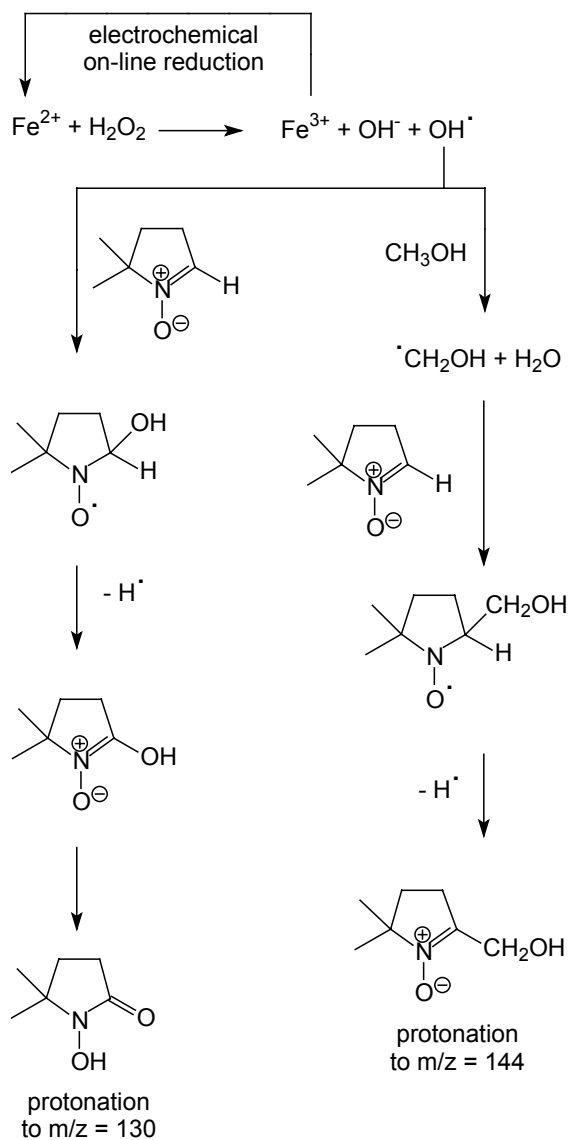
On the other hand, quantitative information on non-polar analytes can best be obtained by LC/electrochemistry/MS, as non-polar analytes may easily be separated under reversed-phase conditions, and the formed more polar species are easier accessible to API-MS detection. While the latter approach also allows the quasi-simultaneous detection of the reaction products of several analytes during one LC run, the earlier approach is preferred in case of a complex product mixture.

### **2.3.5 Combining Electrochemistry with LC and MS**

Both approaches, LC/electrochemistry/MS and electrochemistry/LC/MS have been described in literature. The first report on LC/electrochemistry/MS was described by Volk et al. already in 1989 [44]. Using 6-thiopurine as example, the oxidation of thiopurines was studied using a glassy carbon working electrode with a large surface area, and subsequent reversed-phase LC separation with thermospray-MS detection. Further investigations on the electrochemical reaction pathways of 6-thiopurine and 6-thioxanthine were published later by the same authors using the detection system described above [45]. The same experimental arrangement was also used to compare the electrochemical oxidation of uric acid with its enzymatic oxidation using hydrogen peroxide as oxidant and peroxidase as biocatalyst [46]. Iwahashi and Ishii described a similar approach for the electrochemistry/LC/MS detection of the tryptophan metabolite 3-hydroxy-*dl*-kynurenine. Again, a porous glassy carbon cell was used to ensure high analyte turnover, but detection was performed by ESI-MS [47]. The same instrumentation was used as well to study the electrochemical oxidation of 3-hydroxyanthranilic acid [48]. Bruins et al. have recently described the use of a system, which allows the LC/MS/MS observation of products of the Fenton reaction [49]. Hydroxyl radicals are electrochemically



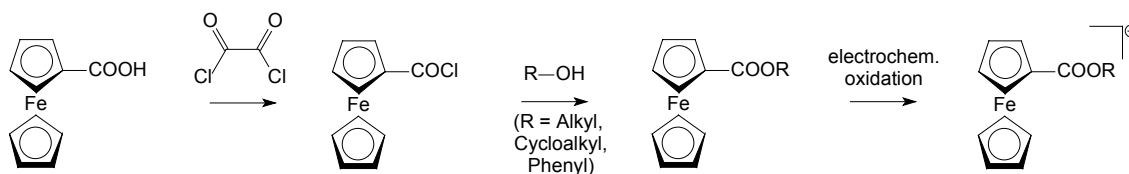
generated in a porous glassy carbon cell, react with xenobiotics, and the products are characterized in the LC/ESI-MS/MS instrument. The respective reaction pathways including the electrochemical generation of hydroxyl radicals and subsequent chemical reactions are presented in Figure 2.3 [49].



**Figure 2.3:** Reaction scheme for the electrochemically assisted Fenton reaction with subsequent radical scavenging by 5,5-dimethyl-1-pyrrolidone-N-oxide (DMPO) and LC/MS analysis of the protonated products [49].

The first report on LC/electrochemistry/MS was described by Dewald et al., who separated phenolic isoflavones by reversed-phase LC, and used a thin-layer cell for electrochemical and a thermospray-MS for subsequent mass spectrometric detection [50]. In this work, the electrochemical cell was not used to improve the MS detection. The method suffered from non-optimum interfacing between the two detectors. Although it is advantageous to obtain data from the two detectors simultaneously, the limited compatibility of gradient elution with electrochemical detection is valid for this method as well. A porous glassy carbon cell was used for the post-column oxidation of various phenols to the respective fluorescent bisphenols [51]. Based on this oxidation, a LC/electrochemistry/fluorescence method for the quantification of phenols was developed, and oligomers of ethylphenol with two, three and four monomers were observed by on-line LC/electrochemistry/APCI(-)-MS.

Recently, Karst et al. [52] presented a method for the determination of ferrocene-labelled alcohols and phenols, in which the analytes were derivatized with ferrocenecarboxylic acid chloride according to literature procedures [53,54]. The derivatives were separated by reversed-phase HPLC and subsequently oxidized in a porous glassy carbon electrode under formation of the charged ferrocinium products. The respective chemical reactions are presented in Figure 2.4.



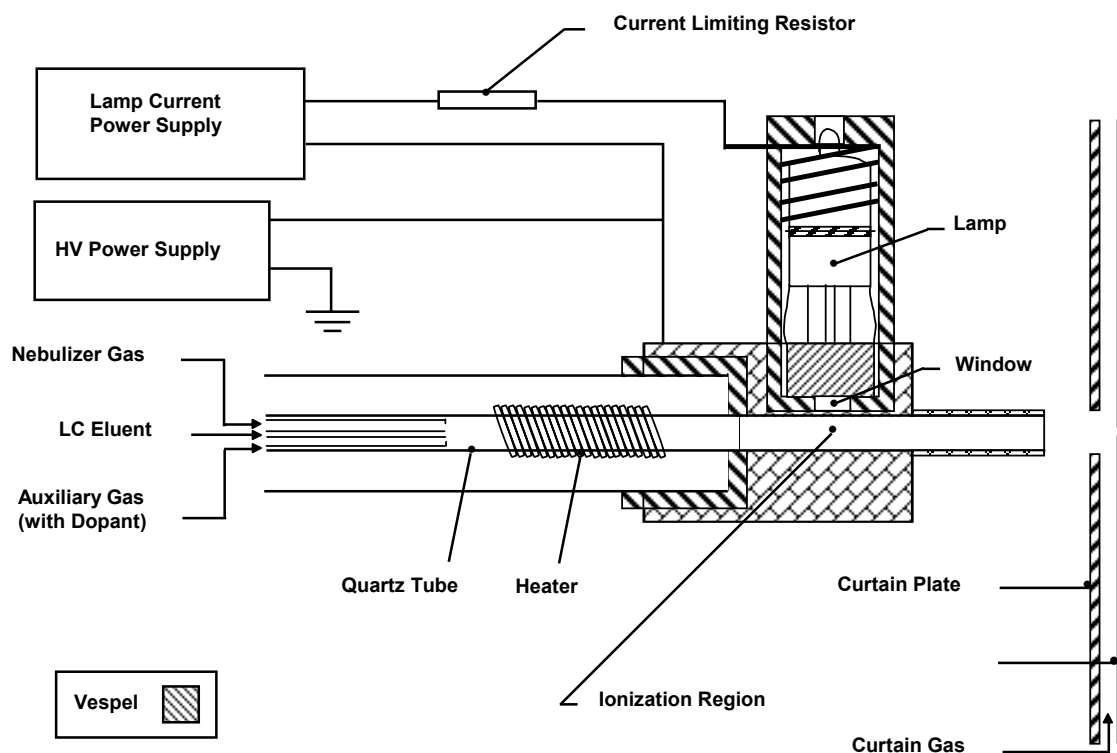
**Figure 2.4:** Derivatization [53,54] and LC/electrochemistry/MS analysis [52,55] of alcohols and phenols using ferrocenecarboxylic acid chloride.

The ferrocenium derivatives were detected in a "heated nebulizer" or thermospray mode using a commercial APCI interface with the corona discharge switched off. The method has also been combined with very fast separations using reversed-phase columns of only 20 mm length [55]. Thus, a series of nine phenol derivatives was separated in less than 1.5 min, and a series of six alcohol derivatives in less than one minute. It can be expected that this and similar labelling strategies will further broaden the applicability of LC/electrochemistry/MS.

Three decades after the first coupling between electrochemistry and MS, this field of research is currently experiencing a dynamic development, as described in this chapter and, with different focus, in previous reviews [11-13,56]. It can be expected that bioanalytical applications of electrochemistry and MS will strongly gain importance in the near future. The groups of Bischoff and Bruins, for example, have recently presented a method for the specific electrochemical cleavage of peptides with on-line mass spectrometric detection [57]. This and related methods are likely to be used either directly or coupled with liquid chromatography in proteomics and related fields.

## 2.4 Atmospheric Pressure Photoionization (APPI)

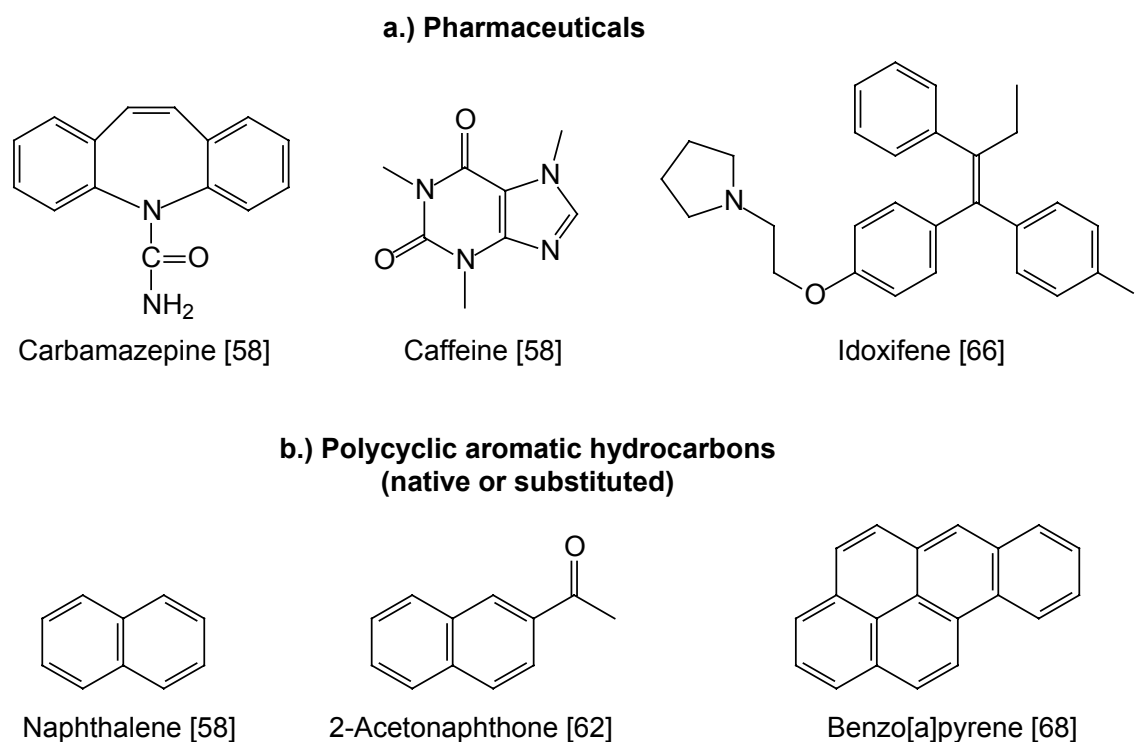
As an alternative ionization technique for API-MS of non-polar compounds, atmospheric pressure photoionization (APPI) has been introduced recently by Bruins et al. [58]. The APPI interface can be considered as a modified APCI source, with the corona discharge being replaced by a gas discharge lamp, which emits photons in the vacuum UV region of the electromagnetic spectrum. The set-up of the APPI interface is presented in Figure 2.5.



**Figure 2.5:** Set-up of the APPI source, including heated nebulizer probe, photoionization lamp and lamp mounting bracket [58].

When the energy of the photons is higher than the first ionization potential of a species in solution, their absorbance leads to single-photon ionization. As the

common LC solvents are characterized by high first ionization potentials, selective ionization of the analytes may occur [58]. The addition of a dopant, an additive to the mobile phase that is first ionized itself and then leads to the ionization of the analytes in further reactions, resulted in greatly enhanced signals [58]. Toluene and acetone were added post-column to the eluent using a syringe pump. Different non-polar compounds were successfully analyzed using this approach, including polycyclic aromatic hydrocarbons (naphthalene and anthracene), drugs (carbamazepine, caffeine) and various other organics (testosterone, diphenyl sulfide) [58]. The structures of some substances which were successfully analyzed by APPI-MS are depicted in Figure 2.6.



**Figure 2.6:** Structures of selected non-polar substances, which are accessible for APPI-MS.

Mechanistic studies were carried out by Koster and Bruins [59], who concluded that in case of proton accepting, reversed phase eluents proton transfer to the analyte will take place via a protonated solvent cluster. In case of normal phase eluents, which cannot accept protons, radical cation formation by charge transfer is favored.

Syage and co-workers presented low-pressure photoionization (LPPI) and APPI, the latter also in combination with liquid chromatography, as new tools for drug discovery [60,61]. As in the work of Bruins et al. [58], dopants were found to offer increased sensitivity for some classes of compounds, although good results were obtained in many cases as well without the presence of a dopant [60].

Kostiainen et al. thoroughly investigated the ionization mechanism and the effect of solvent on the APPI of naphthalenes [62]. A series of seven naphthalene derivatives with electron-donating and electron-withdrawing substituents was investigated in 13 different solvents. Charge exchange and proton transfer were predominantly observed in the positive ion mode, while in the negative ion mode, electron capture or charge exchange were registered for compounds with high electron affinity and proton transfer for compounds with high gas-phase acidity. Again, the ionization efficiency was significantly higher with dopant than without, which was seen as an indication that photoionization of the dopant initiates the ionization process [62]. The group of Kostiainen applied the APPI technique to the analysis of different groups of compounds, including flavonoids [63], steroids [64] and drug metabolites [65]. In all of these cases, APPI-MS was compared with APCI-MS and ESI-MS or ionspray-MS. The best results for these polar analytes were obtained with ESI-MS or ionspray-MS, respectively.

Drug metabolites are also the subject to a recent publication by Yang and Henion [66], who compared APCI-MS and APPI-MS for the determination of idoxifene and its metabolites. While the sensitivity of APPI for idoxifene is 6-8 times higher compared with the sensitivity of APCI, the sensitivity for the metabolites differs, but still with better data for APPI-MS. Plante et al. evaluated the APPI interface with respect to the ionization of drugs under varying conditions (nature and concentration of dopants, flow rates, temperatures and mobile phase composition) in comparison to an APCI and a "turbo ionspray" (modified ESI) interface [67]. With respect to precision and accuracy, the data obtained were comparable to those obtained with the established ionization techniques.

Impey and co-workers [68] investigated polycyclic aromatic hydrocarbons (PAHs), a group of substances, which should be ideal candidates for APPI-MS. Excellent results with very low limits of detection were obtained for normal phase LC, while still satisfactory results were achieved with reversed-phase LC and addition of a dopant. Ambient aerosol samples were investigated using this technique. Cormia et al. used a similar approach, but achieved similar results for most analytes when comparing reversed-phase and normal-phase separation conditions [69]. Methanol gave excellent results as constituent of the mobile phase, and the addition of toluene as dopant proved to be essential.

Ubiquinones and menaquinones were subject to a comparative study of APPI and APCI by Van Berkel et al. [70]. For ubiquinones, both techniques proved to be equally sensitive. For menaquinones, however, sensitivity for APPI was three times higher. As in other studies, toluene was used as a dopant. Kertesz and Van Berkel

observed a reduction of the oligomers formed in the on-line electropolymerization of aniline and of other substances under suitable conditions in both APCI and APPI [71]. It is assumed that reactive species, possibly hydrogen radicals are involved in a surface-assisted process leading to the reduced compounds.

Fat-soluble vitamins were subject to another study by Miller et al. [72]. Vitamin A and vitamin E were directly ionized in the APPI source without the need for a dopant. Depending on the analytes, the  $[M+H]^+$  or the  $[M]^{*+}$  (vitamin E) or the  $[M-H_2O+H]^+$  are observed. Further reactions, which may complicate the interpretation of the spectra, may be observed as well.

Very recently, the similarity of the APPI and APCI sources, the need for comparisons between the two techniques and the missing possibility to predict the performance differences of APCI and APPI for a given analytical task have led to the development of a combined source [73].

Summarizing, APPI-MS is a very young and promising technique which is likely to help overcoming the problems associated with APCI and especially ESI in the analysis of compounds with very low polarity. However, there are only very few reports in literature on APPI yet, and its performance for the analysis of real samples is still to be proven, because the recent publications in this field are mainly focused on the analysis of model compounds or on mechanistic effects. Furthermore, more thorough comparisons between APPI, APCI and ESI, in which the optimum experimental parameters are determined individually for each of the techniques, are needed to allow fair conclusions on the performance of the interfaces. The



determination of PAHs is likely to become a key application for the APPI source, as the APCI performance is very low, while excellent results are already obtained with APPI. It can be expected that, after a period of a few years, APPI will have reached the same degree of maturity that APCI and ESI have already reached today and that a large fraction of those compounds which are currently considered to be optimal candidates for GC/MS will be well accessible by APPI. Therefore, APPI is likely to become a powerful complementary technique to APCI and ESI for the low end of the polarity scale.

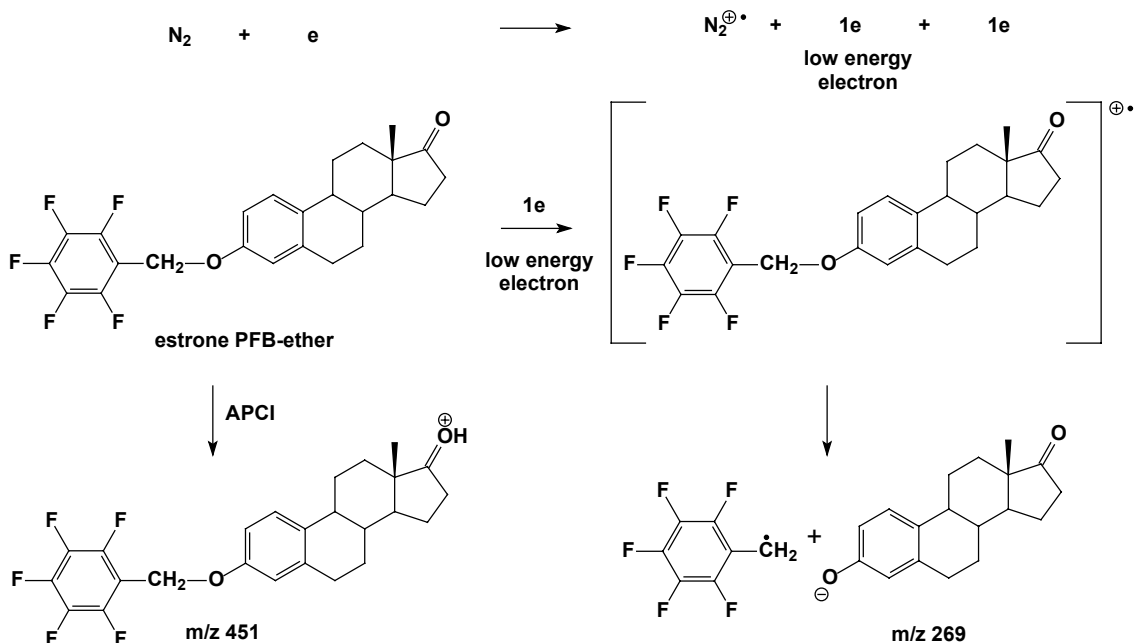
## 2.5 LC/Atmospheric Pressure Electron Capture Negative Ion-MS

When selecting the most selective and sensitive ionization technique for mass spectrometry, electron capture certainly is among the leading candidates. In combination with gas chromatography, attomole amounts of the analyte can be detected. Major prerequisite for electron capture is the presence of an electrophoric group in the molecule to be analyzed. This is mainly introduced using dedicated derivatizing techniques based on polyhalogenated reagents. For analytes bearing polar functionalities, the derivatization does not only improve the detectability, but also the volatility by transferring hydrogen-bond forming functional groups into esters, ethers and related compounds. Recent developments in electron capture MS, with particular focus on GC/MS, are summarized in a review by Giese [74].

In combination with liquid chromatography, only few attempts have been made yet to use electron capture mass spectrometry. The earlier approaches were performed using the particle beam ionization (PBI) interface. Boni et al. derivatized L-tryptophan and L-kynurenine with pentafluorobenzyl bromide, separated them by normal-phase LC and detected them by PBI-MS [75]. The same general strategy was applied by Wang et al., who used 4-pentafluorobenzyl-1,2,4-triazoline-3,5-dione as electron-capture derivatizing agent for dienophiles [76]. Cappiello et al. determined four widely used explosives, 2,4,6-trinitrotoluene (TNT), pentaerythritol tetranitrate (PETN), nitroglycerine (NG) and 1,3,5-trinitro-1,3,5-triazacyclohexane (RDX) by microflow LC-particle beam-NICI-MS [77].

Blair et al. recently realized that, under certain conditions, the corona discharge in commercial APCI interfaces may also be used as a source of low energy electrons,

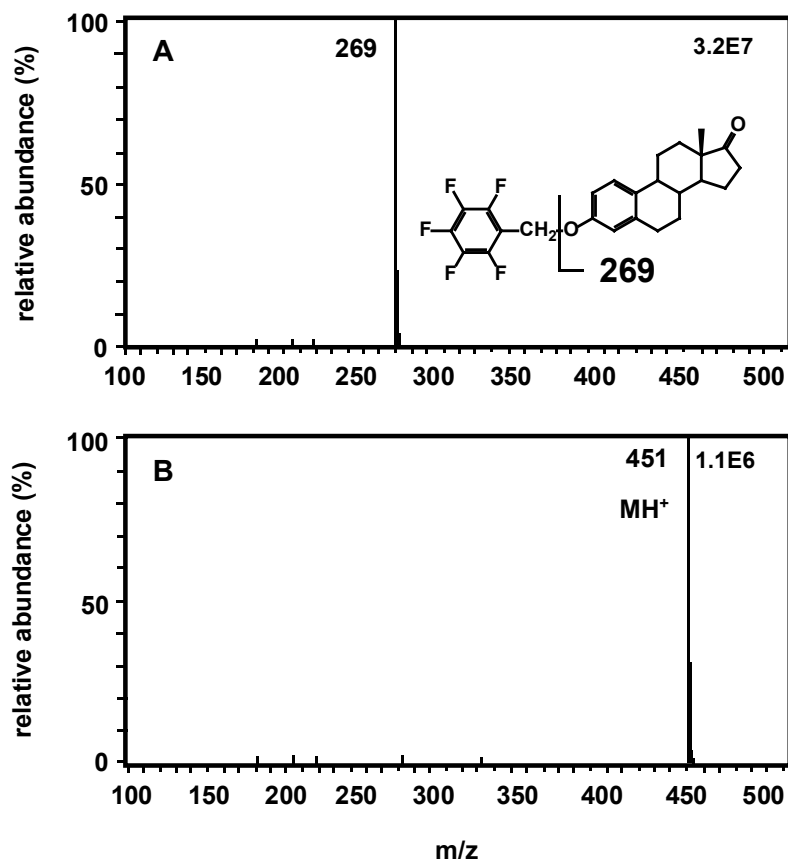
which are generated by displacement of electrons from the nitrogen sheath gas [78]. This way, the known applications of GC/NICI-MS may also be transferred to LC/APCI-MS. Blair et al. used pentafluorobenzyl bromide to derivatize various hydroxy-functionalized biomolecules and drugs. The respective reaction scheme is presented in Figure 2.7.



**Figure 2.7:** Proposed mechanism for electron capture ionization using a commercial APCI interface [78].

The reversed-phase and normal-phase LC separation of the derivatives with subsequent electron capture atmospheric pressure chemical ionization mass spectrometry lead to limits of detection in the attomole range, thus coming close to the limits of detection reported for GC/NICI-MS. In a comparison between negative ion APCI-MS of the underivatized analytes and the new technique, the latter provided an increase in sensitivity of two orders of magnitude [78]. Under dissociative electron capture (loss of the pentafluorobenzyl group), very clear spectra

with a distinct base peak at a mass which corresponds to the  $[M-H]^-$  of the underivatized analytes are obtained, as presented in Figure 2.8.



**Figure 2.8:** Mass spectra of the pentafluorobenzyl-derivative of estrone using an APCI-MS instrument. A: Dissociative electron capture in the negative ion mode. B: Protonation in the positive ion mode [78].

On the basis of APCI(+) experiments, the authors proved that the observed effect is indeed based on electron capture. The structural integrity of the analytes was maintained during the ionization process.

This technique was afterwards used by the same authors and other groups for various new applications. Impey et al. [79] analyzed prostaglandins, estradiol and D-

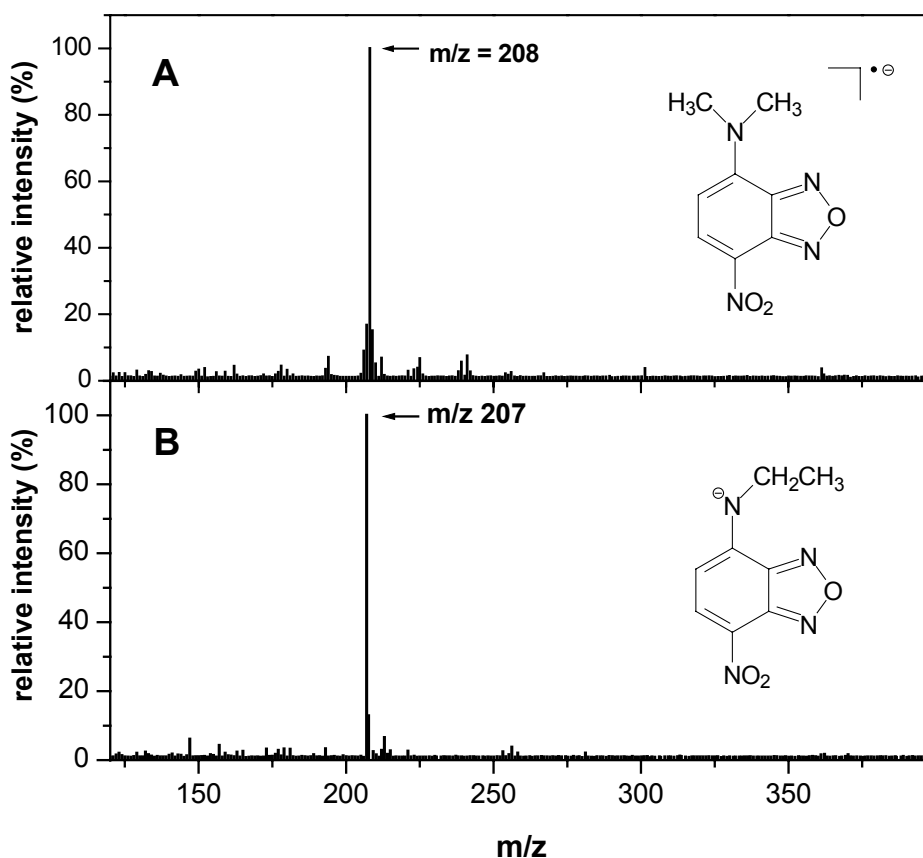
group vitamins using the same methodology, while Fujiwara et al. [80] developed a respective method for the determination of thromboxane in biological samples, with the LC separation performed in the normal-phase mode. Blair et al. again increased the range of applications by a method for the determination of estrogen metabolites [81]. In this work, normal-phase LC was again used with a silica column and a binary isopropanol/hexane gradient.

It can be expected that the range of applications for this methodology will be strongly increasing in the next years. The technique is especially interesting in those cases where multifunctional analytes are derivatized to very large products, which are problematic to be analyzed by GC/NICI-MS.

Even before the pioneering work of Blair et al. on dedicated electron capture derivatizing agents to be used with the APCI interface [78], other authors observed radical anions of nitroaromatics, but obviously without realizing the mechanistic background. Snow et al. determined different nitro-based explosives by LC/MS and detected a significant response for the molecular anion of 2,4,6-trinitrotoluene (TNT) in the negative ion mode [82]. With increasing needle voltage, a strong increase of the abundance of the TNT molecular anion was observed. However, quantification was performed for the stronger peak of the isopropanolate adduct  $\text{TNT} + \text{C}_3\text{H}_7\text{O}^-$ . The authors state that for nitroaromatics, the signals using the APCI interface are generally much stronger compared with the signals using the ESI interface. Palloch and Pelzing observed the radical anion of TNT as well, but with lower abundance than the ion of the deprotonated TNT [83]. No comments were made on the formation of the  $\text{M}^-$  peak. Keely et al. very recently studied the ionization of different

explosives using APCI-MS and ESI-MS more exhaustively [84]. The analytes were transferred into the interface either by infusion or by direct injection, but in all cases without chromatographic separation. In this work, the limit of detection for TNT using APCI-MS surpassed that using ESI-MS by three decades, with both ionization techniques being applied in the negative ion mode. For TNT, Keely et al. [84] detected the radical anion as base peak, and some ions of lower abundance. However, the mechanism of ion formation was not discussed in this case as well.

Karst et al. described unambiguous electron capture effects in the determination of native nitroaromatics and of substances derivatized with nitroaromatics using LC/APCI-MS in the negative ion mode [85]. The electron capture effect was found to be in strong competition with other ionization mechanisms. As soon as easy deprotonation was possible for the nitroaromatics, this was favored in comparison with electron capture. This was demonstrated for the analysis of amines after their derivatization with 4-chloro-7-nitro-2,1,3-benzoxadiazole (NBD chloride). For the derivatives of primary amines, deprotonation at the amino-N occurred. With respect to the derivatives of secondary amines, deprotonation is no longer possible, resulting in a strong signal for the electron capture product, the radical anion. The respective mass spectra for derivatives of a primary and a secondary amine are presented in Figure 2.9.



**Figure 2.9:** APCI(-) mass spectra of the 4-chloro-7-nitrobenzoxadiazole (NBD chloride) derivatives of dimethylamine (A) and ethylamine (B). While non-dissociative electron capture is observed in (A), deprotonation occurs in (B) [85].

It should be mentioned that in this case, non-dissociative electron capture was observed, while dissociative electron capture occurred for example in case of N-methylhydrazino-functionalized aldehydes and ketones [85].

A series of nitrosubstituted and/or halogenated derivatizing agents has recently been introduced by Higashi et al. [86,87]. In [86], a large series of different nitroaromatics and polyhalogenated aromatics was investigated with the goal to find the most suitable backbone molecules for negative ion electron capture-MS in the APCI

interface. It was found that the 2-nitro-4-trifluoromethylphenyl moiety was most effective in improving sensitivity. Reagents based on this backbone were applied to the analysis of steroids in human plasma. In another study, 2-nitro-4-trifluoromethylphenylhydrazine was successfully applied to derivatize 20-oxosteroids for subsequent electron capture in the APCI interface [87].

In this area, the development of new powerful dedicated derivatizing agents based on polyhalogenated compounds or nitroaromatics can be expected. In combination with dissociative or non-dissociative electron capture and tandem mass spectrometry, extremely low limits of detection might be achieved for molecules, which currently cannot be analyzed by GC/MS because of their thermolability even after derivatization. These analytes could include in particular biomolecules with molecular masses of many hundred up to a few thousand g/mol, which are today only accessible by MALDI/MS, but not by MS in combination with separation techniques. Additionally, selected established derivatizing agents, which are applied since a long time in LC with UV or fluorescence detection or in GC with selective detectors may now be used in LC/MS. It should, however, be considered that deprotonation and electron capture are competing processes [85], and that both may occur in parallel for selected compounds. The ratio between both may differ from compound to compound, and strong solvent effects have been observed in own unpublished work of the authors for nitroaromatics. Therefore, individual optimization for any group of analytes will be required to make optimum analytical use of electron capture processes in the APCI interface.



## **2.6 Coordination Ionspray-MS (CIS-MS)**

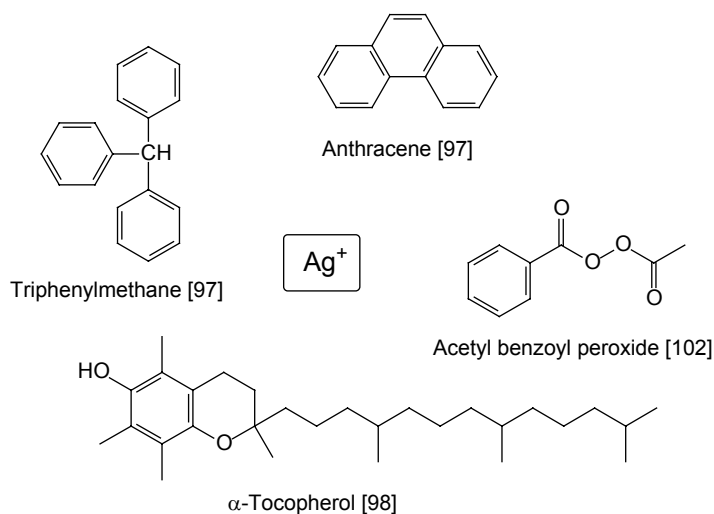
Since many years, the addition of various anions or cations to a solution of the analytes with the purpose to obtain charged adducts is a well-known strategy in various mass spectrometric techniques [88]. This method is mainly applied to polar analytes, which easily form adducts with, e.g., the alkali cations [89], and transition metal cations [90]. Within this chapter, the focus shall exclusively be directed on those methods in combination with ESI-MS or APCI-MS, in which ions are added to non-polar compounds to induce ionization of originally non-charged compounds. One possibility to estimate the usefulness of an added ion to form a complex with the analyte is the application of Pearson's classification of "hard" and "soft" acids and bases [91]. In a simplified summary of Pearson's classification, hard acids or bases are electron pair acceptors or donors, which have comparably high charge and small size. Soft acids or bases, on the other hand, are characterized by low charge and large size. Pearson concludes that hard acids form stable complexes with hard bases, and weak acids form stable complexes with weak bases. As strongly polar compounds will fall under Pearson's definition for hard acids and bases, this chapter will focus on complexes of soft acids (large metal cations with little charge) with soft bases (large, non-polar organics).

As precursor of what is called "coordination ionspray" today, Henderson and Nicholson added silver nitrate to solutions of neutral metal carbonyl complexes [92]. Consequently, their respective silver adducts were detected in the electrospray mass spectrometer. Laakso and Voutilainen analyzed triacylglycerols by LC/MS with silver ions added to the mobile phase [93]. In APCI-MS, protonated and fragmented molecular ions were observed with the highest abundance, and silver adducts were

detected only with lower intensities. On the other hand, the separation of equally unsaturated triacylglycerols was improved. Schuyt et al. investigated the same analytes and detected silver(I) complexes as well, but again the major focus was the improvement of the LC separation by addition of silver ions [94].

In 1997, Siu et al. described the formation of complexes of peptides and proteins with silver(I) cations [95]. The latter were directly added to the solution of the analytes, and electrospray analysis was carried out by infusion of the mixture directly into the ESI interface. No separation was carried out within this work. For proteins as insulin, multiple coordination was observed, resulting in multiple charging of the analytes. According to Pearson's classification, the "soft" methionine sulfur acts as coordination site for the silver(I) ions. Roussis and Prouix [96] used a similar approach to determine the molecular weight distribution of heavy aromatic petroleum fractions by ESI-MS. The addition of  $\text{Ag}^+$  lead to intense signals of the respective complexes. Although in principle possible, no separation was carried out.

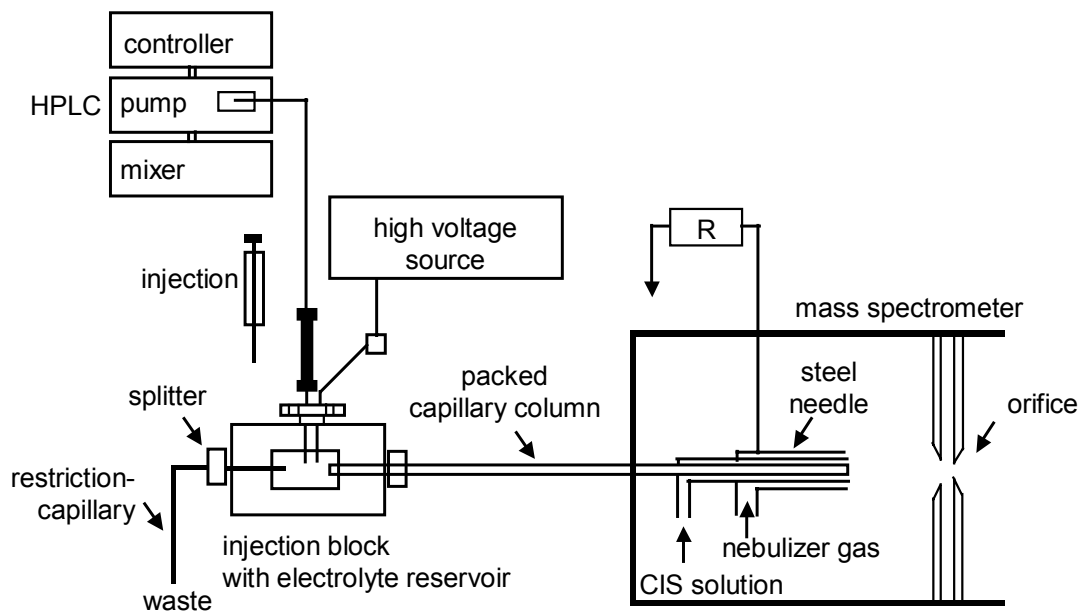
The term "coordination ionspray-MS" was introduced by Bayer et al. in 1999 [97]. They investigated a series of truly non-polar compounds and added, after liquid chromatographic separation of the analytes, various ionic reagents to induce coordination and therefore charging of the subjects of investigation. While Ag(I) was added in order to ionize arenes, olefins, polyolefins and carotinoids, Pd(II) was used to ionize vitamins A, D and E as well as estrogens. The structures of selected non-polar compounds, which may be detected based on their adduct formation with Ag(I) ions are depicted in Figure 2.10.



**Figure 2.10:** Selection of substances which can be analyzed by coordination ionspray-MS with addition of silver(I) ions.

More polar compounds could be analyzed as well, e.g., sugars by addition of boric acid, or peptides, sugars and alcohols by addition of lithium halogenides. It should, however, be noted that the more polar analytes typically may be well detected by ESI-MS, while the less polar compounds are detected with inferior limits of detection or not at all. The solution of the ions to be coordinated is added by a simple set-up in a sheath-flow stream. The respective experimental set-up is presented in Figure 2.11. A previous paper of the same group already described the application of a similar technique to the determination of tocopherols and carotenoids in LC/ESI-MS [98]. In this case,  $\text{Ag(I)}$  ions were added to ionize the analytes. Femtomole amounts of selected carotenoids could be detected. In a combined approach with LC/MS and LC/NMR, the tocotrienol isomers could be separated and identified in crude palm oil extract [99]. As in the previous work, coordination ionspray was carried out using  $\text{Ag(I)}$ . Bayer et al. demonstrated that the coordination ionspray method can also be applied in combination with capillary electrochromatography (CEC) [100]. In this

work, unsaturated fatty acid methyl esters, vitamins of the D group and estrogenic compounds were investigated.



**Figure 2.11:** Instrumental set-up for direct coupling of capillary separation techniques with CIS-MS by adding the solution of the coordinating ion in a sheath-flow stream [97].

Porter et al. expanded the coordination ionspray technique to peroxidation products of cholesterol linoleate and cholesterol arachidonate [101]. Complex peroxide mixtures were successfully investigated by this method. As in the original method of Bayer et al., Ag(I) was added after liquid chromatographic separation of the peroxides. The same group subsequently determined diacyl peroxides by coordination ionspray with tandem mass spectrometry [102]. The site-directed fragmentation of neutral and polar lipids by Ag<sup>+</sup> in coordination ionspray was subject of a more recent report by Porter and co-workers [103]. Rudzinski and Zhang recently reported the analysis of organosulfur compounds in petroleum products by addition of Pd(II) [104]. Dibenzothiophene and related compounds could be

determined by coordination ionspray-tandem mass spectrometry. Takino et al. described the determination of PAHs with post-column addition of Ag(I) [105].

Very recently, coordination ionspray has been applied to triglycerides in vegetable oils after separation by supercritical fluid chromatography. Sandra et al. obtained an increase of sensitivity by a factor of 100 compared with UV detection [106]. For saturated triglycerides, only the  $[M+Ag]^+$  peaks were observed, while unsaturated triglycerides were detected as  $[M+H]^+$  and  $[M+Ag]^+$ .

Coordination ionspray is therefore comparable to the previously discussed techniques, because the method has been introduced very recently, and significant new applications are likely to be presented by an increasing number of scientific groups in the near future. These may occur for example in the field of the analysis of non-polar compounds of biological relevance or in environmental analysis of heteroaromatic substances. Although no respective effects have been reported in literature yet, the addition of Ag(I) salts may lead to the deposition of significant amounts of silver in the instrument. This will depend on the characteristics of the individual interface, but should be considered prior to the application of high silver salt concentrations. A possible strategy to overcome respective problems would be the use of nanospray interfaces at as low flow rates as possible, which would drastically reduce the total silver amount introduced into the system.

## **2.7 Conclusions**

A series of four different new techniques for the LC/MS analysis of non-polar compounds has been presented. From the current point of view, none of these will achieve the status of an “universal” ionization technique for non-polar compounds, but all show a very high potential to be useful tools for particular applications. The coupling of electrochemistry and MS will be limited to electroactive analytes, but the exploitation of this technique may deliver exciting new insights into biological redox reactions, and extremely low limits of detection may be achieved in combination with dedicated derivatizing agents. The APPI approach is probably the most generally applicable of those presented within this paper. APPI is already on the way to be a complementary technique to APCI for even less polar compounds. Especially for the analysis of aromatic compounds with few polar functionalities, APPI is likely to be superior in comparison to APCI. Electron capture ionization may be carried out on an existing LC/APCI-MS instrument, but its application is limited to compounds with strongly electron-withdrawing substituents, e.g., polyhalogenated and nitroaromatic compounds. In the bioanalytical field, an increasing development of dedicated derivatizing agents for electron capture APCI-MS can be expected. For coordination ionspray-MS, the consequent application of Pearson’s classification is likely to lead to new and currently unexpected applications for the analysis of non-polar compounds.

## **2.8 References**

- [1] M. Yamashita, J.B. Fenn, *J. Phys. Chem.* 88 (1984) 4451.
- [2] C. M. Whitehouse, R. N. Dreyer, M. Yamashita, J. B. Fenn, *Anal. Chem.* 57 (1985) 675.
- [3] A. P. Bruins, T. R. Covey, J. D. Henion, *Anal. Chem.* 59 (1987) 2642.
- [4] J. F. Banks, J. P. Quinn, C. M. Whitehouse, *Anal. Chem.* 66 (1994) 3688.
- [5] D. I. Carroll, I. Dzidic, R. N. Stillwell, K. D. Haegele, E. C. Horning, *Anal. Chem.* 47 (1975) 2369.
- [6] B. A. Thomson, *J. Am. Soc. Mass Spectrom.* 9 (1998) 187.
- [7] W. M. A. Niessen, *J. Chromatogr. A* 856 (1999) 179.
- [8] E. Gelpí, *J. Mass Spectrom.* 37 (2002) 241.
- [9] R. Willoughby, E. Sheehan, S. Mitrovich, *A Global View of LC/MS*, 2nd Edition, Global View Publishing, Pittsburgh (2002).
- [10] S. Bruckenstein, R. R. Gadde, *J. Am. Chem. Soc.* 93 (1971) 793.
- [11] H. Chang, D. C. Johnson, R. S. Houk, *Trends Anal. Chem.* 8 (1989) 328.
- [12] B. Bittens-Cattaneo, E. Cattaneo, P. Konigshoven, W. Vielstich, in: A.J. Bard (ed.), *Electroanalytical chemistry*, Vol. 17, Marcel Dekker, New York (1991).
- [13] K. J. Volk, R. A. Yost, A. Brajter-Toth, *Anal. Chem.* 64 (1992) 21A.
- [14] G. Hambitzer, J. Heitbaum, *Anal. Chem.* 58 (1986) 1067.
- [15] G. J. Van Berkel, S. A. McLuckey, G. L. Glish, *Anal. Chem.* 63 (1991) 1098.
- [16] T. Blades, M. G. Ikonomou, P. Kebarle, *Anal. Chem.* 63 (1991) 2109.
- [17] G. J. Van Berkel, F. Zhou, *Anal. Chem.* 67 (1995) 2916.
- [18] G. J. Van Berkel, S. A. McLuckey, G. L. Glish, *Anal. Chem.* 64 (1992) 1586.
- [19] G. J. Van Berkel, F. Zhou, *Anal. Chem.* 67 (1995) 3958.
- [20] X. Xu, S. P. Nolan, R. B. Cole, *Anal. Chem.* 66 (1994) 119.

- [21] T. D. McCarley, M. W. Lufaso, L. S. Curtin, R. L. McCarley, *J. Phys. Chem. B* 102 (1998) 10078.
- [22] K. Jinno, Y. Sato, H. Nagashima, K. Itoh, *J. Microcolumn Sep.* 10 (1998) 79.
- [23] G. Khairalla, J. B. Peel, *J. Phys. Chem. A* 101 (1997) 6770.
- [24] G. Khairalla, J. B. Peel, *Chem. Phys. Lett.* 296 (1998) 545.
- [25] D. Felder, H. Nierengarten, J. P. Gisselbrecht, C. Boudon, E. Leize, J. F. Nicoud, M. Gross, A. Van Dorsselaer, J. F. Nierengarten, *New J. Chem.* 24 (2000) 687.
- [26] M. P. Barrow, X. D. Feng, J. I. Wallace, O. V. Boltalina, R. Taylor, P. J. Derrick, T. Drewello, *Chem. Phys. Lett.* 330 (2000) 267.
- [27] G. J. Van Berkel, J. M. E. Quirke, R. A. Tigani, A. S. Dilley, T. R. Covey, *Anal. Chem.* 70 (1998) 1544.
- [28] J. M. E. Quirke, Y. - L. Hsu, G. J. Van Berkel, *J. Nat. Prod.* 63 (2000) 230.
- [29] J. M. E. Quirke, G. J. Van Berkel, *J. Mass. Spectrom.* 36 (2001) 179.
- [30] G. J. Van Berkel, J. M. E. Quirke, C.L. Adams, *Rapid Commun. Mass Spectrom.* 14 (2000) 849.
- [31] D. Williams, M. K. Young, *Rapid Commun. Mass Spectrom.* 14 (2000) 2083.
- [32] D. Williams, S. Chen, M. K. Young, *Rapid Commun. Mass Spectrom.* 15 (2001) 182.
- [33] K. J. Volk, M. S. Lee, R. A. Yost, A. Brajter-Toth, *Anal. Chem.* 60 (1988) 720.
- [34] K. J. Volk, R. A. Yost, A. Brajter-Toth, *Anal. Chem.* 61 (1989) 1709.
- [35] M. C. S. Regino, A. Brajter-Toth, *Anal. Chem.* 69 (1997) 5067.
- [36] F. Zhou, G. J. Van Berkel, *Anal. Chem.* 67 (1995) 3643.
- [37] X. Xu, W. Lu, R. B. Cole, *Anal. Chem.* 68 (1996) 4244.



- [38] R. B. Cole, X. Xu, U.S. Patent 5 879 949 (1999).
- [39] W. Lu, X. Xu, R. B. Cole, *Anal. Chem.* 69 (1997) 2478.
- [40] H. Deng, G. J. Van Berkel, *Anal. Chem.* 71 (1999) 4284.
- [41] V. Kertesz, G. J. Van Berkel; *Electroanalysis* 13 (2001) 1425.
- [42] H. Deng, G. J. Van Berkel, *Electroanalysis* 11 (1999) 857.
- [43] U. Jurva, H. V. Wikström, A. P. Bruins, *Rapid Commun. Mass Spectrom.* 14 (2000) 529.
- [44] K. J. Volk, R. A. Yost, A. Brajter-Toth, *J. Chromatogr.* 474 (1989) 231.
- [45] K. J. Volk, R. A. Yost, A. Brajter-Toth, *J. Electrochem. Soc.* 137 (1990) 1764.
- [46] K. J. Volk, R. A. Yost, A. Brajter-Toth, *J. Pharm. Biomed. Anal.* 8 (1990) 205.
- [47] H. Iwahashi, T. Ishii, *J. Chromatogr. A* 773 (1997) 23.
- [48] H. Iwahashi, *J. Chromatogr. B.* 736 (1999) 237.
- [49] U. Jurva, H. V. Wikström, A. P. Bruins, *Rapid Commun. Mass Spectrom.* 16 (2002) 1934.
- [50] H. D. Dewald, S. A. Worst, J. A. Butcher, E. F. Saulinskas, *Electroanalysis* 3 (1991) 777.
- [51] J. Meyer, A. Liesener, S. Götz, H. Hayen, U., Karst, *Anal. Chem.* 75 (2003) 922.
- [52] G. Diehl, A. Liesener, U. Karst, *Analyst* 126 (2001) 288.
- [53] J. Rolfes, J. T. Andersson, *Anal. Commun.* 33 (1996) 429.
- [54] J. Rolfes, J. T. Andersson, *Anal. Chem.* 73 (2001) 3073.
- [55] G. Diehl, U. Karst, *J. Chromatogr. A.* 974 (2002) 103.
- [56] G. Diehl, U. Karst, *Anal. Bioanal. Chem.* 373 (2002) 390.

- [57] H. P. Permentier, J. U. Jurva, M. B. Barroso, R. Bischoff, A. P. Bruins, Proceedings of the 50th ASMS Conference on Mass Spectrometry and Allied Topics, Poster TPA 002 (2002).
- [58] D. B. Robb, T. R. Covey, A. P. Bruins, *Anal. Chem.* 72 (2000) 3653.
- [59] G. Koster, A. P. Bruins, Proceedings of the 49th ASMS Conference on Mass Spectrometry and Allied Topics, Poster TPC 071 (2001).
- [60] J. A. Syage, M. D. Evans, *Spectroscopy* 16 (2001) 14.
- [61] J. A. Syage, M. D. Evans, K. A. Hanold, *Amer. Lab.* 32 (2000) 42.
- [62] T. J. Kauppila, T. Kuuranne, E. C. Meurer, M. N. Eberlin, T. Kotiaho, R. Kostianen, *Anal. Chem.* 74 (2002) 5470.
- [63] J. - P. Rauha, H. Vuorela, R. Kostianen, *J. Mass Spectrom.* 36 (2001) 1269.
- [64] A. Leinonen, T. Kuuranne, R. Kostianen, *J. Mass Spectrom.* 37 (2002) 693.
- [65] H. Keski-Hynnälä, M. Kurkela, E. Elovaara, L. Antonio, J. Magdalou, L. Luukkanen, J. Taskinen, R. Kostianen, *Anal. Chem.* 74 (2002) 3449.
- [66] C. M. Yang, J. Henion, *J. Chromatogr. A* 970 (2002) 155.
- [67] G. Plante, E. Tessier, R. Guilbaud, Proceedings of the 49th ASMS Conference on Mass Spectrometry and Allied Topics, Poster TPI 217 (2001).
- [68] G. Impey, B. Kieser, J. - F. Alary, Proceedings of the 49th ASMS Conference on Mass Spectrometry and Allied Topics, Poster TPH 187 (2001).
- [69] P. H. Cormia, S. M. Fischer, C. A. Miller, Proceedings of the 49th ASMS Conference on Mass Spectrometry and Allied Topics, Poster ThPH176 (2001).
- [70] C. A. Lytle, G. J. Van Berkel, D. C. White, Proceedings of the 49th ASMS Conference on Mass Spectrometry and Allied Topics, Poster TPC 074 (2001).
- [71] V. Kertesz, G. J. Van Berkel, *J. Am. Soc. Mass Spectrom.* 13 (2002) 109.

- [72] C. A. Miller, P. H. Cormia, S. M. Fischer, Proceedings of the 49th ASMS Conference on Mass Spectrometry and Allied Topics, Poster TPC 072 (2001).
- [73] K. A. Hanold, J. A. Syage, Proceedings of the 50th ASMS Conference on Mass Spectrometry and Allied Topics, Presentation WOBam 11:15 (2002).
- [74] R. W. Giese, J. Chromatogr. A 892 (2000) 329.
- [75] R. L. Boni, J. T. Simpson, D. B. Naritsin, K. Saito, S. P. Markey, Biol. Mass Spectrom. 23 (1994) 27.
- [76] K. Wang, P. P. Davis, T. Crews, L. Gabriel, R. W. Edom, Anal. Biochem. 243 (1996) 28.
- [77] A. Cappiello, G. Famiglini, A. Lombardozzi, A. Massari, G. G. Vadala, J. Am. Soc. Mass Spectrom. 7 (1996) 753.
- [78] G. Singh, A. Gutierrez, K. Xu. I. A. Blair, Anal. Chem. 72 (2000) 3007.
- [79] G. A. Impey, T. Covey, T. Sakuma, H. Fujiwara, J. Muhammad, K. Duffin, Proceedings of the 50th ASMS Conference on Mass Spectrometry and Allied Topics, Poster MPL 368 (2002).
- [80] H. Fujiwara, J. Muhammad, K. L. Duffin, M. Splendore, M. Amad, R. Thakur, Proceedings of the 50th ASMS Conference on Mass Spectrometry and Allied Topics, Poster TPH 186 (2002).
- [81] A. Gutierrez, S. Tilve, P. O'Dwyer, R. Boston, I. A. Blair, Proceedings of the 49th ASMS Conference on Mass Spectrometry and Allied Topics, Poster ThPM 321 (2001).
- [82] D. A. Cassada, S. J. Monson, D. D. Snow, R. F. Spalding, J. Chromatogr. A 844 (1999) 87.

- [83] P. Palloch, M. Pelzing, Proceedings of the 25th International Symposium on High Performance Liquid Phase Separations and Related Techniques, Poster P1410 (2001).
- [84] C. S. Evans, R. Sleeman, J. Luke, B. J. Keely, Rapid Commun. Mass Spectrom. 16 (2002) 1883.
- [85] H. Hayen, N. Jachmann, M. Vogel, U. Karst, Analyst 127 (2002) 1027.
- [86] T. Higashi, N. Takido, A. Yamauchi, K. Shimada, Anal. Sci. 18 (2002) 1301.
- [87] T. Higashi, N. Takido, K. Shimada, Analyst 128 (2003) 130.
- [88] L. M. Teesch, J. Adams, Org. Mass. Spectrom., 27 (1992) 931.
- [89] K. - E. Karlsson, J. Chromatogr. A 794 (1998) 359.
- [90] J. Shen, J. S. Brodbelt, Rapid Commun. Mass Spectrom., 13 (1999) 1381.
- [91] R. G. Pearson, J. Am. Chem. Soc. 85 (1963) 3533.
- [92] W. Henderson, B. K. Nicholson, J. Chem. Soc., Chem. Commun. 24 (1995) 2531.
- [93] P. Laakso, P. Voutilainen, Lipids 31 (1996) 1311.
- [94] P. J. W. Schuyl, T. de Joode, M. A. Vasconcellos, G. S. M. J. E. Duchateau, J. Chromatogr. A 810 (1998) 53.
- [95] H. Li, K. W. M. Siu, R. Guevremont, J. C. Y. Le Blanc, J. Am. Soc. Mass Spectrom. 8 (1997) 781.
- [96] S. G. Roussis, R. Prouix, Anal. Chem. 74 (2002) 1408.
- [97] E. Bayer, P. Gfrörer, C. Rentel, Angew. Chem. Int. Ed. 38 (1999) 992.
- [98] C. Rentel, S. Strohschein, K. Albert, E. Bayer, Anal. Chem. 70 (1998) 4394.
- [99] S. Strohschein, C. Rentel, T. Lacker, E. Bayer, K. Albert, Anal. Chem. 71 (1999) 1780.
- [100] C. Rentel, P. Gfrörer, E. Bayer, Electrophoresis 20 (1999) 2329.

- [101] C. M. Havrilla, D. L. Hachey, N. A. Porter, *J. Am. Chem. Soc.* 122 (2000) 8042.
- [102] H. Yin, D. L. Hachey, N. A. Porter, *J. Am. Soc. Mass Spectrom.* 12 (2001) 449.
- [103] M. L. Manier, C. M. Havrilla, G. J. Lohr, N. A. Porter, D. L. Hachey, Proceedings of the 49th ASMS Conference on Mass Spectrometry and Allied Topics, Poster MPM 310 (2001).
- [104] W. E. Rudzinski, Y. Zhang, Proceedings of the 50th ASMS Conference on Mass Spectrometry and Allied Topics, Presentation ThOCam 11:15 (2002).
- [105] M. Takino, S. Daishima, K. Yamaguchi, T. Nakahara, *J. Chromatogr. A* 928 (2001) 53.
- [106] P. Sandra, A. Medvedovici, Y. Zhao, F. David, *J. Chromatogr. A* 974 (2002) 231.



# Chapter 3

## Analysis of Phenothiazine and its Derivatives using LC/Electrochemistry/MS and LC/Electrochemistry/Fluorescence\*

### 3.1 Abstract

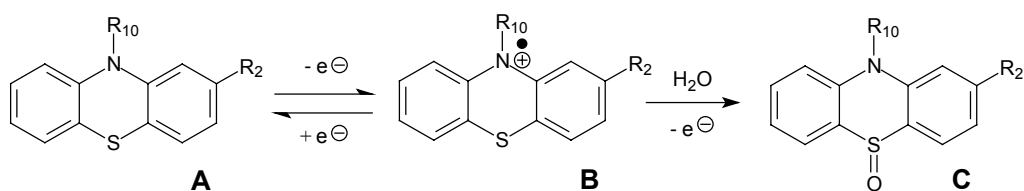
The on-line electrochemical conversion of phenothiazine and its derivatives after liquid chromatographic separation has been studied by mass spectrometry and fluorescence spectroscopy. In an electrochemical cell consisting of porous glassy carbon, the phenothiazines are readily converted to oxidized products, which can be detected by on-line fluorescence spectroscopy and mass spectrometry. The method allows rapid investigations on the electrochemical oxidation pathways, as demonstrated for phenothiazine itself. The phenothiazine derivatives are transferred into their strongly fluorescent sulfoxides. Based on this reaction, an LC/electrochemistry/fluorescence method was developed giving limits of detection between  $5 \times 10^{-9}$  mol/L and  $4 \times 10^{-8}$  mol/L and limits of quantification between  $2 \times 10^{-8}$  mol/L and  $1 \times 10^{-7}$  mol/L for the individual phenothiazines. The linear ranges comprised three decades starting at the limit of quantification.

\*H. Hayen, U. Karst, *Anal. Chem.*, in press

### 3.2 Introduction

Phenothiazine and its derivatives are an important group of pharmaceuticals that are used for the treatment of psychic diseases [1]. Their antihistaminic and antiemetic properties have also found clinical use [2]. For this reason, the determination of phenothiazines in pharmaceutical formulations and in body fluids is important. The large variety of analytical techniques used for this purpose confirms this statement [3]. Titration [4], photometry [5], fluorimetry [6], chemiluminescence [7], electroanalysis [8], enzyme inhibition assays [9], mass spectrometry [10], gas chromatography [11], supercritical fluid chromatography [12], liquid chromatography [13,14], and capillary electrophoresis [15] have been applied for the determination of phenothiazines. Recently, some liquid chromatography/mass spectrometry methods have been developed for the determination of the phenothiazine derivatives with basic side chains [16,17]. Protonation of the nitrogen atoms in the side chains provides for high ionization yields and therefore for low limits of detection. The selectivity of these methods is excellent, but the use of expensive instrumentation is required.

A characteristic property of phenothiazine and its derivatives is the ease of electrochemical oxidation, which is owing to their low ionization potential [18-22], and which has been exploited using chemical, photochemical, enzymatic and electrochemical oxidation techniques under the following reaction scheme (Figure 3.1):



**Figure 3.1:** Reaction scheme of the oxidation of phenothiazines.



The first step is a reversible electron abstraction from the phenothiazine (A) to an intermediate radical cation (B). Its stability is strongly dependent on the substituents  $R_2$  and  $R_{10}$  as well as on kind and pH of the solvent used. While the radical cation of the unsubstituted phenothiazine is comparably stable and can be detected photometrically, the respective radical cations of the derivatives are not stable [18]. The second step comprises the formation of the phenothiazine sulfoxide (C), which is, in contrast to the native phenothiazine, strongly fluorescent. Numerous analytical methods for the determination of phenothiazines make use of their oxidation, including photochemical or chemical oxidation steps [23]. All of these methods are characterized by an inherently low selectivity, with a sum signal being obtained for all phenothiazines in solution. Coupling a chromatographic procedure with an oxidation step is therefore an attractive option to increase selectivity and to gain sensitivity, for example in conjunction with a post-column derivatization to the fluorescent product. High-performance liquid chromatographic (HPLC) methods for the post-column oxidation of phenothiazines with subsequent fluorimetric detection is known since a long time [24-27]. A method for the determination of phenothiazine and 11 of its derivatives with post-column chemical oxidation by peroxyacetic acid to the respective sulfoxides has been published recently [14].

Based on this method, our goal was to simplify the technical set-up without sacrificing sensitivity. The phenothiazines are separated by HPLC, post-column oxidation is carried out in an on-line electrochemical flow cell and the reaction products are detected fluorimetrically. The substitution of the oxidation with peroxyacetic acid by an electrochemical oxidation leads to the following advantages: No unstable chemicals have to be used, and the complexity of the required

instrumentation is significantly reduced. Instead of additional pumps, mixing unit, reaction loop and oven, only a commercially available electrochemical flow cell is implemented. As detection is performed exclusively by fluorescence detection and not by cell signal, the set-up can be used for both isocratic and gradient elution, respectively. To the best of our knowledge, the only related techniques reported so far are dedicated to the determination of nitro-substituted polycyclic aromatic hydrocarbons [28] and phenols [29].

Oxidation with subsequent mass spectrometric detection is also an interesting tool to study on-line oxidation products of phenothiazines generated in the electrochemical cell. Several groups coupled electrochemical cells on-line with particle beam [30,31], thermospray [22,32,33] or electrospray [34-38] mass spectrometry for various analytes. More recently, Kertesz and Van Berkel studied the electropolymerization of methylene blue, a dye with phenothiazine backbone, by on-line electrochemistry/electrospray mass spectrometry [39]. In earlier work, Van Berkel et al. demonstrated that radical cations of different analytes including phenothiazine may be generated electrochemically within the electrospray needle [40].

Surprisingly, there is no thorough study available yet on the electrochemical oxidation with on-line mass spectrometric detection of phenothiazine drugs. We have therefore investigated the on-line coupling of reversed-phase liquid chromatography and electrochemical conversion to study the oxidation process of phenothiazine by mass spectrometric detection and to quantify its derivatives by fluorescence spectroscopy.

### **3.3 Experimental**

#### *Chemicals*

All chemicals used for these experiments were purchased from Aldrich (Steinheim, Germany) and Merck (Darmstadt, Germany) in the highest quality available. As mobile phase for HPLC, acetonitrile "LiChroSolv gradient grade" (Merck) was used. Water for liquid chromatography was from Merck eurolab (Briare le Canal, France).

#### *Electrochemical instrumentation*

The equipment used for post-column electrochemical derivatization was obtained from ESA, Inc. (Chelmsford, MA, USA). It comprised a GuardStat potentiostat and a model 5021 conditioning cell. The working electrode material was glassy carbon with a Pd counter and a Pd/H<sub>2</sub> reference electrode. For protection of the working electrode, a PEEK in-line filter (ESA, Inc.) was mounted between column and electrode.

#### *LC/electrochemistry/UV-vis/fluorescence instrumentation*

Gradient elution was performed on a Shimadzu (Duisburg, Germany) HPLC-system consisting of: two LC-10AS pumps, a SUS mixing chamber (0.5 mL volume), a GT-154 degasser unit, a SIL-10A autosampler and a CBM-10A controller unit with class LC-10 software Version 1.6. Detection was performed with a SPD-M10Avp diodearray detector and a RF-10AXL fluorescence detector connected in series. The on-line coupling of the electrochemical cell to HPLC with diodearray and fluorescence detection was accomplished by inserting the electrochemical flow cell between column and diodearray detector.

*LC/electrochemistry/MS instrumentation*

For HPLC/MS measurements, the following equipment from Shimadzu was used: SCL-10Avp controller unit, DGU-14A degasser, two LC-10ADvp pumps, SIL-10A autosampler, SPD10AV UV-vis detector, LCMS QP8000 single quadrupole mass spectrometer with electrospray ionization (ESI) and atmospheric pressure chemical ionization (APCI) probes and Class 8000 software Version 1.20. Post-column electrochemical derivatization was accomplished by inserting the coulometric flow cell between the column and the interface of the mass spectrometer as described earlier by Diehl et al. for the oxidation of ferrocene derivatives [38].

*HPLC conditions*

As stationary phases, base deactivated Discovery RP-18 columns from Supelco (Deisenhofen, Germany) were used. Column dimensions were 150 mm x 3.0 mm for LC/electrochemistry/UV-vis/fluorescence and LC/electrochemistry/APCI-MS experiments and 150 mm x 2.1 mm for LC/electrochemistry/ESI-MS experiments. Particle size was 5  $\mu\text{m}$  and pore size 100 Å for both columns. Flow rates of the mobile phase were 0.6 mL/min for the 3.0 mm id column and 0.3 mL/min for the 2.1 mm id column. A binary gradient consisting of acetonitrile and aqueous buffer (600  $\mu\text{L}$  formic acid and 265 mg ammonium formate in 1 L water; pH 3) with the following profile was used:

time (min)	0.01	12	13	15	16	20
c (CH <sub>3</sub> CN) (%)	40	45	90	90	40	stop

The concentration of the organic phase was not raised above 90% to ensure sufficient concentration of the base electrolyte.

The injection volume was set to 10  $\mu\text{L}$  for LC/electrochemistry/UV-vis/fluorescence and LC/electrochemistry/APCI-MS and 5  $\mu\text{L}$  for LC/electrochemistry/ESI-MS experiments.

For time-programmed fluorescence detection, the following program was used:

time (min)	0.01	4.6	7.5	9.5	11.5	14.0
$\lambda$ (excitation) (nm)	378	344	345	352	351	344
$\lambda$ (emission) (nm)	502	380	391	400	436	389

The excitation and emission wavelengths of the respective phenothiazine sulfoxides were obtained from Diehl and Karst [14].

#### *MS conditions*

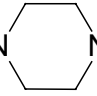
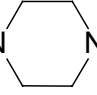
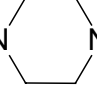
For all measurements, a curved desolvation line (CDL) voltage of  $-5$  V, a CDL temperature of  $280$  °C, a deflector voltages of  $40$  V and a detector voltage of  $1.6$  kV were used. The APCI experiments were carried out with probe voltage  $3$  kV and  $0$  kV, respectively. Nebulizer gas flow rate was  $2.5$  L/min and probe temperature was adjusted to  $450$  °C. The ESI parameters were: Probe voltage  $3$  kV and nebulizer gas flow rate  $4.5$  L/min.

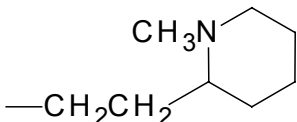
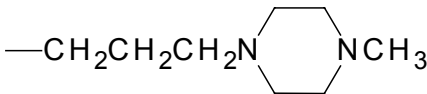
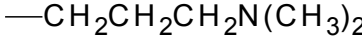
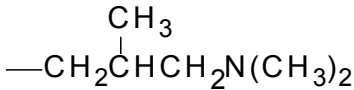
### 3.4 Results and Discussion

#### *Studies on the electrochemical oxidation of phenothiazines*

The two-step oxidation of phenothiazines is an attractive subject to electrochemical studies. Here, a series of 11 phenothiazines, including the unsubstituted phenothiazine and derivatives with basic side chains in R<sub>10</sub> and various substituents in R<sub>2</sub> have been selected. The abbreviations, structures and monoisotopic molecular masses of the substances are provided in Table 3.1.

Table 3.1: Abbreviations, structures and monoisotopic masses of selected phenothiazines.

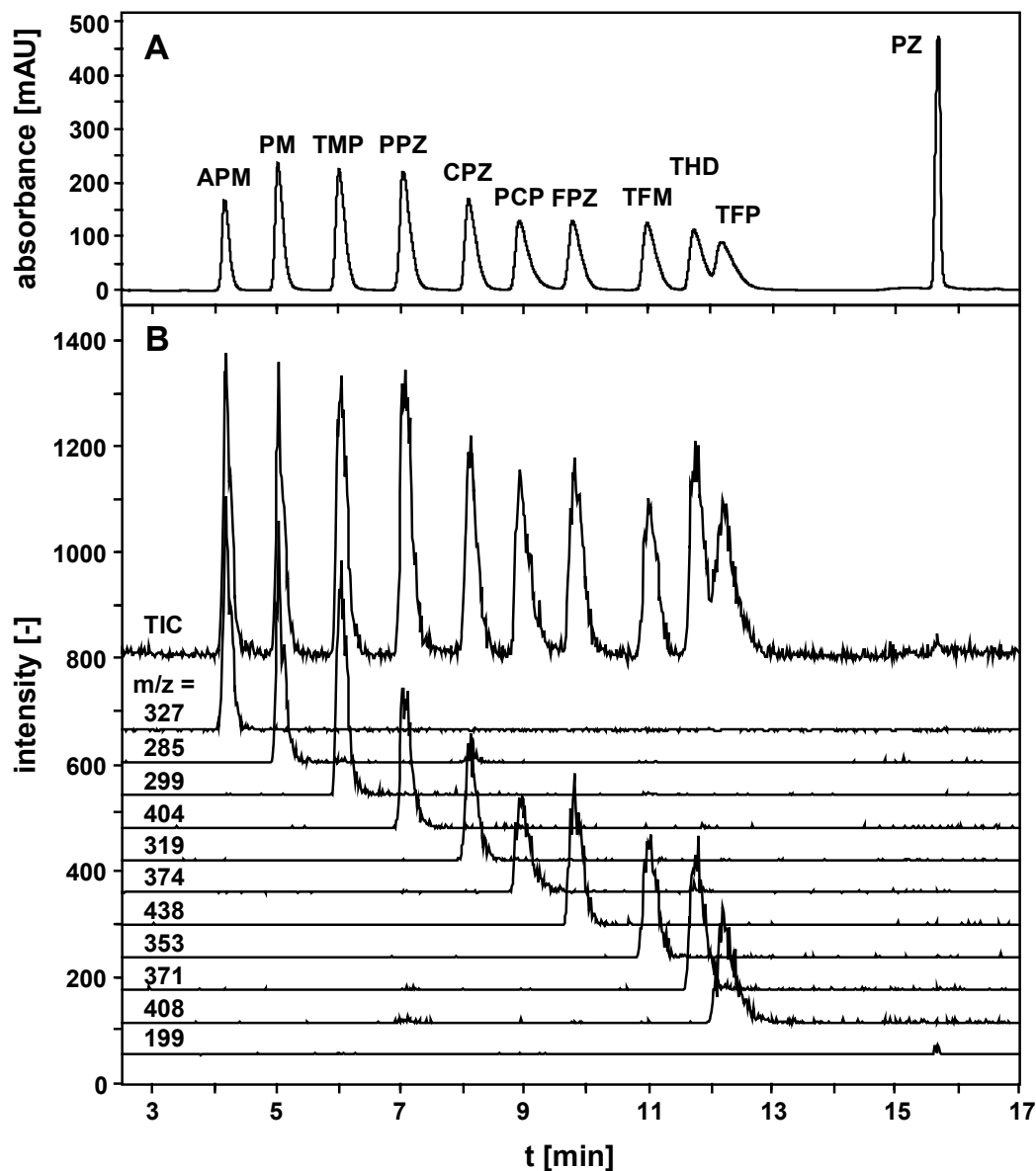
Substance	Substitution		M [Da]
	R <sub>10</sub>	R <sub>2</sub>	
Acetopromazine (APM)	—CH <sub>2</sub> CH <sub>2</sub> CH <sub>2</sub> N(CH <sub>3</sub> ) <sub>2</sub>	—COCH <sub>3</sub>	326.1
Chloropromazine (CPZ)	—CH <sub>2</sub> CH <sub>2</sub> CH <sub>2</sub> N(CH <sub>3</sub> ) <sub>2</sub>	—Cl	318.1
Fluphenazine (FPZ)	—CH <sub>2</sub> CH <sub>2</sub> CH <sub>2</sub> N  NCH <sub>2</sub> CH <sub>2</sub> OH	—CF <sub>3</sub>	437.2
Perphenazine (PPZ)	—CH <sub>2</sub> CH <sub>2</sub> CH <sub>2</sub> N  NCH <sub>2</sub> CH <sub>2</sub> OH	—Cl	403.1
Phenothiazine (PZ)	—H	—H	199.0
Prochloroperazine (PCP)	—CH <sub>2</sub> CH <sub>2</sub> CH <sub>2</sub> N  NCH <sub>3</sub>	—Cl	373.1
Promazine (PM)	—CH <sub>2</sub> CH <sub>2</sub> CH <sub>2</sub> N(CH <sub>3</sub> ) <sub>2</sub>	—H	284.2

Thioridazine (THD)		—SCH <sub>3</sub>	370.2
Trifluoperazine (TFP)		—CF <sub>3</sub>	407.2
Triflupromazine (TFM)		—CF <sub>3</sub>	352.1
Trimeprazine (TMP)		—H	298.2

---

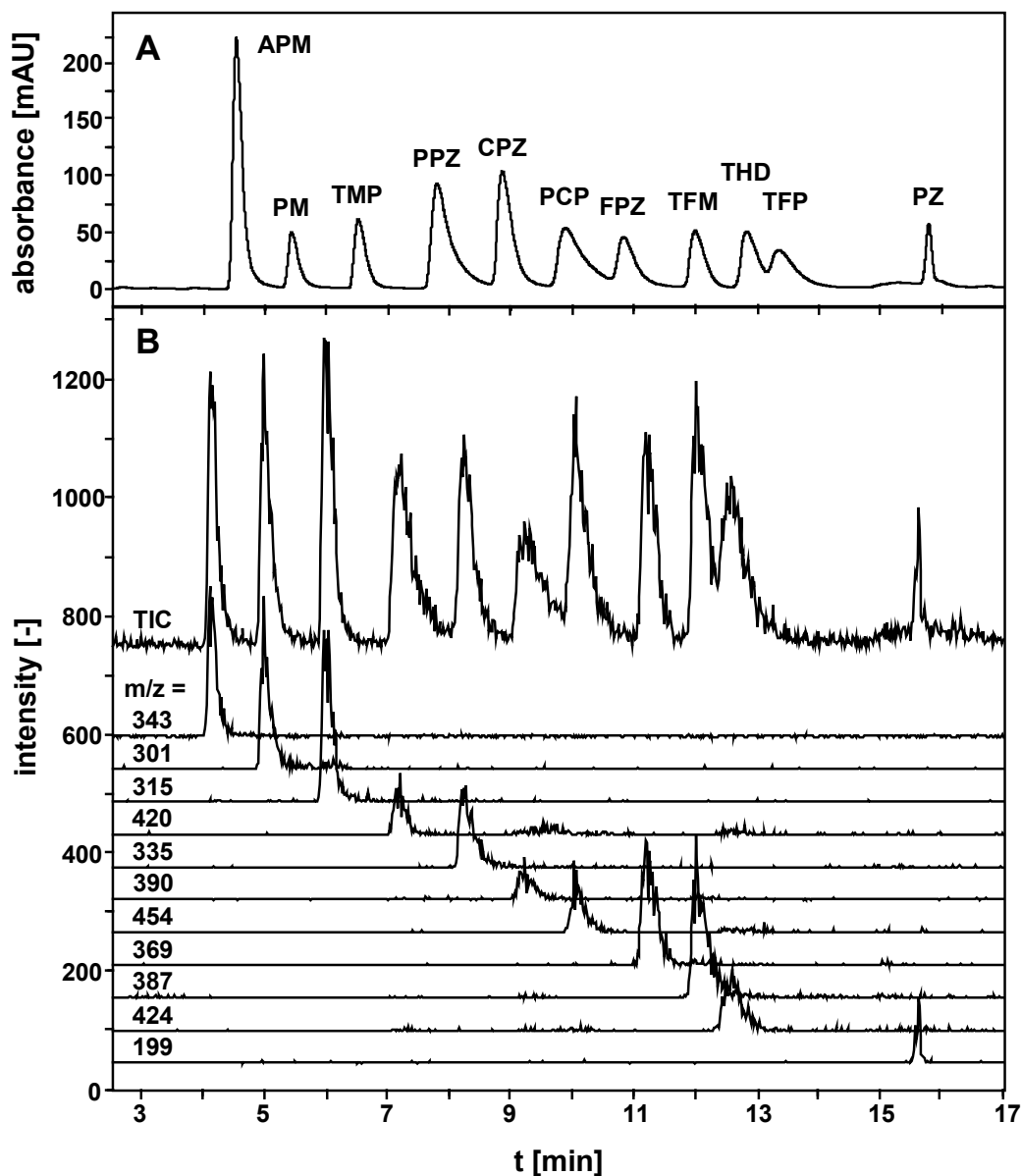
First, a reversed-phase liquid chromatographic separation for the investigated compounds was developed on a base-deactivated Supelco Discovery<sup>®</sup> C18 column at ambient temperature using a binary gradient consisting of acetonitrile and aqueous formic acid/ammonium formate buffer (pH 3). The respective chromatogram with photometric detection at 254 nm is presented in Figure 3.2, chromatogram A. Under these conditions, excellent peak shapes are observed even for the strongly basic substances.

Recently, methods for the LC/MS determination of the pharmaceutically relevant derivatives have been developed [16,17]. It is not surprising that these compounds allow easy detection under electrospray conditions in the positive ion mode (ESI(+)), because the basic side chain is readily protonated. Under these considerations, it should be harder to detect the non-substituted phenothiazine by ESI(+), because there are no basic side chains in the molecule.



**Figure 3.2:** Chromatogram of a mixture of phenothiazine and selected derivatives with UV-Vis detection at 254 nm (chromatogram A) and mass spectrometric detection with electrospray ionization (chromatogram B) recorded in SCAN mode ( $m/z = 100 - 500$ ). Displayed are the baseline-shifted extracted mass traces corresponding to the protonated derivatives of phenothiazine and the radical cation of phenothiazine. For abbreviations of the analytes, refer to Table 3.1. Concentrations range from  $1.0 - 1.3 \times 10^{-4}$  mol/L.

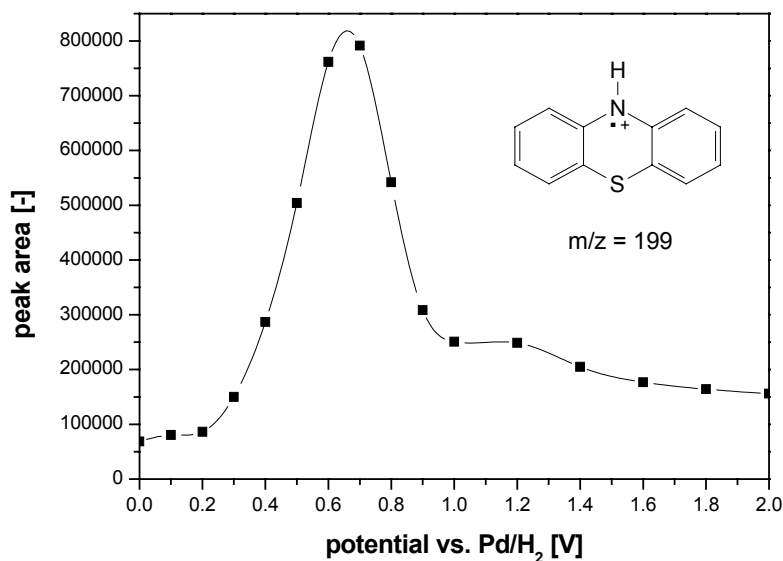




**Figure 3.3:** Chromatogram of a mixture of phenothiazine and selected derivatives with on-line electrochemical oxidation (0.8 V vs. Pd/H<sub>2</sub>) and UV-Vis detection at 254 nm (chromatogram A) and mass spectrometric detection with electrospray ionization (chromatogram B) recorded in SCAN mode ( $m/z = 100 - 500$ ). Displayed are the baseline-shifted extracted mass traces corresponding to the protonated sulfoxides of the derivatives and the radical cation of phenothiazine. For abbreviations of the analytes, refer to Table 3.1. Concentrations range from  $1.0 - 1.3 \times 10^{-4}$  mol/L.

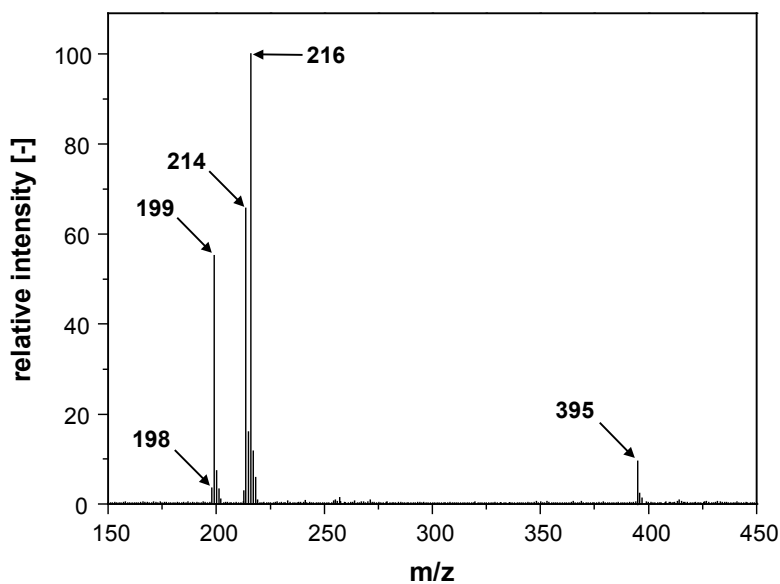
The effect of the electrochemical oxidation on phenothiazine and its derivatives in an on-line LC/electrochemistry/MS system is shown in Figures 3.2 and 3.3. In Figure 3.2, chromatogram B, the total ion current (TIC) and the extracted mass traces of the protonated phenothiazines ( $[M+H]^+$ ) without using the electrochemical cell is shown. Under these conditions, phenothiazine is detected with low sensitivity as radical cation with  $m/z = 199$  ( $[M]^+$ ). The respective chromatogram with an applied cell potential of 0.8 V vs. Pd/H<sub>2</sub> is presented in Figure 3.3. Chromatogram B shows the TIC and the extracted mass traces of the protonated sulfoxides of the basic phenothiazine derivatives and of the radical cation of phenothiazine. In comparison to Figure 3.2, some band broadening caused by the insertion of the electrochemical cell is observed.

At a concentration of  $1 \times 10^{-5}$  mol/L, phenothiazine is not detected at all in the full scan mode ( $m/z = 150 - 500$ ) using either the ESI or the APCI interface without applying a potential at the electrochemical cell. Enhanced sensitivity is achieved by electrochemical on-line oxidation. The dependency of the signal intensity of the radical cation ( $m/z = 199$ ) on the applied cell potential is depicted in Figure 3.4. The signal increases significantly from 0.3 V, and reaches a maximum between 0.6 and 0.8 V vs. Pd/H<sub>2</sub>. At higher potentials, the signal decreases again and reaches a plateau at 1.0 V vs. Pd/H<sub>2</sub>.



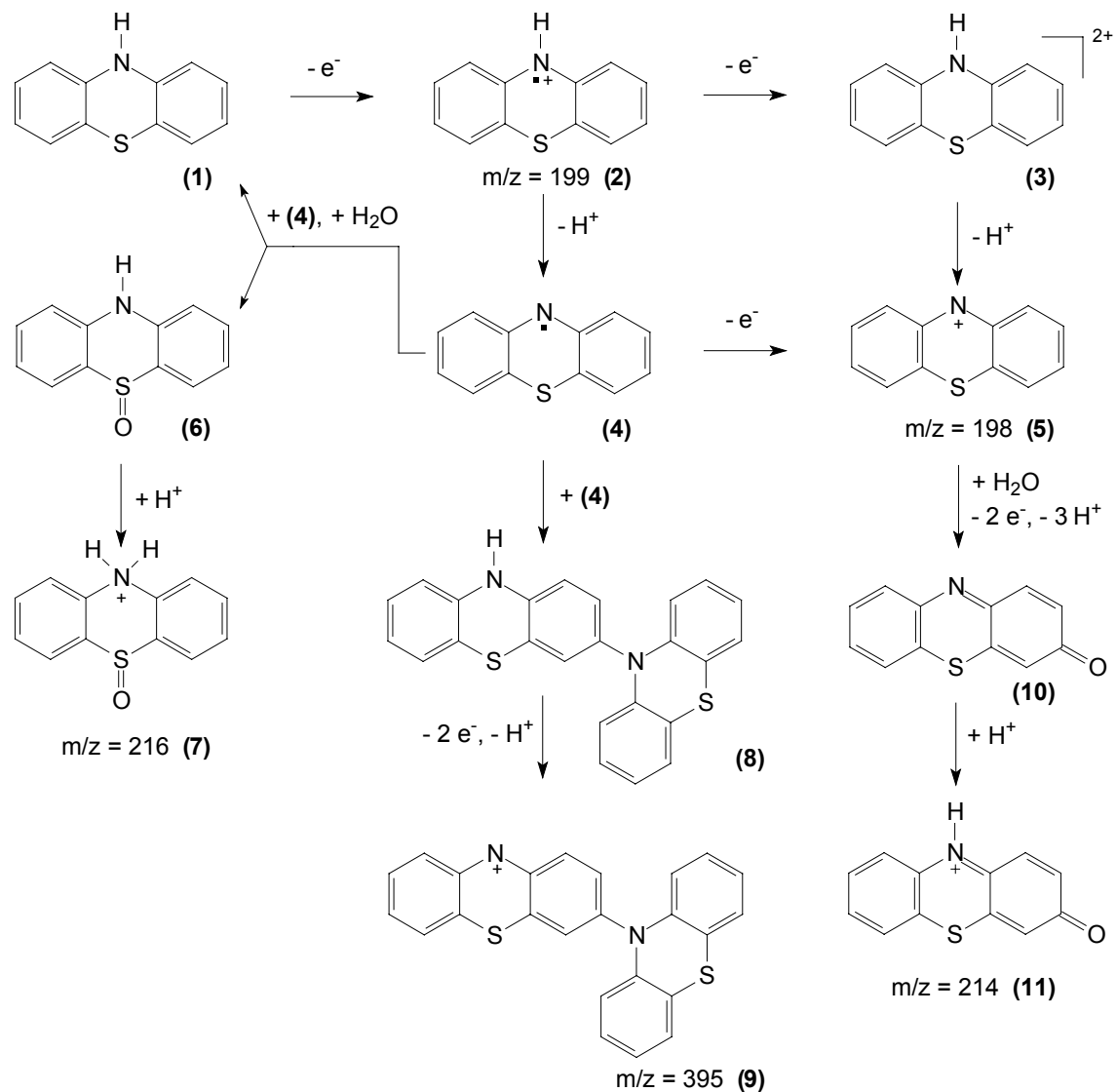
**Figure 3.4:** Dependency of the signal of the radical cation generated by the electrochemical oxidation of phenothiazine on the applied electrochemical potential with APCI-MS detection.  $c_{\text{phenothiazine}} = 1.3 \times 10^{-4} \text{ mol/L}$ .

In the mass spectrum obtained with APCI(+)-MS after electrochemical on-line oxidation of phenothiazine (Figure 3.5), several peaks are observed.



**Figure 3.5:** LC/electrochemistry/APCI(+) mass spectrum of phenothiazine after electrochemical oxidation. Cell potential = 0.8 V vs. Pd/H<sub>2</sub>;  $c_{\text{phenothiazine}} = 1.3 \times 10^{-4} \text{ mol/L}$ .

The most abundant peaks are at  $m/z = 198$ ,  $199$ ,  $214$ ,  $216$  and  $395$ . A reaction scheme explaining these peaks can be seen in Figure 3.6.



**Figure 3.6:** Reaction scheme summarizing the oxidation of phenothiazine in the LC/electrochemistry/MS system.

The signal at  $m/z = 199$  is related to the radical cation of phenothiazine (**2**), which is obtained after the loss of one electron from phenothiazine (**1**). This confirms that the radical cation of phenothiazine is much more stable than that of the respective  $R_2$  and  $R_{10}$ -substituted derivatives, where the radical cation is not observed at all under these conditions.

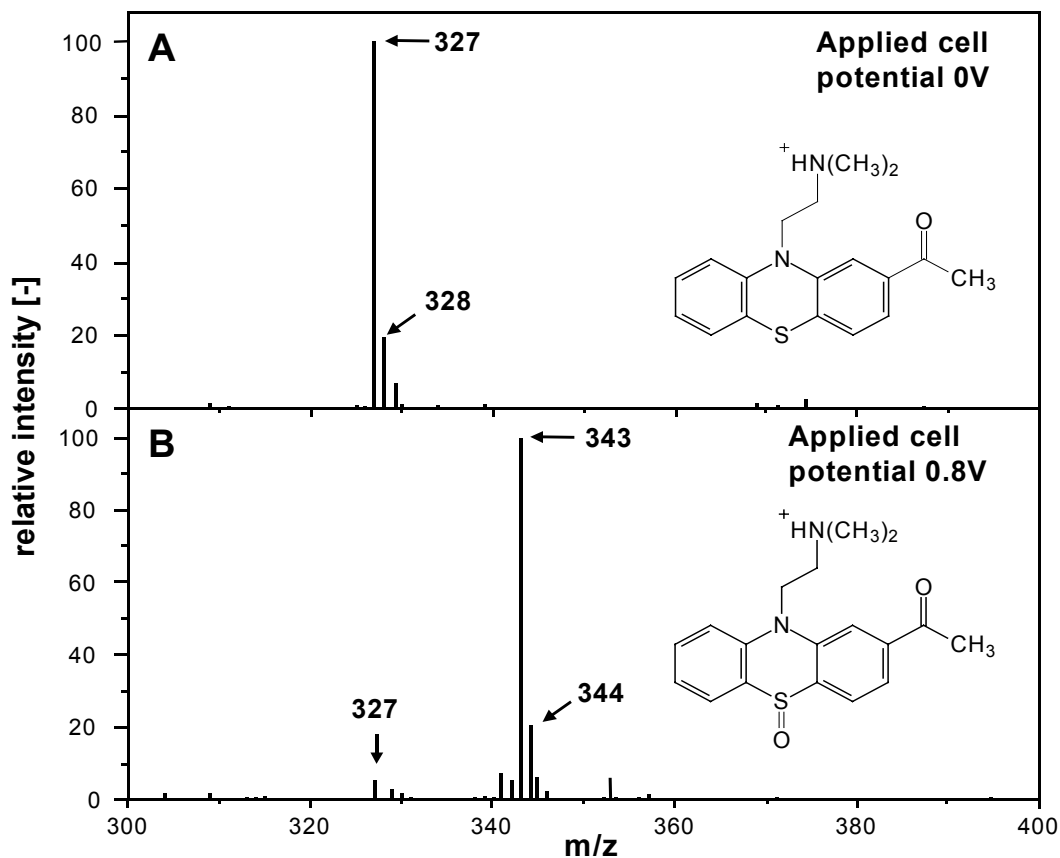
In respect of the peak with  $m/z = 198$  (**5**), two alternative reaction pathways are possible. Either, (**2**) is first oxidized to the dication (**3**) and then deprotonated to (**5**), or (**2**) is first deprotonated to the radical (**4**) and then oxidized to (**5**). This interpretation was first made by Cauquis et al. [19] for voltammetric measurements of phenothiazine and selected derivatives and is in accordance with the mass spectrometric data reported here.

Two molecules of the radical (**4**) react with one water molecule under formation of one molecule phenothiazine (**1**) and one molecule phenothiazine sulfoxide (**6**). This reaction is consistent with data from earlier voltammetric measurements by Merkle and Discher [21]. Protonation of (**6**) in the ESI or APCI interface leads to the formation of the  $[M+H]^+$  pseudomolecular ion with  $m/z = 216$  (**7**).

The dimerization of (**4**) leads, in accordance with literature [20,21], to the formation of (**8**), 3,10'-bisphenothiazinyl, or its isomer 1,10'-bisphenothiazinyl, which is not shown. After two one-electron oxidation steps and deprotonation, the cation (**9**) is obtained, which is detected in the mass spectrometer at  $m/z = 395$ . As above for the oxidation of (**2**) to (**5**), there are alternatives for the exact sequence of the individual reaction steps.

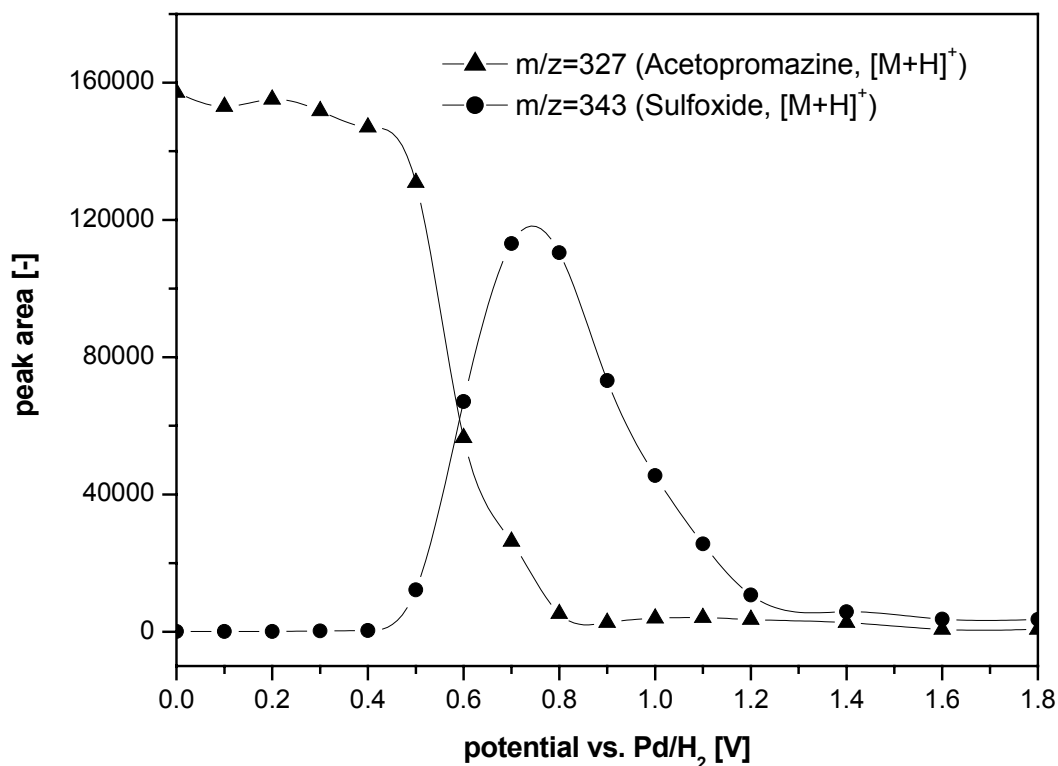
Nucleophilic attack of **(5)** by water, deprotonation, a two-electron oxidation and abstraction of two protons yields the quinoid system **(10)**. Protonation of the latter leads to its radical cation **(11)**, which is observed in the mass spectrum with  $m/z = 214$ . Again, these data correlate well with voltammetric data obtained previously by other groups [19].

Compared with the unpolar phenothiazine, the derivatives with basic side chains in position 1 are easily ionized by protonation. As expected, the  $[M+H]^+$  peak with  $m/z = 327$  is observed for acetopromazine in Figure 7A when using the APCI interface without electrochemical oxidation. In Figure 7B, the base peak in the experiment with an electrochemical cell potential of 0.8 V vs. Pd/H<sub>2</sub> is the respective protonated sulfoxide with an  $m/z = 343$ . Only a very small fraction of the sulfide is still present, indicating a very high turnover in the electrochemical cell. It should be noted that, according to a literature report [21], the mechanism of the oxidation of the phenothiazines leads first to the radical cations, two of which disproportionate in the presence of water under formation of one molecule of phenothiazine and one molecule of phenothiazine sulfoxide. This means that several oxidation cycles must have occurred in the cell to obtain the conversion rate observed here.



**Figure 3.7:** LC/electrochemistry/APCI(+) mass spectrum of acetopromazine without electrochemical oxidation (A) and after on-line electrochemical conversion to the respective sulfoxide at a cell potential of 0.8 V (B).  $c_{\text{acetopromazine}} = 1.0 \times 10^{-5}$  mol/L.

The dependency of the peak areas of  $m/z = 327$  ( $[M+H]^+$  of the sulfide) and  $m/z = 343$  ( $[M+H]^+$  of the sulfoxide) on the applied potential at the electrochemical cell has been investigated, as demonstrated in Figure 3.8.



**Figure 3.8:** Dependency of the oxidation of acetopromazine to the respective sulfoxide on the applied electrochemical potential.

The signal of the sulfide is declining already at 0.4 V vs. Pd/H<sub>2</sub>, and reaches zero at 0.9 V. The signal for the sulfoxide starts at zero, increases significantly from 0.5 V, and reaches a maximum between 0.7 and 0.8 V vs. Pd/H<sub>2</sub>. At higher potentials, the signal decreases again due to further electrochemical oxidation and reaches zero at 1.4 V vs. Pd/H<sub>2</sub>. For all other phenothiazine drugs with basic side-chains investigated in this study, similar mass spectra were obtained for the on-line oxidation with equal or lesser intensities of the sulfoxide peaks compared to the native phenothiazines. It is obvious that the on-line LC/electrochemistry/MS method allows the rapid and convenient investigation of electrochemical reaction pathways of phenothiazines.



*Quantification of phenothiazine derivatives*

The high conversion rate in combination with the fact that the phenothiazine sulfoxides fluoresce stronger than the respective sulfides indicate that there should be a possibility to develop a sensitive method for the determination of phenothiazines by means of LC/electrochemistry/fluorescence. In the following, the fluorescence intensity of the phenothiazine derivatives depending on the applied potential was studied. The fluorescence intensity of acetopromazine is increasing from almost zero at a potential of 0 V vs. Pd/H<sub>2</sub> to a maximum at 0.8 V. At higher potentials, the fluorescence intensity is decreasing again, most likely due to further conversion of the fluorescent sulfoxide to other species. The same tendency is observed for all other basic phenothiazine derivatives investigated, although there are different fluorescence excitation and emission maxima for all derivatives. The data correlate well with the respective investigation by LC/electrochemistry/MS (see above).

Quantitative measurements were carried out for the LC/ESI-MS, LC/APCI-MS and LC/electrochemistry/fluorescence methods. The respective data are summarized in Table 3.2.

**Table 3.2:** *Analytical figures of merit for the determination of selected phenothiazine derivatives using LC/ESI-MS, LC/APCI-MS and LC/electrochemistry/fluorescence. (LOD = limit of detection; RSD = relative standard deviation; R<sup>2</sup> = regression coefficient).*

Chapter 3

Substance	LC/ESI-MS					LC/APCI-MS					LC/Electrochemistry/Fluorescence				
	LOD [mol/L]	RSD (n=3)			R <sup>2</sup>	LOD [mol/L]	RSD (n=3)			R <sup>2</sup>	LOD [mol/L]	RSD (n=3)			R <sup>2</sup>
		1x10 <sup>-7</sup> mol/L	1x10 <sup>-6</sup> mol/L	1x10 <sup>-5</sup> mol/L		1x10 <sup>-7</sup> mol/L	1x10 <sup>-6</sup> mol/L	1x10 <sup>-5</sup> mol/L			1x10 <sup>-7</sup> mol/L	1x10 <sup>-6</sup> mol/L	1x10 <sup>-5</sup> mol/L		
Acetopromazine	2x10 <sup>-8</sup>	7.5%	3.2%	1.3%	0.9986	2x10 <sup>-8</sup>	6.4%	4.4%	1.8%	0.9968	5x10 <sup>-9</sup>	4.5%	3.2%	1.3%	0.9992
Chlorpromazine	5x10 <sup>-8</sup>	8.0%	2.8%	1.4%	0.9990	2x10 <sup>-8</sup>	5.6%	3.8%	3.6%	0.9944	4x10 <sup>-8</sup>	3.8%	0.8%	1.4%	0.9982
Fluphenazine	2x10 <sup>-8</sup>	7.3%	3.9%	1.0%	0.9990	2x10 <sup>-8</sup>	11.4%	7.2%	3.4%	0.9964	6x10 <sup>-9</sup>	7.3%	3.9%	1.0%	0.9986
Perphenazine	2x10 <sup>-8</sup>	1.4%	1.0%	2.3%	0.9970	2x10 <sup>-8</sup>	5.5%	5.4%	4.3%	0.9932	8x10 <sup>-9</sup>	1.2%	1.1%	1.0%	0.9980
Prochloroperazine	2x10 <sup>-8</sup>	7.1%	1.3%	1.2%	0.9982	4x10 <sup>-8</sup>	5.0%	5.5%	5.4%	0.9928	1x10 <sup>-8</sup>	7.1%	1.3%	1.2%	0.9980
Promazine	2x10 <sup>-8</sup>	8.3%	1.2%	1.6%	0.9982	2x10 <sup>-8</sup>	4.8%	11.4%	6.3%	0.9956	3x10 <sup>-8</sup>	5.0%	1.1%	1.2%	0.9978
Thioridazine	1x10 <sup>-8</sup>	5.0%	1.0%	1.9%	0.9974	2x10 <sup>-8</sup>	6.1%	9.2%	4.3%	0.9956	4x10 <sup>-8</sup>	4.9%	0.8%	0.9%	0.9976
Trifluoperazine	1x10 <sup>-8</sup>	10.0%	1.1%	1.0%	0.9980	2x10 <sup>-8</sup>	8.2%	3.8%	2.3%	0.9948	6x10 <sup>-9</sup>	4.8%	1.0%	0.9%	0.9994
Triflupromazine	2x10 <sup>-8</sup>	7.4%	1.0%	1.3%	0.9992	4x10 <sup>-8</sup>	4.3%	11.2%	5.2%	0.9964	6x10 <sup>-9</sup>	7.4%	0.9%	0.5%	0.9982
Trimeprazine	2x10 <sup>-8</sup>	3.1%	5.2%	1.2%	0.9984	2x10 <sup>-8</sup>	9.4%	7.7%	4.8%	0.9962	5x10 <sup>-9</sup>	3.2%	5.2%	1.1%	0.9998

As the basic phenothiazine derivatives are readily protonated without the use of an electrochemical cell, and as the oxidation products do not exhibit superior properties with respect to LC/MS determination, only the data from LC/MS (without electrochemical oxidation) and LC/electrochemistry/fluorescence at a cell potential of 0.8 V vs. Pd/H<sub>2</sub> are listed in Table 3.2. The LC/MS measurements were carried out in selected ion monitoring (SIM) mode for quantification purposes. Limits of detection (LOD) were determined as a signal to noise ratio of 3 and the limit of quantification (LOQ) as a signal to noise ratio of 10. Fluorescence detection has been done in a time-programmed manner to ensure the optimum selection of excitation and emission wavelengths for each individual compound. Limits of detection for LC/MS range from  $1 \times 10^{-8}$  mol/L to  $5 \times 10^{-8}$  mol/L for ESI-MS and from  $1 \times 10^{-8}$  mol/L to  $4 \times 10^{-8}$  mol/L for APCI-MS. For LC/electrochemistry/fluorescence, the limits of detection are slightly lower with  $5 \times 10^{-9}$  mol/L to  $4 \times 10^{-8}$  mol/L. Limits of quantification for LC/MS range from  $3 \times 10^{-8}$  mol/L to  $2 \times 10^{-7}$  mol/L for ESI-MS and from  $3 \times 10^{-8}$  mol/L to  $1 \times 10^{-7}$  mol/L for APCI-MS. The LC/electrochemistry/fluorescence method is characterized by slightly lower LOQs ( $1 \times 10^{-8}$  mol/L to  $1 \times 10^{-7}$  mol/L). The linear ranges comprise three decades starting at the limits of quantification. The relative standard deviations for multiple subsequent analysis ( $n = 3$ ) of the same solutions were calculated for the concentrations of  $1 \times 10^{-7}$  mol/L,  $1 \times 10^{-6}$  mol/L and  $1 \times 10^{-5}$  mol/L. As could be expected, the relative standard deviations (RSDs) are in general lower for fluorescence detection than for mass spectrometric detection. At lower concentrations, the RSDs are typically higher than at higher concentrations.

The calibration data of the determination of phenothiazine derivatives by HPLC/electrochemistry/fluorescence are in good agreement with the post-column

oxidation with peroxyacetic acid. Limits of detection ranged from  $4 \times 10^{-9}$  mol/L of triflupromazine (20 pg on column) to  $2 \times 10^{-8}$  mol/L of thioridazine (148 pg on column) with post-column oxidation using peroxyacetic acid [14]. Applying electrochemical oxidation, LODs ranged from  $5 \times 10^{-9}$  mol/L of trimeprazine (15 pg on column) to  $4 \times 10^{-8}$  mol/L of thioridazine (148 pg on column). That indicates that the electrochemical oxidation is as sensitive as the chemical oxidation, but requires much less effort. Additionally, this is another indication for a very high turnover at the electrochemical cell.

In Table 3.3, the described HPLC/electrochemistry/fluorescence method is compared with other techniques reported in literature with respect to the analysis of thioridazine.

**Table 3.3:** Comparison of HPLC methods for the determination of thioridazine with post-column oxidation and fluorescence detection (NP = normal-phase HPLC, RP = reversed-phase HPLC).

Separation	Detection	Post-column oxidation	Limit of detection [ng]	Reference
NP	Fluorescence, filters	Permanganate/ H <sub>2</sub> O <sub>2</sub>	0.8	24
RP	Fluorescence, 340/378 nm	Photochemical Oxidation	0.5	25
RP	Fluorescence, 345/425 nm	Bromine	0.5	27
RP	Fluorescence, 351/436 nm	Peroxyacetic acid	0.2	14
RP	Fluorescence, 351/436 nm	Electrochemical Oxidation	0.2	This work

Again, the obtained data correspond well with the post-column oxidation with peroxyacetic acid [14]. Limits of detection for both methods were 0.2 ng thioridazine on column in pure standard solutions, whereas the other methods are characterized by higher LODs but in plasma samples. Wells et al. obtained a LOD of 0.5 ng after oxidation with permanganate [24]. The sample was concentrated as part of the clean-up procedure. Thioridazine was determined in plasma without enrichment [25,27]. Scholten et al. received a LOD of 0.5 ng applying photochemical oxidation [25]. Electrochemically generated bromine was used as oxidizing agent by Kok et al. and the LOD was 0.8 ng [27].

*Quantification of phenothiazine*

For phenothiazine, there is a stable colored radical cation as well as a fluorescent sulfoxide. Thus, it should be possible to develop methods for LC/electrochemistry/fluorescence and for LC/electrochemistry with UV-vis detection. The dependency of the UV-vis signal at 517 nm (absorption maximum of the radical cation) and the fluorescence signal using the excitation maximum of 344 nm and the emission maximum of 389 nm of the sulfoxide on the applied electrochemical cell potential was investigated between 0 V and 2 V vs. Pd/H<sub>2</sub>. As slight fluorescence is already observed from the native phenothiazine, the fluorescence increases only by a factor of 10, while the absorbance is increasing by a factor of 100. While the maximum intensity for the absorbance method is already observed at 0.7 V vs. Pd/H<sub>2</sub>, the maximum fluorescence intensity is registered not before a potential of 1.4 V. The absorbance signal decreases only slightly with further increasing potential, while the fluorescence signal stays constant until a potential of 2.0 V. These data indicate the chemical stability of both species formed.

Quantitative measurements have been carried out for the determination of phenothiazine by LC/electrochemistry/MS, LC/electrochemistry/fluorescence and LC/electrochemistry/UV-vis. The analytical figures of merit for all methods, including limits of detection, limits of quantification, relative standard deviations at selected concentrations and regression coefficients for the plot of signal vs. concentration are summarized in Table 3.4.

**Table 3.4:** Analytical figures of merit for the determination of phenothiazine by LC/electrochemistry/ESI-MS, LC/electrochemistry/APCI-MS, LC/electrochemistry/fluorescence and LC/electrochemistry/UV-vis detection.

	LC/EC/ESI-MS		LC/EC/APCI-MS			LC/EC/ Flu	LC/EC/ UV-vis
Probe voltage [kV]	3	3	3	3	0	/	/
Applied cell potential [mV]	0	800	0	800	1600	1600	1600
Detected m/z	199	216	199	216	198	/	/
LOD [mol/L]	$1 \times 10^{-5}$	$2 \times 10^{-7}$	$1 \times 10^{-6}$	$5 \times 10^{-8}$	$2 \times 10^{-8}$	$1 \times 10^{-7}$	$5 \times 10^{-7}$
LOQ [mol/L]	$3 \times 10^{-5}$	$7 \times 10^{-7}$	$3 \times 10^{-6}$	$2 \times 10^{-7}$	$7 \times 10^{-7}$	$3 \times 10^{-7}$	$2 \times 10^{-6}$
RSD (n = 3) at $1 \cdot 10^{-6}$ mol/L	/	10.7%	/	8.0%	10.2%	1.9%	4.3%
RSD (n = 3) at $1 \cdot 10^{-5}$ mol/L	6.0%	5.3%	4.8%	6.7%	4.0%	2.0%	1.9%
RSD (n = 3) at $1 \cdot 10^{-4}$ mol/L	2.6%	2.0%	4.0%	3.9%	3.3%	0.3%	1.0%
Regression coefficient ( $R^2$ )	0.9493	0.9924	0.9956	0.9950	0.9821	0.9998	0.9992

Owing to the low polarity of phenothiazine, LC/MS analysis using ESI or APCI results in poor limits of detection. The limit of detection for the determination of phenothiazine by LC/ESI-MS without electrochemical oxidation is  $1 \times 10^{-5}$  mol/L in the selected ion monitoring (SIM) mode. The sensitivity of this method is improved applying electrochemical on-line oxidation at 0.8 V vs. Pd/H<sub>2</sub> by a factor of 50. The

native phenothiazine is converted to the corresponding sulfoxide ( $m/z = 216$  for the protonated sulfoxide), which can then be detected with a LOD of  $2 \times 10^{-7}$  mol/L.

Compared with electrospray ionization, APCI is characterized by lower limits of detection for the determination of phenothiazine. Without electrochemical oxidation, the radical cation is detected at  $m/z = 199$  with a LOD of  $1 \times 10^{-6}$  mol/L. At a cell potential of 0.8 V vs. Pd/H<sub>2</sub>, the sulfoxide is generated and detected at  $m/z = 216$  with 20-fold improved sensitivity (LOD =  $5 \times 10^{-8}$  mol/L).

Additionally, the APCI probe voltage was set to 0 kV to ensure that ions, which are observed are generated in the electrochemical cell and not by the APCI process. Thus, the APCI interface has been operated as "heated nebulizer" or "thermospray" interface for these experiments. The most abundant peak in the spectrum is that of the phenothiazine radical cation with  $m/z = 198$ . Optimization of the applied cell potential resulted in highest signals at 1.6 V vs. Pd/H<sub>2</sub>. The LOD for this method with  $2 \times 10^{-8}$  mol/L is even lower than with applied APCI probe voltage of 3 kV. As the ions are exclusively generated in the electrochemical cell and not in the APCI interface, which is only used for heated nebulization, noise is reduced and sensitivity is improved. These measurements were not possible with the electrospray interface, because the spraying process in ESI depends on a high voltage at the ESI capillary.

The determination of phenothiazine with fluorescence and UV-vis detection was carried out at a cell potential of 1.6 V vs. Pd/H<sub>2</sub>. For LC/electrochemistry/fluorescence, the limit of detection is  $1 \times 10^{-7}$  mol/L, whereas photometrical detection at 517 nm resulted in a slightly higher value ( $3 \times 10^{-7}$  mol/L). These results are



comparable to the post-column oxidation with peroxyacetic acid [14]. The chemical oxidation to the radical cation with photometric detection at 525 nm resulted in the same LOD ( $3 \times 10^{-7}$  mol/L), whereas chemical oxidation to the sulfoxide is characterized by a slightly higher value (LOD =  $1 \times 10^{-7}$  mol/L). The data indicate the same effectiveness of both oxidation procedures: On the one hand electrochemical on-line oxidation in a coulometric flow-cell and on the other hand chemical oxidation with peroxyacetic acid.

The relative standard deviations for multiple subsequent analysis ( $n = 3$ ) of the same solutions were determined for the concentrations of  $1 \times 10^{-6}$  mol/L,  $1 \times 10^{-5}$  mol/L and  $1 \times 10^{-4}$  mol/L. As could be expected, the relative standard deviations (RSDs) are in general lower for UV-vis and fluorescence detection than for mass spectrometric detection. At lower concentrations, the RSDs are typically higher than at higher concentrations.

Despite the large number of over 1000 injections in the HPLC system for this study, the electrochemical cell required no maintenance during this complete work, and there was no decay of the MS or fluorescence signals observed with increasing lifetime of the cell. This is another confirmation for the statement that phenothiazines are excellent redox systems that do not tend to form insoluble polymer films on the electrode surfaces.

### 3.4 Conclusions

A powerful hyphenated technique for the determination of phenothiazines based on the combination of HPLC, electrochemical on-line oxidation and different detection methods of the formed oxidation products has been developed. The coupling of electrochemistry to LC/MS offers the possibility to elucidate on-line the reaction pathways of the oxidation of phenothiazines. The oxidation of phenothiazine leads to the formation of a radical cation and other oxidized products which can be detected by means of photometry, fluorimetry and mass spectrometry. The conversion to more polar or even charged species improves sensitivity in mass spectrometry by a factor of 50 compared to conventional LC/MS. Quantification can also be carried out by UV-vis spectroscopy at 517 nm or fluorescence spectroscopy with limits of detection of  $3 \times 10^{-7}$  mol/L and  $1 \times 10^{-7}$  mol/L, respectively.

The basic phenothiazine derivatives are transferred into strongly fluorescent sulfoxides. This offers possibilities to quantify phenothiazines at very low limits of detection in the nanomolar range using fluorescence detection with simple, robust and readily available instrumentation and avoiding laborious derivatization procedures. Further research will be directed to the analysis of phenothiazines in real samples as blood or urine.

### **3.5 References**

- [1] S. G. Dahl in: E. Usdin, S. G. Dahl, L. F. Gram (Eds.), *Clinical Pharmacology and Psychiatry, Neuroleptic Antidepressants Research (2nd International Meeting 1980)*, Macmillan, London (1981) 125.
- [2] R. J. Baldessarini in: A. G. Gilman, L. S. Goodman, T. W. Rall, F. Murad (Eds.), *The Pharmacological Basis of Therapeutics*, 7th ed., Macmillan, New York (1985) 391.
- [3] M. M. Hefnawy, *J. Pharmaceut. Biomed.* 27 (2002) 661.
- [4] K. Basavaiah, J. M Swamy, *Oxid. Commun.* 24 (2001) 619.
- [5] C. C. Nascentes, S. Cardenas, M. Gallego, M. Valcarcel, *Anal. Chim. Acta* 462 (2002) 275.
- [6] B. Laassis, J. J. Aaron, M. C. Mahedero, *Anal. Chim. Acta* 290 (1994) 27.
- [7] J. Cepas, M. Silva, D. Perez-Bendito, *Anal. Chem.* 66 (1994) 4079.
- [8] C. Petit, K. Murakami, A. Erdem, E. Kilinc, G. O. Borondo, J. - F. Liegeois, J. - M. Kauffmann, *Electroanal.* 10 (1998) 1241.
- [9] T. Ghous, A. Townshend, *Anal. Chim. Acta* 387 (1999) 47.
- [10] Y. Ishikawa, O. Suzuki, H. Hattori, *Forensic Sci. Int.* 44 (1990) 93.
- [11] H. Hattori, S. Yamamoto, M. Iwata, E. Takashima, T. Yamada, O. J. Suzuki, *Chromatogr.-Biomed.* 579 (1992) 247.
- [12] T. A. Berger, W. H. Wilson, *J. Pharm. Sci.* 83 (1994) 281.
- [13] K. Shimada, T. Mino, M. Nakajima, H. Wakabayashi, S. Yamato, J. *Chromatogr. B* 661 (1994) 85.
- [14] G. Diehl, U. Karst, *J. Chromatogr. A* 890 (2000) 281.
- [15] R. Y. Wang, X. N. Lu, H. J. Xin, M. Wu, *Chromatographia* 51 (2000) 29.

- [16] M. F. Sauvage, P. Marquet, A. Rousseau, J. Buxeraud, C. Raby, G. Lachatre, J. Liq. Chromatogr. 21 (1998) 3173.
- [17] H. Seno, H. Hattori, A. Ishii, T. Kumazawa, K. Watanabe-Suzuki, O. Suzuki, Rapid Commun. Mass Spectrom. 13 (1999) 2394.
- [18] A. N. Pankratov, I. M. Uchaeva, A. N. Stepanov, Can. J. Chem. 71 (1993) 674.
- [19] G. Cauquis, A. Deronzier, J. - L. Lepage, D. Serve, Bull. Soc. Chim. France (1977) 295.
- [20] G. Cauquis, A. Deronzier, J. - L. Lepage, D. Serve, Bull. Soc. Chim. France (1977) 303.
- [21] F. H. Merkle, C. A. Discher, Anal. Chem. 36 (1964) 1639.
- [22] G. Hambitzer, P. P. Heinz, I. Stassen, J. Heitbaum, Synthetic Metals 55 (1993) 1317.
- [23] A. Kojlo, J. Karpinska, L. Kuzmicka, W. Misiuk, H. Puzanowska-Tarasiewicz, M. Tarasiewicz, J. Trace Microprobe Techn. 19 (2001) 40.
- [24] C. E. Wells, E. C. Juenge, W. B. Fuman, J. Pharm. Sci. 72 (1983) 622.
- [25] A. H. M. T. Scholten, P. L. M. Welling, U. A. T. Brinkman, R. W. J. Frei, Chromatogr. A 199 (1980) 239.
- [26] B. Mann, M. Grayeski, Biomed. Chromatogr. 5 (1991) 47.
- [27] W. T. Kok, W. H. Voogt, U. A. T. Brinkman, R. W. Frei, J. Chromatogr. A 354 (1986) 249.
- [28] M. Murayama, P. K. Dasgupta, Anal. Chem. 68 (1996) 1226.
- [29] J. Meyer, A. Liesener, S. Götz, H. Hayen U. Karst, Anal. Chem. 75 (2003) 922.
- [30] M. C. S. Regino, A. Brajter-Toth, Anal. Chem. 69 (1997) 5067.

- [31] T. Zhang, A. Brajter-Toth, *Anal. Chem.* 72 (2000) 2533.
- [32] G. Hambitzer, J. Heitbaum, *Anal. Chem.* 58 (1986) 1067.
- [33] K. J. Volk, R. A. Yost, A. Brajter-Toth, *Anal. Chem.* 61 (1989) 1709.
- [34] F. Zhou, G. J. Van Berkel, *Anal. Chem.* 67 (1995) 3643.
- [35] X. Xu W. Lu, R. B Cole, *Anal. Chem.* 69 (1997) 2478.
- [36] H. Deng, G. J. Van Berkel, *Anal. Chem.* 71 (1999) 4284.
- [37] U. Jurva, H. V. Wikström, A. P. Bruins, *Rapid Commun. Mass Spectrom.* 14 (2000) 529.
- [38] G. Diehl, A. Liesener, U. Karst, *Analyst* 126 (2001) 288.
- [39] V. Kertesz, G. J. Van Berkel, *Electroanalysis* 13 (2001) 1425.
- [40] G. J. Van Berkel, S. A. McLuckey, G. L. Glish, *Anal. Chem.* 64 (1992) 586.



# Chapter 4

## Liquid Chromatography/Electrochemistry/ Mass Spectrometry of Polycyclic Aromatic Hydrocarbons\*

### 4.1 Abstract

An efficient way for the fast elucidation of electrochemical reactions of polycyclic aromatic hydrocarbons (PAHs) has been set-up by applying post-column electrochemistry in liquid chromatography/mass spectrometry (LC/MS). With this set-up, a strong improvement of sensitivity in the LC/MS analysis of PAHs is observed. Due to their low redox potentials, the non-polar PAHs are converted into the respective radical cations, which may further react with constituents of the mobile phase and in additional electrochemical oxidation steps. Among other products, mono-, di- and trioxygenated species are observed in aqueous solutions, alkoxyated compounds in alcohols and solvent adducts in the presence of acetonitrile. While more different products are observed by using atmospheric pressure chemical ionization in the positive ion mode (APCI(+)), the deprotonation of hydroxylated species results in very clear spectra in the negative ion mode (APCI(-)). Deuterated PAHs and deuterated solvents were used to gain additional information on the formation of the reaction products.

\*S. M. van Leeuwen, H. Hayen, U. Karst, *Anal. Bioanal. Chem.*, in press

## 4.2 Introduction

The coupling of liquid chromatography (LC) and mass spectrometry (MS) has been established as one of the most powerful tools in analytical chemistry since the mid 1980s and has given access to important advances especially in biomedical and biochemical research [1,2]. The predominantly used interfaces are electrospray ionization (ESI) and atmospheric pressure chemical ionization (APCI). As ionization of the analytes typically occurs on the basis of acid/base reactions, ESI and APCI are particularly well-suited for the analysis of pharmaceuticals, peptides and other polar compounds. The determination of non-polar analytes with these techniques, however, leads to unfavorable results. In the last years, some new approaches, which shall improve the applicability of ESI and APCI for non-polar compounds have been presented. These include electron capture ionization in a commercial APCI interface [3-5], atmospheric pressure photoionization (APPI) [6], coordination ionspray [7], and electrochemical conversions [8-15].

In the latter of these new approaches, the goal is the electrochemical conversion of the non-polar compounds to more polar or even charged products, which are accessible to ESI- and APCI-MS [8,11-15]. Cole and co-workers coupled electrochemistry on-line with ESI-MS for the detection of PAHs using a self-constructed electrochemical flow cell inside the electrospray probe [8]. Van Berkel et al. have extensively studied electrochemical reactions in the ESI interface, considering the electrospray interface itself as an electrochemical reactor [16]. It was found that the ability to produce radical cations in the ESI process expands the possibilities of ESI, thus including compounds that are normally not amenable to electrospray ionization. The structure and the electroactivity of the analytes are



important factors for the formation of radical cations in electrochemical oxidation processes. To demonstrate the applicability of this method they investigated different metal porphyrins and PAHs, N,N,N',N'-tetramethyl-1,4-phenylenediamine and the heteroaromatic phenothiazine which all could be detected as radical cations.

Another possibility to ionize non- or less polar compounds is the use of an external electrochemical flow cell that is placed ahead of the interface. On-line electrochemistry/MS has been used for investigations on the generation of reaction intermediates and products as well as for studying biological redox reactions [17,18]. Recently, Diehl et al. have presented an external electrochemical flow cell coupled on-line with LC/MS [19]. A "coulometric" cell was inserted between HPLC and MS for the analysis of ferrocene-labeled alcohols and phenols. With this approach, the effects of electrochemical pretreatment, forming oxidized species that are either already ionized or are subsequently ionized in the APCI or ESI interface could be demonstrated. In contrast to electrochemical detection, there is full compatibility with gradient elution in liquid chromatography. The applied cell contained a porous glassy carbon working electrode, the large surface area of which allows the quantitative oxidative turnover of the analytes.

Another important group of non-polar compounds are the polycyclic aromatic hydrocarbons (PAHs). Extensive studies have been carried out with respect to their electrochemical oxidation under various conditions [20,21]. As their liquid chromatographic separation is carried out since long [22], the current study was undertaken to evaluate the possibilities for LC/electrochemistry/MS investigations on PAHs. This paper presents the results of LC/electrochemistry/MS studies performed

for sixteen priority pollutant PAHs as assigned by the EPA, focusing the technique on the elucidation of the electrochemical reactions taking place, and secondary applying it for identification of the analytes in a mixture.

## 4.3 Experimental

### *Chemicals*

The non-deuterated PAHs were ordered as EPA PAH Kit 610-N from Supelco (Bellefonte, PA, USA), containing the following priority pollutant PAHs: naphthalene, acenaphthylene, acenaphthene, fluorene, phenanthrene, anthracene, fluoranthene, pyrene, benzo[a]anthracene, chrysene, benzo[b]fluoranthene, benzo[k]fluoranthene, benzo[a]pyrene, dibenzo[a,h]anthracene, benzo[ghi]perylene, and indeno[1,2,3-cd]pyrene. Deuterated PAHs (d<sub>10</sub>-anthracene, d<sub>12</sub>-benzo[a]pyrene, d<sub>10</sub>-phenanthrene and d<sub>10</sub>-pyrene) were purchased from Aldrich Chemical Co. (Milwaukee, WI, USA). Formic acid (p.a. grade) was obtained from Merck (Darmstadt, Germany). Ammonium formate was purchased from Aldrich Chemie (Steinheim, Germany) in the highest quality available.

Solvents for LC were acetonitrile (Chromasolv<sup>®</sup>, gradient grade), methanol (Chromasolv<sup>®</sup>, gradient grade), both purchased from Sigma Aldrich (Seelze, Germany) and water (gradient grade) obtained from Biosolve LTD (Valkenswaard, The Netherlands). Additional LC solvents were ethanol (LiChroSolv<sup>®</sup>, gradient grade), from Merck (Darmstadt, Germany) and deuterated water (D<sub>2</sub>O), acetonitrile (CD<sub>3</sub>CN) and methanol (CD<sub>3</sub>OD), all obtained from Aldrich Chemical Co. (Milwaukee, WI, USA, 99.8%). All PAH solutions used for both single compound and multi-component investigation in direct-injection electrochemistry/MS and LC/electrochemistry/MS were ca. 1·10<sup>-4</sup> M in acetonitrile. Fluorescence detection was applied to 5·10<sup>-5</sup> molar solutions in acetonitrile.

*Instrumentation*

The electrochemical system from ESA Inc. (Chelmsford, MA, USA) used for direct-injection electrochemistry/MS and on-line HPLC/electrochemistry/MS consisted of a GuardStat potentiostat and a model 5021 conditioning cell with an in-line polyether-etherketone (PEEK) filter placed in front of the inlet. The cell contains a glassy carbon working electrode, a Pd counter electrode, and a pH sensitive Pd/H<sub>2</sub> reference electrode, which is a special type of standard hydrogen electrode (SHE). For the coupling of LC/MS on-line with electrochemistry, the electrochemical cell was inserted between the LC column and the APCI interface of the existing LC/MS system, according to Diehl [15]. All potentials mentioned in this work are vs. the Pd/H<sub>2</sub> reference electrode. The LC/MS system from Shimadzu (Duisburg, Germany), consisted of a SCL-10Avp controller unit, a DGU-14A degasser, two LC-10ADvp pumps, a SUS mixing chamber (0.5 mL), a SIL-10A autosampler, a LCMS QP8000 single quadrupole mass spectrometer with atmospheric pressure chemical ionization (APCI) probe and Class 8000 Version 1.20 software. Part of the MS interface is the CDL (curved desolvation line), which serves for further evaporation of the solvent and introduction of the sample from the low vacuum into the high vacuum region of the MS.

For the experiments with individual compounds, direct-injection analysis was carried out. For the mechanistic studies in deuterated solvents, a single HPLC pump was used with premixed eluent instead of the two pumps with mixing chamber to reduce the consumption of deuterated solvents to the lowest possible extent.

The HPLC/UV-vis/fluorescence system from Shimadzu (Duisburg, Germany) consisted of a CBM-10A communications bus module, a GT-154 degasser, two LC-10AS pumps, a SIL-10A autosampler, a SUS mixing chamber (0.5 mL), a CTO-10ACvp column oven, a SPD-M10Avp diode array detector, a RF-10Axl fluorescence detector and Class LC10 software version 1.6.

#### *Cleaning procedure*

It should be noted that upon use of the electrochemical cell, the backpressure of the device increased significantly. As the cell is limited to a back pressure of about 48 bar, cleaning procedures were required every 70 injections, including flushing the cell off-line with 100% acetonitrile, 100% toluene, and again 100% acetonitrile. The fact of increasing pressure indicates that the analytes (PAHs) and products, especially the polymerization products tend to adsorb at the working electrode to block the flow path. The high analyte concentrations of  $10^{-4}$  M are a major reason for these phenomena. The use of a state-of-the-art mass spectrometer with higher sensitivity would allow analyte concentrations at or below  $10^{-5}$  M, thus largely increasing the mean time between cleaning procedures. However, the complete mechanistic work described in this manuscript was performed with only one electrochemical cell, indicating the effectiveness of the cleaning procedure.

#### *Analysis*

Separations were performed using a Supelcosil LC-PAH column (Supelco, Deisenhofen, Germany) with the following dimensions: 5  $\mu$ m particle size, 3 mm id, 25 cm length, and a 2 cm x 3 mm guard column (Supelguard<sup>TM</sup> LC-18). Eluent A of the mobile phase was a solution of 260 mg ammonium formate and 0.6 mL formic

acid in 1 L HPLC-grade water (pH  $\approx$  3), containing 1% of acetonitrile to prevent for bacteria growth. Eluent B was acetonitrile containing 5% of methanol. Injection volumes were 10  $\mu$ L. Flow rates of 0.6 mL/min with the following gradient profile were applied:

time (min)	0.01	10	20	35	35.5	45
c (CH <sub>3</sub> CN) (%)	60	60	95	95	60	stop

For the direct-injection experiments, the conditions were: 10  $\mu$ L injection volume, flow rate 0.4 mL/min, isocratic 30% eluent A/70% organic solvent (v/v), where the employed organic solvents are acetonitrile, methanol, ethanol, and those eluents in fully deuterated form.

UV chromatograms were recorded at 220 and 254 nm when using the LC/MS system. When using the LC/UV-vis/fluorescence system, UV-vis spectra were recorded in the range from 200 to 600 nm.

The conditions used for the direct-injection/electrochemistry/MS experiments (after general optimization of the parameters) are presented in Table 4.1.

**Table 4.1:** Applied MS parameters for direct-injection electrochemistry/MS experiments.

	needle voltage [kV]	deflector voltages [V]	CDL voltage [V]	APCI temp. [°C]	CDL temp. [°C]
APCI(+)	+5	+75	-5	450	300
APCI(-)	-5	-75	+5	450	300

In the HPLC/electrochemistry/MS experiments those MS conditions were the same, except for the needle voltage that was then set to  $\pm 3$  kV. In the scan mode, experiments were carried out in a mass range from  $m/z = 150$  to  $m/z = 400$ . SIM mode experiments were performed for selected ions as presented in the respective figures.

## 4.4 Results and Discussion

### *Optimization*

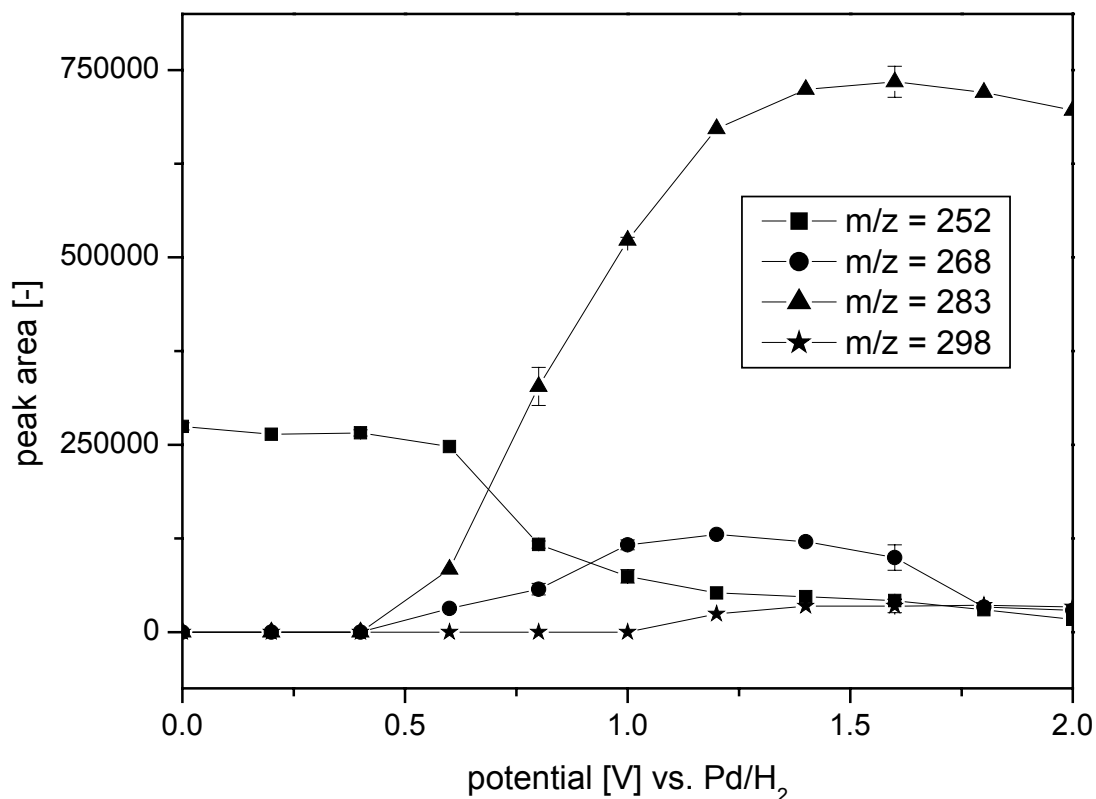
The first measurements were performed using the following conditions: needle 5 kV; deflectors 75 V; CDL voltage -5 V; APCI and CDL temp. 450 and 300 °C, respectively; cell potential 1 V vs. Pd/H<sub>2</sub>; LC flow 0.4 mL/min, consisting of 20% buffer and 80% acetonitrile. A selected number of different PAHs was investigated. Benzo[a]pyrene was used as model compound to optimize several conditions, listed in Table 4.2.

**Table 4.2:** *Experimental conditions used for optimization.*

Parameter	Values
cell potential (V)	0-2; 0.2 V intervals
needle voltage (kV)	0; 1; 3; 5
Deflector voltage (V)	0-100; 25 V intervals

Reproducibility measurements have been performed for 0 and 1.6 V (5 injections each) and 0.4, 0.8 and 1.0 V (3 injections each) at the electrochemical cell. The respective error bars for the peak areas are shown in Figure 4.1. The relative standard deviation varies between 1 and 5% for 0 and 1.6 V and between 1 and 10% for 0.4, 0.8 and 1.0 V.





**Figure 4.1:** Occurrence of different oxidation products of perylene depending on the potential of the electrochemical cell ranging from 0 to 2.0 V versus Pd/H<sub>2</sub>. MS conditions: APCI needle voltage 5 kV, deflector voltage 75 V, APCI temp. 450 °C and CDL temp. 300 °C. The error bars represent relative standard deviations ( $n = 5$  at 0 V and 1.6 V;  $n = 3$  at 0.4, 0.8, and 1.0 V).

First, the electrochemical cell potential (varied in the range from 0 V to +2 V vs. Pd/H<sub>2</sub>), was optimized. As Figure 4.1 shows, increasing potential up to 0.5 V does not lead to changes in the products. Further increase of the potential leads to a decrease of the abundance of the molecular radical cation ( $m/z = 252$ ) but to an increase for the mono- ( $m/z = 268$ ), di- ( $m/z = 283$ ) and tri- ( $m/z = 298$ ) oxygenated products, for which the pathway of formation is explained below. The highest total ion current was obtained with 2 V applied at the cell. However, the spectrum which

revealed most information on the reaction pathways by showing the largest number of different oxidation products was obtained at 1 V vs. Pd/H<sub>2</sub>. Applying this voltage to the electrochemical cell, further fine-tuning of the most important MS parameters was performed, for which 3 kV at the APCI needle and 50 V at the deflectors turned out to be the optimal settings. Applying harder conditions, e.g., higher voltages at the discharge needle and the deflectors, respectively, the main differences observed are the changing intensity ratios of the oxidation and fragmentation products, but the influence on the total ion current is negligible.

When examining other PAHs, the optimum is found at different conditions. Most of the PAHs show better response using harder conditions. Hence, for further experiments the cell voltage was set to 1.6 V, the needle voltage to 5 kV and the deflector voltages to 75 V.

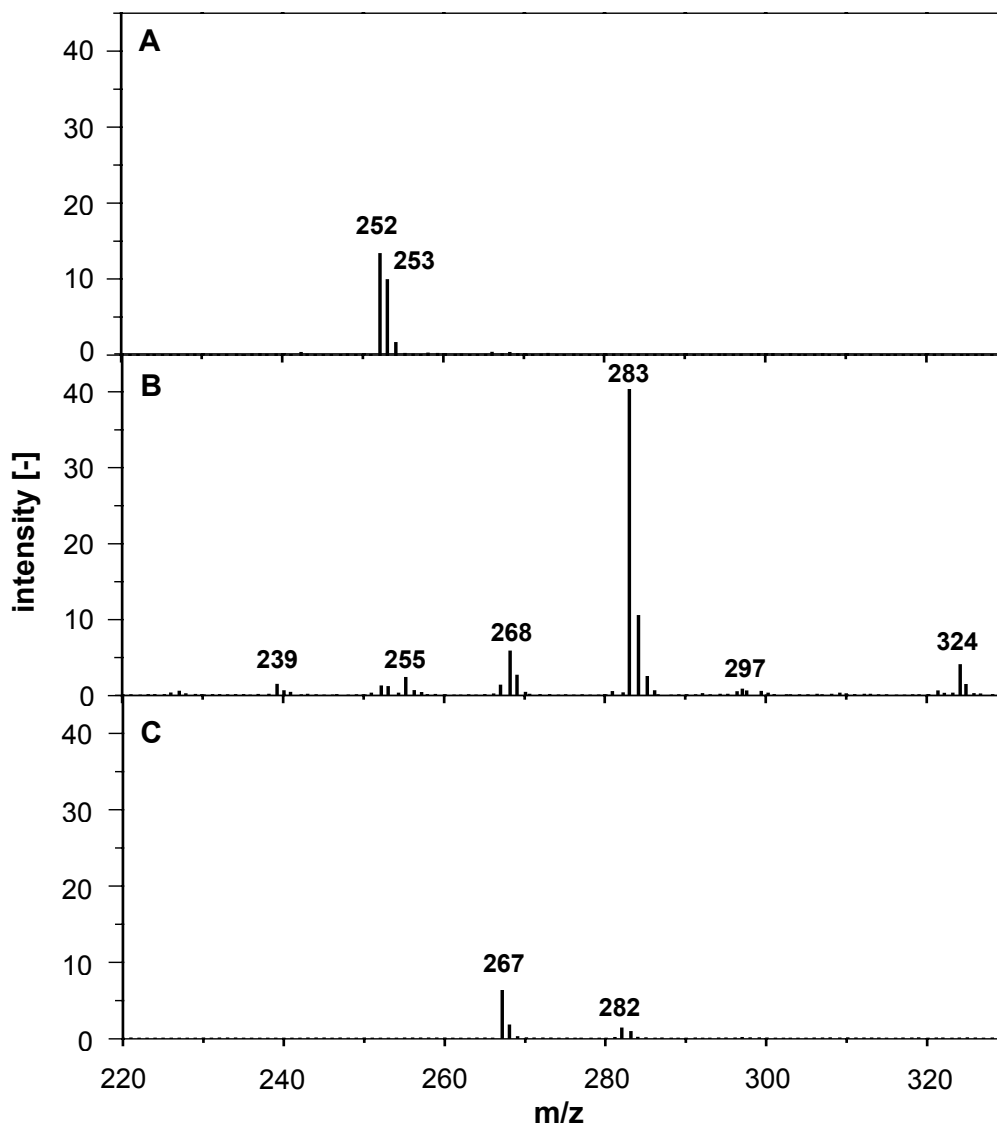
#### *Mechanistic studies*

All PAHs turned out to follow the same general principle for electrochemical oxidation. BaP, being one of the most potent carcinogens among the PAHs yielded the highest signals and was therefore selected as model compound to study the oxidation behavior of PAHs. For this purpose, several experiments have been conducted for BaP using different solvents.

Direct-injection/electrochemistry/mass spectra were recorded for BaP and BaP-*d*<sub>12</sub> in acetonitrile, deuterated acetonitrile, methanol, deuterated methanol and ethanol. All organic solvents were applied in combination with aqueous buffers (70/30, v/v). When using deuterated acetonitrile or methanol, a buffer on the basis of deuterated

water replaced the non-deuterated buffer. In all solvents, measurements were made both in the positive and negative ion detection modes and with the electrochemical cell off as well as with a potential applied at the cell. In the positive ion mode, measurements with the corona discharge needle without potential were carried out as well to study the formation of charged species directly in the electrochemical cell. This effect was observed earlier for ferrocene derivatives [19]. As hardly any signal was obtained in case of the PAHs without applied needle voltage, the conclusion is drawn that the majority of the electrochemical oxidation products are uncharged and therefore have to be ionized first in the APCI interface prior to mass spectrometric detection.

To describe the oxidation reactions taking place in the electrochemical cell, a selected series of direct-injection electrochemistry/MS experiments with their resulting spectra are shown in Figures 4.2, 4.3 and 4.5. Symbols in between brackets assigned to the discussed products refer to the symbols in Figure 4.4.



**Figure 4.2:** Electrochemistry/MS spectra for benzo[a]pyrene ( $2.4 \times 10^{-4}$  M) in acetonitrile/ammonium formate buffer. (A): Electrochemical flow cell off, APCI(+) mode; (B): 1.6 V at the electrochemical cell, APCI(+) mode; (C): 1.6 V at the electrochemical cell, APCI(-) mode.

Figure 4.2A shows the formation of the molecular radical cation  $[M]^{\bullet+}$  and the protonated molecule in the APCI interface ( $m/z = 252$  and  $253$ ) in acetonitrile/buffer without an electrochemical potential applied at the cell. The  $m/z = 253$  signal is too

high for the calculated  $^{13}\text{C}$ -satellite peak and is thus partly assigned to the protonated parent molecule. It should be noticed that without any oxidation prior to the ionization in the interface, the ionization yield is already relatively high for BaP compared to the other PAHs. Figure 4.2B shows a spectrum recorded at the same conditions, but with a potential of 1.6 V vs. Pd/H<sub>2</sub> applied at the electrochemical cell. Significant differences compared to the spectrum of the unoxidized BaP are observed in this case: The molecular radical cation and the protonated molecular cation almost disappear, while the spectrum is dominated by the mono- and dioxygenated species. The signal  $m/z = 268$  can be explained with the formation of BaP-ol [B<sub>1</sub>], which means an oxidation of the BaP to its radical cation, subsequent nucleophilic attack of one H<sub>2</sub>O molecule and the final loss of two H<sup>+</sup> and one electron, yielding the alcohol having a mass of  $[M+O] = 268$  Da. In the interface, one electron is removed resulting in the formation and detection of the respective radical cation at  $m/z = 268$ .

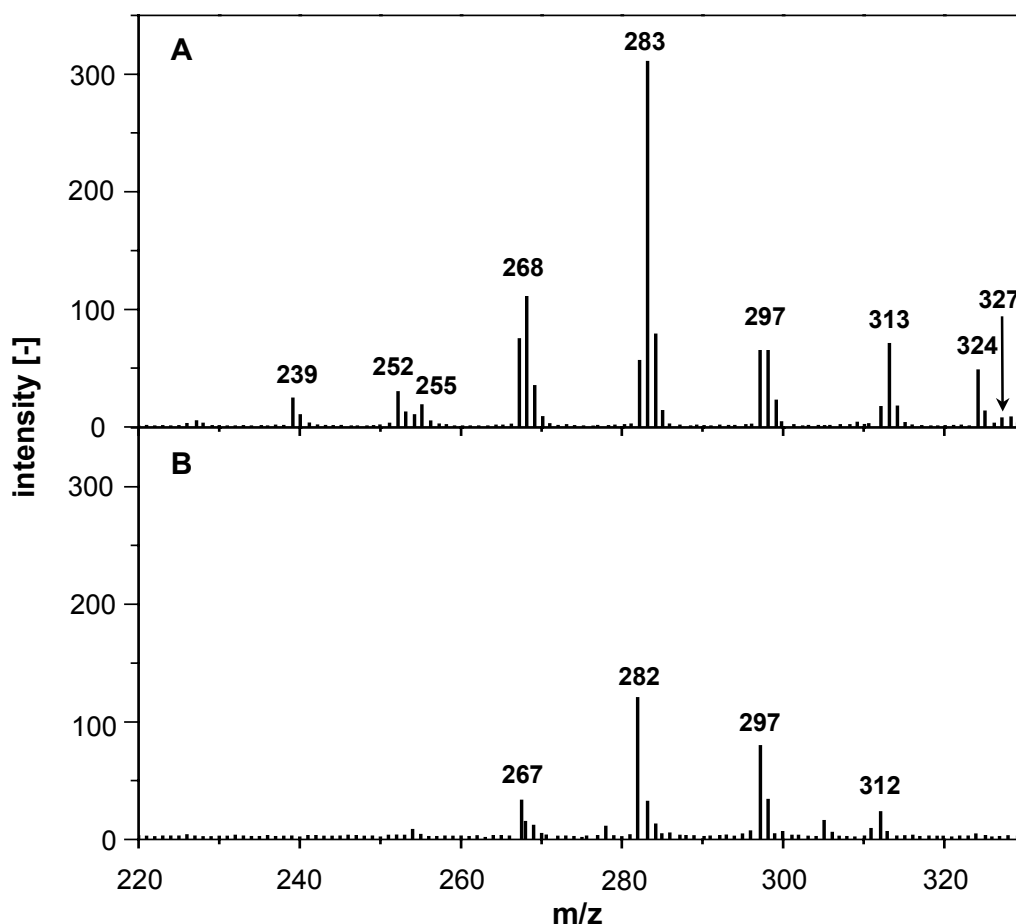
In the electrochemical cell, the alcohol is further oxidized, first removing two electrons and one proton to yield a positively charged ketone [B<sub>2</sub>] with  $m/z$  of 267 in the MS. A peak of  $m/z = 267$  is present in the spectrum, but as it was not in the spectrum obtained without needle voltage, the formation of the final product is assigned to APCI processes rather than electrochemical processes in the additional cell. This positively charged ketone rapidly undergoes the next step to form BaP-diol [B<sub>3</sub>] by adding water and losing a H<sup>+</sup> ( $M = 284$  Da), which leads after oxidation in the interface to the signal of its radical cation at  $m/z = 284$ . As this signal is only about one fourth as intense as the  $m/z = 283$  signal, it indicates that under the applied conditions, the diol is rapidly oxidized losing two electrons and two protons

to end up as BaP-quinone [A<sub>1</sub>]. This product, having a molecular mass of 282 Da, is easily protonated in the interface to give an intense signal of  $m/z = 283$ . The protonated quinone forms an acetonitrile adduct, which is detected at  $m/z = 324$ . To a very small amount, the quinone undergoes another oxidation step. Attack of water, and withdrawal of two electrons and two protons yields the hydroxyquinone [A<sub>2</sub>] with a mass of 298 Da. This product is further oxidized to yield the positively charged oxoquinone [B<sub>4</sub>] at  $m/z = 297$ .

Under these relatively hard MS conditions, fragmentation of the oxidation products occurs as well, mainly resulting in a neutral loss of CO, which has been observed before in LC/MS studies of partially oxidized PAHs [23,24,25]. Hence, the peak at  $m/z = 255$  is assigned to a product resulting from loss of CO from [BaP-quinone +H]<sup>+</sup>. Analogue to this fragmentation, the signal at  $m/z = 239$  is assigned to the protonated BaP ketone ( $m/z = 267$ ) after loss of CO.

Figure 4.2C presents signals for anions with  $m/z = 267$ , 282 and 283. The first one shows the deprotonation of the BaP-ol [B<sub>1</sub>] (M = 268 Da), to yield [M-H]<sup>-</sup>. The  $m/z = 283$  results from the deprotonated BaP-diol [B<sub>3</sub>] [M-H]<sup>-</sup>. The BaP-quinone [A<sub>1</sub>] leads to the  $m/z = 282$  peak after capturing one electron in the APCI interface, which may in the negative ion mode be considered as source of low energy electrons [3-5].

Figure 4.3A presents the mass spectrum of BaP in a methanol/buffer solution, obtained in the APCI(+) mode after electrochemical pretreatment.



**Figure 4.3:** *Electrochemistry/MS spectra for benzo[a]pyrene ( $2.4 \times 10^{-4}$  M) in methanol/ammonium formate buffer. (A): 1.6 V at the electrochemical cell, APCI(+) mode; (B): 1.6 V at the electrochemical cell, APCI(-) mode.*

Signals at  $m/z = 252, 267, 268, 283, 297,$  and  $324$  already have been explained in Figure 4.2. In methanol, the peak at  $m/z = 268$  is higher than the peak at  $m/z = 267$ , suggesting the BaP-ol radical cation being favored in methanol. The presence of the acetonitrile adduct at  $m/z = 324$  in the methanol environment is explained from the 1% acetonitrile in the buffer solution. Additionally to the spectrum obtained from BaP in acetonitrile, peaks occur at  $m/z = 282, m/z = 298, m/z = 313$  and  $m/z = 327$ . These mass-to-charge ratios are explained on the basis of a nucleophilic attack of methanol

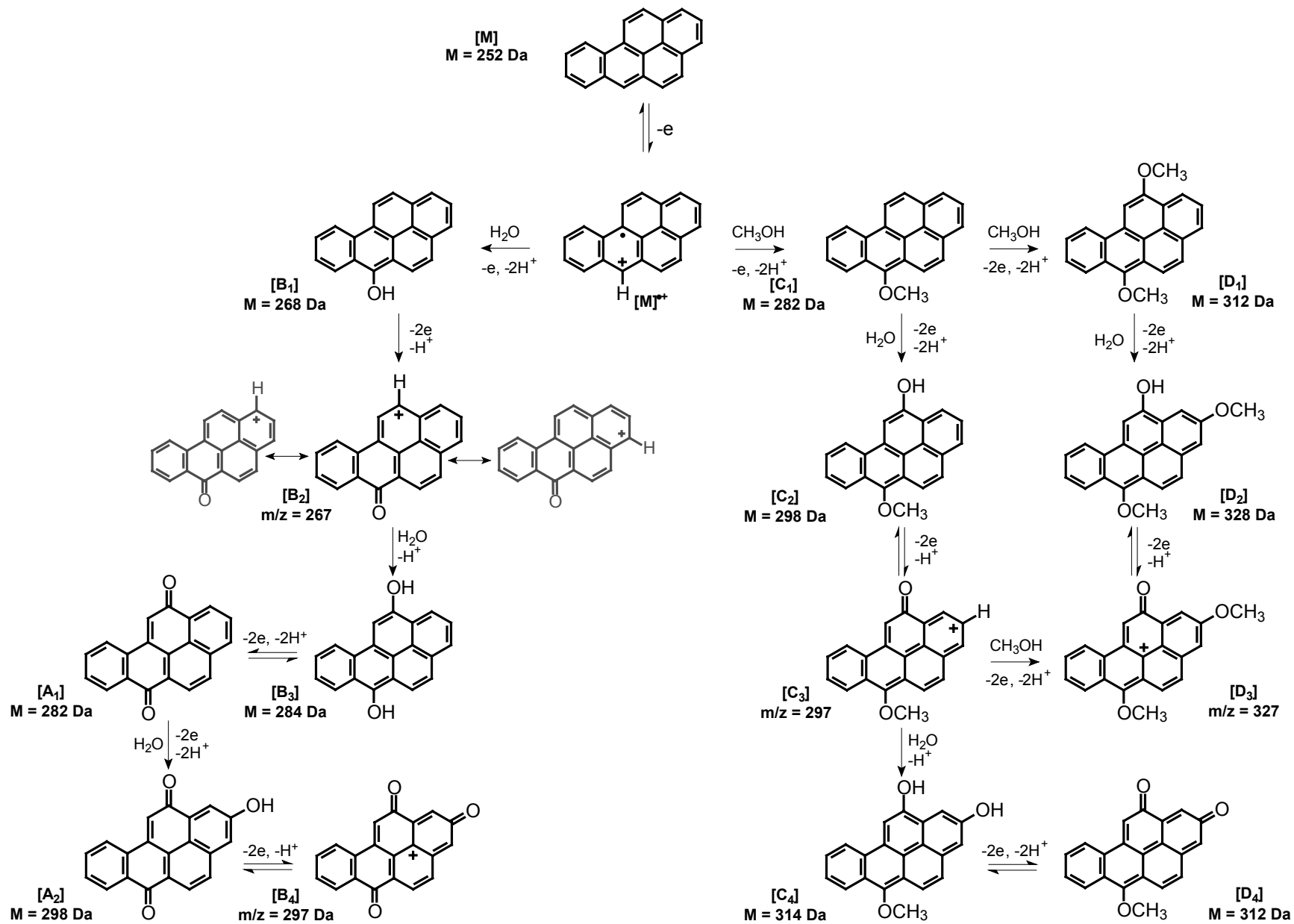
on the radical cation instead of water, resulting in the formation of methoxy-BaP [C<sub>1</sub>] parallel to hydroxy-BaP [B<sub>1</sub>] and furthermore dimethoxy-BaP [D<sub>1</sub>], methoxy-BaP-ketone [C<sub>3</sub>], methoxy-BaP-ol [C<sub>2</sub>], methoxy-BaP-quinone [D<sub>4</sub>], dimethoxy-BaP-ol [D<sub>2</sub>] and dimethoxy-BaP-ketone [D<sub>3</sub>].

Similar to the spectrum for BaP in acetonitrile obtained in the negative ion mode (Figure 4.2C), Figure 4.3B shows the peaks at  $m/z = 267$  and  $m/z = 282$  for the deprotonated BaP-ol [B<sub>1</sub>] and radical anion of BaP-quinone [C<sub>2</sub>]. The signal intensity for the BaP-quinone in methanol is much higher than in acetonitrile, due to the better ionization efficiency of methanol. The peaks present at  $m/z = 297$ ,  $298$  and  $312$  are explained by hydroxy-BaP-quinone [A<sub>2</sub>] (M = 298 Da), observed as both the deprotonated species and the radical anion, and methoxy-BaP-quinone [D<sub>4</sub>] (M = 312 Da), observed as the radical anion.

All the above discussed reaction products for the electrochemical process lead to the overall reaction pathways for the electrochemical oxidation of BaP as depicted in Figure 4.4.

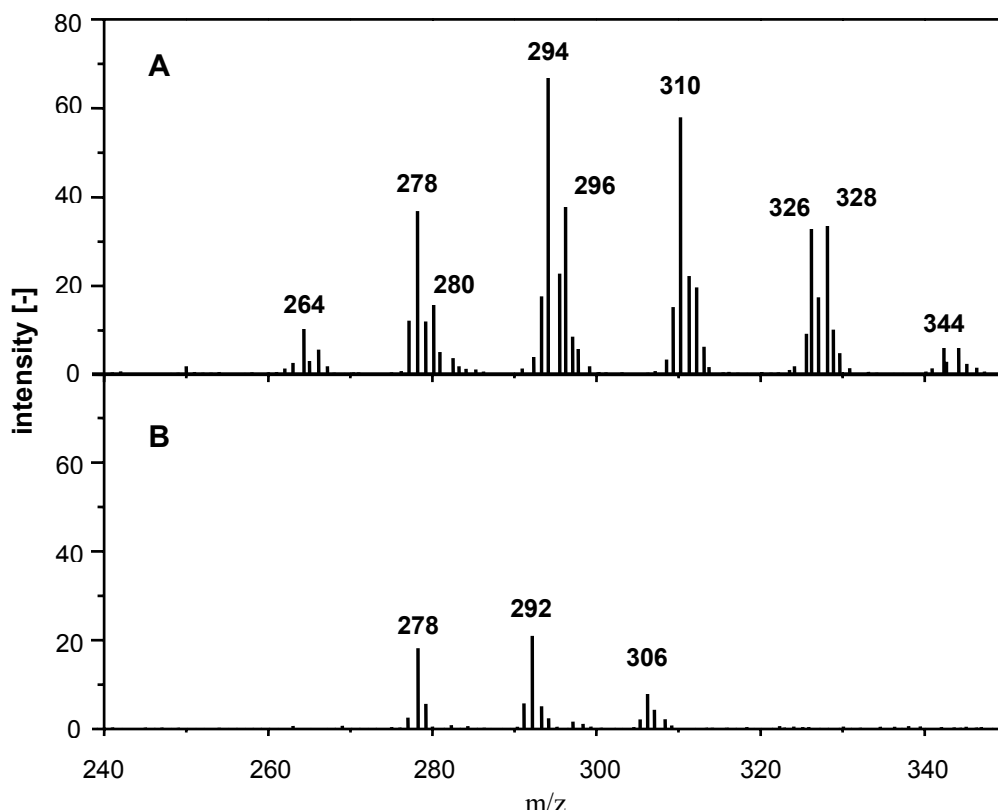


...Electrochemistry/Mass Spectrometry of Polycyclic Aromatic Hydrocarbons



**Figure 4.4:** Reaction scheme for the oxidation of BaP in methanol/ammonium formate buffer in the electrochemical flow cell. The structural formulas in grey are an example of possible mesomeric oxidation products.

To provide for additional evidence for this oxidation scheme, experiments were carried out in ethanol, deuterated solvents and with deuterated BaP as well, for which most of the obtained spectra are not presented in this chapter. The obtained mass spectra for BaP- $d_{12}$  in deuterated methanol/deuterated water in the positive and negative APCI mode are presented in Figure 4.5. The expected masses calculated for the different products assumed in the former spectra fit to the observed masses.



**Figure 4.5:** Electrochemistry/MS spectra for benzo[a]pyrene- $d_{12}$  ( $8.9 \times 10^{-5}$  M) in deuterated methanol/ammonium formate buffer. (A): 1.6 V at the electrochemical cell, APCI(+) mode; (B): 1.6 V at the electrochemical cell, APCI(-) mode.

It has to be mentioned that the positions of the inserted functional groups may vary, as there are several possible isomers. With the equipment available for this study, the exact positions of the substituents at the aromatic rings could not be allocated. However, the most reactive sites (referring to the highest electron density, and overall charge delocalization in the radical cations) are known from literature [12,16,20,21], according to which the structures in Figure 4.4 are drawn.

The observed products as discussed for acetonitrile/buffer corroborate those found in off-line investigations by Jeftić and Adams [21]. They did not observe the hydroxyquinone or the corresponding oxo-quinone. But as discussed, these products are hardly formed in acetonitrile and more favored in methanol (or ethanol), which they did not use as solvent in their studies. Jeftić and Adams, however, additionally observed a BaP-dimer, being adsorbed to the electrode, which could not be detected in our MS-experiments. It is likely that, under the electrochemical conditions used and considering that a large surface glassy carbon electrode was applied, adsorption of dimers or higher oligomers at the electrode surface occurs in this study as well. However, the major advantage of this approach is the possibility for the on-line investigation of the reaction products of several PAHs in one single LC run without the need to isolate the reaction products and to identify them off-line. The use of an ion trap or triple quadrupole mass spectrometer might furthermore allow to determine the allocation of the oxygen-based substituents at the aromatic rings. Cole and co-workers recently detected the radical cations of PAHs using an electrochemical system, which was constructed in the electrospray probe [16]. However, this set-up is limited to comparably low flow rates and may theoretically be coupled only to

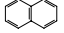
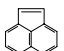
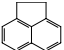
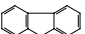
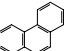
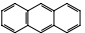
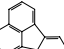
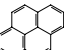
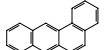
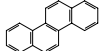
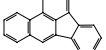
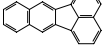
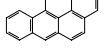
microbore LC, while the approach presented in this study may be used in conjunction with LC in standard dimensions using commercially available equipment.

In contrast to the work of Jeftić and Adams [21] and of Cole et al. [8], organic solvents are used in combination with an aqueous buffer in this study. To detect the radical cations, the other groups used pure organic solvents, which did not contain nucleophiles. Jeftić and Adams found out that the overall reaction scheme is deemed to be rather insensitive to the employed organic solvent. The presence of oxygenated reaction products is then due to impurities (water traces), and, as Cole et al. found [8], is significantly increased by adding a few millimoles per liter of water to the organic solvent. As discussed in this chapter present paper, the insensitivity to the solvent is not observed for the nucleophilic alcoholic solvents. Methanol and ethanol are strongly involved in the follow-up reactions in the electrochemical cell, and beyond this, methanol significantly increases the ionization efficiency to yield much larger total ion currents than in acetonitrile. Experiments performed in deuterated solvents and with deuterated PAHs provide even more evidence for the formation of the discussed products.

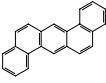

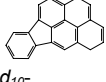
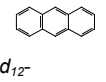
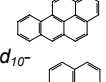
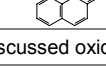
The results of investigations on PAHs in different solvents using different electrochemistry and MS conditions are summarized in Table 4.3.

**Table 4.3:** Structures and properties of the investigated PAHs, total ion currents obtained mass spectrometrically with and without oxidation in the electrochemical cell and observed mass traces in electrochemistry/MS, in positive and negative ion mode. Electrochemical cell potential: 1.6 V, APCI needle voltage:  $\pm 5$  kV, APCI temperature: 450 °C, deflector voltage:  $\pm 75$  V, CDL temperature: 300 °C.

...Electrochemistry/Mass Spectrometry of Polycyclic Aromatic Hydrocarbons

No	Compound	Abbr.	FW	Structure	Total Ion Current [-] APCI(+)			Prominent Observed Masses (rel. int.) in MeOH [m/z (%)]	
					without cell	with cell, AcN	with cell, MeOH	APCI(+)	APCI(-)
1	Naphtalene	Naph	128.2		150,000	350,000	600,000	184.3* (15), 210.1* (15), 227.3* (30), 254.3 (9), 326.2* (25), 338.4* (100)	--
2	Acenaphthylene	ANy	152.2		nd	nd	120,000	140.0 (100), 168.1 (60), 212.9 (30), 318.9 (25)	--
3	Acenaphthene	ANe	154.2		nd	nd	70,000	140.0, 168.1, 335.8* (100)	167.0
4	Fluorene	Fle	166.2		75,000	300,000	420,000	227.2 (25), 326.4* (20), 338.4* (100), 379.4* (10)	--
5	Phenanthrene	Phen	178.2		nd	nd	nd	--	--
6	Anthracene	Ant	178.2		4,000	250,000	450,000	152.1 (5), 165.2 (40), 178.1 (100), 194.2 (40), 208.3 (5), 235.3 (5)	193.0 (100)
7	Fluoranthene	Fla	202.3		nd	nd	55,000	178.0 (35), 205.2 (70), 217.0 (85), 232.9 (100), 248.0 (85), 265.0 (40), 262.0 (40)	217.0 (100),
8	Pyrene	Pyr	202.3		30,000	130,000	650,000	205.1 (10), 218.1 (15), 233.2 (55), 247.1 (100), 263.1 (55), 277.1 (25), 293.4 (10)	219.0 (30), 232.0 (45), 247.0 (100), 262.4 (10)
9	Benzo[a]anthracene	BaA	228.3		6,000	600,000	1,000,000	202.2 (5), 216.2 (15), 228.1 (100), 244.2 (60), 259.1 (10)	243.2 (100)
10	Chrysene	Chr	228.3		150,000	225,000	400,000	210.1 (25), 227.2* (35), 245.3 (30), 273.1 (55), 283.3* (25), 326.3* (35), 338.4* (100), 379.4* (15)	243.0 (100)
11	Benzo[b]fluoranthene	BbF	252.3		200,000	400,000	500,000	227.2 (35), 255.1 (15), 268.1 (20), 283.2 (100), 297.9 (20), 313.1 (60), 338.4* (80)	--
12	Benzo[k]fluoranthene	BkF	252.3		50,000	150,000	600,000	239.0 (20), 252.1 (70), 255.1 (25), 268.1 (90), 283.1 (100), 298.1 (50), 313.1 (40), 327.1 (20), 343.2 (5)	267.1 (100), 282.1 (15), 296.9, (10)
13	Benzo[a]pyrene	BaP	252.3		450,000	1,000,000	1,500,000	239.2 (5), 252.2 (15), 267.2 (30), 268.2 (30), 283.1 (100), 297.1 (30), 313.1 (60), 327.1 (20), 324.2 (20)	267.0 (35), 281.9 (100), 297.2 (80), 312.1 (20)

Chapter 4

No	Compound	Abbr.	FW	Structure	Total Ion Current [-] APCI(+)			Prominent Observed Masses (rel. int.) in MeOH [m/z (%)]	
					without cell	with cell, AcN	with cell, MeOH	APCI(+)	APCI(-)
14	Dibenzo[ <i>a,h</i> ]anthracene	dBA	278.3		35,000	200,000	800,000	264.9 (15), 278.1 (100), 294.1 (55), 309.2 (30), 325.0 (10), 339.1 (5)	293.1 (100)
15	Benzo[ <i>ghi</i> ]perylene	B <i>ghi</i> P	276.3		350,000	450,000	850,000	227.2 (25), 279.1 (20), 291.9 (30), 307.1 (85), 322.1 (85), 338.4 (100), 352.3 (25)	291.1 (100), 306.1 (75), 321.0 (35), 337.1 (10)
16	Indeno[1,2,3- <i>cd</i> ]pyrene	I <i>cd</i> P	276.3		300,000	450,000	100,000	227.2 (10), 276.1 (15), 292.1 (50), 307.1 (95), 321.1 (100), 336.3 (90), 352.1 (40), 367.3 (20), 383.4 (10)	291.3 (100), 305.9 (85), 320.9 (50), 337.4 (15)
17	Anthracene- <i>d</i> <sub>10</sub>	Ant- <i>d</i> <sub>10</sub>	188.3	 <i>d</i> <sub>10</sub> -	3,000	150,000	460,000	159.3 (5), 174.1 (20), 187.2 (100), 203.1 (50), 219.3 (5), 244.1 (5)	--
18	Benzo[ <i>a</i> ]pyrene- <i>d</i> <sub>12</sub>	BaP- <i>d</i> <sub>12</sub>	264.4	 <i>d</i> <sub>12</sub> -	40,000	700,000	750,000	278.3 (25), 293.2 (80), 307.2 (100), 322.1 (85), 337.3 (30)	278.0 (25), 292.3 (100), 306.2 (85)
19	Pyrene- <i>d</i> <sub>10</sub>	Pyr- <i>d</i> <sub>10</sub>	212.3	 <i>d</i> <sub>10</sub> -	50,000	160,000	750,000	213.3 (10), 225.3 (20), 241.1 (60), 253.8 (100), 269.9 (75), 284.3 (20), 299.1 (10)	226.0 (25), 240.0 (55), 254.2 (100), 268.0 (15)

\* mass traces which cannot be explained from the discussed oxidation pathways

Except for phenanthrene, which could not be detected at all, all PAHs of the sixteen priority PAHs of the EPA show significantly increased sensitivity in direct-injection/electrochemistry/MS compared with the approach without electrochemical cell. Comparing the oxidation and the ionization yields in methanol and acetonitrile, higher signal intensities are obtained in methanol.

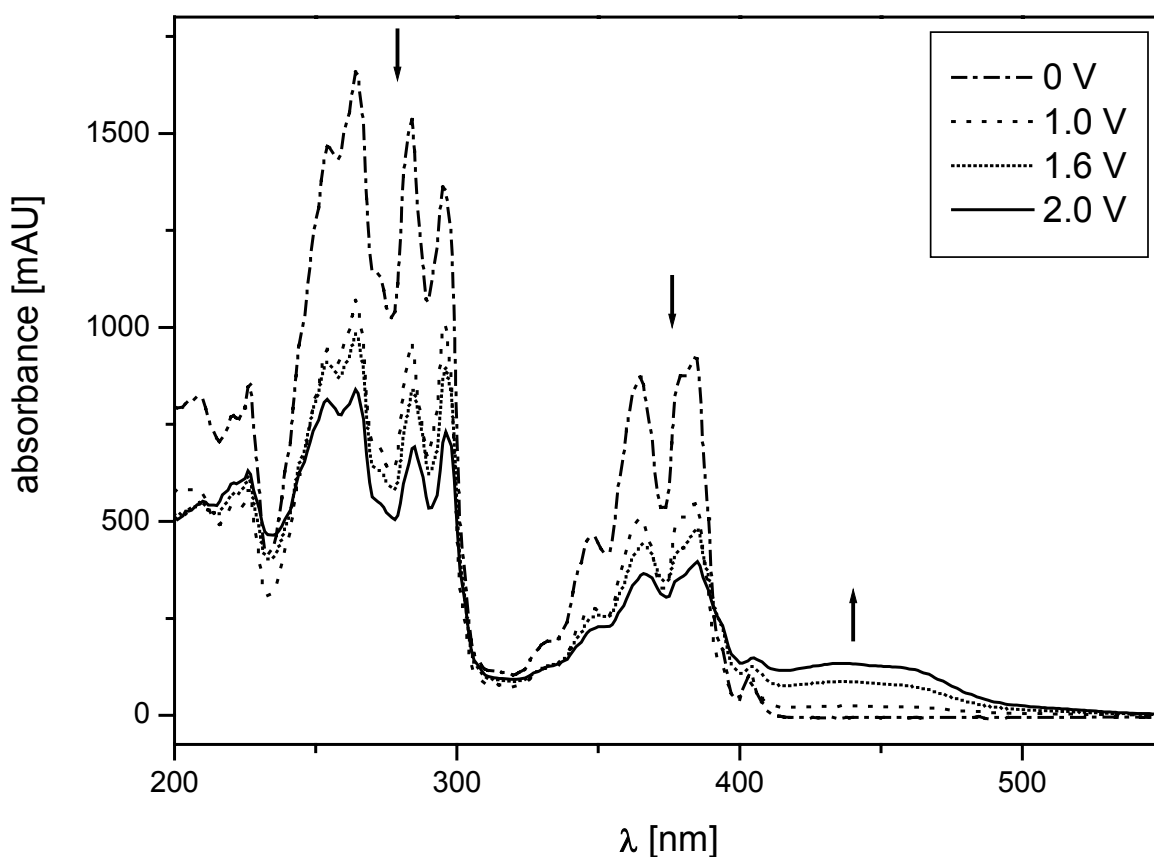
When comparing the oxidation results for the other PAHs to the oxidation of BaP, the initial oxidation to a radical cation was observed in all cases. Following reactions were first the addition of water or methanol, then the formation of hydroxy-PAHs and PAH-ketones. Differences arise when looking at the number of inserted substituents at one molecule, the stage in which the product is detected (radical cation, protonated cation, or ketone), and in which ratio the oxidation products are formed. All those differences in oxidation depend on size and structure of the PAHs, which determine the over-all charge delocalization in the radical cation and thus influence the stability of the radical and the possibilities for oxidation. The smaller PAHs, containing two or three condensed aromatic rings (naphthalene, acenaphthene and fluorene), are hardly detected as direct oxidation products of the molecule, but rather as dimerization products, which are then oxygenated.

In respect of other compounds, anthracene, benzo[a]anthracene, chrysene, benzo[b]fluoranthene, and dibenzo[a,h]anthracene show up to doubly substituted products, whereas fluoranthene, pyrene, benzo[k]fluoranthene, benzo[a]pyrene, benzo[ghi]perylene, and indeno[1,2,3-cd]pyrene even show triply substituted products. The electroactivity is not only size dependent, but also structure dependent: The more compact the molecule, the higher the electron density, the

higher the activity, which means higher ability to form multiply substituted electrochemical oxidation products. Secondly, the electron density of the PAH enables good charge delocalization in the radical, which allows for stable radicals and thus good possibilities for further oxidation.

As additional evidence for the formation of oxygenated products in the electrochemical cell, UV-vis spectra were recorded for the compounds both with and without on-line pretreatment in the electrochemical cell and at different potentials.

Figure 4.6 shows the respective UV-vis spectra for BaP.



**Figure 4.6:** Red-shift of the electrochemistry/UV-vis spectra for benzo[a]pyrene ( $2.4 \times 10^{-4}$  M) at increasing cell potential at the electrochemical cell (arrows indicate the direction of the intensity upon increasing potential at the electrochemical cell).

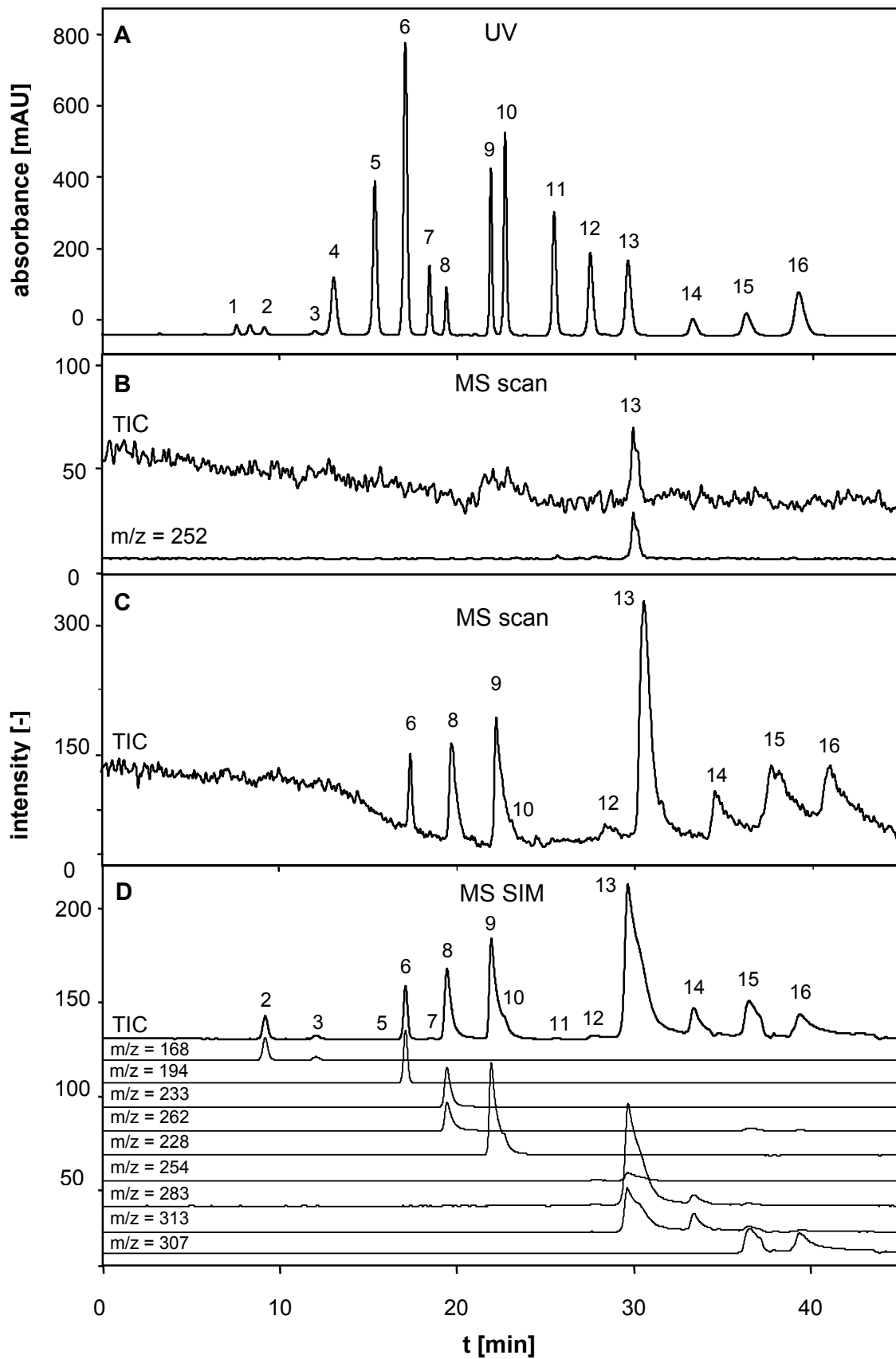


An increase of the cell potential leads to a red-shift, which demonstrates the formation of ketones and quinones, as carbonyl-substituted PAHs tend to absorb at higher wavelengths than unsubstituted PAHs do. Furthermore, these results show the applicability of on-line LC/electrochemistry/UV-vis spectrometry.

#### *On-line LC/electrochemistry/MS*

After an intensive study on the oxidation of the single compounds, the HPLC system and the electrochemistry/MS setup were coupled to study the separation with on-line detection of the sixteen EPA priority PAHs. First of all, separation was carried out using LC/UV-vis (Figure 4.7A). The obtained parameters were used to set up the separation in the LC/electrochemistry/MS system. Optimization of the APCI interface conditions for the on-line set-up lead to best LC/electrochemistry/MS results when applying 3 kV at the APCI needle, 75 V at the deflectors and temperatures of 450 and 300 °C for the APCI-interface and CDL, respectively. All other parameters were kept as before.

Figure 4.7B shows a LC/MS chromatogram without post-column electrochemical conversion. Concentrations for all PAHs are between  $9.9 \times 10^{-5}$  and  $1.1 \times 10^{-4}$  M, except for BaP ( $9.6 \times 10^{-5}$  M), BbF, BkF, IcdP ( $9.7 \times 10^{-5}$  M), Fla ( $1.3 \times 10^{-4}$  M), and Fle ( $1.8 \times 10^{-4}$  M). Obviously, the sensitivity is insufficient under these conditions. Only one peak is observed for BaP at a retention time of close to 30 min. When exploring the traces for the known compounds, some more of the larger PAHs (>4 fused aromatic rings) can be detected with very low signals. The signals observed here result from the respective  $[M]^{++}$  and  $[M+H]^+$  ions.



**Figure 4.7:** LC/electrochemistry/UV-vis and LC/electrochemistry/MS chromatograms for a mixture of the sixteen priority pollutant PAHs, concentrations between  $9.9 \times 10^{-5}$  and  $1.1 \times 10^{-4}$  M, except for BaP ( $9.6 \times 10^{-5}$  M), BbF, BkF, IcdP ( $9.7 \times 10^{-5}$  M), Fla ( $1.3 \times 10^{-4}$  M), and Fle ( $1.8 \times 10^{-4}$  M), positive ion mode. Naphtalene (1), acenaphtylene (2), acenaphtene (3), fluorene (4), phenanthrene (5), anthracene (6), fluoranthene (7), pyrene (8), benzo[a]anthracene (9), chrysene (10), benzo[b]fluoranthene (11), benzo[k]fluoranthene (12), benzo[a]pyrene (13), dibenzo[a,h]anthracene (14), benzo[ghi]perylene (15), indeno[1,2,3-cd]pyrene (16). (A): UV chromatogram recorded at 254 nm; (B): MS chromatogram, scan mode  $m/z$  150 – 400, electrochemical flow cell off; (C): MS chromatogram, scan mode  $m/z$  150 – 400, electrochemical flow cell 1.6 V; (D): MS chromatogram, selected ion monitoring (SIM) mode, electrochemical flow cell 1.6 V.

First LC/electrochemistry/MS chromatograms were obtained in the scan mode, both in the positive and negative ion mode, for which Figure 4.7C depicts the increase in sensitivity when changing from LC/MS to LC/electrochemistry/MS. It clearly shows nine of the sixteen PAHs in contrast to only one peak in the chromatogram obtained without electrochemical conversion (Figure 4.7B). Higher sensitivity is achieved when applying the selected ion-monitoring (SIM) mode, a chromatogram of which is presented in Figure 4.7D. The chromatograms show peaks for ANy (9.1 min), ANe (12.0 min), Phen (15.4 min), Ant (17.1 min), Fla (18.4 min), Pyr (19.4 min), BaA (21.9 min), Chr (22.6 min; as shoulder in BaA peak) BbF (25.6 min) BkF (27.6 min), BaP (29.6 min), dBA (33.4 min), BghiP (36.5 min), IcdP (39.4 min). Only two out of the 16 PAHs are not detectable at all, phenanthrene only could be detected (barely) in the negative ion mode, and acenaphtylene is only seen in the positive ion mode.

The slight shift to the larger retention times compared to the UV chromatograms is explained by the additional retention of the higher PAHs in the electrochemical cell, as they tend to have fairly strong interactions with the glassy carbon electrode. While some peak broadening in the HPLC column already occurs at the increasing retention times, the retention in the electrochemical cell leads to broad tailing and overlapping peaks at the end of the MS chromatogram. Summarizing, the set-up is well-suited for the investigation of reaction pathways, but the sensitivity cannot compete with the established methods for the quantitative analysis of PAHs.

## 4.5 Conclusions

The coupling of LC/electrochemistry/MS has been applied to the determination of polycyclic aromatic hydrocarbons (PAHs). This LC/electrochemistry/MS setup is well-suited for the analysis of PAHs and has especially been versatile for the elucidation of the respective electrochemical reaction pathways.

The obtained spectra clarify the reaction pathways for PAHs in electrochemical oxidation. Different solvents lead to different mass spectra for the same compound as the solvent is here involved in following reactions after the electrochemical oxidation. However, the solvent also influences the ionization processes in the APCI interface, as the ratio for formation of the radical ions and (de)protonated ions turns out to be different in different solvent systems. Whether the oxidation products are detected as radical ions or (de)protonated ions, the obtained spectra still confirm the reaction pathways, inserting hydroxy or methoxy groups subsequently to and accompanied by losses of electrons to yield mono-, di- and trisubstituted alcohols, ketones and methoxylated PAHs. For measurements in acetonitrile/buffer, relative standard deviations for the intensities of  $m/z = 252$  and  $m/z = 283$  are found between 1 and 5% ( $n=5$ ) at 0 V and 1.6 V and between 1 and 10% ( $n=3$ ) at 0.4, 0.8 and 1.0 V.

Application of the LC/electrochemistry/MS set-up to determine PAHs in a mixture lead to chromatograms where fourteen out of sixteen compounds could be identified, both in the positive and in the negative ion mode. The obtained sensitivity is quite different for different PAHs, but for all of these fourteen PAHs, the sensitivity is much better than in LC/MS without electrochemical pretreatment. For more quantitative data, see Table 4.3.

Sensitivity cannot compete yet with fluorescence detection, but electrochemistry/MS-detection is much more selective than fluorescence and UV detection and provides much more structural information of the analytes and the oxidation processes. It offers good possibilities in the on-line elucidation of oxidation pathways and is much more rapid and efficient as the currently used off-line methods on this purpose.

The experienced tailing and overlapping of the peaks is disadvantageous for integration. As this fact is mainly due to the adsorption of the PAHs on the graphite electrode of the electrochemical cell, future work concerning employment of other electrode materials (metals) may reduce this obstacle and lead to large improvements with respect to applications in quantitative analysis.

## 4.6 References

- [1] E. Gelpí, *J. Chromatogr. A* 703 (1995) 59.
- [2] W. M. A. Niessen, *J. Chromatogr. A* 856 (1999) 179.
- [3] G. Singh, A. Gutierrez, K. Xu, I. A. Blair, *Anal. Chem.* 72 (2000) 3007.
- [4] H. Hayen, N. Jachmann, M. Vogel, U. Karst, *Analyst* 127 (2002) 1027.
- [5] C. S. Evans, R. Sleeman, J. Luke, B. J. Keely, *Rapid Commun. Mass Spectrom.* 16 (2002) 1883.
- [6] D. B. Robb, T. R. Covey, A. P. Bruins, *Anal. Chem.* 72 (2000) 3653.
- [7] E. Bayer, P. Gfrörer, C. Rentel, *Angew. Chem. Int. Ed.* 38 (1999) 992.
- [8] X. M. Xu, W. Z. Lu, R. B. Cole, *Anal. Chem.* 68 (1996) 4244.
- [9] T. Y. Zhang, S. P. Palii, J. R. Eyler, A. Brajter-Toth, *Anal. Chem.* 74 (2002) 1097.
- [10] G. Diehl, U. Karst, *Anal. Bioanal. Chem.* 373 (2002) 390.
- [11] G. J. Van Berkel, J. M. E. Quirke, R. A. Tigani, A. S. Dilley, T. R. Covey, *Anal. Chem.* 70 (1998) 1544.
- [12] G. J. Van Berkel, K. G. Asano, *Anal. Chem.* 66 (1994) 2096.
- [13] H. Moriwaki, *Analyst* 125 (2000) 417.
- [14] F. Zhou, G. J. Van Berkel, *Anal. Chem.* 67 (1995) 3643.
- [15] M. Regino, C. Weston, A. Brajter-Toth, *Anal. Chim. Acta* 369 (1998) 253.
- [16] G. J. Van Berkel in: R. B. Cole (ed) *Electrospray Ionization Mass Spectrometry*, Wiley, New York (1997) 65.
- [17] K. J. Volk, R. A. Yost, A. Brajter-Toth, *Anal. Chem.* 64 (1992) 21A.
- [18] T. Zhang, A. Brajter-Toth, *Anal. Chem.* 72 (2000) 2533.
- [19] G. Diehl, A. Liesener, U. Karst, *Analyst* 126 (2001) 228.
- [20] L. S. Marcoux, J. M. Fritsch, R. N. Adams, *J. Am. Chem. Soc.* 89 (1967) 5766.

- [21] L. Jeftić, R. N. Adams, *J. Am. Chem. Soc.* 92 (1970) 1332.
- [22] D. L. Poster, L. C. Sander, S. A. Wise in: A.H. Neilson (ed) *PAHs and Related Compounds: Chemistry*. Springer, Berlin Heidelberg (1998) 77.
- [23] T. Letzel, E. Rosenberg, R. Wissiack, M. Grasserbauer, R. Niessner, *J. Chromatogr. A* 855 (1999) 501.
- [24] T. Letzel, U. Pöschl, R. Wissiack, E. Rosenberg, M. Grasserbauer, R. Niessner, *Anal. Chem.* 73 (2001) 1634.
- [25] T. Letzel, U. Pöschl, E. Rosenberg, M. Grasserbauer, R. Niessner, *Rapid Commun. Mass Spectrom.* 13 (1999) 2456.



## **Chapter 5**

### **LC/Electron Capture APCI-MS for the Determination of Nitroaromatic Compounds**

## 5.1 Introduction

In recent years, the coupling of high-performance liquid chromatography (HPLC) to mass spectrometry (MS) using electrospray ionization (ESI) and atmospheric pressure chemical ionization (APCI) has turned out to be a versatile tool for the analysis of environmental and biological samples [1-5]. Although other ionization principles have been introduced only recently, e.g., atmospheric pressure photoionization (APPI) by Bruins and co-workers [6], the most commonly used interfaces in HPLC/MS are ESI and APCI. For both techniques, ionization of the analytes is mostly based on protonation (in the positive ion mode) and deprotonation (in the negative ion mode). In contrast to gas chromatography (GC), where ionization by means of electron capture mechanisms is frequently used for the mass spectrometric detection of, e.g., halogenated analytes [7-9], only few examples for electron capture ionization in conjunction with HPLC/MS have been reported yet [10]. A pioneering paper of Blair et al. described that the pentafluorobenzyl (PFB) derivatives of some biomolecules and drug substances undergo a dissociative electron capture when being determined by means of HPLC/APCI(-)-MS [11]. It could be shown that the PFB derivatives yielded  $[M-PFB]^-$  anions through the loss of a PFB radical. Within the APCI interface, low-energy (thermal) electrons are generated, which are able to interact with compounds that comprise electron-attracting moieties. Provided that the latter are present, negative ions may either be formed by resonance capture (reaction 1) or dissociative capture (reaction 2).



In a preliminary study, Karst and co-workers have recently published a paper on dissociative and non-dissociative electron capture observed during the APCI(-)-MS determination of several nitroaromatic compounds [12]. Depending on the structural backbone of the analytes, either deprotonation or electron capture - dissociative as well as non-dissociative - has been observed. Ionization based on deprotonation turned out to be preferred to electron capture ionization in all those cases where the compounds of interest possessed an acidic hydrogen atom [13,14]. However, predictions regarding the occurrence of either non-dissociative or dissociative electron capture could not be made. In the following, further examples for non-dissociative electron capture in the field of HPLC/APCI(-)-MS have been published. Higashi et al. reported non-dissociative electron capture for steroids that had been derivatized by means of different dihydroxyborane and hydrazine reagents [15-17].

Owing to their advantageous spectroscopic properties, derivatization reagents that are based on the 2,1,3-benzoxadiazole backbone have gained significant importance both for the analysis of environmental and biological samples [18,19]. Subsequent to liquid chromatographic separation of the reagents and the respective derivatives, detection is mostly performed by means of UV-vis or fluorescence spectroscopy. Within the group of benzoxadiazole reagents, especially 4-nitro-2,1,3-benzoxadiazoles (NBD) find widespread use in analytical chemistry [20-25].

NBD-based derivatizing agents have been applied to, e.g., the determination of carbonyl compounds in air [20,21], the quantification of amines [22,23] or the workplace monitoring of isocyanates [24,25]. Due to the electron-attracting nitro group and oxadiazole ring, NBD reagents and derivatives are also prone to be

detected by means of electron capture APCI(-)-MS. Mainly dissociative electron capture was reported for the carbonyl derivatives of MNBDH, while either deprotonation or non-dissociative electron capture were observed for the amine derivatives of NBDCI [12]. However, no detailed studies on the parameters significantly influencing the occurrence of electron capture ionization in conjunction with LC/MS have been published yet.

The first part of this chapter deals with the first observations of electron capture ionization in conjunction with LC/APCI(-)-MS. On the basis hereof, a first screening of organic compounds, which may be prone to undergo electron capture within the APCI interface has been performed. Analytes comprised the amine derivatives of 4-chloro-7-nitro-2,1,3-benzoxadiazole (NBDCI), *N*-methyl-2,4-dinitrophenylhydrazine (MDNPH) and *N*-methyl-7-hydrazino-4-nitro-2,1,3-benzoxadiazole (MNBDH) as well as Sanger's reagent (2,4-dinitrofluorobenzene), 2,4-dinitrophenylazide and several nitromusk compounds.

In the second part a thorough investigation with respect to instrumental and solvent parameters influencing the electron capture ionization is presented for NBDCI and its amine derivatives as well as for 4-nitro-7-piperazino-2,1,3-benzoxadiazole (NBDPZ) and its mono- and diisocyanate ureas [23,24]. The parameters favoring electron capture mechanisms have been studied thoroughly under consideration of the competing deprotonation mechanism. Thus, a better understanding of the electron capture process is to be obtained in order to improve the selectivity and sensitivity of the analysis.

### **5.3 First Observations of Electron Capture Phenomena in Conjunction with HPLC/APCI(-)-MS\***

#### **5.2.1 Abstract**

The determination of selected nitroaromatic compounds in liquid chromatography/mass spectrometry with electron capture ionization using a commercial atmospheric pressure chemical ionization (APCI) interface in the negative ion mode is described. The electron capture effect is observed for nitroaromatics which do not easily undergo deprotonation under these conditions. Depending on the structure of the analytes, either dissociative or non-dissociative electron capture is observed. Limits of detection and linear range for the determination of the analytes match those obtained for nitroaromatics which undergo deprotonation. The investigated substances comprise numerous substituted nitrobenzenes and nitrobenzoxadiazoles.

*\*H. Hayen, N. Jachmann, M. Vogel, U. Karst, Analyst 127 (2002) 1027.*

## 5.2.2 Experimental

### *Chemicals*

Solvents for LC were acetonitrile (elution grade) and methanol (elution grade) from Merck eurolab (Fontenau S/Bois, France). Water for liquid chromatography was from Merck eurolab (Briare le Canal, France). Nitromusks were obtained from Promochem (Wesel, Germany) in the highest purity available. 2,4-Dinitrofluorobenzene, m-dinitrobenzene and 4-chloro-7-nitro-2,1,3-benzoxadiazole (NBDCI) were purchased from Aldrich Chemie (Steinheim, Germany). MDNPH [26], MNBDH [20] and the respective hydrazones [26,20], 2,4-dinitrophenylazide [27], and the amine derivatives of NBDCI [23] were synthesized according to literature studies.

### *LC/MS instrumentation*

The LC/MS system was from Shimadzu (Duisburg, Germany) and consisted of a SCL-10Avp controller unit, a DGU-14A degasser, two LC-10ADvp pumps, a SUS mixing chamber (0.5 ml volume), a SIL-10A autosampler, a SPD-10AV UV/vis detector, a LCMS QP8000 single quadrupole mass spectrometer with atmospheric pressure chemical ionization and electrospray ionization probes and Class 8000 Version 1.20 software.

### *LC conditions*

For the LC separation of the different classes of compounds, the following columns were used:

*Column A:* LiChrospher RP-18 ec (Macherey-Nagel, Düren, Germany), 5  $\mu\text{m}$  particle size, 100 Å pore size, 3.0 mm id, 250 mm length; guard column of the same material: 3.0 mm id, 20 mm length.

Column B: Discovery C18 (Supelco, Deisenhofen, Germany), 5 µm particle size, 100 Å pore size, 3.0 mm id, 150 mm length; guard column of the same material: 3.0 mm id, 20 mm length.

For the liquid chromatographic separation of nitromusks, 2,4-dinitrofluorobenzene, m-dinitrobenzene and NBDCl, the following binary gradient consisting of acetonitrile and water with a flow rate of 0.62 mL/min was used:

t (min)	0	1	8	10	11	14
c (CH <sub>3</sub> CN) (%)	50	50	100	100	50	stop

Separation was performed on column A and the injection volume was set to 10 µL.

For the separation of MDNPhydrazones and MNBDhydrazones, the following gradient consisting of methanol and water with a flow rate of 0.6 mL/min was used:

t (min)	0	0.5	10	12	13	15
c (CH <sub>3</sub> CN) (%)	40	40	100	100	40	stop

Separation was performed on column B and the injection volume was set to 10 µL.

For the separation of NBDamine derivatives, the following gradient consisting of methanol and water with a flow rate of 0.6 mL/min was used:

t (min)	0	0.5	30	32	35	36	40
c (CH <sub>3</sub> CN) (%)	35	35	70	100	100	35	stop

Separation was performed on column B and the injection volume was set to 10 µL.

DNPA was determined on column A using a binary gradient which consisted of acetonitrile and water. The flow rate was set to 0.62 mL/min:

t (min)	0	1	6.5	8	11.5	14.5	19.5
c (CH <sub>3</sub> CN) (%)	49	49	65	80	80	49	stop

The injection volume was 10  $\mu$ L.

### MS conditions

The instrumental parameters used for mass spectrometric detection of different compounds are summarized in Table 5.1. The nebulizer gas-flow rate for all measurements was set to 2.5 L/min.

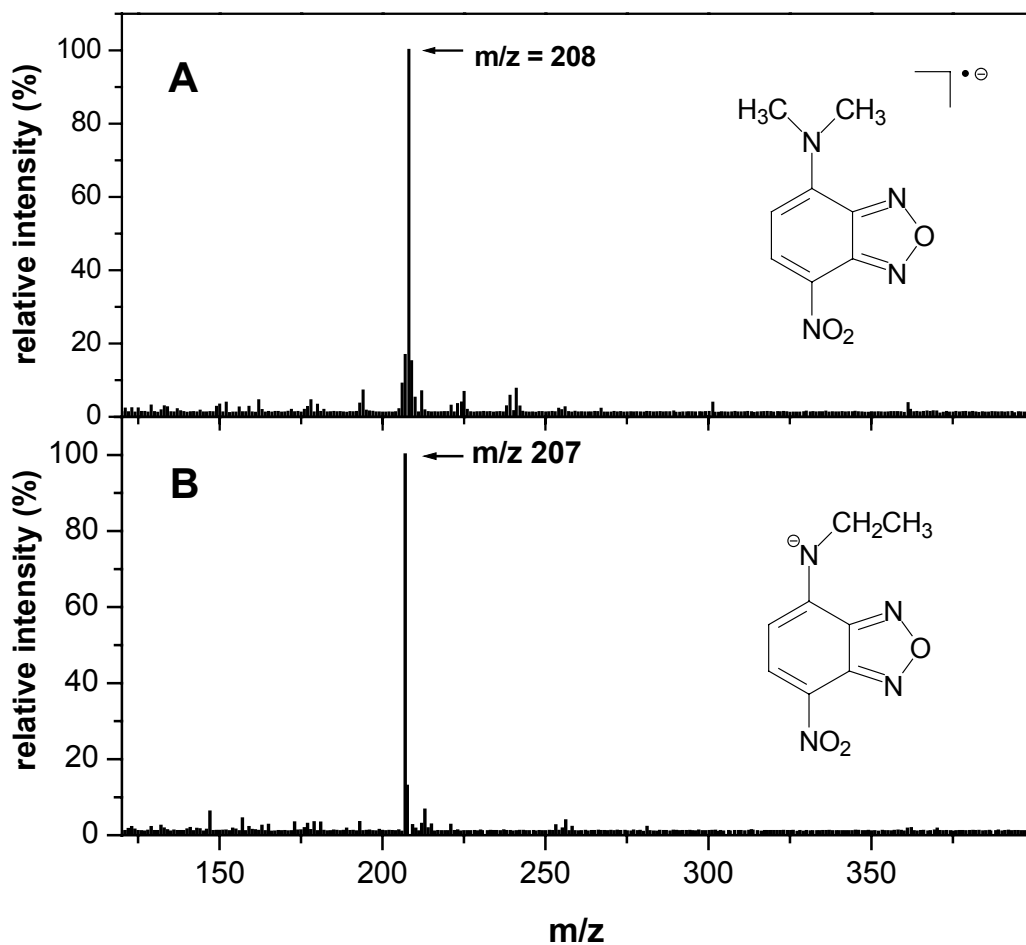
**Table 5.1:** Mass spectrometric parameters applied for the detection of different classes of analytes.

	CDL Voltage [V]	CDL Temp. [°C]	Deflector Voltages [kV]	Detector Voltage [V]	Probe Voltage [kV]	Probe Temp. [°C]
NBDamine Derivatives	30	300	-30	1.7	-2.6	450
MNBDhydrazones	0	300	-40	1.7	-4.5	400
MDNPhydrazones	0	300	-40	1.7	-4.5	400
m-dinitrobenzene (DNPA)	-20	250	-35	1.7	-3.0	300
Sanger's reagent (2,4-dinitrofluorobenzene)	5	300	0	1.7	-2.3	450
Nitromusks	5	300	0	1.7	-2.3	450



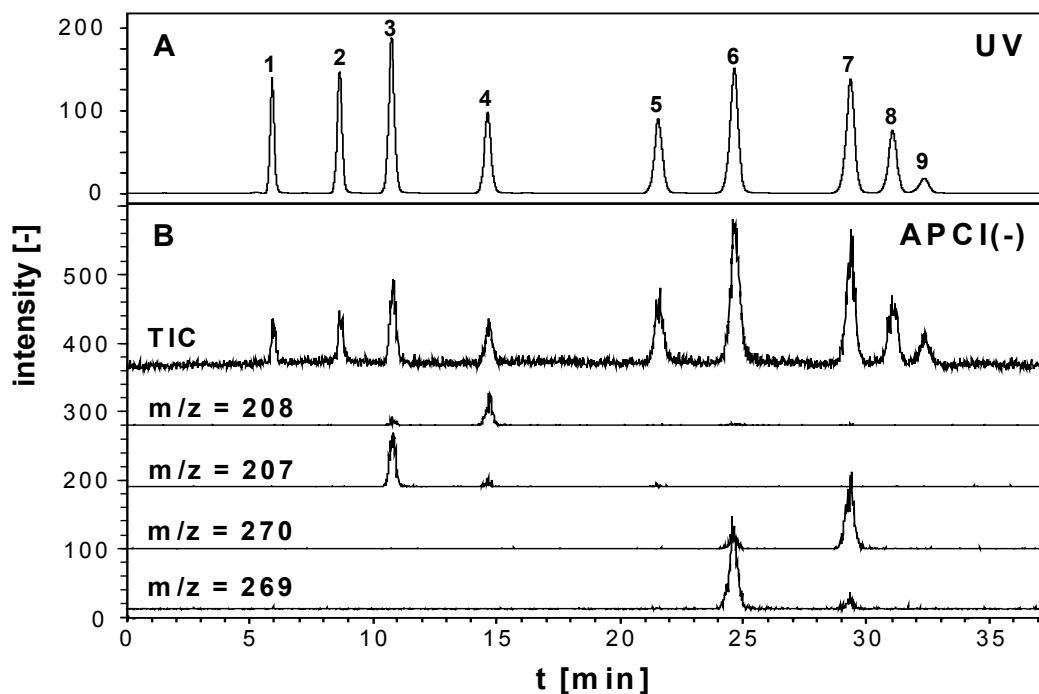
### 5.2.3 Results and Discussion

Figure 5.1A shows the APCI(-) mass spectrum of the dimethyl amine (DMA) derivative of 4-chloro-7-nitro-2,1,3-benzoxadiazole (NBDCI), NBDDMA. The observed base peak with  $m/z = 208$  corresponds to the molecular radical anion  $[M]^{-\bullet}$  the formation of which can only be explained on the basis of a non-dissociative electron capture process. The electron capture occurs owing to the strongly electron-attracting nitro function and the benzoxadiazole backbone.



**Figure 5.1:** APCI(-) mass spectra of the 4-chloro-7-nitro-2,1,3-benzoxadiazole (NBDCI) derivatives of dimethylamine (A) and ethylamine (B). While non-dissociative electron capture is observed in (A), deprotonation occurs in (B).

Comparing the ionization of the ethylamine (EA) derivative of NBDCI, NBDEA, with that of NBDDMA obtained under the same conditions which is presented in Figure 5.1B, no electron capture but deprotonation is observed, thus yielding the  $[M-H]^-$  ion. This is due to the fact that, in contrast to NBDDMA, NBDEA contains an acidic  $\alpha$ -hydrogen. This difference in ionization mechanisms was used for the identification of NBDDMA and NBDEA after liquid chromatographic separation. Figure 5.2 presents the liquid chromatographic separation of several NBD amine derivatives with subsequent photometric detection at 460 nm and mass spectrometric detection.



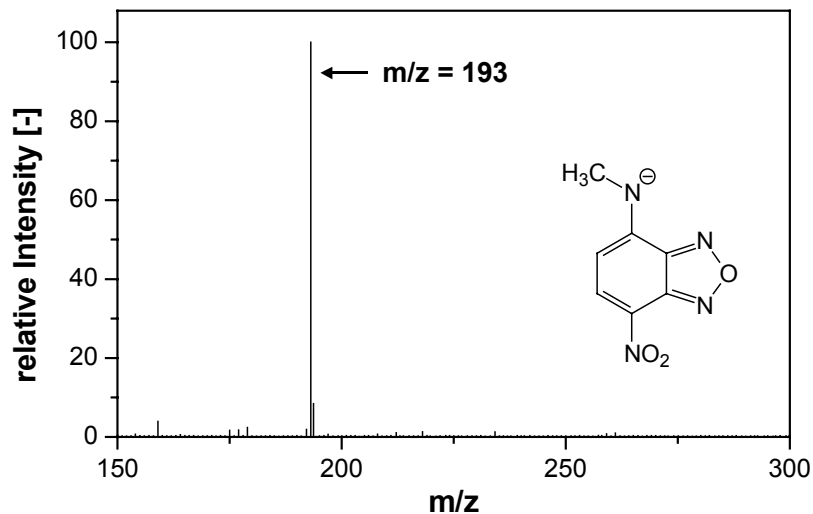
**Figure 5.2:** Liquid chromatographic separation of 9 NBD amine derivatives. A: UV-Vis chromatogram ( $\lambda = 460$  nm). Peaks: (1) ammonia (A); (2) methylamine (MA); (3) ethylamine (EA); (4) dimethyl amine (DMA); (5) diethyl amine (DEA); (6) benzylamine (BzA); (7) N-methyl aniline (NMA); (8) dipropyl amine (DPA); (9) ethylanilin (EAn)-derivative of NBDCI. B: Total ion current (TIC,  $m/z = 120 - 500$ ) and the extracted mass traces for NBDDMA ( $m/z = 208$ ), NBDEA ( $m/z = 207$ ), NBDNMA ( $m/z = 270$ ) and NBDBzA ( $m/z = 269$ ).

Both the dimethylamine and the ethylamine derivative have the same molecular mass of 208 g/mol. Based on the different ionization processes applying APCI(-), the extracted mass traces of  $m/z = 208$  (electron capture) and  $m/z = 207$  (deprotonation) allow to elucidate the identity of the respective peaks apart from simple retention time comparison. It is obvious from the small signal at  $m/z = 207$  for NBDDMA that even in this case, some deprotonation is observed, which is, however, negligible compared with the peak of  $m/z = 208$ . For NBDEA, the small peak at  $m/z = 208$  represents the natural abundance of the  $^{13}\text{C}$  isotope.

With respect to the aromatic primary amine derivative (NBDBzA), similar effects as for NBDEA were observed. Again, deprotonation in the interface led to the formation of the  $[\text{M}-\text{H}]^-$  ion with an  $m/z = 269$ , while the  $m/z = 270$  corresponds to the  $^{13}\text{C}$  satellite. The ionization of the secondary amine derivative (NBDNMA<sub>n</sub>) showed main MS signals based on non-dissociative electron capture, thus yielding  $[\text{M}]^-$  with an  $m/z = 270$ .

The assumption that the NBD backbone is responsible for the electron capture processes observed could be verified by investigating NBDCI ( $M = 199$  g/mol) in the APCI(-) mode. Again, the base peak in the respective mass spectrum resulted from the radical anion ( $m/z = 199$ ).

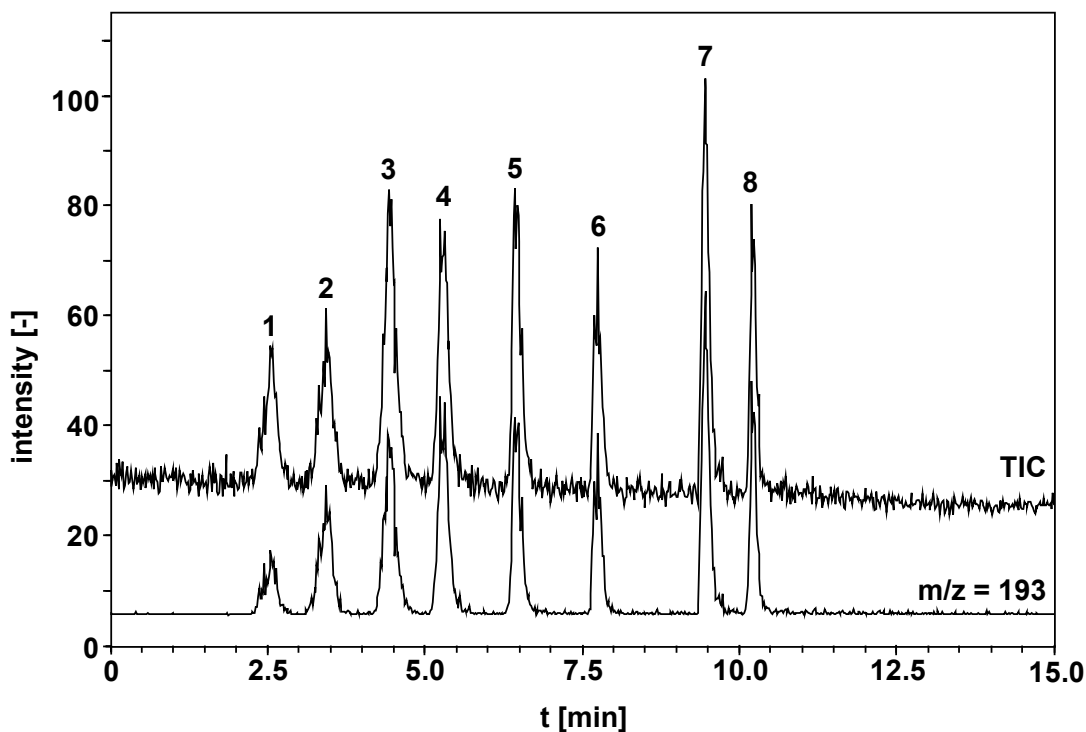
When ionizing the hydrazones of *N*-methyl-7-hydrazino-4-nitro-2,1,3-benzooxadiazole (MNBDH), mainly dissociative electron capture is observed. The respective mass spectrum of the formaldehyde-MNBDH derivative is depicted in Figure 5.3.



**Figure 5.3:** APCI(-) mass spectrum of the formaldehyde derivative of MNBDH with a base peak of  $m/z = 193$  resulting from dissociative electron capture. The applied needle voltage was -2.6 kV.

Although the signal at  $m/z = 193$  is the base peak in the mass spectrum, deprotonation as a competitive reaction leading to the formation of  $[M-H]^-$  can also be detected.

A liquid chromatographic separation of *N*-methyl-7-hydrazino-4-nitro-2,1,3-benzoxadiazole (MNBDH), *N*-methyl-7-hydrazino-4-amino-2,1,3-benzoxadiazole (MNBDA) and some MNBD-derivatives applying APCI(-)-MS detection is presented in Figure 5.4.



**Figure 5.4:** Liquid chromatographic separation of *N*-methyl-7-hydrazino-4-nitro-2,1,3-benzoxadiazole (MNBDH), *N*-methyl-7-hydrazino-4-amino-2,1,3-benzoxadiazole (MNBDH) and 6 MNBD-derivatives with mass spectrometric detection. The TIC ( $m/z = 100 - 500$ ) and the extracted mass trace of  $m/z = 193$  are presented. Peaks: (1) *N*-methyl-7-hydrazino-4-nitro-2,1,3-benzoxadiazole (MNBDH); (2) *N*-methyl-7-hydrazino-4-amino-2,1,3-benzoxadiazole (MNBDH); (3) acetone (MNBD-Ac); (4) formaldehyde (MNBD-FA); (5) acetaldehyde (MNBD-AA); (6) acrolein (MNBD-Acr); (7) benzaldehyde (MNBD-BA); (8) *p*-tolaldehyde (MNBD-TA)-derivative of MNBDH.

A comparison of the TIC and the extracted mass trace of  $m/z = 193$  shows that the ionization of MNBDH derivatives (peaks 3 – 8) is mainly characterized by dissociative electron capture yielding fragments of  $m/z = 193$ . In contrast to MNBD-hydrazones, MNBDH ( $M = 209$  g/mol) possesses an acidic  $\alpha$ -hydrogen at the hydrazine function. Both deprotonation ( $m/z = 208$ ) and dissociative electron capture ( $m/z = 193$ ) are observed with almost equal signal intensities. Owing to the amino

function, MNBDA ( $M = 194$  g/mol) is easy to deprotonate. Thus, hydrogen abstraction yielding the  $[M-H]^-$  pseudo molecular ion with  $m/z = 193$  is the main ionization mechanism.

Analytical figures of merit for a series of MNBDH, MNBDA and some MNBD-derivatives are summarized in Table 5.2.

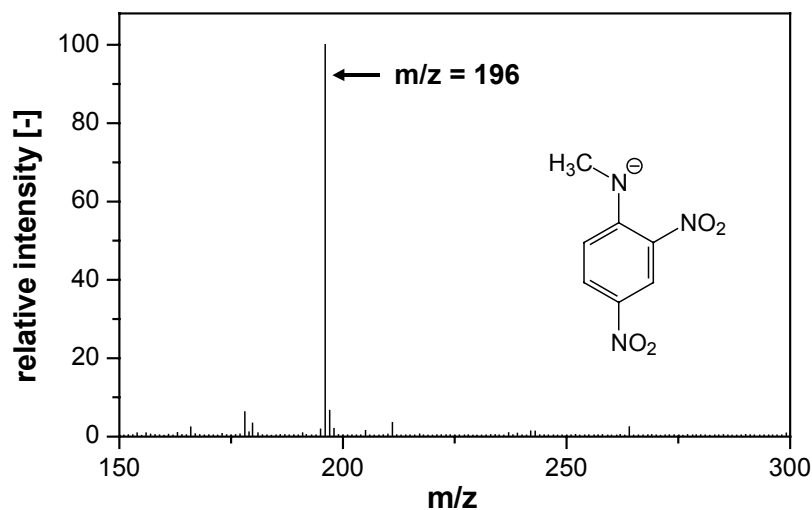
**Table 5.2:** Analytical figures of merit for the APCI(-) determination of MNBDH, MNBDA and six carbonyl derivatives of MNBDH

abbreviation	M [Da]	detected m/z	LOD [nmol/L]	LOQ [nmol/L]	RSD (n=3)			R <sup>2</sup>
					$5 \times 10^{-7}$ mol/L	$5 \times 10^{-6}$ mol/L	$5 \times 10^{-5}$ mol/L	
MNBDH	209	193	80	260	5.5	1.6	1.8	0.9996
MNBDA	194	193	40	200	2.5	3.0	1.2	0.9984
MNBD-Ac	249	193	40	130	3.7	2.0	0.6	0.9984
MNBD-FA	221	193	20	70	3.5	2.8	3.3	0.9990
MNBD-AA	235	193	10	70	2.8	4.2	1.6	0.9997
MNBD-Acr	247	193	10	30	3.1	2.3	2.5	0.9995
MNBDH-BA	297	193	10	30	3.2	2.2	2.5	0.9988
MNBDH-TA	311	193	40	130	6.3	4.3	3.6	0.9970

As discussed, all MNBDH derivatives undergo dissociative electron capture in the APCI interface yielding the fragment with  $m/z = 193$ . APCI(-) detection results in instrumental limits of detection (LOD) ranging from 10 nmol/L to 40 nmol/L. The LOD obtained for the MNBDA by means of deprotonation is as sensitive as the electron capture mechanism (40 nmol/L). In contrast to the latter, the ionization of MNBDH is characterized by both deprotonation and electron capture. Thus, a higher LOD (80 nmol/L) is achieved.

The linear ranges extend from the limit of quantification up to  $1 \times 10^{-4}$  mol/L for all derivatives. Thus, APCI(-) has turned out to be a selective and sensitive tool for the determination of MNBDH derivatives. Relative standard deviations (RSD) are given for three different concentrations. Increasing with decreasing concentrations, values range from ~ 1% to ~ 6%.

A further proof for the fact that organic nitro compounds easily undergo an electron capture mechanism during the APCI(-) process is provided with the investigation of N-methyl-2,4-dinitrophenylhydrazine derivatives (MDNPhydrazones). Similar to the MNBDhydrazones, dissociative electron capture is observed as presented in Figure 5.5.

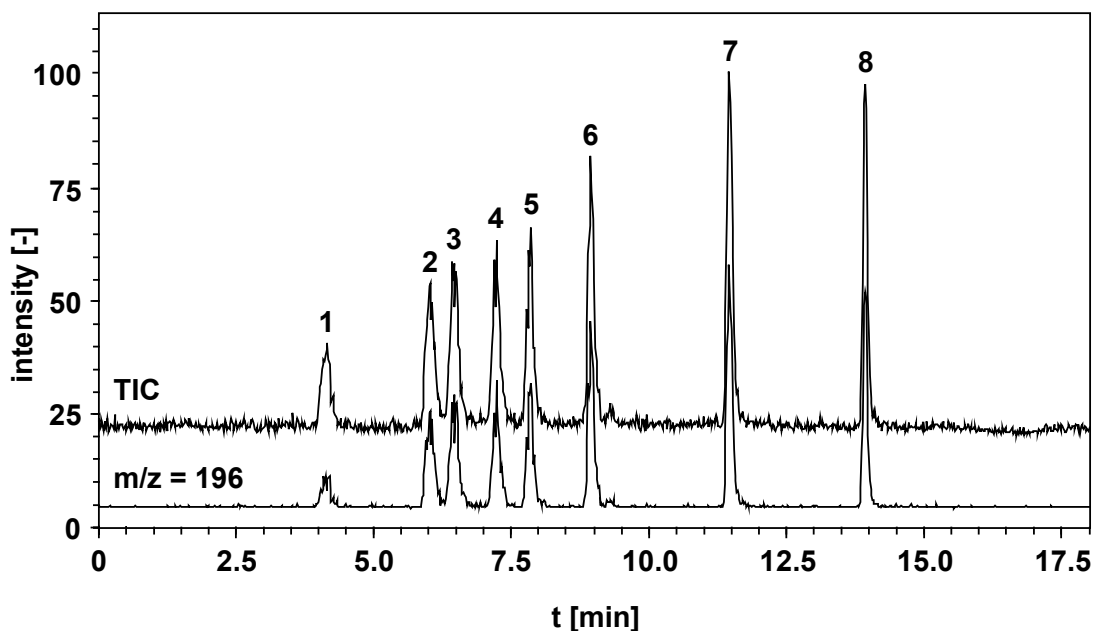


**Figure 5.5:** APCI(-) mass spectrum of the formaldehyde derivative of MDNPH (MDNPF) with a base peak of  $m/z = 196$  resulting from dissociative electron capture. The applied needle voltage was -2.6 kV.

In a first step, radical anions of the respective hydrazones are formed. This is immediately followed by a cleavage of the N-N bond, thus finally yielding anions with

$m/z = 196$ . Similar to the MNBDH derivatives, MDNPhydrazones show signals from deprotonation.

A liquid chromatographic separation of MDNPH, N-methyl-2,4-dinitroaniline (MDNA) and some MDNPhydrazones applying APCI(-)-MS detection is presented in Figure 5.6.



**Figure 5.6:** Liquid chromatographic separation of N-methyl-2,4-dinitrophenylhydrazine (MDNPH), N-methyl-2,4-dinitroaniline (MDNA) and 6 MDNPhydrazones with mass spectrometric detection. The TIC ( $m/z = 100 - 500$ ) and the extracted mass trace of  $m/z = 196$  are presented. Peaks: (1) N-methyl-2,4-dinitrophenylhydrazine (MDNPH), (2) N-methyl-2,4-dinitroaniline (MDNA); (3) formaldehyde (MDNP-FA); (4) acetone (MDNP-Ac); (5) acetaldehyde (MDNP-AA); (6) acrolein (MDNP-Acr); (7) p-tolulaldehyde (MDNP-TA); (8) decanal (MDNP-Dec) derivative of MDNPH.



Analytical figures of merit for a series of MDNPH, MDNA and some MDNP-derivatives are summarized in Table 5.3.

**Table 5.3:** Analytical figures of merit for the APCI(-) determination of MDNPH, MDNA and six carbonyle derivatives of MDNPH

abbreviation	M [Da]	detected m/z	LOD [nmol/L]	LOQ [nmol/L]	RSD (n=3)			R <sup>2</sup>
					5 x 10 <sup>-7</sup> mol/L	5 x 10 <sup>-6</sup> mol/L	5 x 10 <sup>-5</sup> mol/L	
MDNPH	212	196	50	170	2.0	1.8	1.5	0.9997
MDNA	197	196	20	70	3.3	1.0	1.6	0.9996
MDNP-FA	224	196	20	70	4.4	2.4	1.7	0.9998
MDNP-Ac	252	196	20	70	1.6	2.8	1.1	0.9996
MDNP-AA	238	196	20	70	2.3	3.7	1.7	0.9996
MDNP-Acr	250	196	20	70	2.7	4.1	1.2	0.9995
MNBD-TA	314	196	10	30	4.4	1.6	1.8	0.9996
MNBD-Dec	350	196	10	30	5.2	2.1	2.5	0.9990

Analogue to MNBDhydrazones, all derivative of MDNPH undergo dissociative electron capture in the APCI interface yielding the fragment with m/z = 196. APCI(-) detection results in instrumental limits of detection (LOD) ranging from 10 nmol/L to 20 nmol/L. The LOD obtained for MDNA by means of deprotonation is as sensitive as the electron capture mechanism (20 nmol/L). Due to ionization by both deprotonation and electron capture the LOD for the determination of MNBDH is higher (50 nmol/L) compared to its derivatives.

The linear ranges extend from the limit of quantification up to  $1 \times 10^{-4}$  mol/L for all derivatives. Relative standard deviations (RSD) are increasing with decreasing concentrations. The values range from ~ 1% to ~ 5%.

The results regarding the investigation of m-dinitrobenzene, 2,4-dinitrofluorobenzene (Sanger's reagent) and 2,4-dinitrophenylazide (DNPA) are summarized in Table 5.4.

**Table 5.4:** Summary of results for the APCI(-) determination of m-dinitrobenzene, Sanger's reagent (2,4-dinitrofluorobenzene) and 2,4-dinitrophenylazide.

	M [Da]	Base peak	Diss. electron capture	Non-diss. electron capture
m-Dinitrobenzene	168	m/z = 168	-	+
Sanger's Reagent	186	m/z = 186	[M-NO] <sup>-</sup>	+
DNPA	209	m/z = 181	[M-N <sub>2</sub> ] <sup>-</sup>	-

While atmospheric pressure chemical ionization in the negative ion mode for m-dinitrobenzene (M = 168 g/mol) shows a pure non-dissociative electron capture (base peak m/z = 168), Sanger's reagent exhibits both dissociative (loss of NO) and non-dissociative electron capture (m/z = 186) while DNPA only yields m/z = 181 which is in accordance with a dissociative electron capture process [M-N<sub>2</sub>]<sup>-</sup>.

With respect to the APCI(-) determination of the three nitromusk compounds, the base peaks in the respective mass spectra result from a dissociative electron capture. While musk ketone and musk moskene predominantly yield the [M-NO]<sup>-</sup>

ions, the most intense signal for musk ambrette is caused by the  $[M-CH_3]^+$  ion. Although for all three analytes signals of the deprotonated species are detected, the latter may be neglected when compared to the dissociative electron capture peaks.

Additionally, all analytes described were also investigated by means of electrospray ionization in the negative ion mode. Only very weak signals were observed for deprotonation, and, in no case, electron capture occurred. This is in good accordance with the assumption that the corona discharge is a source of low-energy electrons which are inevitable for an ionization mechanism on the basis of electron capture. These low-energy electrons are not generated within the ESI interface unit.

#### **5.2.4 Conclusions**

The electron capture mechanism significantly broadens the applicability of APCI-MS to nitroaromatic compounds of low polarity which do not contain acidic hydrogen atoms. Deprotonation and electron capture are competitive mechanisms, and deprotonation will be predominantly observed when acidic hydrogen atoms are present.

## **5.4 Investigations on the Electron Capture Effects during LC/APCI(-)-MS Determination of Nitrobenzoxadiazole Derivatives\***

### **5.3.1 Abstract**

Nitrobenzoxadiazole (NBD) derivatives are determined with limits of detection ranging down to 20 nmol/L using liquid chromatography/mass spectrometry (LC/MS) with electron capture ionization. An atmospheric pressure chemical ionization (APCI) interface operated in the negative ion mode is used as ionization source. Amine derivatives of 4-chloro-7-nitro-2,1,3-benzoxadiazole (NBDCI) as well as the isocyanate derivatives of 4-nitro-7-piperazino-2,1,3-benzoxadiazole (NBDPZ) have been analyzed using this technique. The parameters favoring electron capture mechanisms have been thoroughly investigated under consideration of the competing mechanism of deprotonation to allow a better understanding of the electron capture process and to improve selectivity of the analysis.

*\*H. Hayen, N. Jachmann, M. Vogel, U. Karst, Analyst, submitted for publication*

### **5.3.2 Experimental**

#### *Chemicals*

Solvents for LC were acetonitrile (elution grade) and methanol (elution grade) from Merck eurolab (Fontenau S/Bois, France). Water for liquid chromatography was from Merck eurolab (Briare le Canal, France). The amine derivatives of 4-chloro-7-nitro-2,1,3-benzoxadiazole (NBDCI) [23] and the isocyanate derivatives of 4-nitro-7-piperazino-2,1,3-benzoxadiazole (NBDPZ) [24] were synthesized according to literature studies. Nitrogen gas used for LC-MS analyses was grade 3.0.

#### *LC/MS instrumentation*

The LC/MS system was from Shimadzu (Duisburg, Germany) and consisted of a SCL-10Avp controller unit, a DGU-14A degasser, two LC-10ADvp pumps, a SUS mixing chamber (0.5 mL volume), a SIL-10A autosampler, a SPD-10AV UV/Vis detector, a LCMS QP8000 single quadrupole mass spectrometer with atmospheric pressure chemical ionization and electrospray ionization probes and Class 8000 Version 1.20 software.

#### *LC conditions*

As stationary phases, base deactivated Discovery<sup>®</sup> RP-18 columns from Supelco (Deisenhofen, Germany) were used. Column dimensions were 150 mm x 3.0 mm for LC/APCI-MS experiments and 150 mm x 2.1 mm for LC/ESI-MS experiments. Particle size was 5  $\mu\text{m}$  and pore size 100 Å for both columns. Flow rates of the mobile phase were 0.6 mL/min for the 3.0 mm id column and 0.3 mL/min for the 2.1 mm id column.

For the separation of NBD amine derivatives, the following gradient consisting of methanol and water was used:

t (min)	0	0.5	7	11	13	14	18
c (MeOH) (%)	35	35	50	100	100	35	stop

For the separation of NBDPZ isocyanate derivatives, the following gradient consisting of methanol and water was used:

t (min)	0	0.5	38	39	41	42	45
c (MeOH) (%)	55	55	85	100	100	55	stop

The injection volume was set to 10  $\mu\text{L}$  for LC/APCI-MS and 5  $\mu\text{L}$  for LC/ESI-MS experiments.

#### *MS conditions*

The optimized conditions for the APCI(-) measurements were the following: Probe voltage  $-2.6$  kV, curved desolvation line (CDL) voltage 10 V, CDL temperature 300  $^{\circ}\text{C}$ , deflector voltages  $-35$  V and detector voltage 1.6 kV, nebulizer gas flow rate 2.5 L/min and probe temperature 450  $^{\circ}\text{C}$  for the determination of NBD amine derivatives and 500  $^{\circ}\text{C}$  for NBDPZ isocyanate derivatives.

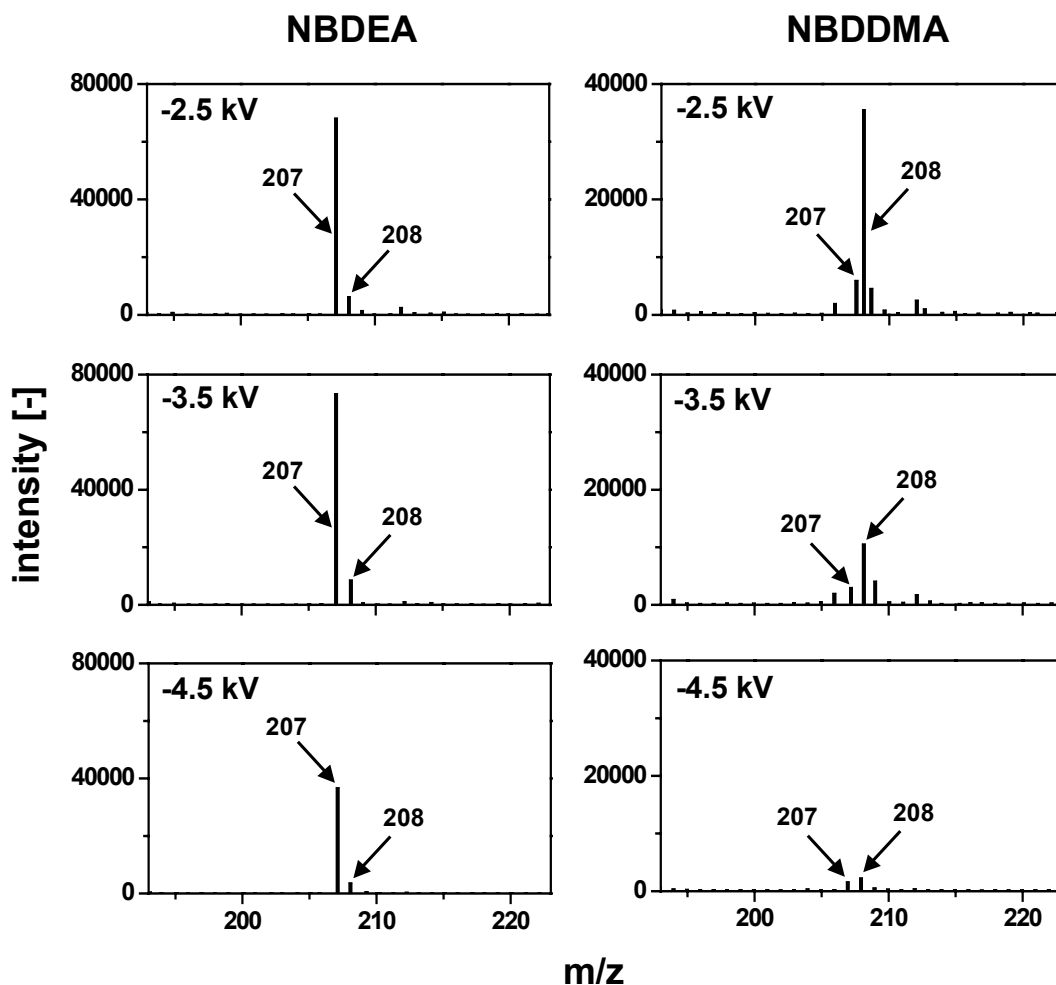
#### *Investigation of solvent influences*

For the investigation of solvent influences on the occurrence of either deprotonation or electron capture ionization, flow-injection analysis was applied. LC/MS instrumentation was as mentioned above. Regarding MS conditions, the optimized conditions for APCI(-) measurements as mentioned above were applied. The

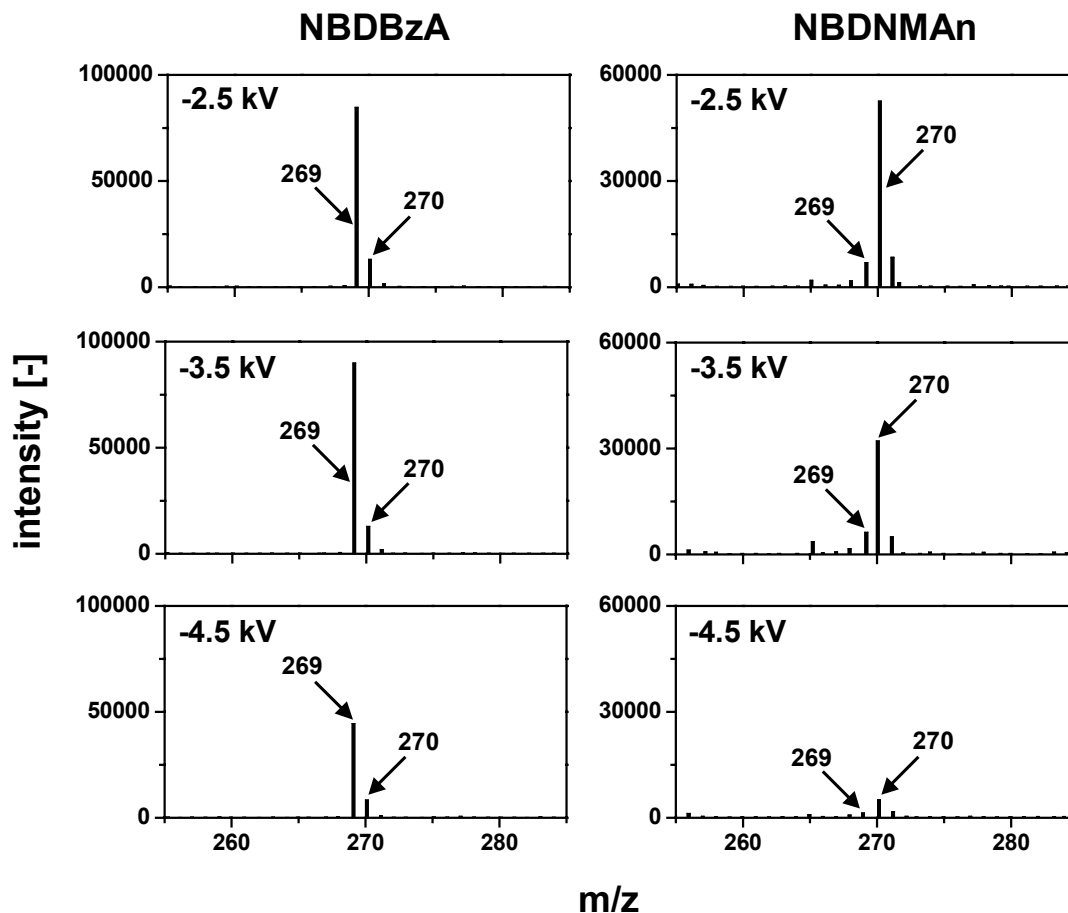
injection volume was adjusted to 5  $\mu$ L. The flow rate of the eluent was 0.4 mL/min. Eluents were methanol, acetonitrile, methanol/acetonitrile (50:50; v/v) or methanol/water (50:50; v/v).

### 5.3.3 Results and Discussion

Applying a negative needle voltage, atmospheric pressure chemical ionization of primary and secondary amine derivatives of NBDCI results in different ionization mechanisms. In contrast to secondary amine analytes, which mainly yield  $[M]^+$  ions based on non-dissociative electron capture, mass spectra of the primary amine compounds are characterized by signals based on deprotonation, thus yielding  $[M-H]^-$  ions as described in preliminary investigations [12]. The influence of probe voltage on the ionization of different NBDCI derivatives is shown in Figure 5.7.







**Figure 5.7:** The influence of probe voltage on the occurrence of electron capture (EC) ionization vs. deprotonation for a series of NBDCI derivatives. The instrumental parameters for liquid chromatography as well as for MS detection are given in the Experimental section. NBDEA: ethyl amine; NBDDMA: dimethyl amine; NBDBzA: benzyl amine; NBDNMA: *N*-methyl aniline derivative of NBDCI.

Subsequent to liquid chromatographic separation on an ODS-modified reversed-phase column using a binary methanol/water gradient (see Experimental section), the derivatives of a primary aliphatic amine (ethylamine, EA), a secondary aliphatic amine (dimethylamine, DMA), a primary aromatic amine (benzylamine, BzA) and a secondary aromatic amine (*N*-methylaniline, NMA) were ionized at three different probe voltages. The potential at the needle was adjusted to -2.5 kV, -3.5 kV and -4.5

kV, respectively. The APCI(-)-MS spectrum of NBDEA shows a main signal resulting from the deprotonated species  $[M-H]^-$  with an  $m/z = 207$ . Calculations based on the isotopic ratios have proven that the observed  $m/z = 208$  is related to the  $^{13}C$  satellite. Increasing the probe voltage from -2.5 kV up to -3.5 kV did neither change the intensity nor the ratio of the signals. When adjusting a needle voltage of -4.5 kV, the signal intensities were significantly decreased. This may be owing to the fact that the high potential caused in-source fragmentation, thus leading to a decrease of the intensity of the  $[M-H]^-$  peak. With respect to the aromatic primary amine derivative (NBDBzA), similar effects as for NBDEA were observed. Again, deprotonation in the interface led to the formation of  $[M-H]^-$  ions with an  $m/z = 269$ , while the  $m/z = 270$  corresponds to the  $^{13}C$  satellite.

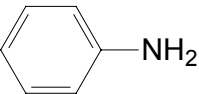
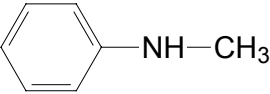
In contrast, both the secondary aliphatic (dimethylamine, DMA) as well as the aromatic (*N*-methyl aniline, NMA<sub>n</sub>) NBD derivative showed main MS signals based on non-dissociative electron capture, thus yielding  $[M]^-$  with an  $m/z = 208$  and 270, respectively. Although both derivatives do not possess acidic hydrogen atoms, deprotonation giving  $m/z = 207$  and  $m/z = 269$  was observed to a smaller extent. Furthermore, the influence of probe voltage on signal intensity was much stronger than for the primary amine derivatives. Decreased signals were already observed at -3.5 kV. At a potential of -4.5 kV, both the signals of NBDDMA and NBDNMA<sub>n</sub> were reduced to a fraction of their initial values at -2.5 kV. This is due to the fact that electron capture is the preferred way of ionization, while deprotonation is hardly possible. However, with increasing probe voltage, thermal electrons generated at the corona discharge needle of the APCI interface will pick up more and more energy. Being beyond a voltage maximum, the electrons of higher energy will - in average -

be too fast to be captured by analyte molecules. With respect to secondary amine derivatives, deprotonation is hardly a competitive ionization mechanism. Thus, signal intensities are distinctly decreasing.

Analytical figures of merit for a series of NBDCI amine derivatives are summarized in Table 5.5. As discussed, all secondary amines undergo electron capture within the APCI interface and the mass-to-charge ratios correspond to the radical anion of the respective analytes. APCI(-) detection results in instrumental limits of detection (LOD) ranging from 20 nmol/L for NBDAn to 50 nmol/L for NBDMA. This is in the same range as for UV-vis detection, where instrumental LOD between 16 nmol/L and 36 nmol/L were determined [23]. Although fluorescence detection for NBDCI amine derivatives giving LOD between 4 nmol/L and 28 nmol/L is more sensitive than MS or UV-vis detection, only aliphatic compounds possess fluorescence characteristics. The linear ranges extend from the limit of quantification up to  $1 \times 10^{-4}$  mol/L for all derivatives. Thus, APCI(-) has proven to be a selective and sensitive tool for the determination of NBDCI amines. Relative standard deviations (RSD) are given for three different concentrations. Increasing with decreasing concentrations, values range from ~ 2% to ~ 8%.

**Table 5.5:** Analytical figures of merit for the APCI(-) determination of nine amine derivatives of NBDCI.

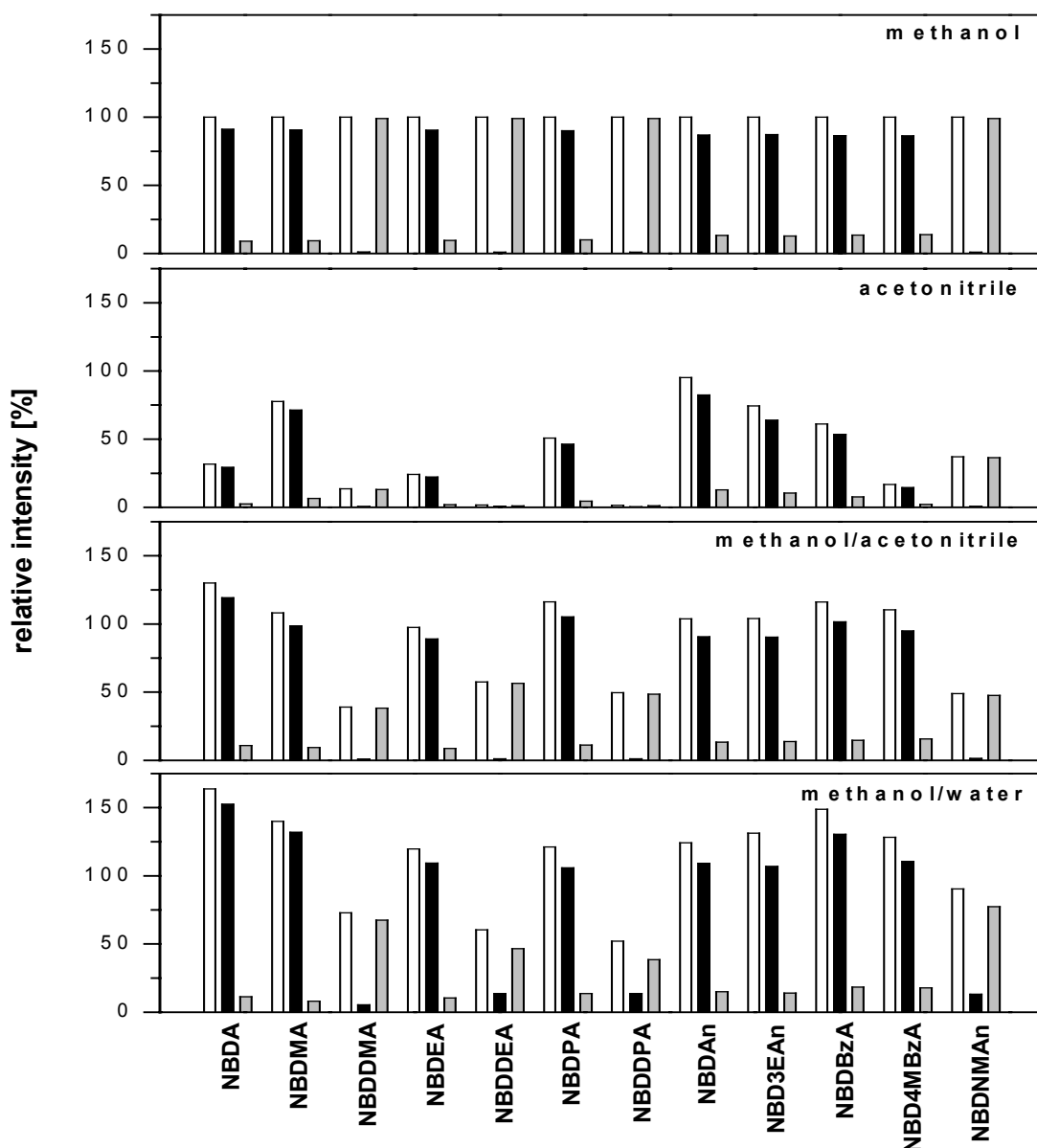
Chapter 5

abbreviation	NBD-Cl derivative of	M [Da]	detected m/z	LOD [nmol/L]	LOQ [nmol/L]	RSD (n=3)			R <sup>2</sup>
						$5 \times 10^{-7}$ mol/L	$5 \times 10^{-6}$ mol/L	$5 \times 10^{-5}$ mol/L	
NBDA	NH <sub>3</sub>	180	179	30	100	6.3	5.2	3.6	0.9990
NBDMA	H <sub>3</sub> C—NH <sub>2</sub>	194	193	50	170	5.0	6.2	3.0	0.9978
NBDDMA	H <sub>3</sub> C—NH—CH <sub>3</sub>	208	208	40	130	6.1	5.9	2.0	0.9980
NBDEA	H <sub>5</sub> C <sub>2</sub> —NH <sub>2</sub>	208	207	30	100	4.8	4.8	3.3	0.9970
NBDPA	H <sub>7</sub> C <sub>3</sub> —NH <sub>2</sub>	222	221	20	70	3.5	3.3	1.8	0.9990
NBDDEA	H <sub>5</sub> C <sub>2</sub> —NH—C <sub>2</sub> H <sub>5</sub>	236	236	30	100	7.6	5.4	5.0	0.9986
NBDDPA	H <sub>7</sub> C <sub>3</sub> —NH—C <sub>3</sub> H <sub>7</sub>	264	264	20	70	2.3	2.6	1.6	0.9976
NBDAn		256	255	20	70	3.9	4.1	3.1	0.9974
NBDNMAAn		270	270	30	100	5.6	4.3	4.0	0.9990

Different deflector voltages and their influence on ionization were investigated. Within the MS system used, the deflectors are to induce fragmentation of the analyte ions. The following deflector voltages were investigated: 0 V, -20 V, -30 V, -40 V and -60 V. The maximum signal intensity was observed at -30 V. However, the variation of the deflector voltage had no influence on the electron capture to deprotonation intensity ratio  $[M]^\bullet/[M-H]^-$ . This gives further evidence that electron capture ionization within the APCI interface is mainly dependent on the applied needle voltage, and thus on the energy of the thermal electrons that are generated at the needle tip.

The strong influence of different mobile phases used for the liquid chromatographic separation of a series of 12 NBD amines on the competition of proton abstraction and electron capture as well as on the total intensity of MS signals is presented in Figure 5.8. The sum of peak areas ( $[M]^\bullet + [M-H]^-$ ) obtained with an eluent consisting of pure methanol was arbitrarily set to 100%. Regarding a pure methanol eluent, electron capture was favored for secondary amine derivatives. However, weak signals based on proton abstraction reaching ~ 1% of the electron capture signal were detected. Regarding primary amine derivatives of NBDCI,  $[M-H]^-$  ions contributed between 86 and 91% to the total signal intensity while the rest is traced back to the  $^{13}\text{C}$  satellite. Using pure acetonitrile as the mobile phase, ionization efficiency was significantly decreased. Analytes prone to undergo electron capture ionization gave only rather weak (NBDDMA and NBDNMA<sub>n</sub>) or even negligible (NBDDEA and NBDDPA) MS signals. Reaching ~ 0.5 to 1%, contribution of  $[M-H]^-$  ions was comparable to that observed for methanol separation. Although ionization for primary amine derivatives was much more efficient than for secondary analytes, signal intensities related to deprotonation only reached between 15 and 82% of the

total value observed for methanol separation. With respect to a binary eluent consisting of methanol and acetonitrile (50:50; v/v), ionization characteristics of primary analytes derivatives were similar to those, which had been observed for pure methanol. Again, electron capture signal intensities of secondary NBD amines were lower than those obtained in conjunction with methanol separation, thus showing a decreased  $[M]^{*}/[M-H]^{-}$  ratio. However, signals based on proton abstraction were again in the range of 1% (related to the total intensity in methanol). Using a solvent composition of methanol and water, significant deprotonation was observed for the NBDCl derivatives of secondary amines. Signal intensities ranged from 5 to 13%. Primary amines also gave stronger deprotonation, thus showing total intensities higher than those observed for methanol separation. Increased deprotonation of analytes comprising an acidic hydrogen atom may be explained on the basis of gas-phase proton affinities of the eluents used. Within the series of mobile phases for high-performance liquid chromatography, the hydroxide ion  $OH^{-}$  is the strongest base in the gas phase. This is followed by methanolate  $CH_3O^{-}$  and the carbanion of acetonitrile  $^{-}CH_2CN$  [28]. Thus, the use of the weaker gas-phase base  $^{-}CH_2CN$  instead of methanolate leads to decreased proton abstraction reactions. In contrast, the application of the stronger gas-phase base  $OH^{-}$  leads to improved deprotonation. However, this does not explain why the highest signals based on electron capture ionization are observed applying a pure methanol eluent.

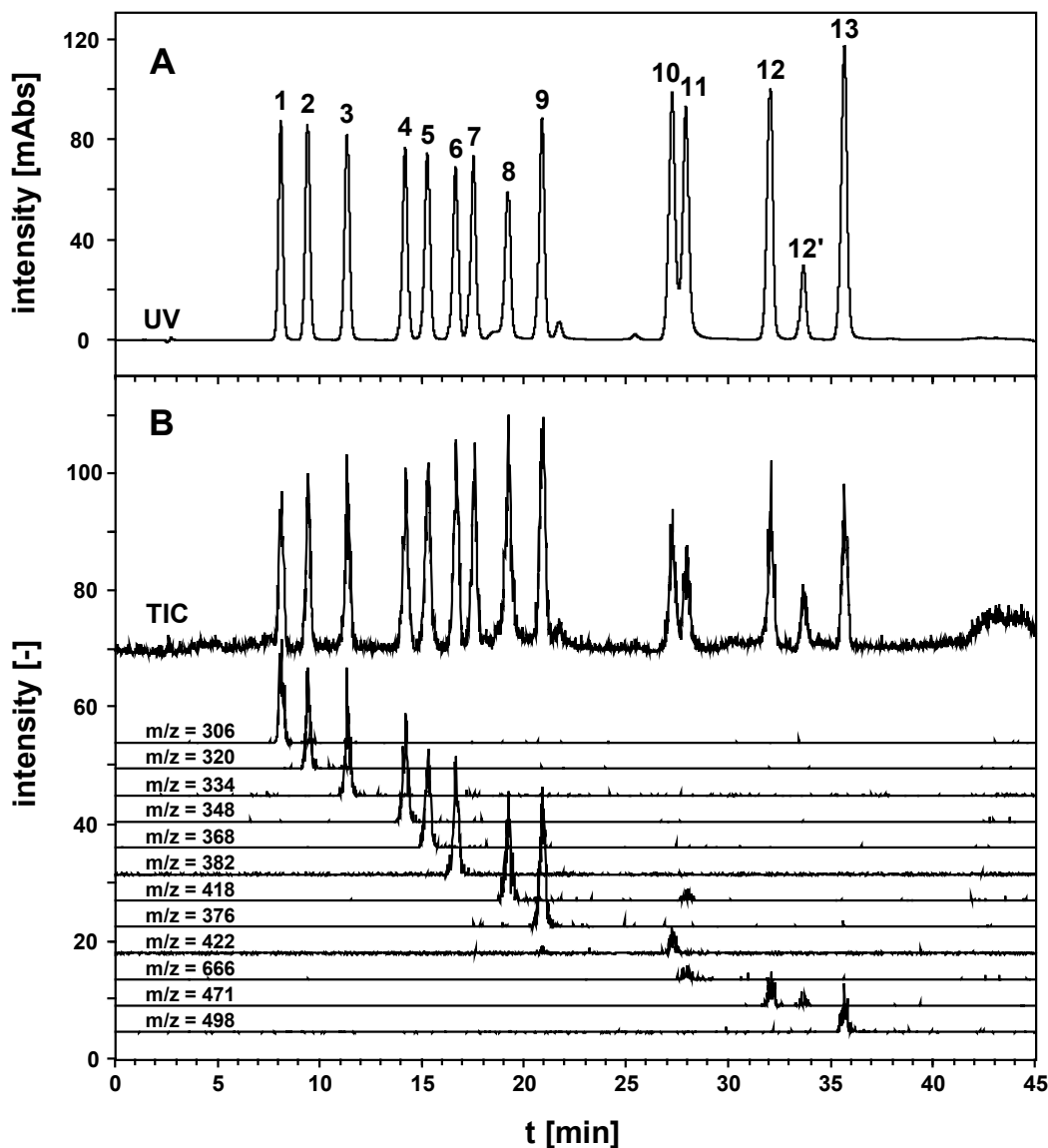


**Figure 5.8:** The influence of different eluents on the ratio of electron capture to proton abstraction  $[M]^+/[M-H]$ . White bars indicate the sum of signal intensities from  $[M]^+$  and  $[M-H]$ . The sum parameter obtained with methanol has arbitrarily been set to 100%. Black bars are related to  $[M-H]$ , while grey bars refer to the radical anions  $[M]^+$ . NBDA: ammonia; NBDMA: methyl amine; NBDDMA: dimethyl amine; NBDEA: ethyl amine; NBDDEA: diethyl amine; NBDPA: propyl amine; NBDDPA: dipropyl amine; NBDAn: aniline; NBD3EAn: 3-ethyl aniline; NBDBzA: benzyl amine; NBD4MBzA: 4-methylbenzyl amine; NBDNMAAn: N-methyl aniline derivative of NBDCI.

Comparative measurements using  $10^{-4}$  mol/L solutions of NBD amines have been performed by electrospray ionization in the negative ion mode. Capillary voltage was adjusted to  $-2.5$  kV,  $-3.5$  kV and  $-4.5$  kV, respectively. As could be expected, MS signals were only observed for those analytes possessing an  $\alpha$ -hydrogen atom bound to the nitrogen atom, thus yielding  $[M-H]^-$  ions. As the ESI probe cannot serve as a source of low-energy thermal electrons, no electron capture ionization was observed for NBDCl amine derivatives.

Further investigations on electron capture ionization in conjunction with LC/APCI(-)-MS have been performed with respect to 4-nitro-7-piperazino-2,1,3-benzoxadiazole (NBDPZ) and a series of corresponding mono- and diisocyanate urea derivatives. The liquid chromatographic separation of 13 isocyanate derivatives of NBDPZ (NPDPZ ureas) is depicted in Figure 5.9. Both the UV chromatogram and the total ion current (TIC) chromatogram are shown. Best separation of the urea compounds was obtained on phenyl-modified RP columns [24]. However, owing to significant column bleeding under release of compounds interfering with the  $m/z$  ratios to be detected, liquid chromatography/mass spectrometry had to be performed on C18 reversed-phase columns. Thus, the derivatives of 2,6-toluene diisocyanate (2,6-TDI) and hexamethylene diisocyanate (HDI) revealed co-elution.





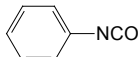
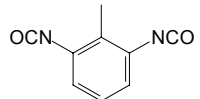
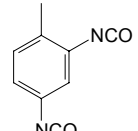
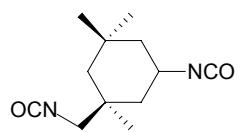
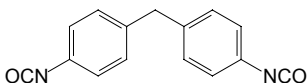
**Figure 5.9:** Liquid chromatographic separation of 13 NBDPZ isocyanate derivatives. A: UV-Vis chromatogram ( $\lambda = 460$  nm). B: Total ion current (TIC) chromatogram (probe voltage -2.5 kV); extracted mass traces for each analyte were chosen according to the signal of highest intensity. Peaks: (1) methyl isocyanate (MI); (2) ethyl isocyanate (EI); (3) propyl isocyanate (PI); (4) butyl isocyanate (BI); (5) phenyl isocyanate (PhI); (6) benzyl isocyanate (BzI); (7) pentyl isocyanate (PeI); (8) naphthyl isocyanate (NI); (9) hexyl isocyanate (HI); (10) 2,6-toluene diisocyanate (2,6-TDI); (11) hexamethylene diisocyanate (HDI); (12/12') trans/cis isophorone diisocyanate (IPDI); (13) 4,4'-methylene bis(phenyl isocyanate) (MDI) derivative of NBDPZ.

As for the MS chromatogram, a number of mass traces extracted from the TIC chromatogram is presented. Strong signals related to electron capture ionization yielding mainly  $[M]^{-}$  were observed for the NBDPZ derivatives of aliphatic monoisocyanates (methyl isocyanate MI, ethyl isocyanate EI, propyl isocyanate PI, butyl isocyanate BI, pentyl isocyanate PeI). Aromatic monoisocyanate ureas mainly resulted signals from deprotonation,  $[M-H]^{-}$ , while, prior to ionization, both aliphatic and aromatic diisocyanate derivatives additionally had undergone thermal degradation, as discussed in more detail below.

Structures and analytical figures of merit for the mass spectrometric detection of NBDPZ ureas are summarised in Table 5.6. Instrumental limits of detection (LOD) obtained by APCI(-)-MS ranged from 20 nmol/L for NBDPZ-EI to 100 nmol/L for NBDPZ-2,4-TDI for the employed single quadrupole instrument in selected ion monitoring (SIM) mode. This is in the same range as for photometric detection showing LOD between 11 nmol/L and 35 nmol/L [24]. Actually, highest sensitivity regarding NBDPZ derivatives could be obtained by means of fluorescence detection. Relative standard deviations for MS detection are given for three different concentrations. Largest values of RSD were determined for the positional isomers 2,4-TDI and 2,6-TDI.

**Table 5.6:** *Analytical figures of merit and molecular structures for a series of mono- and diisocyanate derivatives of NBDPZ.*

*LC/APCI-MS for the Determination of Nitroaromatic Compounds*

abbreviation	NBDPZ derivative of	M [Da]	detected m/z	LOD [nmol/L]	LOQ [nmol/L]	RSD (n=3)			R <sup>2</sup>
						5 × 10 <sup>-7</sup> mol/L	5 × 10 <sup>-6</sup> mol/L	5 × 10 <sup>-5</sup> mol/L	
NBDPZ-MI	H <sub>3</sub> C—NCO	306.1	306	30	100	3.5	2.8	3.3	0.9990
NBDPZ-EI	H <sub>5</sub> C <sub>2</sub> —NCO	320.1	320	20	70	2.8	4.2	1.6	0.9991
NBDPZ-PrI	H <sub>7</sub> C <sub>3</sub> —NCO	334.1	334	30	100	3.1	4.0	2.6	0.9989
NBDPZ-PhI		368.1	367	30	100	4.5	4.3	3.1	0.9980
NBDPZ-2,6-TDI		672.2	422	90	300	8.1	7.8	6.2	0.9952
NBDPZ-2,4-TDI		672.2	422	100	330	6.9	7.6	4.8	0.9946
NBDPZ-IPDI		720.3	471	50	170	5.2	5.0	3.7	0.9962
NBDPZ-MDI		748.2	498	50	170	4.3	4.3	2.9	0.9948

As in the case of the amine derivatives of NBDCI, atmospheric pressure chemical ionization in the negative ion mode has been thoroughly studied also for NBDPZ compounds with respect to solvent influences and instrumental parameters. Table 5.7 surveys the ionization observed in methanol, acetonitrile, methanol/ acetonitrile (50:50; v/v) and methanol/water (50:50; v/v) for a series of NBDPZ isocyanates.

On the basis of the results obtained, NBDPZ derivatives can be divided into four groups: 1. Aliphatic monoisocyanate derivatives, 2. aromatic monoisocyanate derivatives, 3. aliphatic diisocyanate derivatives and 4. aromatic diisocyanate derivatives. In Table 5.7, for each analyte the signal of the dominating ion was arbitrarily set to 100%. Using a methanol eluent, aliphatic monoisocyanates have undergone mainly electron capture ionization. Only for the long-chain derivatives of pentyl and hexyl isocyanate, significant signals from proton abstraction (28% and 24%, respectively) were observed. An opposite behavior was observed in acetonitrile. Here, spectra were dominated by signals resulting from  $[M-H]^-$  ions. Nevertheless, electron capture ionization ranged from 20 to 36%. Changing the solvent composition to methanol/acetonitrile, again more electron capture ionization than deprotonation was observed. The only exception was observed for hexyl isocyanate NBDPZ. In methanol/acetonitrile, deprotonation was competitive to electron capture ionization yielding signal intensities between 24 and 52% of the main signal's intensity.

**Table 5.7:** *Investigation of solvent influences on the negative atmospheric pressure chemical ionization of NBDPZ derivatives. Relative signal intensities are given in brackets and are related to the base peak of the respective mass spectrum.*

*LC/APCI-MS for the Determination of Nitroaromatic Compounds*

substance	M [Da]	methanol	acetonitrile	methanol/acetonitrile	methanol/water
NBDPZ-MI	306.1	305 (6), 306 (100)	305 (100), 306 (34)	305 (31), 306 (100)	305 (100), 306 (76)
NBDPZ-EI	320.1	319 (8), 320 (100)	319 (100), 320 (29)	319 (25), 320 (100)	319 (100), 320 (91)
NBDPZ-PrI	334.1	333 (14), 334 (100)	333 (100), 334 (30)	333 (45), 334 (100)	333 (100), 334 (64)
NBDPZ-Bul	348.2	347 (10), 348 (100)	347 (100), 348 (37)	347 (24), 348 (100)	347 (100), 348 (86)
NBDPZ-Pel	362.2	361 (28), 362 (100)	361 (100), 362 (20)	361 (52), 362 (100)	361 (100), 362 (84)
NBDPZ-HI	376.2	375 (24), 376 (100)	375 (100), 376 (36)	375 (100), 376 (73)	375 (100), 376 (82)
NBDPZ-PhI	368.1	367 (100), 368 (20)	367 (100), 368 (20)	367 (100), 368 (22)	367 (100), 368 (23)
NBDPZ-BzI	382.1	381 (100), 382 (44)	381 (100), 382 (30)	381 (100), 382 (56)	381 (100), 382 (81)
NBDPZ-NI	418.1	417 (100), 418 (20)	417 (100), 418 (25)	417 (100), 418 (38)	417 (100), 418 (18)
NBDPZ-HDI	666.3	416 (87), 417 (30)	416 (66), 417 (20)	416 (74), 417 (24)	416 (77), 417 (31)
		665 (64), 666 (100)	665 (100), 666 (66)	665 (100), 666 (27)	665 (100), 666 (92)
NBDPZ-IPDI	720.3	470 (42), 471 (100)	470 (100), 471 (69)	470 (100), 471 (49)	470 (100), 471 (84)
		719 (8), 720 (10)	719 (13), 720 (11)	719 (13), 720 (8)	719 (11), 720 (7)
NBDPZ-MDI	748.2	498 (100), 499 (65)	498 (100), 499 (33)	498 (100), 499 (34)	498 (100), 499 (31)
		747 (4), 748 (5)	747 (5), 748 (8)	747 (1), 748 (9)	747 (10), 748 (12)
NBDPZ-2,6-TDI	672.2	422 (100), 423 (61)	422 (100), 423 (29)	422 (100), 423 (40)	422 (100), 423 (35)
		671 (5), 672 (3)	671 (72), 672 (38)	671 (3), 672 (1)	671 (1), 672 (2)

Although electron capture was the dominating process, for a binary mixture of methanol and water, proton abstraction as well as electron capture ionization occurred nearly to the same extent.

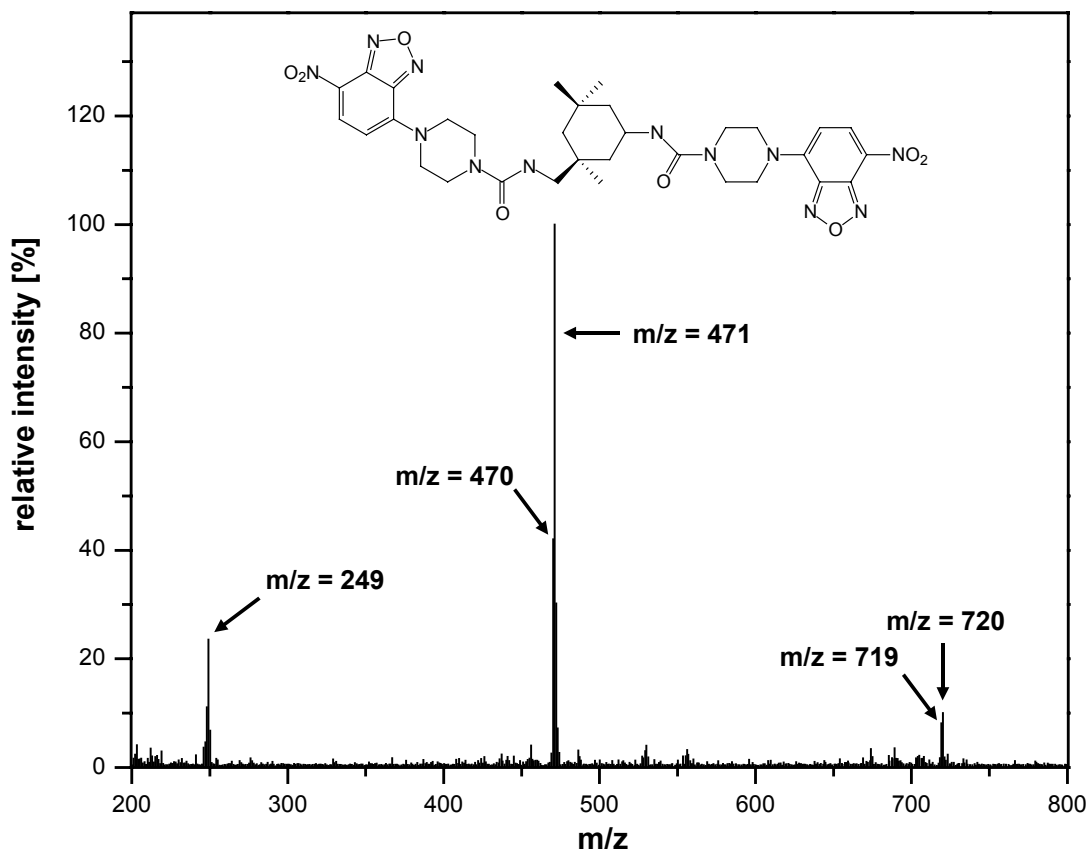
In contrast to aliphatic monoisocyanate derivatives, aromatic monoisocyanates (NBDPZ-PhI, NBDPZ-BzI, NBDPZ-NI) turned out to mainly undergo deprotonation in the APCI interface. Actually, no general tendency for electron capture ionization in different solvents could be seen with respect to this class of NBDPZ derivatives. It can be concluded that, for all solvents, deprotonation for these compounds is favored. This is owing to the fact that the aromatic system is able to stabilize the generated  $[M-H]^-$  ions by resonance stabilization.

Compared to monoisocyanate compounds, APCI(-)-MS of diisocyanate derivatives revealed more complex mechanisms. As can be seen from Table 5.7, the aliphatic NBDPZ-HDI mainly yielded  $m/z = 666$  when methanol was used as the mobile phase. This signal is related to the  $[M]^-$  ion resulting from electron capture ionization. Additionally, signals based on deprotonation ( $m/z 665$ ) were observed. Owing to APCI probe temperatures of around  $500\text{ }^\circ\text{C}$ , a significant amount of the HDI derivative has undergone thermal degradation in the interface, thus losing one NBDPZ functionality. Thermal degradation was also observed for monoisocyanate derivatives, but to a much smaller extent. Compared to  $500\text{ }^\circ\text{C}$ , almost no thermal degradation of the monoisocyanate derivatives was observed at  $250\text{ }^\circ\text{C}$ . However, sufficient evaporation of the diisocyanate derivatives of NBDPZ is only achieved above  $400\text{ }^\circ\text{C}$ . The maximum signal intensity for all selected isocyanate derivatives

was observed at 500 °C. The variation of the probe temperature had no influence on the electron capture to deprotonation ratio  $[M]^{*\cdot}/[M-H]^{-}$ .

Within the APCI interface, the remaining [M-NBDPZ] fragments were ionized on the basis of either deprotonation yielding  $[M-NBDPZ-H]^{-}$  ( $m/z = 416$ ) or electron capture yielding  $[M-NBDPZ]^{*\cdot}$  ( $m/z = 417$ ). After having changed the eluent from methanol to acetonitrile, ionization of NBDPZ-HDI by means of proton abstraction ( $m/z = 665$ ) was favoured. Again, significant fragmentation was observed. Similar effects were seen for binary eluents consisting either of methanol/acetonitrile or methanol/water. With the isophorone diisocyanate derivative of NBDPZ, another aliphatic diisocyanate has been investigated. An APCI(-) mass spectrum of NBDPZ-IPDI in methanol is shown in Figure 5.10.

In contrast to NBDPZ-HDI, thermal degradation in the interface was much more abundant for NBDPZ-IPDI. Only weak signals from  $[M]^{*\cdot}$  ( $m/z = 720$ ) or  $[M-H]^{-}$  ( $m/z = 719$ ) ions were observed. In pure methanol, MS spectra were dominated by  $[M-NBDPZ]^{*\cdot}$  ( $m/z = 471$ ) ions, which were related to an electron capture ionization of the fragments that had been generated owing to thermal degradation. As for NBDPZ-HDI, weaker signals from deprotonated fragment ions  $[M-NBDPZ-H]^{-}$  ( $m/z = 470$ ) were detected. Signals from  $m/z = 249$  were related to NBDPZ fragments. When changing the eluent from methanol to either acetonitrile or binary mixtures, the IPDI derivative exhibited the same behaviour as the HDI derivative. Signals based on electron capture ionization were decreasing, and proton abstraction became the favored ionization mechanism.

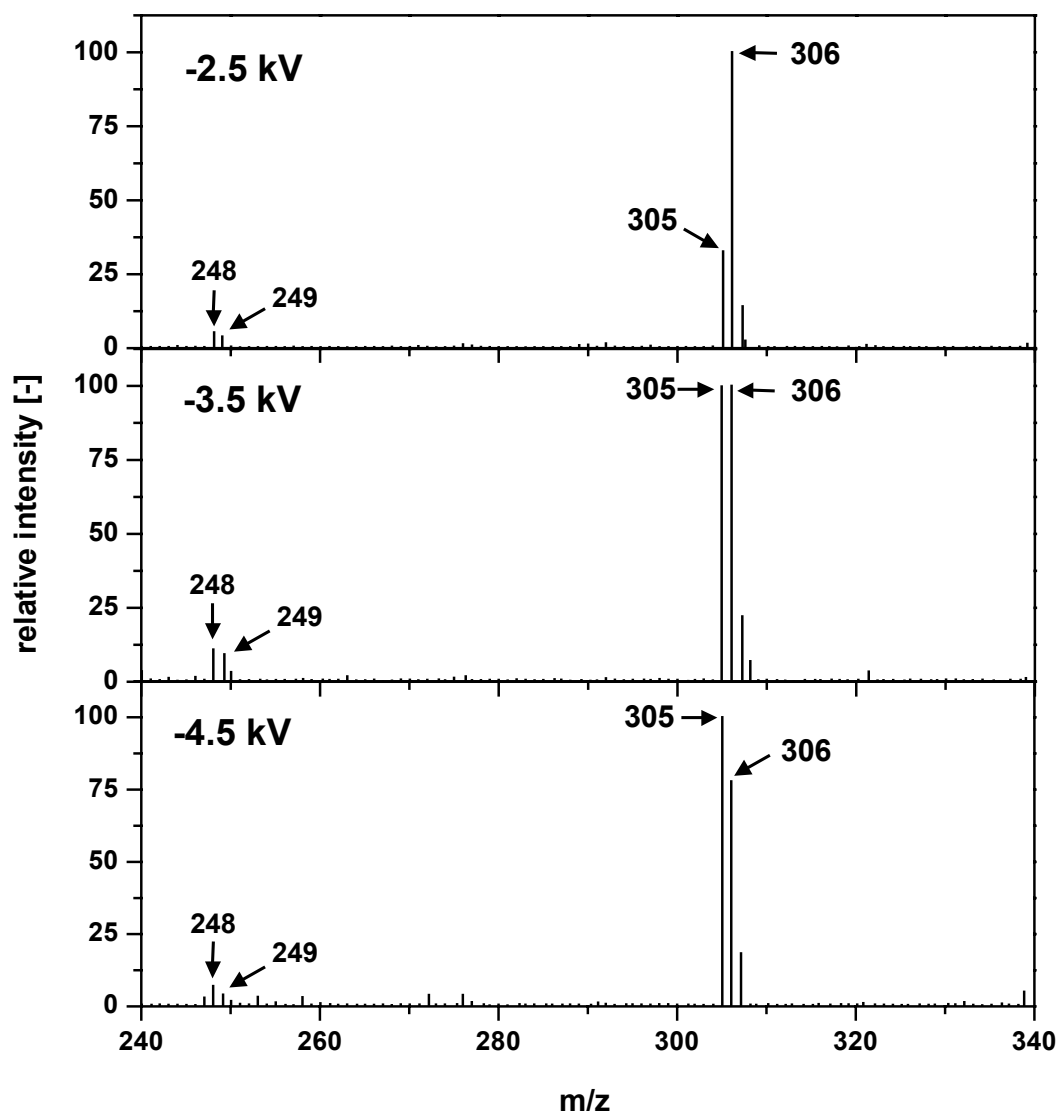


**Figure 5.10:** APCI(-) mass spectrum of the isophorone diisocyanate derivative of NBDPZ (NBDPZ-IPDI) with a base peak at  $m/z = 471$  corresponding to the  $[M-NBDPZ]^{\bullet-}$  radical anion. The applied needle voltage was -2.6 kV.

Besides resulting thermal degradation in the APCI interface, aromatic diisocyanate derivatives of NBDPZ have shown ionization similar to those of the mono-functionalized aromatic analytes. As can be concluded from Table 5.7, for both the MDI and 2,6-TDI derivatives, proton abstraction results in the formation of  $[M-NBDPZ-H]^{-}$  ions ( $m/z$  498 and  $m/z$  422, respectively). Again, electron capture ionization turned out to be a competing reaction being most abundant in a pure methanol eluent. In acetonitrile, methanol/acetonitrile or methanol/water, the signal intensities were significantly lower.



The influence of probe voltage on either deprotonation or electron capture of NBDPZ derivatives is shown in Figure 5.11.



**Figure 5.11:** The influence of APCI needle voltage on electron captures ionization vs. deprotonation. APCI(-) mass spectra of the methyl isocyanate derivative of NBDPZ are shown at three different probe voltages. The peak at  $m/z = 306$  corresponds to the  $[M]^-$  species, while the peak at  $m/z = 305$  is related to the deprotonated  $[M-H]^-$  ion. The signals at  $m/z = 248$  and  $m/z = 249$  correspond to NBDPZ fragments obtained from thermal decomposition.

The methyl isocyanate NBDPZ derivative (NBDPZ-MI) has been investigated applying APCI needle voltages of -2.5 kV, -3.5 kV and -4.5 kV. While electron capture ionization dominates at -2.5 kV, both mechanisms are observed with almost equal signal intensities of the respective products at -3.5 kV. The application of higher voltages led to increased deprotonation. Apart from the signals related to either electron capture or proton abstraction, weak signals from NBDPZ fragments ( $m/z$  248 and  $m/z$  249, respectively) were observed. Similar investigations have been performed for the NBDPZ derivatives of EI, PI, BI, PhI, BzI, PeI, NI, 2,6-TDI, HDI, IPDI and MDI. For all of them, similar behavior was observed.

Furthermore, deflector voltages were varied from 0 V to -80 V. As for the NBDCI amine derivatives, no influence on the electron capture/deprotonation ratio  $[M]^{-}/[M-H]^{-}$  was determined. Actually, maximum signal intensity was observed at -40 V. In accordance with the results obtained for NBDCI derivatives, the effect of electron capture in the APCI interface is mainly dependent on the energy of the thermal electrons generated. On the one hand, this process is closely related to the probe voltage; on the other hand, solvent parameters play a significant role with respect to the occurrence of electron capture ionization.

Comparative experiments for NBDPZ analytes have been performed with electrospray ionization in the negative ion mode.  $1 \times 10^{-4}$  mol/L solutions of a mixture of NBDPZ standards were measured applying capillary voltages of -2.5 kV, -3.0 kV, -4.0 kV and -5.0 kV. Only weak signals from deprotonated species were detected. As expected for ESI, no electron capture was observed.

#### **5.3.4 Conclusions**

Both NBDCI amine derivatives and NBDPZ isocyanate derivatives were detected by means of APCI(-) mass spectrometry with good sensitivity. Electron capture ionization and ionization based on proton abstraction are mostly competitive reactions. Electron capture is supposed to occur owing to the presence of an electron-attracting nitro function and the oxadiazole backbone for all NBD derivatives. This competition between electron capture ionization and proton abstraction was mainly affected by different mobile phases applied for liquid chromatography. Predominantly, methanol increased the abundance of electron capture processes. However, the mechanism of solvent influences has not been elucidated yet, and the influence of other eluents has to be studied. In principle, non-polar solvents for normal-phase LC could be investigated, but the chromatographic separation would not be as easy as for RP-LC. Regarding instrumental parameters, e.g., probe voltage, deflector voltage or probe temperature, mainly the potential applied at the corona discharge needle within the APCI interface determines the energy of the generated electrons. Beyond an optimum potential, electron capture efficiency decreases because the energy of the electrons is too high to serve for electron capture ionization.

## 5.4 References

- [1] E. Gelpí, *J. Chromatogr. A* 703 (1995), 59.
- [2] W. M. A. Niessen, *J. Chromatogr. A* 1000 (2003) 413.
- [3] T. Reemtsma, *J. Chromatogr. A* 1000 (2003) 477.
- [4] M. Kohler, N. V. Heeb, *Anal. Chem.* 75 (2003), 3115.
- [5] L. Bonnington, E. Eljarrat, M. Guillamón, P. Eichhorn, A. Taberner, D. Barceló, *Anal. Chem.* 75 (2003) 3128.
- [6] D. B. Robb, T. R. Covey, A. P. Bruins, *Anal. Chem.* 72 (2000) 3653.
- [7] R. W. Giese, *J. Chromatogr. A* 892 (2000) 329.
- [8] S. G. Chu, A. Covaci, K. Haraguchi, P. Schepens, *Analyst* 127 (2003) 1621.
- [9] W. Vetter, *Anal. Chem.* 73 (2001) 4951.
- [10] H. Hayen, U. Karst, *J. Chromatogr. A* 1000 (2003) 549.
- [11] G. Singh, A. Gutierrez, K. Xu, I. A. Blair, *Anal. Chem.* 72 (2000) 3007.
- [12] H. Hayen, N. Jachmann, M. Vogel, U. Karst, *Analyst* 127 (2002) 1027.
- [13] S. Kölliker, M. Oehme, C. Dye, *Anal. Chem.* 70 (1998) 1979.
- [14] G. Zurek, H. Luftmann, U. Karst, *Analyst* 124 (1999) 1291.
- [15] T. Higashi, N. Takido, A. Yamauchi, K. Shimada, *Anal. Sci.* 18 (2002) 1301.
- [16] T. Higashi, N. Takido, K. Shimada, *Analyst* 128 (2003) 130.
- [17] T. Higashi, A. Yamauchi, K. Shimada, *Anal. Sci.* 19 (2003) 941.
- [18] S. Uchiyama, T. Santa, N. Okiyama, T. Fukushima, K. Imai, *Biomed. Chromatogr.* 15 (2001) 295.
- [19] A. A. Al-Majed, F. Belal, M. A. Abounassif, N. Y. Khalil, *Microchim. Acta* 141 (2003) 1.
- [20] A. Büldt, U. Karst, *Anal. Chem.* 71 (1999) 1893.
- [21] M. Vogel, A. Büldt, U. Karst, *Fresenius' J. Anal. Chem.* 366 (2000) 781.

- [22] P. B. Ghosh, M. W. Whitehouse, *Biochem. J.* 108 (1968) 155.
- [23] N. Jachmann, Doctoral Thesis, University of Münster, Münster/Germany, 2001.
- [24] M. Vogel, U. Karst, *Anal. Chem.* 74 (2002) 6418.
- [25] H. Henneken, R. Lindahl, A. Östin, M. Vogel, J.-O. Levin, U. Karst, *J. Environ. Monit.* 5 (2003)100.
- [26] A. Büldt, U. Karst, *Anal. Chem.* 69 (1997) 3617.
- [27] A. S. Bailey, J. R. Case, *Tetrahedron* 3 (1958) 113.
- [28] A. P. Bruins, *Mass Spectrom. Rev.* 10 (1991) 53.



# Chapter 6

## Liquid Chromatography/Coordination Ion-spray-Mass Spectrometry (LC/CIS-MS) for the Analysis of Rubber Vulcanization Products\*

### 6.1 Abstract

Liquid chromatography/coordination ion-spray-mass spectrometry (LC/CIS-MS) has been used for the identification of reaction products in a model rubber vulcanization process. After LC separation using reversed-phase conditions,  $\text{AgBF}_4$  in acetonitrile was added, and strong signals were observed for silica-rubber coupling agents and products of the reaction between these and alkenes. The method performs best for substances containing sulfur chains with chainlengths between two and eight sulfur atoms, but sulfur-free compounds containing triethoxysilyl groups were detected as well. For the latter, the post-column addition of  $\text{NaBF}_4$  proved to be a suitable alternative. Besides the coupling agents, various reaction products, including sulfur-chain bridged alkenes were identified.

*\*H. Hayen, M. M. Álvarez-Grima, S. C. Debnath, J. W. M. Noordermeer, U. Karst, Anal. Chem., submitted for publication*

## 6.2 Introduction

The invention of electrospray ionization (ESI) [1,2] is the major reason for the evolution of liquid chromatography/mass spectrometry (LC/MS) as one of the most powerful analytical techniques currently available [3,4]. As acid/base reactions or the addition of ions from the mobile phase are the most frequently observed ionization mechanisms, it is obvious that best results are obtained for the analysis of highly polar or even charged molecules by ESI-MS. Atmospheric pressure chemical ionization (APCI) [5] expands the range of applications to less polar compounds, but the analysis of non-polar compounds is still difficult. Within the last few years, a series of different strategies to overcome these limitations of ESI-MS and APCI-MS has evolved [6]. One alternative is coordination ionspray-mass spectrometry (CIS-MS) [7]. The addition of ions, typically of  $\text{Ag}^+$ , which form stable complexes with compounds of low polarity, leads to the ionization of the analytes [7-12]. Only few papers describe the use of this method, and applications for the determination of tocopherols and carotenoids [8], tocotrienols [9], lipid peroxidation products [10], diacyl peroxides [11], polycyclic aromatic hydrocarbons [12], jojoba oil constituents [13] and endocannabinoids [14] have been presented.

Bis(3-triethoxysilylpropyl)tetrasulfide (TESPT) is a widely used coupling agent for silica reinforced rubber compounds [15-17]. To understand the mode of action of this compound and to optimize the respective processes, sound knowledge on the chemical reactions taking place with TESPT during rubber vulcanization is essential. Due to the three-dimensional network of polymeric chains of vulcanized rubber, which is insoluble in most solvents, the investigation of the wide range of vulcanization products is difficult. Therefore, model compound vulcanization (MCV)



is carried out, which is based on the vulcanization of a low-molecular weight model for rubber, e.g., squalene or 2,3-dimethyl-2-butene [18].

Looking only at their polarity, TESPT and related compounds should be ideal candidates for gas chromatographic analysis with subsequent mass spectrometric detection (GC/MS). However, their known thermolability leads to significant problems during gas chromatographic analysis [19]. Matrix assisted laser desorption/ionization-mass spectrometry (MALDI-MS) has been applied to investigate reactions of other sulfur-donating reagents with squalene as model compound [20]. However, the major strength of MALDI-MS is in the higher mass range, as the matrix constituents may interfere with the determination of low molecular weight reaction products. Furthermore, additional information with respect to chromatographic retention times cannot be obtained. Rodriguez et al. have analyzed the reaction products of squalene with a sulfur-based acceleration system with LC/particle beam-MS [21]. Although some reaction products could be identified, the authors concluded that the drastic ionization conditions readily lead to breaking S-S bonds [21].

Up to now, the use of LC/MS using atmospheric pressure ionization (API) techniques has not been described in conjunction with the analysis of rubber vulcanization products. Based on the assumption that TESPT and related compounds as well as their reaction products are non-polar compounds, which are not likely to be detected using ESI-MS or APCI-MS, the addition of  $\text{Ag}^+$  to the sulfur-containing compounds was considered to be a promising alternative. The respective results on coordination ionspray-MS for the determination of the vulcanization coupling agents and their reaction products are described in this chapter.

## 6.3 Experimental

### *Chemicals*

Bis(3-triethoxysilylpropyl)tetrasulfide (Silquest<sup>®</sup> A-1289 Silane, TESPT) was obtained from Osi Crompton Corporation (South Charleston, WV, USA). Bis(3-trimethylsilylpropyl)tetrasulfide (TMeSPT) and 1,10-bis(triethoxysilyl) decane (TESD) were synthesized according to ref. [22]. Trans-3-hexene (T-3-H) and 2,3-dimethyl-2-butene (tetramethylethylene, TME) were obtained from Merck (Darmstadt, Germany). Silver tetrafluoroborate and sodium tetrafluoroborate were purchased from Aldrich Chemie (Steinheim, Germany) in the highest quality available. As mobile phase for HPLC, acetonitrile (elution grade) from Merck eurolab (Fontenau S/Bois, France) and water for liquid chromatography from Merck eurolab (Briare le Canal, France) was used.

### *Model Vulcanization*

Two different reaction mixtures were weighed into a glass ampoule: Sample A contained 7 g TESPT/100 g trans-3-hexene. Sample B consisted of 8 g TESPT/ 100 g 2,3-dimethyl-2-butene. Before closing the ampoules by melting the glass neck, a flow of nitrogen was passed through the ampoule to remove the oxygen. The closed ampoules were then placed in a thermostated oil bath ( $T = 140\text{ }^{\circ}\text{C}$ ) for 30 min. During the reaction time, the mixtures were constantly stirred with a magnetic stirrer inside the ampoule. The ampoule was also covered with aluminium foil to protect the reaction mixture from UV irradiation. The reaction was stopped by immersion in an ice bath.

### *Sample Preparation*

After opening the ampoules, the reaction mixtures were filtered through a 0.45  $\mu\text{m}$  membrane filter. Of the filtered sample, 100  $\mu\text{L}$  were diluted with 900  $\mu\text{L}$  acetonitrile.

Prior to LC/MS analysis, TESPT, TMeSPT and TESD were diluted by a factor of 500 with acetonitrile and filtered as well through a 0.45  $\mu\text{m}$  membrane filter.

### *Instrumentation*

For HPLC/MS measurements, the following equipment from Shimadzu (Duisburg, Germany) was used: SCL-10Avp controller unit, DGU-14A degasser, two LC-10ADvp pumps, SIL-10A autosampler, SPD10AV UV-Vis detector, LCMS QP8000 single quadrupole mass spectrometer with electrospray ionization (ESI) probe and Class 8000 software Version 1.20.

### *HPLC Conditions*

As stationary phase, a base deactivated Discovery<sup>®</sup> RP-18 column from Supelco (Deisenhofen, Germany) was used. Column dimensions were 150 mm x 2.1 mm. Particle size was 5  $\mu\text{m}$  and pore size 100 Å. Flow rate of the mobile phase was 300  $\mu\text{L}/\text{min}$ . A binary gradient consisting of acetonitrile and water with the following profile was used:

time (min)	0.01	0.5	30	35	36	40
c (CH <sub>3</sub> CN) (%)	70	70	100	100	70	stop

A syringe pump model 74900 (Cole Parmer Instrument Company, Illinois, USA) equipped with a 500  $\mu\text{L}$  syringe (SGE GmbH, Darmstadt, Deutschland) was used to deliver a solution of  $\text{AgBF}_4$  (2.92 mg/mL acetonitrile) or  $\text{NaBF}_4$  (1.65 mg/mL acetonitrile) at 10  $\mu\text{L}/\text{min}$  via a zero dead volume mixing Tee post-column into the mobile phase to obtain a concentration in the HPLC eluent of 0.5 mmol/L. Ahead of the electrospray interface, a flow splitter (split ratio = 1:10) was implemented.

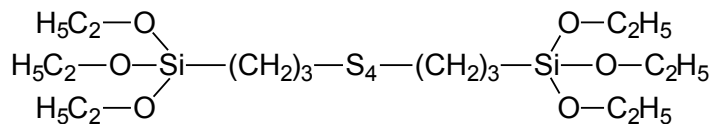
The injection volume was set to 5  $\mu\text{L}$  and the detection wavelengths in the dual-wavelength UV-Vis detector were 251 and 300 nm, respectively.

#### *MS Conditions*

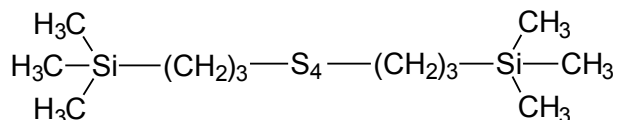
All mass spectrometry measurements were recorded using electrospray in the positive ion mode under the following conditions: Probe voltage 3 kV, curved desolvation line (CDL) voltage -50 V, CDL temperature 250  $^{\circ}\text{C}$ , nebulizer gas ( $\text{N}_2$ ) flow rate 4.5 L/min, deflector voltages 35 V and detector voltage 1.6 kV were used. For SCAN mode measurements, a mass range from  $m/z$  100 – 1000 was chosen and the integration time was 1 s.

## 6.4 Results and Discussion

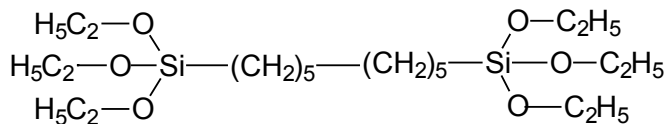
Initial studies with electrospray LC/MS were carried out using the three coupling agents TESPT, TMeSPT and TESD. The soft ionization process associated with the electrospray interface typically leads to protonation in the positive ion mode or deprotonation in the negative ion mode. In many cases, adducts with ammonium or sodium ions in the positive ion mode and chloride, formate or acetate in the negative ion mode are observed as well. From the structural formula of the compounds in Figure 6.1 and considering Pearson's classification [23], it can be concluded that protonation or the formation of adducts with ammonium or sodium ions is only likely for TESPT and TESD due to an adduct formation with the triethoxysilyl group, but not for TMeSPT.



Bis-(3-triethoxysilylpropyl)tetrasulfide (**TESPT**)



Bis-(3-trimethylsilylpropyl)tetrasulfide (**TMeSPT**)

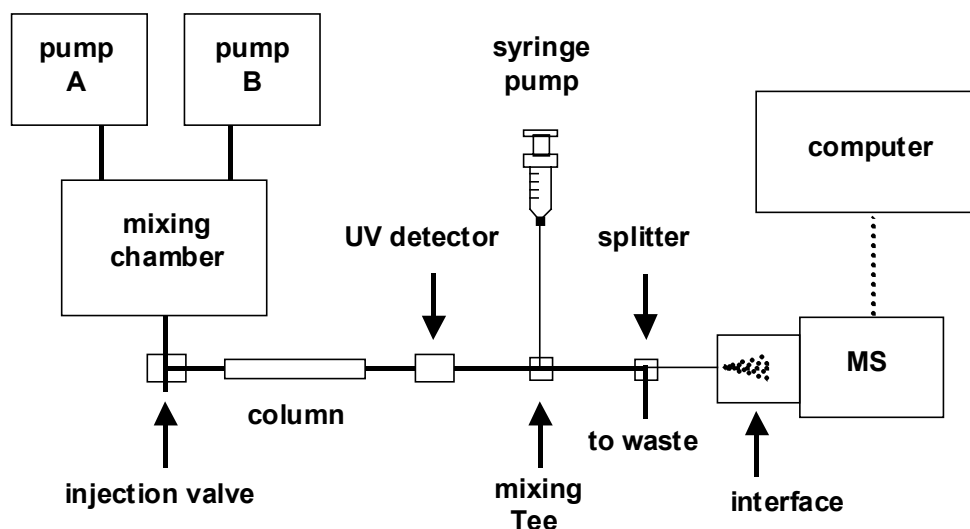


1,10-Bis(triethoxysilyl)decane (**TESD**)

**Figure 6.1:** Structural formula of the coupling agents TESPT, TMeSPT and TESD.

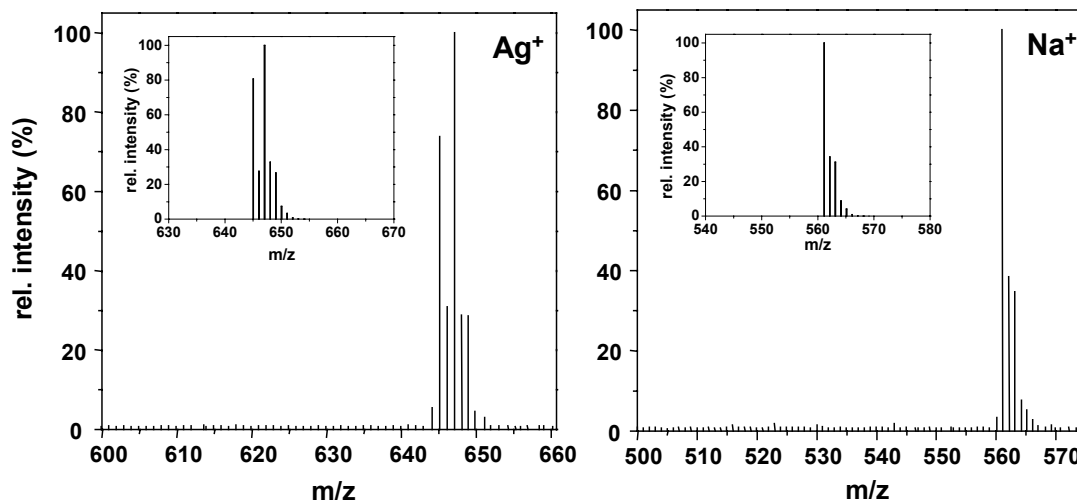
Deprotonation or the formation of adducts in the negative ion mode are not likely at all. First measurements using a mobile phase without additives confirmed these assumptions. Only poor signals of sodium adducts were observed for TESPT and TESD in the positive ion mode. TMeSPT was not detected at all. In the negative ion mode, no signals were observed for any of the compounds. According to Pearson's classification, those of the vulcanization coupling agents, which contain sulfur chains may be considered as "soft electron pair donors" or "soft bases" [23]. These compounds are known to form stable complexes with "soft electron pair acceptors" or "soft acids", which are large cations with low charge. Silver(I) ions are typical "soft acids", and silver has been used before to form complexes with comparably non-polar compounds with the goal to improve their ionization in the so-called coordination ionspray approach, as discussed above [7]. In the presence of  $\text{Ag}^+$  in the mobile phase, strong signals are observed for both TESPT and much weaker signals for TMeSPT.

Therefore, an experimental set-up as described in Figure 6.2 was selected: To a binary gradient HPLC system with dual-wavelength UV detector, a reagent solution consisting of either  $\text{NaBF}_4$  or  $\text{AgBF}_4$  in acetonitrile was delivered using a syringe pump and a low dead volume mixing Tee. A splitter was used to minimize the amount of silver(I) ions, which were transferred into the mass spectrometer. Therefore, the contamination of the mass spectrometer with  $\text{Ag}^+$  was reduced as far as possible. It should, however, be noted that even after long series of samples, no contamination was detected in the system, if atmospheric pressure parts of the system were cleaned thoroughly.



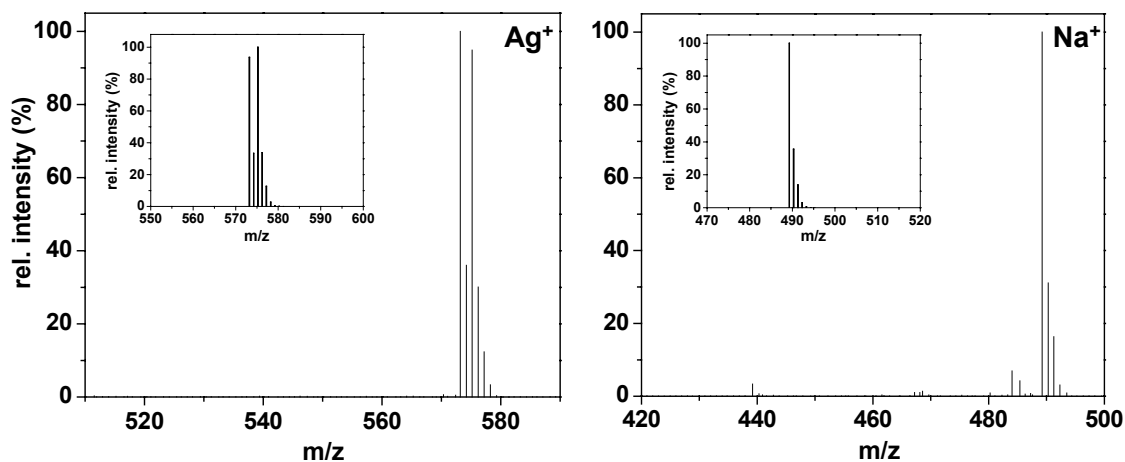
**Figure 6.2:** Experimental set-up used for LC/CIS-MS measurements.

In Figure 6.3, the mass spectra of TESPT with a sulfur chain of four atoms are presented after addition of  $\text{Ag}^+$  (left) and  $\text{Na}^+$  (right). In both cases, the characteristic isotopic patterns of the compounds are observed, and the inserts prove that the measured spectra (large) correlate well with the calculated spectra (inserted).

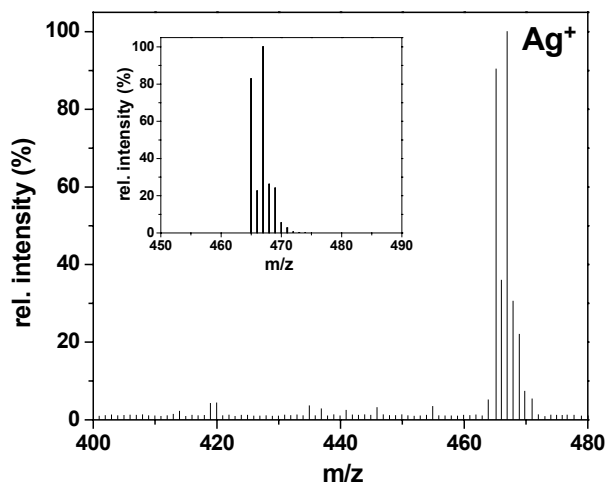


**Figure 6.3:** Mass spectra of TESPT after addition of  $\text{Ag}^+$  and  $\text{Na}^+$ , respectively. Inserted: Calculated isotopic pattern.

In Figure 6.4, the same spectra are presented for TESD, and in Figure 6.5, the respective spectrum of TMeSPT after addition of  $\text{Ag}^+$  is presented, again for a sulfur chain of four atoms. In this case, no sodium adduct was observed.



**Figure 6.4:** Mass spectra of TESD after addition of  $\text{Ag}^+$  and  $\text{Na}^+$ , respectively. Inserted: Calculated isotopic pattern



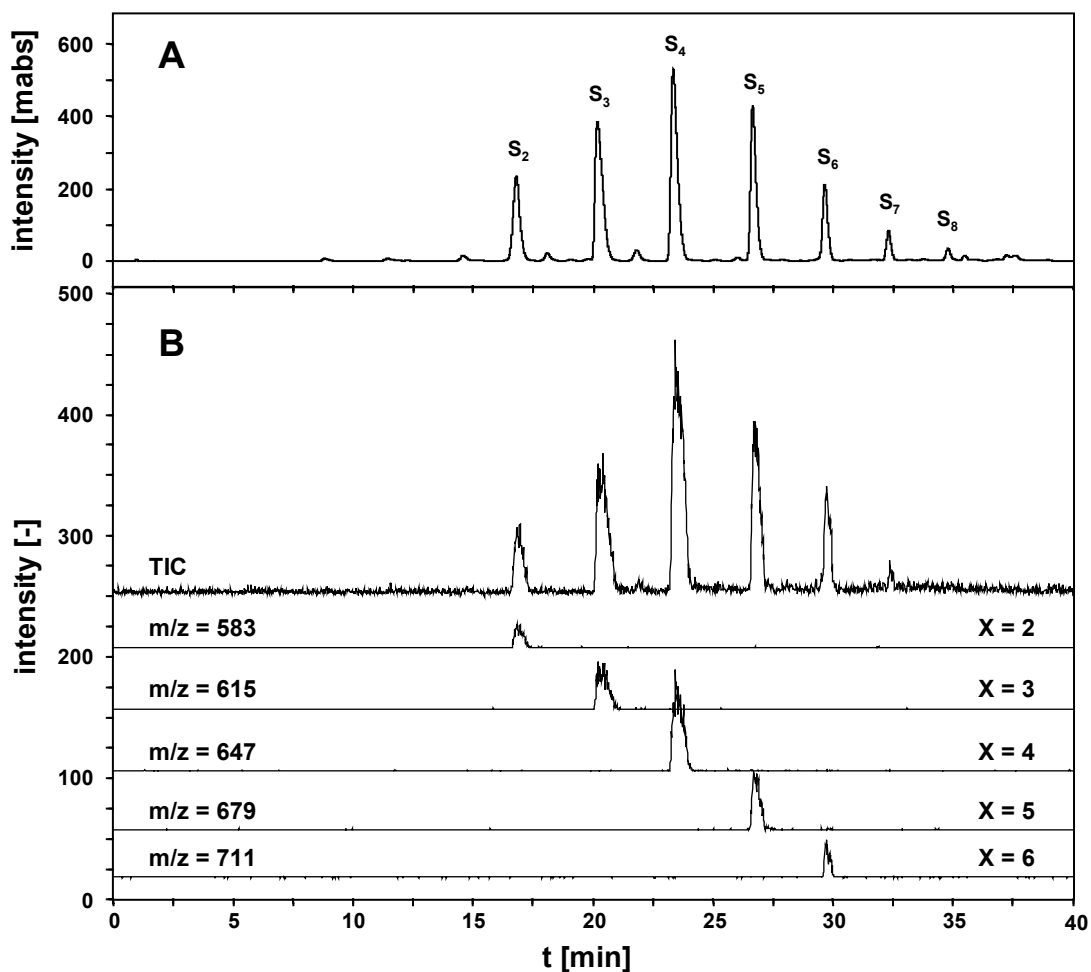
**Figure 6.5:** Mass spectrum of TMeSPT after addition of  $\text{Ag}^+$ . Inserted: Calculated isotopic pattern.

From Figures 6.3 - 6.5 it may be concluded that for this group of compounds, the addition of silver ions is preferred over the addition of sodium ions, because all three



coupling agents were detected after silver addition, but only two after sodium addition. It is obvious that the  $\text{Ag}^+$  ion coordinates preferably with the sulfur chains, but to a lesser extent with the triethoxysilyl groups as well. On the other hand, the triethoxysilyl groups are required to observe sodium adducts. As the major goal of this work is not to detect the vulcanization coupling agents themselves, but their reaction products with alkenes, which will most likely not all contain triethoxysilyl groups, the addition of silver was selected for all further studies on the reaction products.

A good separation of the starting materials and the reaction products in liquid chromatography is important to use retention times and UV/vis spectroscopic data in addition to the MS data and to reduce complexity of the mass spectra of the technical products in comparison with direct injection mass spectrometry without LC separation. In Figure 6.6, the chromatograms of technical TESPT with UV/vis (A) and mass spectrometric (B) detection are presented. Obviously, the homologues of TESPT are well separated using reversed-phase LC and strong signals are observed for the TESPT homologues with between two and six sulfur atoms.



**Figure 6.6:** Chromatographic separation of a technical TESPT mixture with two to eight sulfur atoms. Detection is performed by UV spectroscopy at  $\lambda = 251$  nm (A) and by mass spectrometry after addition of  $Ag^+$  (B). The total ion current (TIC) plus several extracted mass traces are displayed.

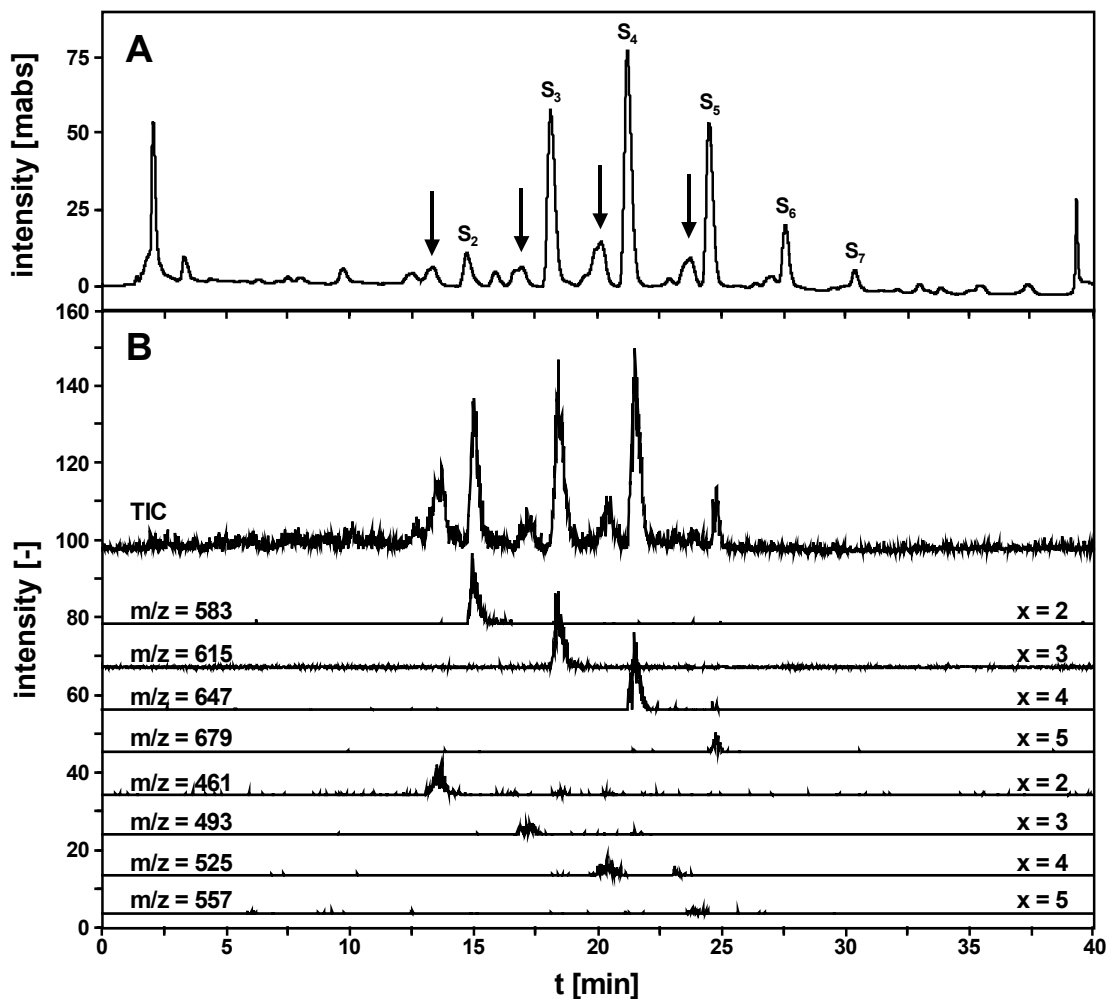
Looking closer at the individual extracted masses from the total ion current (TIC), it can be concluded that, as presented in Table 6.1, different series of  $Ag^+$  and  $Na^+$  adducts are observed. For the lower homologues of TESPT, the addition of  $Na^+$  is favorable, but for the higher homologues, better signals are observed for the addition of  $Ag^+$ . However, due to the reasons provided above, all further measurements were carried out using the addition of  $Ag^+$ .

**Table 6.1:** Ions observed with LC/CIS-MS for the analysis of technical mixtures of TESPT, TMeSPT and TESD.

number of sulfur atoms	TESPT			TMeSPT			TESD		
	M [Da]	observed [M+Na] <sup>+</sup> m/z	observed [M+ <sup>107</sup> Ag] <sup>+</sup> m/z	M [Da]	observed [M+Na] <sup>+</sup> m/z	observed [M+ <sup>107</sup> Ag] <sup>+</sup> m/z	M [Da]	observed [M+Na] <sup>+</sup> m/z	observed [M+ <sup>107</sup> Ag] <sup>+</sup> m/z
0	410.2	433.2	n. d.	230.2	n. d.	n. d.	466.3	489.2	573.2
1	442.2	465.2	n. d.	262.2	n. d.	n. d.	/	/	/
2	474.2	497.2	581.1	294.1	n. d.	401.1	/	/	/
3	506.2	529.2	613.1	326.1	n. d.	433.1	/	/	/
4	538.1	561.1	645.0	358.1	n. d.	465.0	/	/	/
5	570.1	593.1	677.0	390.0	n. d.	497.0	/	/	/
6	502.1	625.1	709.0	422.0	n. d.	529.0	/	/	/
7	634.0	657.0	740.9	454.0	n. d.	561.0	/	/	/
8	666.0	n. d.	772.9	486.0	n. d.	593.0	/	/	/

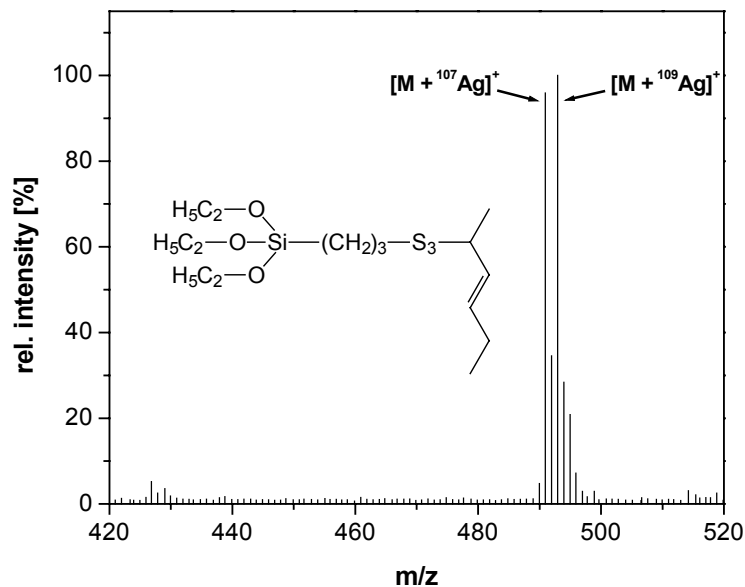
In the following, model reactions between the vulcanization coupling agents and selected alkenes were carried out with the goal to improve the understanding of the rubber vulcanization process.

In Figure 6.7, the chromatogram of a reaction mixture of TESPT with T-3-H (reaction temperature: 140°C) is presented. Already in the UV trace (A), the TESPT peaks are still present, but additional peaks have been formed. In part B this is confirmed by the mass spectra when looking at the mass traces of TESPT with between two and five sulfur atoms. In the lower parts, a homologous series of a reaction product with two to five sulfur atoms is observed with their characteristic mass traces. These compounds were identified as adducts formed after thermal cleavage of TESPT and subsequent addition of the formed (EtO)<sub>3</sub>Si(CH<sub>2</sub>)<sub>3</sub>S<sub>x</sub> to a molecule of T-3-H.



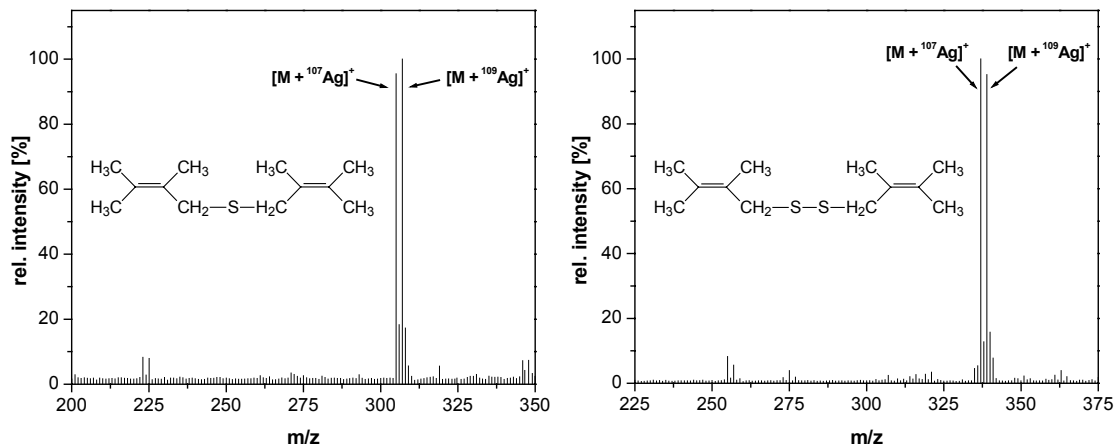
**Figure 6.7:** Chromatographic separation of a reaction mixture of TESPT and T-3-H using LC/CIS-MS with post-column addition of Ag<sup>+</sup>. Detection with UV spectroscopy at  $\lambda = 251\text{nm}$  (A) and mass spectrometry (B). The TIC and several extracted mass traces are presented.

The extracted mass spectrum for the reaction product with three sulfur atoms as well as its structural formula is presented in Figure 6.8. Under the selected experimental conditions, no other series of products could be detected.



**Figure 6.8:** Mass spectrum for the reaction product at  $t_R = 17$  min in Figure 6.7. The structural formula of the product is inserted. The measured isotopic pattern fits well to the calculated pattern.

The situation is different for the reaction of TESPT with TME. In this case, no adducts of parts of TESPT with the alkene were observed, but sulfur-bridged alkenes, which represent higher products in the vulcanization process. From the mass spectra with inserted structural formula in Figure 6.9, one can conclude that for these two products, two TME molecules are bridged by one or two sulfur atoms, respectively. As in the other cases, the observed isotopic patterns fit well to the calculated patterns, providing additional evidence for the provided sum formula.



**Figure 6.9:** Mass spectra of two reaction products between TESPT and TME. The structural formula of the products are inserted. The measured isotopic patterns fit well to the calculated patterns.

## 6.5 Conclusions

Coordination-ion-spray mass spectrometry has been proven to be a valuable tool for investigations on the rubber vulcanization process, in which thermolabile and non-polar sulfur-containing compounds are involved. The addition of  $\text{Ag}^+$  ions allows to detect the reaction products rapidly, using a simple post-column reagent addition set-up. Reaction products, which were only suspected to be formed could be identified unambiguously using this method. Future work will focus on the use of an ion trap mass spectrometer, which will allow to perform  $\text{MS}^n$  experiments to identify the reaction products from more complex mixtures and to improve structure elucidation of the products.

## **6.6 References**

- [1] M. Yamashita, J. B. Fenn, *J. Phys. Chem.* 88 (1984) 4451.
- [2] C. M. Whitehouse, R. N. Dreyer, M. Yamashita, J. B. Fenn, *Anal. Chem.* 57 (1985) 675.
- [3] W. M. A. Niessen, *J. Chromatogr. A* 856 (1999) 179.
- [4] E. Gelpí, *J. Mass Spectrom.* 37 (2002) 241.
- [5] D. I. Carroll, I. Dzidic, R. N. Stillwell, K. D. Haegele, E. C. Horning, *Anal. Chem.* 47 (1975) 2369.
- [6] H. Hayen, U. Karst, *J. Chromatogr. A* 1000 (2003) 549.
- [7] E. Bayer, P. Gfrörer, C. Rentel, *Angew. Chem. Int. Ed.* 38 (1999) 992.
- [8] C. Rentel, S. Strohschein, K. Albert, E. Bayer, *Anal. Chem.* 70 (1998) 4394.
- [9] S. Strohschein, C. Rentel, T. Lacker, E. Bayer, K. Albert, *Anal. Chem.* 71 (1999) 1780.
- [10] C. M. Havrilla, D. L. Hachey, N. A. Porter, *J. Am. Chem. Soc.* 122 (2000) 8042.
- [11] H. Yin, D. L. Hachey, N. A. Porter, *J. Am. Soc. Mass Spectrom.* 12 (2001) 449.
- [12] M. Takino, S. Daishima, K. Yamaguchi, T. Nakahara, *J. Chromatogr. A* 928 (2001) 53.
- [13] A. Medvedovici, K. Lazou, A. d'Oosterlinck, Y. Zhao, P. Sandra, *J. Sep. Sci.* 25 (2002) 173.
- [14] P. J. Kingsley, L. Marnett, *J. Anal. Biochem.* 314 (2003) 8.
- [15] J. W. ten Brinke, S. C. Debnath, L. A. E. M. Reuvekamp, J. W. M. Noordermeer, *Compos. Sci. Technol.* 63 (2003) 1165.
- [16] H.-D. Luginsland, *Kautsch. Gummi Kunstst.* 53 (2000) 10.

- [17] L. A. E. M. Reuvekamp, J. W. ten Brinke, P. J. van Swaaij, J. W. M. Noordermeer, *Kautsch. Gummi Kunstst.* 55 (2002) 41.
- [18] P. J. Niewenhuizen, J. G. Haasnoot, J. Reedijk, *Kautsch. Gummi Kunstst.* 53 (2000) 144.
- [19] U. Görl, J. Münzenberg, D. Luginsland, A. Müller, *Kautsch. Gummi Kunstst.* 52 (1999) 588.
- [20] M. Gros, S. Borrós, D. B. Amabilino, J. Veciana, I. Folch, *J. Mass Spectrom.* 36 (2001) 294.
- [21] S. Rodriguez, C. Masalles, N. Agulló, S. Borrós, L. Comellas, F. Broto, *Kautsch. Gummi Kunstst.* 52 (1999) 438.
- [22] L. A. E. M. Reuvekamp, *Reactive mixing of silica and rubber for tyres and engine*, PhD thesis, Twente University Press 2003, Enschede, The Netherlands
- [23] R. G. Pearson, *J. Am. Chem. Soc.* 85 (1963) 3533.



# Chapter 7

## LC/MS Studies on the *In Vitro* Degradation of Poly(ether ester) Block Copolymers\*

### 7.1 Abstract

A detailed study on the *in vitro* degradation of a biocompatible poly(ether ester) block copolymer, which is based on poly(ethylene glycol) and poly(butylene terephthalate), was carried out using liquid chromatography/electrospray-mass spectrometry. All major degradation products and several side-products were identified using both the positive and the negative ion mode. The data indicate that degradation does not only occur in the “soft”, but also in the “hard” segment of the polymer. Liquid chromatographic separation is required to distinguish between isomers. The addition of ammonium and sodium ions provided important complementary information on the number of monomer units.

\*A. A. Dechamps, A. A. van Appeldorn, H. Hayen, J. D. de Bruijn, U. Karst, D. W. Grijpma, J. Feijen, *Biopolymers*, accepted for publication

\*H. Hayen, A. A. Deschamps, D. W. Grijpma, J. Feijen, U. Karst, *J. Chromatogr. A*, submitted for publication

## 7.2 Introduction

Favorable thermal and mechanical properties are distinct features of aromatic polyesters as, e.g., poly(ethylene terephthalate) (PET) and poly(butylene terephthalate) (PBT). They are biocompatible [1] and often used as biomaterials [1,2]. Their relative stability under physiological conditions is, however, a significant drawback when biodegradability is required [3,4]. In contrast to aromatic polyesters, aliphatic polyesters turned out to be biodegradable. However, these lack sufficient mechanical strength. Therefore, aliphatic-aromatic copolyesters have been developed to serve as biodegradable polymers [4]. The copolymerization of poly(ethylene terephthalate) with lactic acid,  $\epsilon$ -caprolactone or ethylene oxide to form block and random copolymers are the modifications that have been mainly investigated in the development of biodegradable polymers [5]. The degradation of the latter has been investigated *in vitro* by Nagata et al. [6,7] and Reed and Gilding [8]. They found that *in vitro* degradation was due to hydrolysis of the ester bonds, which could be enhanced by the addition of enzymes.

The group of poly(ether ester) copolymers consisting of poly(ethylene oxide) (PEO) and PBT has been thoroughly studied regarding degradation processes and potential medical applications [9,10]. The *in vivo* degradation of PEOT/PBT segmented copolymers was described [11]. Two degradation pathways are expected *in vivo*: On the one hand, hydrolysis of ester bonds in the PBT part or hydrolysis of the ester bonds connecting PEO segments and terephthalate units. On the other hand, oxidative degradation of PEO based on a radical mechanism [12,13]. Both mechanisms were observed *in vitro*. While oxidation of PEO was observed in

H<sub>2</sub>O<sub>2</sub>/CoCl<sub>2</sub> solution [14], hydrolysis was most abundant in respect of PEOT/PBT degradation under non-oxidative conditions [14,15].

The extent of biodegradability can be estimated by the weight loss of copolymer films incubated in buffer solutions [7,8]. Apart from weight loss and water uptake, material properties as, e.g., glass transition temperature and intrinsic viscosity, can be used to investigate the degradation behavior of the polymer [14,15]. The hydrolytic degradation of the polyesters involves cleavage of ester bonds. Therefore, this reaction can be followed by measuring the increasing amount of carboxyl end groups. Zhang and Ward determined the rate of formation of carboxyl end groups using infrared spectroscopy [16]. Furthermore, <sup>1</sup>H-NMR has turned out to be a helpful tool for the determination of degradation products in solution [14,15].

However, all these methods have in common that they give an indication of the remaining products, but not on the variety of degradation products that become soluble in the buffer solution. To overcome this limitation, mass spectrometric (MS) methods may be applied. Mass spectrometry, in the present case mainly matrix assisted laser desorption/ionization (MALDI)-MS and electrospray ionization (ESI)-MS, has turned out to be a versatile tool for the analysis of copolymers [17]. These techniques are also applied with respect to polymer characterization [18,19]. In order to enhance selectivity, these MS methods may also be coupled to liquid chromatography [17-19].

In a preliminary study of 1000 PEOT71/PBT29 (a copolymer based on PEG with a molecular weight of 1000 g/mol and 71 wt% of PEO-containing soft segments)

degradation products, which are soluble in PBS buffer, liquid chromatographic separation with subsequent photometric and mass spectrometric detection was performed [15]. Atmospheric pressure chemical ionization (APCI) was applied both in the positive and the negative ion mode. In APCI(-), terephthalic acid and the monoester of terephthalic acid and butanediol were identified. In the positive ion mode, PEG and PEG linked to one molecule of terephthalate were found as degradation products. Although more degradation products were visible by photometric detection, higher degradation products could not be identified. As APCI applies high temperatures to evaporate both eluent and analyte molecules, some drawbacks were observed while analyzing PEOT/PBT degradation products: On the one hand, application of low probe temperatures (below 400 °C) is insufficient for the evaporation of terephthalate linked to PEG or higher mass degradation products. On the other hand, the application of high temperatures in the range of 500 °C causes thermal degradation. Fragmentation of both the PEG starting material and the terephthalate-PEG species, respectively, was observed. Whereas the latter predominately revealed a loss of one terephthalate unit, the fragmentation of PEG was mainly characterized by the loss of ethylene glycol moieties. Thus, identification of higher degradation products was not possible. In contrast to APCI, ESI induces less thermal stress to the analytes. Therefore, ESI-MS detection was applied for the identification of higher degradation products of the 1000 PEOT71/PBT29 block copolymer. Especially, the nature of cleaved bond (ether or ester bond) and the part of the polymer where cleavage takes place (soft or hard segment) should be elucidated.

### 7.3 Experimental

#### *Chemicals*

Poly(ethylene glycol) of average molecular weight 1000 g/mol (PEG 1000) (Fluka, Switzerland), poly(butylene terephthalate) (PBT) (Aldrich, Milwaukee, Wisconsin, USA), titanium tetrabutoxide ( $\text{Ti}(\text{OBU})_4$ ) (Merck, Darmstadt, Germany), dimethyl terephthalate (Merck, Darmstadt, Germany), 1,4-butanediol (Acros organics, Geel, Belgium) and Irganox 1330 from (Ciba-Geigy, Basel, Switzerland) were used without further purification. All solvents used were analytical grade (Biosolve, Valkenswaard, The Netherlands). As buffer for degradation experiments, phosphate buffered saline (PBS, NPBI, Emmer-Compascuum, The Netherlands) was applied. Solvents for liquid chromatography were acetonitrile (elution grade) and methanol (elution grade) from Merck Eurolab (Fontenau S/Bois, France). Water for liquid chromatography was purchased from Merck (Briare le Canal, France). Terephthalic acid (Acros organics, Geel, Belgium) was used as a standard for HPLC measurements.

#### *Polymer synthesis and processing*

The PEOT/PBT multiblock copolymers were synthesized on a 50 g scale by a two-step polycondensation of PEG, 1,4-butanediol and dimethyl terephthalate in the presence of titanium tetrabutoxide as catalyst and Irganox 1330 as antioxidant [14,15]. Polymer films were prepared by compression molding (laboratory press THB008, Fontijne, The Netherlands) at a temperature of 140 °C. For the degradation experiments, discs of a thickness of 400-600  $\mu\text{m}$  and a diameter of 15 mm were prepared.

*In vitro degradation*

Hydrolysis of the PEOT/PBT discs was accelerated by refluxing the materials for 14 days in phosphate buffered saline. The polymer discs became very brittle and were recovered from the PBS solution by filtering. The soluble degradation products were characterized by LC/electrospray-MS as described in detail below.

*Analytical instrumentation*

For HPLC/MS measurements, the following equipment from Shimadzu (Duisburg, Germany) was used: SCL-10Avp controller unit, DGU-14A degasser, two LC-10ADvp pumps, SIL-10A autosampler, SPD10AV UV-vis detector, LCMS QP8000 single quadrupole mass spectrometer with electrospray ionization (ESI) probe and Class 8000 software Version 1.20.

*HPLC conditions*

All separations were performed using a Merck LiChroSher RP-18ec column with ChromCart cartridges (Macherey Nagel, Düren, Germany) of the following dimensions: Particle size, 5  $\mu\text{m}$ ; pore size, 100  $\text{\AA}$ ; 125 mm x 2 mm i.d. Flow rate of the mobile phase was 300  $\mu\text{L}/\text{min}$ .

With respect to the LC/electrospray-MS experiments in the positive ion mode, a binary gradient consisting of acetonitrile and buffer (either aqueous 20 mM ammonium formate/formic acid or aqueous 20 mM sodium formate/formic acid) was used. The gradient profile was the following:

LC/MS Studies on the in Vitro Degradation of Poly(ether ester) Block Copolymers

time (min)	0.01	1	100	108	112	114	120
c (CH <sub>3</sub> CN) (%)	10	10	70	100	100	10	stop

A binary gradient consisting of methanol and water was used for the electrospray-MS experiments in the negative ion mode. The gradient profile was the following:

time (min)	0.01	1	100	108	112	114	120
c (CH <sub>3</sub> CN) (%)	20	20	80	100	100	20	stop

The injection volume was set to 5  $\mu$ L and detection wavelengths were 251 and 300 nm, respectively.

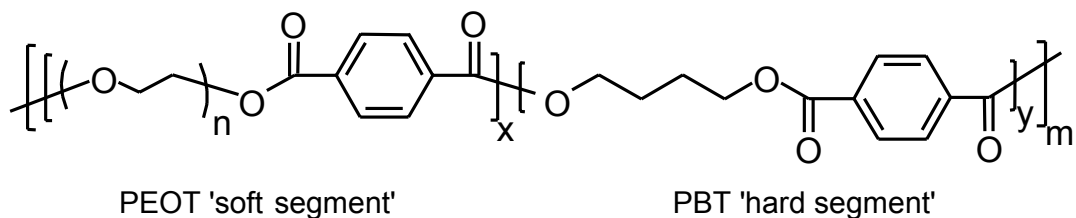
*MS conditions*

Electrospray-mass spectrometry measurements were performed in the positive ion mode using the following conditions: Probe voltage 3 kV, curved desolvation line (CDL) voltage -55 V, CDL temperature 250 °C, nebulizer gas (N<sub>2</sub>) flow rate 4.5 L/min, deflector voltages 35 V and detector voltage 1.7 kV. For SCAN mode measurements, a mass range from m/z 200 – 1600 was chosen, and the integration time was 1 s.

Electrospray-mass spectrometry measurements in the negative ion mode were carried out applying the following conditions: Probe voltage -5 kV, curved desolvation line (CDL) voltage 50 V, CDL temperature 250 °C, nebulizer gas (N<sub>2</sub>) flow rate 4.5 L/min, deflector voltages -55 V and detector voltage 1.7 kV were used. For SCAN mode measurements, a mass range from m/z 100 – 500 was chosen, and the integration time was 1 s.

## 7.4 Results and Discussion

The structure of a 1000 PEOT71/PBT29 segmented block copolymer is presented in Figure 7.1.



**Figure 7.1:** Chemical structure of 1000 PEOT71/PBT29 block copolymer.

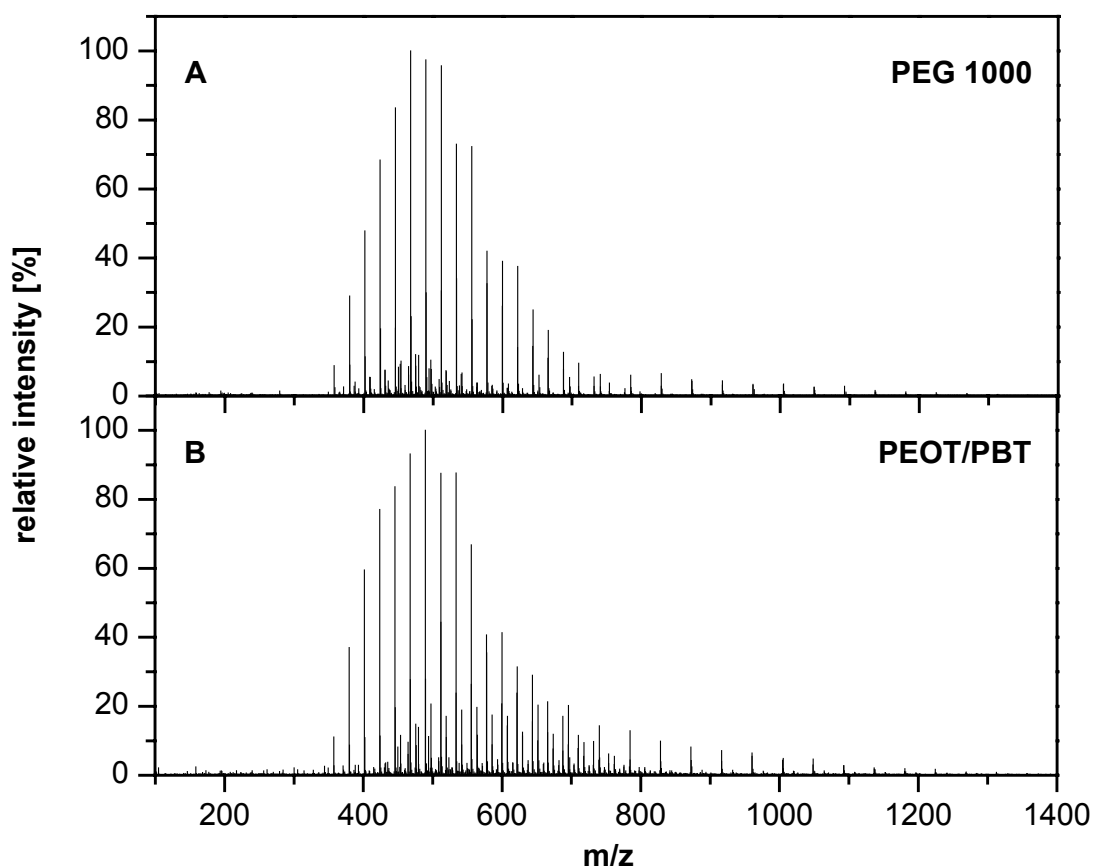
The composition of the block copolymer is abbreviated as  $a\text{PEOT}b/\text{PBT}c$ , in which  $a$  is the starting PEO molecular weight,  $b$ , the weight percentage of PEOT soft segments and  $c$ , the weight percentage of PBT hard segments. It has to be noted that terephthalic acid ester units are present in both the soft and the hard segment. Therefore, the notation PEOT (T for terephthalate) is used to refer to the soft part. The abbreviation PEO is used to refer to the repeating segment in the copolymer, whereas PEG is used to refer to the material applied for the synthesis.

While the hard segment is characterized only by ester bonds, the soft segment with its ether bonds is likely to be cleaved to a large extent under formation of PEG. For this reason, initial experiments focused on a comparison of the PEG 1000, which is used for the synthesis of the block copolymer with the soluble products obtained from the *in vitro* degradation of the block copolymer. These experiments were carried out without LC separation by directly injecting diluted aqueous PEG solutions (0.5 mM) as well as the diluted degradation product solutions in PBS buffer into the mass spectrometer. The latter were diluted 1:10 with water and filtered through a  $0.45\ \mu\text{m}$



membrane filter. For these experiments, the single quadrupole mass spectrometer was operated using the electrospray interface in the positive ion mode, as is typically performed for instrument tuning with PEG standards.

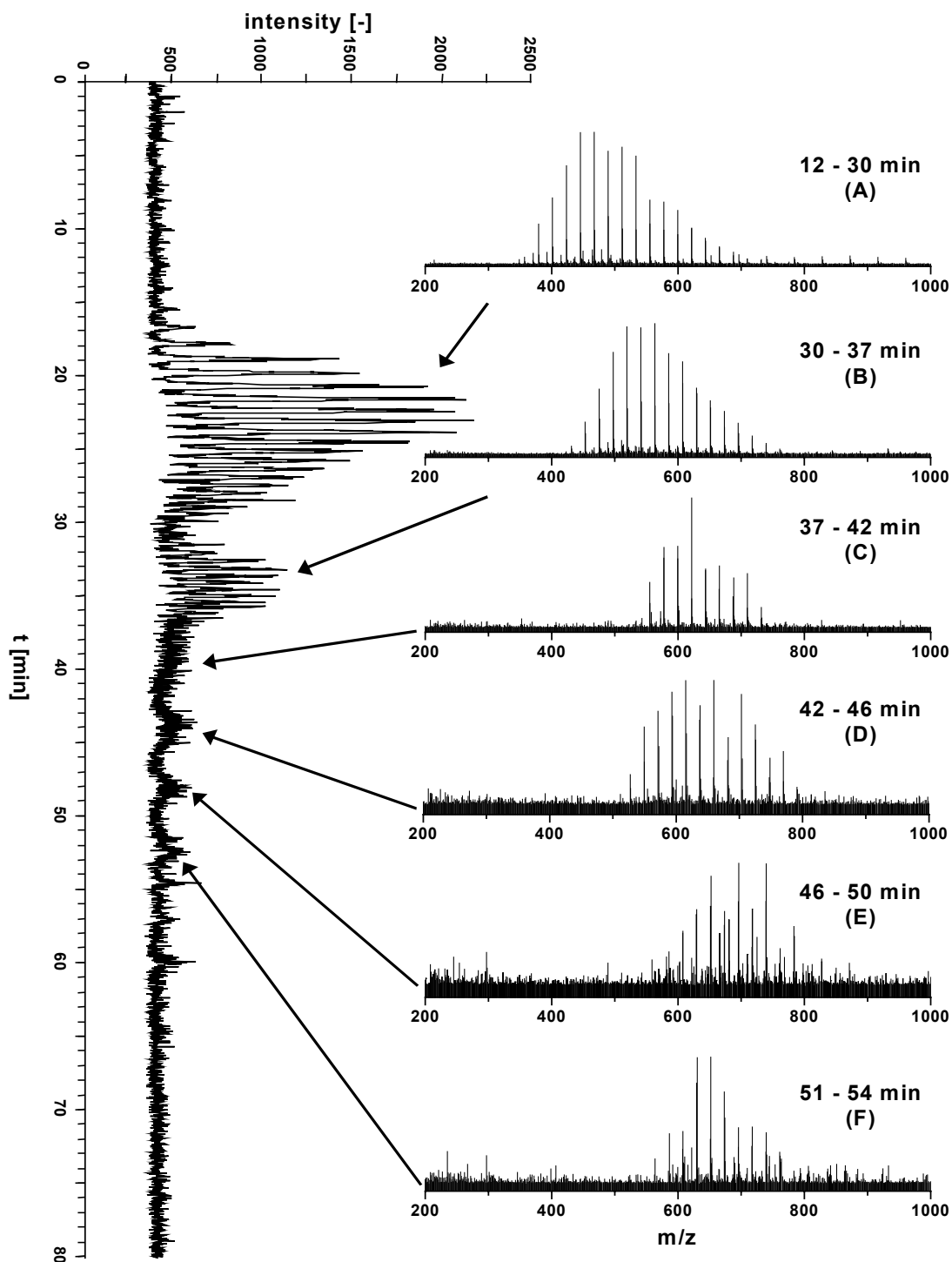
It is obvious from Figure 7.2 that there are strong similarities between the main peak patterns of the PEG standard and the degradation products in solution.



**Figure 7.2:** Mass spectra of PEO 1000 standard (A) and soluble products derived from 1000 PEOT71/PBT29 block copolymer (B) with electrospray ionization in the positive ion mode.

The peak distribution of the main pattern is almost identical for both samples, indicating that a large amount of PEG is released during the hydrolysis experiment. Due to the doubly charged individual substances (see below for interpretation of the mass spectra), the mass difference between the individual major peaks is  $m/z = 22$ , corresponding to one ethylene oxide unit. Interestingly, there is no degradation of the ether groups in the PEG chains, which should result in a peak distribution shifted to maxima at lower  $m/z$  values. On the other hand, it can be seen that several peak distributions with lower intensities are only observed for the degradation products in solution. This is a first indication that different bonds are broken to a significant extent during these experiments.

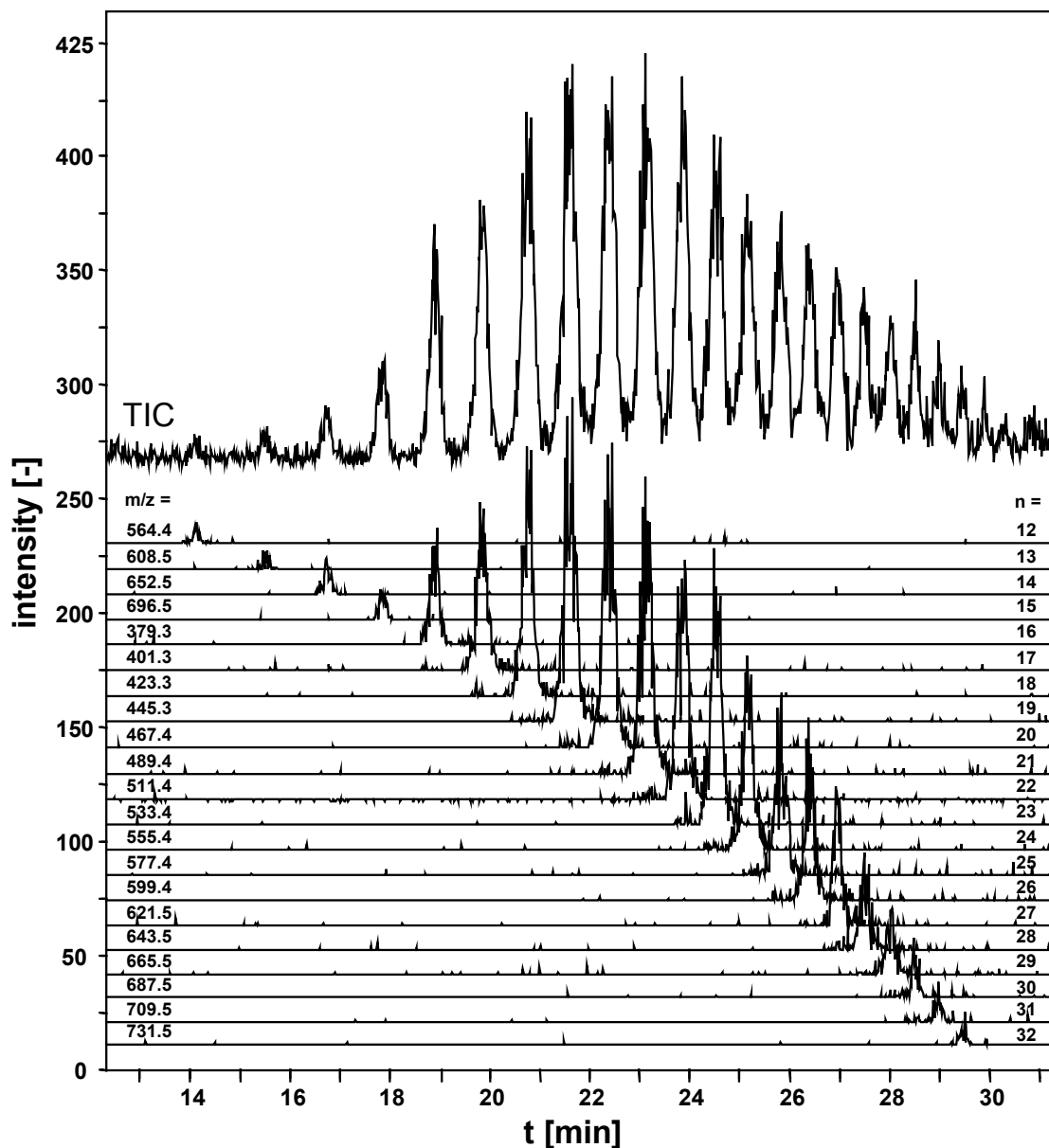
With a single quadrupole mass spectrometer, it is not possible to resolve a sufficient number of peak distributions. For this reason, reversed-phase liquid chromatography was carried out using an endcapped C18 stationary phase in combination with a binary gradient of acetonitrile and aqueous formic acid/ammonium formate buffer. As excellent resolution between the individual oligomers was intended, a long gradient with a total duration of two hours was selected. With respect to direct-injection experiments, the mass spectrometer was operated using the electrospray probe in the positive ion mode. In Figure 7.3, the total ion current (TIC) chromatogram is presented. For the substances eluting between 12 and 30 minutes, an excellent separation is observed already for the individual substances within one distribution. The inserted Figures contain the complete mass spectra of a combined time period, e.g., from 12 to 30 minutes.



**Figure 7.3:** Liquid chromatographic separation of the soluble degradation products derived from 1000 PEOT71/PBT29 with ESI(+)-mass spectrometric detection recorded in SCAN mode ( $m/z = 200 - 1600$ ). Inserted are extracted mass spectra representing six peak series eluting at different retention times.

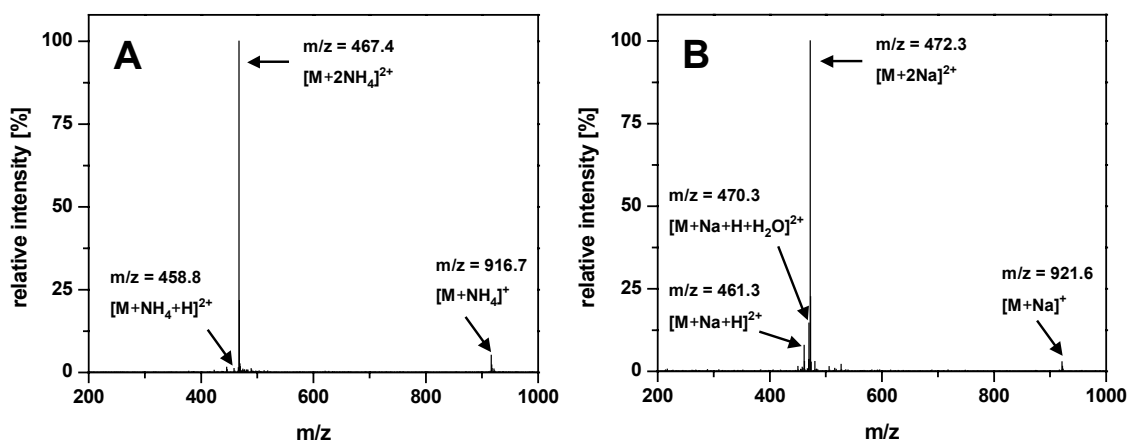
As in Figure 7.2, all major peaks in the mass spectra are associated with doubly charged ions, resulting in variations of  $m/z = 22$ , which correspond to individual ethylene oxide units. A comparison with a PEG 1000 standard proves that peak group A corresponds to the unmodified PEG 1000 itself, while peak groups B to F correspond to higher degradation products, which are discussed below.

The TIC chromatogram in Figure 7.4 is an extract of the chromatogram in Figure 7.3, which covers the retention times from 12 to 31 minutes. Two series of individual mass traces are presented below the TIC chromatogram. All peaks correspond to the PEG oligomers comprising  $n = 12 - 32$  ethylene oxide units. Due to the mobile phase used, the ammonium adducts are observed with the highest abundance. For the lower oligomers with  $n = 12 - 15$ , the singly charged adducts of one  $\text{NH}_4^+$  are most abundant. For the higher oligomers, the doubly charged adducts of two ammonium ions are observed with the highest intensity. While the lower oligomers are baseline separated by LC, there is still a very good separation for the higher oligomers.



**Figure 7.4:** Part of the liquid chromatographic separation (12 - 31 min) of the soluble degradation products derived from 1000 PEOT71/PBT29 with ESI(+)-mass spectrometric detection recorded in SCAN mode ( $m/z = 200 - 1600$ ). Displayed are the base-shifted mass traces corresponding to the PEO oligomers. The peaks correspond to numbers of EO units ranging from 12 to 32.

In Figure 7.5, the mass spectrum of the peak at a retention time of 22 minutes (compare Figure 7.4) is presented on the left side. On the right side, the mass spectrum of the same peak resulting from an LC separation using a different mobile phase containing sodium formate instead of ammonium formate is presented.

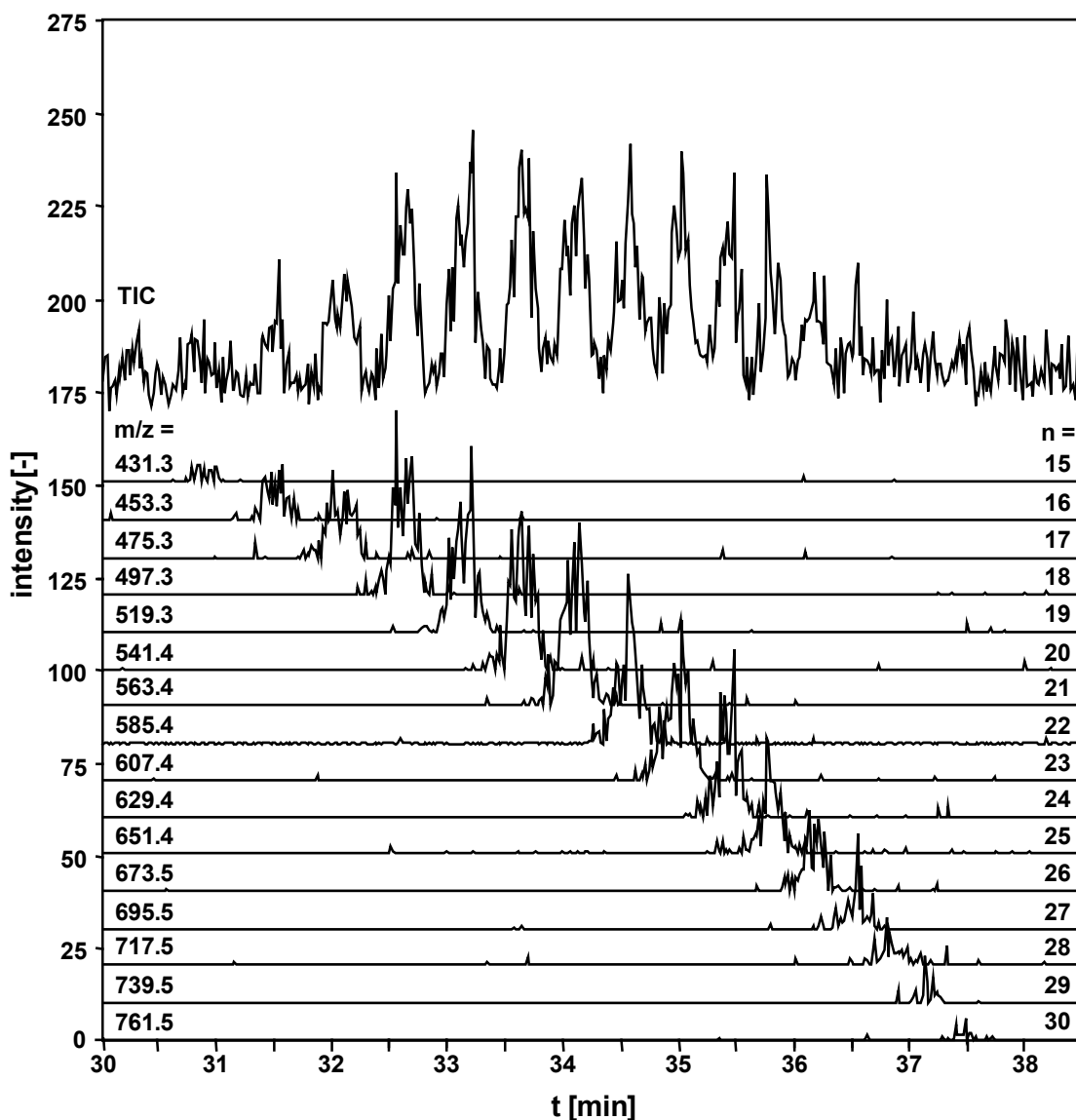


**Figure 7.5:** ESI(+)-mass spectra of the PEO oligomer ( $n = 20$ ) with ammonium ions (A) and sodium ions (B) in the mobile phases.

As expected for the electrospray analysis of PEG distributions, adducts of  $Na^+$ ,  $NH_4^+$  or  $H^+$  are observed. To elucidate the nature of the adducts (kind and number of the associated cations), the comparison between the mobile phases containing sodium or ammonium salts is very helpful. Together with an investigation of the  $^{13}C$  satellite peak to obtain the charge state, these experiments help to obtain the molecular weight information of the species. Regarding the PEG distribution itself, this is not absolutely necessary, because a comparison with the commercially available PEG starting material together with the retention time does already allow an unambiguous identification. For the other decomposition products, this is different. However, to explain the strategy, the procedure is first carried out with PEG itself.

With respect to the ammonium-containing mobile phase, the mass spectrum of the PEG with  $n = 20$  exhibits a  $[M+NH_4]^+$  at  $m/z = 916.7$  as well as a  $[M+2NH_4]^{2+}$  at  $m/z = 467.4$  and a  $[M+H+NH_4]^{2+}$  at  $m/z = 458.8$ . The respective mobile phase containing sodium leads to similar results:  $[M+Na]^+$  at  $m/z = 921.6$  as well as a  $[M+2Na]^{2+}$  at  $m/z = 472.3$  and  $[M+H+Na]^{2+}$  at  $m/z = 461.3$ . The  $m/z$  difference of 5 between  $[M+NH_4]^+$  and  $[M+Na]^+$  already indicates a singly charged species, which is confirmed by the  $^{13}C$  satellite peak. Additionally, the adduct of a proton and a sodium ion can be easily identified compared with the respective ammonium adduct, because the  $m/z$  difference of 2.5 indicates only one exchange between sodium and ammonium ( $m/z$  difference of 5), but a doubly charged PEG, which is also obvious from the  $^{13}C$  satellite peaks. Only for the mobile phase containing sodium ions, a  $[M+Na+H+H_2O]^{2+}$  at  $m/z = 470.3$  is observed as well. A respective peak is not observed for the mobile phase containing ammonium ions. Considering the complete PEG distribution as shown in Figure 7.4, the adduct of one ammonium ion is observed for  $n = 8 - 39$  ( $n = 10 - 30$  for one sodium ion), of two ammonium ions for  $n = 8 - 31$  (sodium:  $n = 13 - 36$ ), of one ammonium ion and one proton for  $n = 16 - 33$  (sodium:  $16 - 29$ ), and for three ammonium ions for  $n = 28 - 40$  (sodium:  $24 - 38$ ). The adduct of one sodium ion, one proton and one water molecule is observed for  $n = 19 - 32$ . Using these considerations, the higher degradation products were characterized as well as described below. The major result of the interpretation of this group of peaks is the fact that there is obviously no cleavage of the ether bonds in the PEG under the degradation conditions.

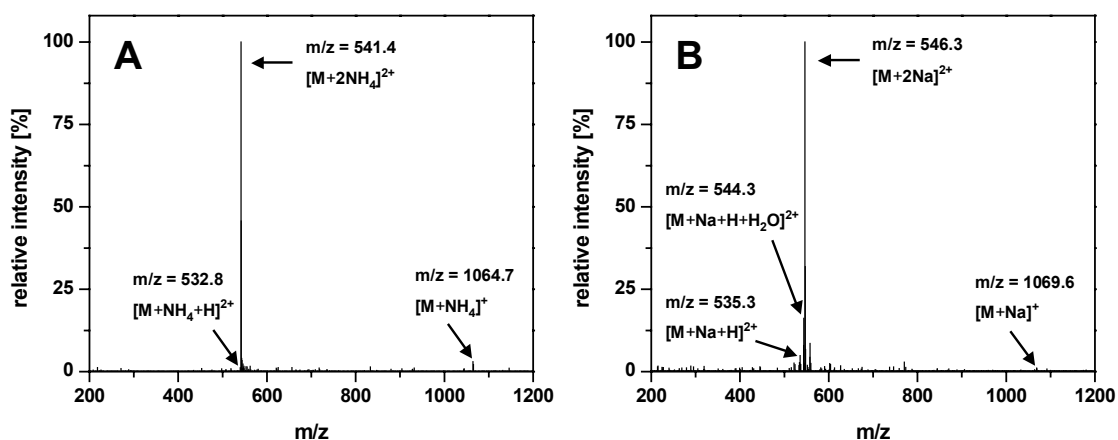
Series B in Figure 7.3 comprises peaks eluting between 30 and 38 minutes, and the peaks are presented in an expanded manner in Figure 7.6.



**Figure 7.6:** Part of the liquid chromatographic separation (30-39 min) of the soluble degradation products derived from 1000 PEOT71/PBT29 with ESI(+)-mass spectrometric detection recorded in SCAN mode ( $m/z = 200 - 1600$ ). Displayed are the base-shifted mass traces corresponding to one terephthalate molecule linked to PEO molecules. For this series, the peaks correspond to numbers of EO units ranging from 15 to 30.



The peak distribution indicates that PEG is involved, and the  $m/z$  ratios allow the conclusion that this series comprises the adducts of the PEG oligomers with one molecule of terephthalate (PEG + T). The  $m/z$  difference of 22 indicates that doubly charged ions are observed again. All extracted mass traces in Figure 7.6 correspond to the respective  $[M+2NH_4]^{2+}$  ions. In Figure 7.7, the mass spectra of the (PEG + T) oligomer with  $n = 20$  are presented with ammonium ions (left) and sodium ions (right) in the mobile phases.

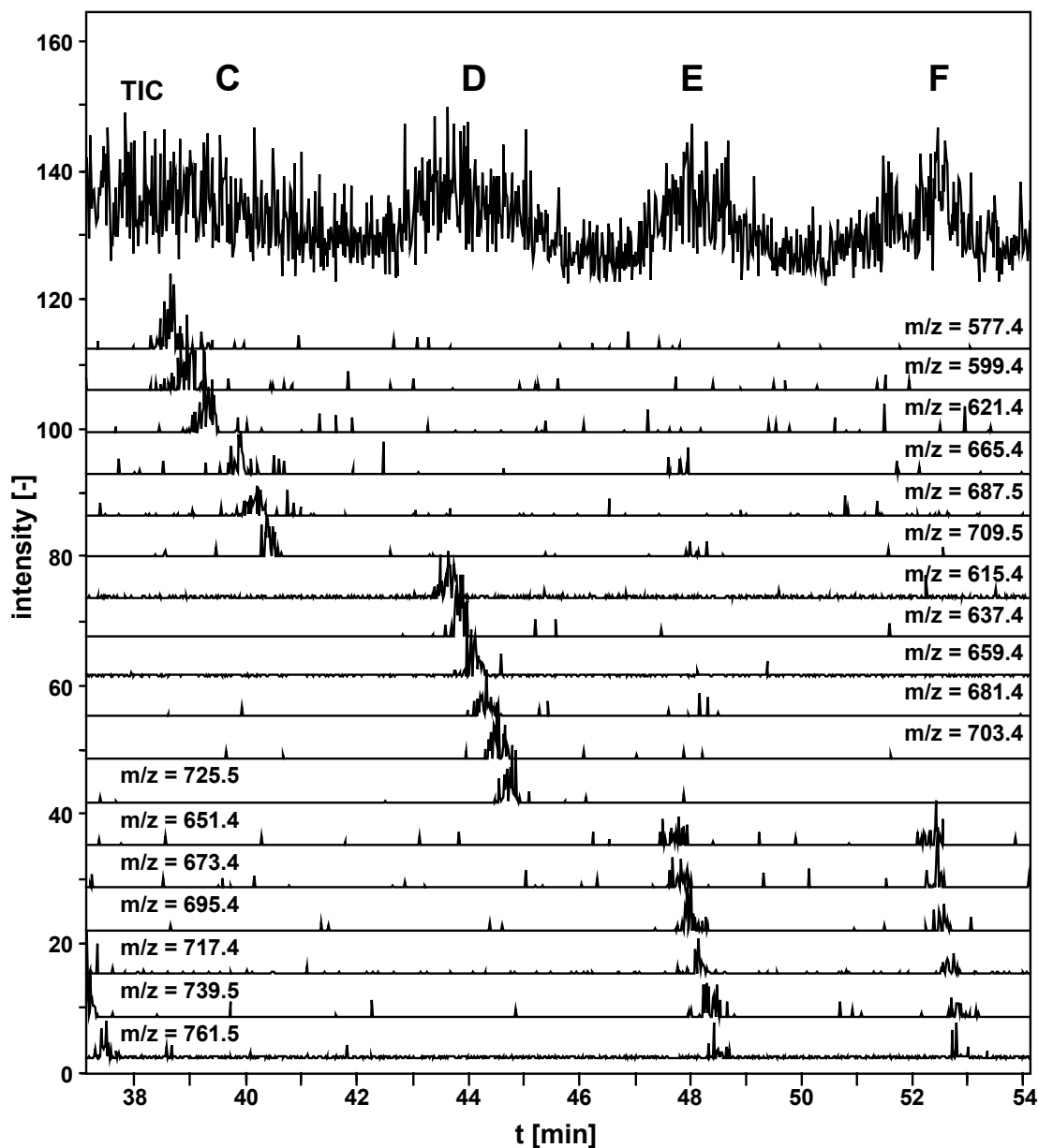


**Figure 7.7:** ESI(+)-mass spectra of terephthalate linked to one PEO oligomer ( $n = 20$ ) with ammonium ions (A) and sodium ions (B) in the mobile phases.

For this compound, the mass spectra are very similar to the mass spectra for the PEG oligomer with  $n = 20$ . However, regarding the (PEG + T) sequence, the sodium adducts are observed with much lower intensity than the ammonium adducts. Therefore, the mobile phase including ammonium formate was applied for all further measurements of the higher degradation products.

In Figure 7.8, it is obvious in the TIC chromatogram (extract of Figure 7.3 from 37 to 54 minutes) that the oligomers of the higher degradation products are not baseline

separated by LC. Nevertheless, the extracted mass traces prove that the distributions may still be detected mass spectrometrically.



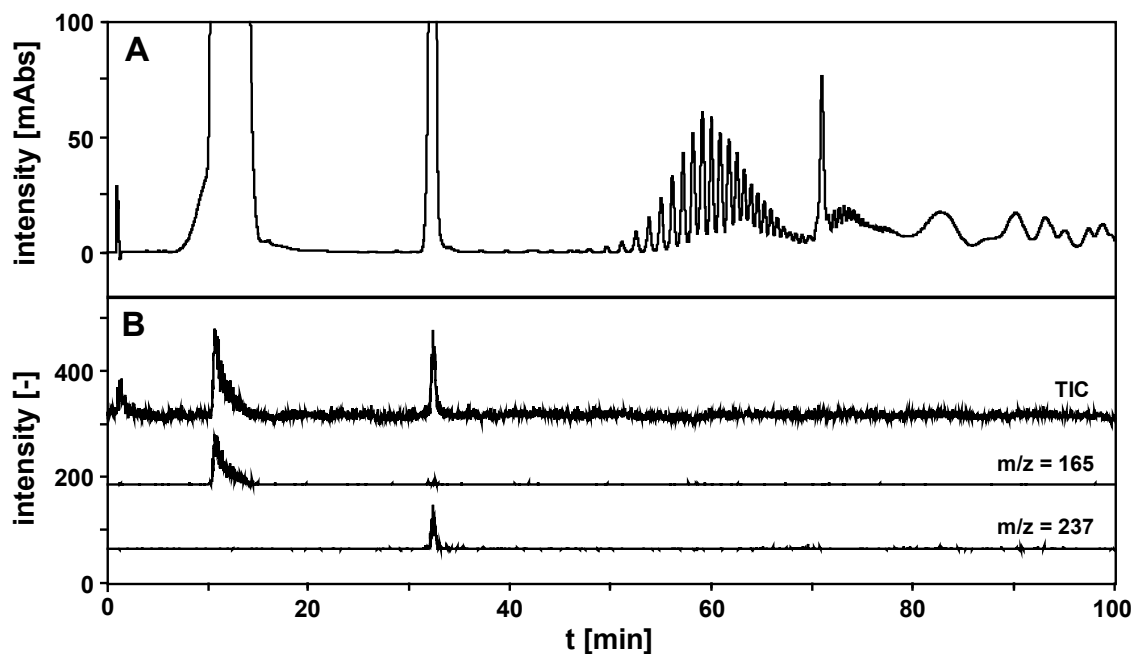
**Figure 7.8:** Part of the liquid chromatographic separation (37–54 min) of the soluble degradation products derived from 1000 PEOT71/PBT29 with ESI(+)-mass spectrometric detection recorded in SCAN mode ( $m/z = 200 - 1600$ ). Displayed are the base-shifted mass traces corresponding to the linked PEO molecules: PEO + T + Bu (series C), T + PEO + T (series D), and PEO + T + Bu + T or Bu + T + PEO + T (series E and F). For the four series, the peaks correspond only for the numbers of EO units ranging from 20 – 25.

The extracted mass traces are the  $[M+2NH_4]^{2+}$  ions in all cases. Peak series C contains the degradation products consisting of one PEG unit, one terephthalate residue and one butanediol rest (PEG + T + Bu) and series D are (T + PEG + T). Series E and F are both composed of one PEG unit, two terephthalate residues and one butanediol rest. However, the two possible different sequences (PEG + T + Bu + T) and (Bu + T + PEG + T) obviously lead to a different chromatographic behavior of the series. It can be assumed that the larger polarity of (PEG + T + Bu + T) results in earlier elution. The LC separation of the two isomers clearly proves that both sequences are present in the sample, thus demonstrating again that the LC separation provides very useful data, which could not be obtained with mass spectrometry alone.

Furthermore, it should be noted that the (PEG + T) peak series (compare to Figure 7.6) and the peak series E and F in Figure 7.8 differ by 220 mass units. It is obvious from the mass traces of  $m/z = 739.5$  and  $m/z = 761.5$  in Figure 7.8 that the higher homologues ( $n = 29$ ,  $n = 30$ ) of the (PEG + T) series are detected at retention times between 37 and 38 minutes. The same  $m/z$  values are observed for series E and F, but in this case for  $n = 24$  and  $n = 25$ , because the mass of the additional (T + Bu) in series E and F equals that of five ethylene oxide units. Under reversed-phase LC conditions, the decomposition product with higher polarity (more ethylene oxide units) elutes first. Without LC separation, it would not be possible to distinguish between these series.

As a significant number of degradation products contains terephthalate, showing strong UV-vis absorption at  $\sim 251$  nm, HPLC separation with subsequent UV

detection had already been performed in an earlier study [15]. In Figure 7.9, a liquid chromatographic separation of the complete mixture of degradation products comparing photometric detection at  $\lambda = 251$  nm (Figure 7.9A) and ESI(-)-MS detection (Figure 7.9B) is presented.



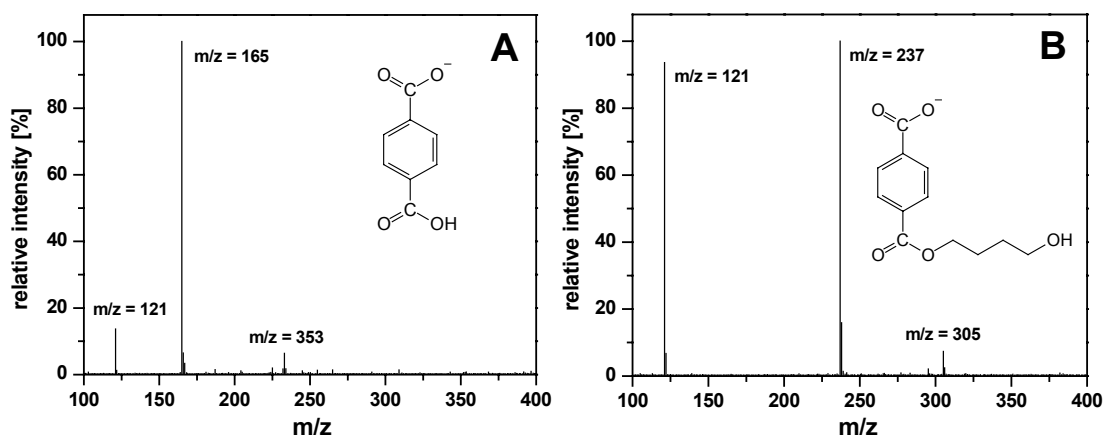
**Figure 7.9:** Liquid chromatographic separation of the soluble degradation products derived from 1000 PEOT71/PBT29 with UV detection at 251 nm (A) and mass spectrometric detection (B) applying ESI(-) conditions recorded in SCAN mode ( $m/z = 100 - 500$ ).

In the negative ion mode, deprotonation of terephthalic acid is expected. This had already been shown in a previous study in which atmospheric pressure chemical ionization (APCI) in the negative ion mode was applied [15].

Initial experiments were carried out with terephthalic acid as a standard in order to optimize the conditions for the ESI(-) detection. Since only small peaks for terephthalic acid were observed using acetonitrile as mobile phase constituent, it

was replaced by methanol. Methanolate,  $\text{CH}_3\text{O}^-$ , is a stronger gas phase base than the carbanion of acetonitrile  $^-\text{CH}_2\text{CN}$ . Thus, the use of the stronger gas phase base methanolate leads to increased proton abstraction and improved sensitivity. Owing to the lower elution strength of methanol, the amount of the latter which was used for the gradient had to be increased. Although the retention times were shifted to higher values, the elution order was not affected at all.

The total ion current (TIC) and two individual mass traces are presented in figure 9B. The signals of  $m/z = 165$  and  $m/z = 237$  correspond to the  $[\text{M}-\text{H}]^-$  peaks of terephthalic acid and the monoesters of butanediol and terephthalic acid, respectively. The full mass spectra of both compounds, recorded in a mobile phase containing methanol and aqueous formic acid/sodium formate, are presented in Figure 7.10.



**Figure 7.10:** ESI(-)-mass spectra of terephthalic acid (A) eluting at 10.8 min and monoester of butanediol and terephthalic acid (B) eluting at 32.4 min.

In Figure 7.10A (terephthalic acid), the  $[\text{M}-\text{H}]^-$  peak is most abundant, but the peaks of  $m/z = 121$  ( $[\text{M}-\text{CO}_2-\text{H}]^-$ ) and  $m/z = 353$  ( $2[\text{M}-\text{H}+\text{Na}]^-$ ) are observed as well. In Figure 10B (T + Bu), the  $[\text{M}-\text{H}]^-$  signal at  $m/z = 237$  is most abundant. The

$[M+HCOONa-H]^-$  peak at  $m/z = 305$  is observed, and the fragment at  $m/z = 121$  ( $[M-COO(CH_2)_4OH-H]^-$ ) is present, too. This ESI-MS data confirm the identification of terephthalic acid and the monoester of terephthalic acid and butanediol obtained with APCI-MS in the earlier study [15].

## 7.5 Conclusions

It can be concluded that the ester bonds within the block copolymer are much easier cleaved than the ether bonds of the PEG part. Due to the very similar chemical nature of all ester bonds within the block copolymer, it is likely that the cleavage is observed in a similar way for all ester bonds. However, the hydrolysis of ester bonds is also dependent on chain mobility and permeability [20-22]. The higher grade of crystallinity in the hard segment hinders the attack of water. In contrast, the amorphous and more hydrophilic PEO containing soft segment is much easier accessible by water. Thus, initial degradation is restricted to the amorphous soft segment. The fact that PEG is detected alone as major degradation product proves this assumption. To obtain these main fragments, both neighbouring ester bonds of PEO - the one within the soft segment and the one coupling it to other soft segments - have to be cleaved. However, cleavage of the ester bond connecting PEO to the hard segment is also possible. For the ester bond between Bu and T in the hard segment, a final proof for cleavage could only be the direct detection of either Bu or (Bu + T + Bu), as both could not be detected under the selected conditions. However, as both series C (PEG + T + Bu) and F (Bu + T + PEG + T) prove, there is at least a cleavage between Bu and T between a hard and a soft segment.

## 7.6 References

- [1] K. G. Dahmen, N. Maurin, H. A. Richter, C. H. Mittermayer, J. Mater. Sci. - Mater. Med. 8 (1997) 239.
- [2] A. J. A. Klomp, G. H. M. Engbers, J. Mol, J. G. A. Terlingen, J. Feijen, Biomaterials 20 (1999) 1203.
- [3] T. E. Rudakova, G. E. Zaikov, O. S. Voronkova, T. T. Daurova. S. M. Degtyareva, J. Polym. Sci. - Polym. Sym. 66 (1979) 277.
- [4] R. J. Muller, I. Kleeberg, W. D. Deckwer, J. Biotechnol. 86 (2001) 87.
- [5] D. Kint, S. Muñoz-Guerra, Polym. Int. 48 (1999) 346.
- [6] M. Nagata, T. Kiyotsukuri, S. Minami, N. Tsutsumi, W. Sakai, Polym. Int. 39 (1996) 83.
- [7] M. Nagata, T. Kiyotsukuri, S. Minami, N. Tsutsumi, W. Sakai, Eur. Polym. J. 33 (1997) 1701.
- [8] A. M. Reed, D. K. Gilding, Polymer 22 (1981) 499.
- [9] A. M. Radder, J. A. van Loon, G. J. Puppels, C. A. Van Blitterswijk, J. Mater. Sci. - Mater. Med. 6 (1995) 510.
- [10] R. Kuijjer, S. J. M. Bouwmeester, M. M. W. E. Drees, D. A. M. Surtel, E. A. W. Terwindt-Rouwenhorst, A. J. van der Linden, C. A. van Blitterswijk, S. K. Bulstra, J. Mater. Sci. - Mater. Med. 9 (1998) 449.
- [11] G. J. Beumer, C. A. van Blitterswijk, M. Ponec, J. Biomed. Mater. Res. 28 (1994) 545.
- [12] Y. Wu, C. Saletti, J. M. Anderson, A. Hiltner, G. A. Lodoen, C. R. Payet, J. Appl. Polym. Sci. 46 (1992) 201.
- [13] G. Botelho, A. Queiros, P. Gijsman, Polym. Deg. Stab. 70 (2000) 299.
- [14] A. A. Deschamps, D. W. Grijpma, J. Feijen, Polymer 42 (2001) 9335.

- [15] A. A. Deschamps, A. A. van Apeldoorn, H. Hayen, J. D. de Bruijn, U. Karst, D. W. Grijpma, J. Feijen, *Biomaterials* (2003) in press.
- [16] H. Zang, I. M. Ward, *Macromolecules* 28 (1995) 7622.
- [17] M. S. Mondaudo, *Mass Spectrom. Rev.* 21 (2002) 108.
- [18] S. D. Hanton, *Chem. Rev.* 101 (2001) 527.
- [19] R. Murgasova, D. M. Hercules, *Anal. Bioanal. Chem.* 373 (2002) 481.
- [19] Y. Wu, J. M. Anderson, A. Hiltner, G. A. Lodoen, C. R. Payet, *J. of Appl. Polym. Sci.* 46 (1992) 201.
- [20] D. Paszun, T. Szychaj, *Ind. Eng. Chem. Res.* 36 (1997) 1373.
- [21] N. S. Allen, M. Edge, M. Mohammadian, K. Jones, *Eur. Polym. J.* 27 (1991) 1701.
- [22] M. E. Cagiao, F. J. Baltá Calleja, C. Vanderdonckt, H. G. Zachmann, *Polymer* 34 (1993) 2024.



# Chapter 8

## Concluding Remarks and Future Perspectives

Three different approaches to expand the applicability of LC/MS to the analysis of non-polar compounds have been presented within this thesis. They comprise the coupling of electrochemistry to mass spectrometry, electron capture ionization in conjunction with APCI and coordination ionspray/mass spectrometry. These methods are complementary to APPI, which is already commercially available for the API mass spectrometers of most major manufacturers. From the current point of view, none of these techniques will achieve the status of an “universal” ionization technique for non-polar compounds, but all show a very high potential to be useful tools for particular applications.

The coupling of electrochemistry and MS will be limited to electroactive analytes, but the exploitation of this technique may deliver exciting new insights into biochemical redox reactions, and extremely low limits of detection may be achieved in combination with dedicated derivatizing agents. It can be expected that more research groups will enter this field soon, and that manufacturers will start developing dedicated instrumentation, e.g., electrochemical cells with low volume and high conversion rate. The development of cells, which are located very close to the electrospray emitter or the heated nebulizer would also be attractive to study fast redox reactions.

Electron capture ionization may be carried out on an existing LC/APCI-MS instrument, but its application is limited to compounds with strongly electron-withdrawing substituents, e.g., polyhalogenated and nitroaromatic compounds. In the bioanalytical field, an increasing development of dedicated derivatizing agents for electron capture APCI-MS can be expected. Future developments will certainly comprise work to better understand the similarities, but also the differences to electron capture ionization in gas chromatography/mass spectrometry. Special focus should be directed to the competition between deprotonation and electron capture, which is characteristic for this method. Sound knowledge on the involved mechanisms will be most important to synthesize and apply new derivatizing agents for electron capture APCI-MS, which would be valuable in fields as doping control, food chemistry and clinical diagnostics. For instrument manufacturers, the development of electron monochromators would be attractive, as it would allow to tune selectivity to a particular reagent and its derivatives.

With respect to coordination ionspray-MS, the consequent application of Pearson's classification is likely to lead to new and currently unexpected applications for the analysis of non-polar compounds. As mainly silver is applied to form charged complexes with the analyte molecule, the use of other cationizing agents certainly will broaden the scope of this technique. A large potential could be expected for  $\text{Ni}^{2+}$  and its coordination to proteins, or for "soft" transition metal cations as  $\text{Cu}^+$ ,  $\text{Pd}^{2+}$ ,  $\text{Au}^+$ , main group ions as  $\text{Pb}^{2+}$  or  $\text{Tl}^+$  and possibly even for small cluster cations with low charge. For the negative ion mode, anions as iodide or picrate could be attractive for coordination ionspray-MS. This technique offers least possibilities for instrument manufacturers, because the post-column set-up is simple and consists of

readily available components. Possible applications may be expected for polycyclic aromatic hydrocarbons, sulfur species in biochemistry and environmental chemistry and for heterocyclic compounds of limited polarity.



# Abbreviations

Å	Ångström
ANe	acenaphthene
Ant	anthracene
ANy	acenaphthylene
APCI	atmospheric pressure chemical ionization
API	atmospheric pressure ionization
APM	acetopromazine
APPI	atmospheric pressure photoionization
BaA	benzo[ <i>a</i> ]anthracene
BaP	benzo[ <i>a</i> ]pyrene
BbF	benzo[ <i>b</i> ]fluoranthene
BghiP	benzo[ <i>ghi</i> ]perylene
BkF	benzo[ <i>k</i> ]fluoranthene
c	concentration
CDL	curved desolvation line
CEC	capillary electrochromatography
Chr	crysene
CIS	coordination ionspray
CPZ	chloropromazine
DAD	diode array detector
dBA	dibenzo[ <i>a,h</i> ]anthracene
DMPO	5,5-dimethyl-1-pyrrolidone-N-oxide

## Abbreviations

---

DNPA	2,4-dinitrophenylazide
EI	electron ionization
EC	electron capture
ESI	electrospray ionization
Fla	fluoranthene
Fle	fluorene
FPZ	Fluphenazine
GC	gas chromatography
HPLC	high performance liquid chromatography
IcdP	indeno[1,2,3- <i>cd</i> ]pyrene
IR	infrared
LC	liquid chromatography
LC/MS	liquid chromatography/mass spectrometry
LOD	limit of detection
LOQ	limit of quantification
LPPI	low-pressure photoionization
MALDI	matrix assisted laser desorption/ionization-mass spectrometry
MDNA	<i>N</i> -methyl-2,4-dinitroaniline
MDNPH	<i>N</i> -methyl-2,4-dinitrophenylhydrazine
NMR	nuclear magnetic resonance
MNBDA	<i>N</i> -methyl-7-hydrazino-4-amino-2,1,3-benzoxadiazole
MNBDH	<i>N</i> -methyl-7-hydrazino-4-nitro-2,1,3-benzoxadiazole
MS	mass spectrometry
Naph	naphthalene
NBD-Cl	4-chloro-7-nitro-2,1,3-benzoxadiazole

NBDPZ	4-nitro-7-piperazino-2,1,3-benzoxadiazole
NICI	negative-ion chemical ionization
NP	normal-phase
ODS	octadecyl silica
PAH	polycyclic aromatic hydrocarbon
PB	particle beam
PBT	poly(butylene terephthalate)
PCP	prochloroperazine
PEEK	polyetheretherketone
PEG	poly(ethylene glycol)
PEO	poly(ethylene oxide)
PEOT/PBT	poly(ethylene oxide) and poly(butylene terephthalate) copolymer
PET	poly(ethylene terephthalate)
PFB	pentafluorobenzyl
Phen	phenanthrene
PM	promazine
PPZ	perphenazine
Pyr	pyrene
PZ	phenothiazine
R <sup>2</sup>	regression coefficient
RP	reversed-phase
RSD	relative standard deviation
SIM	selected ion monitoring
T-3-H	trans-3-hexene
TESD	1,10-bis-(triethoxysilyl)decane

## *Abbreviations*

---

TESPT	bis-(3-triethoxysilylpropyl)tetrasulfide
TFM	triflupromazine
TFP	trifluoperazine
THD	thioridazine
TIC	total ion current
TME	2,3-dimethyl-2-butene, tetramethylene
TMeSPT	bis-(3-trimethylsilylpropyl)tetrasulfide
TMP	trimeprazine
TNT	2,4,6-trinitrotoluene
TOF	time of flight
TSP	thermospray
UV	ultraviolet
Vis	visible



# Summary

Strategies to expand the applicability of LC/MS to the analysis of non-polar compounds are presented within this thesis: The most important techniques presented here are on-line electrochemical conversion of the analytes to more polar reaction products, atmospheric pressure electron capture negative ion-MS and coordination ionspray-MS. These techniques are presented in detail, compared and discussed critically with respect to their current status and future perspectives. Particular focus is directed from a chemical point of view on the substance groups which are accessible by each of the new approaches.

The coupling of electrochemistry to mass spectrometry was used for the on-line conversion of phenothiazines and polycyclic aromatic hydrocarbons (PAHs). LC/atmospheric pressure electron capture negative ion-MS was applied for the analysis of several nitroaromatic compounds, whereas LC/coordination ionspray-MS was used for the identification of reaction products in a model rubber vulcanization process. Soluble degradation products of a poly(ether ester) block copolymer were identified by means of LC/electrospray-MS in conjunction with the addition of ammonium and sodium ions to provide important complementary information on the number of monomer units.

The on-line electrochemical conversion of phenothiazine and its derivatives after liquid chromatographic separation has been studied by mass spectrometry and fluorescence spectroscopy. In an electrochemical cell consisting of a porous glassy

carbon working electrode, the phenothiazines are readily converted to oxidized products, which can be detected by on-line fluorescence spectroscopy and mass spectrometry. The method allows rapid investigations on the electrochemical oxidation pathways, as demonstrated for phenothiazine itself. The phenothiazine derivatives are transferred into their strongly fluorescent sulfoxides. Based on this reaction, an LC/electrochemistry/ fluorescence method was developed.

An efficient way for the fast elucidation of electrochemical reactions of polycyclic aromatic hydrocarbons has been set-up by coupling electrochemistry on-line to mass spectrometry. With this set-up, an improvement of sensitivity in the LC/MS analysis of PAHs is observed. Due to their low redox potentials, the non-polar PAHs are converted into the respective radical cations, which may further react with constituents of the mobile phase and in additional electrochemical oxidation steps. Among other products, mono-, di- and trioxygenated species are observed in aqueous solutions, alkoxyated compounds in alcohols and solvent adducts in the presence of acetonitrile. Deuterated PAHs and deuterated solvents were used to gain additional information on the formation of the reaction products.

The determination of selected nitroaromatic compounds by means of LC/MS with electron capture ionization using a commercial atmospheric pressure chemical ionization (APCI) interface in the negative ion mode was carried out. The electron capture effect is observed for nitroaromatics which do not easily undergo deprotonation under these conditions. Depending on the structure of the analytes, either dissociative or non-dissociative electron capture is observed. Limits of detection and linear range for the determination of the analytes match those

obtained for nitroaromatics which undergo deprotonation. The investigated substances comprise numerous substituted nitrobenzenes and nitrobenzoxadiazols including the amine derivatives of 4-chloro-7-nitro-2,1,3-benzoxadiazole (NBDCI) as well as the isocyanate derivatives of 4-nitro-7-piperazino-2,1,3-nitrobenzoxadiazole (NBDPZ). The parameters favoring electron capture mechanisms have been thoroughly investigated under consideration of the competing mechanism of deprotonation to allow a better understanding of the electron capture process and to improve sensitivity and selectivity of the analysis.

Liquid chromatography/coordination ionspray-mass spectrometry has been used for the identification of reaction products in a model rubber vulcanization process. After LC separation using reversed-phase conditions,  $\text{AgBF}_4$  was used to form a charged cation-analyte complex, which was detected by ESI-MS. Strong signals were observed for vulcanization accelerators and products of the reaction between these and alkenes. The method performs best for substances containing sulfur chains with chainlengths between two and eight sulfur atoms, but sulfur-free compounds containing triethoxysilyl groups were detected as well. For the latter, the post-column addition of  $\text{NaBF}_4$  proved to be a suitable alternative. Besides the vulcanization accelerators, various reaction products, including sulfur-chain bridged alkenes were identified.

A detailed study on the *in vitro* degradation of a biocompatible poly(ether ester) block copolymer, which is based on poly(ethylene glycol) and poly(butylene terephthalate), was carried out using LC/ESI-MS. All major degradation products and several side-products were identified using both the positive and the negative ion mode,

## Summary

---

respectively. The data indicate that degradation does not only occur in the “soft”, but also in the “hard” segment of the polymer. Liquid chromatographic separation is required to distinguish between isomers. The addition of ammonium and sodium ions provided important complementary information on the number of monomer units.

# Samenvatting

In dit proefschrift zijn enkele strategieën voorgelegd ter uitbreiding van de toepasbaarheid van LC/MS voor de bepaling van apolaire verbindingen. De belangrijkste weergegeven technieken zijn: on-line elektrochemische conversie van de te bepalen verbindingen naar polairdere reactieproducten, atmospheric pressure electron capture negative ion-MS en coordination ion spray-MS. Deze technieken zijn gedetailleerd beschreven, vergeleken en kritisch bediscussieerd ten opzichte van hun huidige status en perspectieven. Vanuit chemisch oogpunt is er speciale aandacht gericht op de groepen verbindingen die voor de verschillende nieuwe benaderingen toegankelijk zijn.

De koppeling van elektrochemie aan massaspectrometrie is benut voor de on-line omzetting van phenothiazines en polycyclische aromatische koolwaterstoffen (PAKs). LC/atmospheric pressure electron capture negative ion-MS is benut ter identificatie van reactieproducten in een rubbervulcanisatiemodel. Oplosbare afbraakproducten van een poly(ether-ester) blok copolymeer zijn geïdentificeerd door middel van LC/electrospray-MS, in combinatie met toevoeging van ammonium- en natriumionen aan het eluens om belangrijke aanvullende informatie te leveren over het aantal monomeereenheden.

De na vloeistofchromatografische scheiding on-line elektrochemisch omgezette phenothiazine en zijn derivaten zijn bestudeerd met massaspectrometrie en fluorescentiespectroscopie. In een elektrochemische cell met een werkelektrode van

poreuze koolstof worden de phenothiazines snel omgezet in geoxydeerde producten, die on-line door middel van fluorescentiespectroscopie en massaspectrometrie gedetecteerd kunnen worden. Deze methode maakt een snelle studie mogelijk naar de reactiestappen in elektrochemische oxidatie, zoals is getoond voor phenothiazine zelf. De phenothiazinederivaten worden omgezet in hun sterk fluorescerende sulfoxiden. Gebaseerd op deze reactie is een LC/elektrochemie/fluorescentie methode ontwikkeld.

Voor snelle opheldering van elektrochemische reacties van PAKs is een efficiënte methode opgezet door elektrochemie on-line te koppelen aan massaspectrometrie. Met deze opstelling is verbetering waargenomen in de gevoeligheid van PAKs-detectie in LC/MS analyse. Vanwege hun lage redoxpotentiaal worden de apolaire PAKs geconverteerd naar de respectievelijke radicaalkationen, die in opvolgende elektrochemische oxidatiestappen verder kunnen reageren met onderdelen van de mobiele fase. Als resultaat worden onder andere enkelvoudig, tweevoudig, en drievoudig geoxideerde producten gevonden in waterig milieu, gealkoxylerde verbindingen in alcoholische oplosmiddelen en oplosmiddel-adducten in aanwezigheid van acetonitriël. Gedeuteerde PAKs en gedeuteerde oplosmiddelen zijn gebruikt om aanvullende informatie in te winnen over de vorming van de reactieproducten.

Een selectie van nitroaromatische verbindingen is bepaald door middel van LC/MS met electron capture ionization, gebruik makend van een commerciële atmospheric pressure chemical ionization interface in de negatieve ionenmodus. Het

elektronenvangsteffect is geobserveerd voor nitroaromaten die onder deze omstandigheden niet zo makkelijk deprotonatie ondergaan. Afhankelijk van de structuur van de te bepalen stoffen wordt er of dissociatieve of niet-dissociatieve elektronenvangst waargenomen. De bereikte detectielimieten en lineaire gebieden voor de bepaling van deze verbindingen liggen gelijk aan die voor nitroaromaten die deprotonatie ondergaan. Onder de onderzochte stoffen vallen verschillende gesubstitueerde nitrobenzenen en nitrobenzoxadiazolen, waarbij zowel de aminederivaten van 4-chloro-7-nitro-2,1,3-benzoxadiazole (NBDCI) als de isocyanaatderivaten van 4-nitro-7-piperazino-2,1,3-nitrobenzoxadiazole (NBDPZ) zijn inbegrepen. De variabelen die het elektronenvangstmechanisme ondersteunen zijn grondig onderzocht. Hierbij is ook het concurrerende mechanisme van deprotonatie in beschouwing genomen om een beter begrip te krijgen van het elektronenvangstproces en om de gevoeligheid en selectiviteit van de analyse te verbeteren.

Liquid chromatography/coordination ion spray-mass spectrometry is benut voor de identificatie van reactieproducten in een rubbervulkanizatiemodel. Na reversed-phase LC scheiding is  $\text{AgBF}_4$  gebruikt om een geladen cation-analyt complex te vormen dat met ESI-MS gedetecteerd wordt. Voor vulkanizatiekoppelingsmiddelen en producten van de reactie tussen deze stoffen en alkenen zijn sterke signalen geobserveerd. De methode werkt het best voor stoffen die sulfurketens bevatten met ketenlengtes tussen de twee en acht sulfuratomen, maar sulfurvrije verbindingen met tri-ethoxysilylgroepen zijn ook gedetecteerd. In het laatste geval bleek de post-kolom additie van  $\text{NaBF}_4$  een geschikt alternatief te zijn. Naast de

vulkanizatiekoppelingsmiddelen zijn ook verschillende reactieproducten geïdentificeerd, waaronder met sulfurketens gelinkte alkenen.

Van de *in vitro* afbraak van een biocompatibele poly(ether-ester) blok-copolymeer die gebaseerd is op poly(ethyleenglycol) en poly(butyleenterephthalaat), is een gedetailleerde studie gemaakt middels LC/ESI-MS. De belangrijkste afbraakproducten en verscheidene bijproducten zijn geïdentificeerd, gebruik makend van zowel de positieve als de negatieve ionenmodus. De verworven gegevens wijzen erop dat het verval niet alleen optreedt in de 'zachte' segmenten, maar ook in de 'harde' segmenten van de polymeer. Vloeistofchromatografische scheiding is vereist om onderscheid te kunnen maken tussen isomeren. De toevoeging van ammonium- en natriumionen heeft belangrijke complementaire informatie geleverd over het aantal monomeereenheden.



# Curriculum Vitae

## *Personal Details*

- **Name:** Heiko Hayen
- **Nationality:** German
- **Date of Birth:** September 13<sup>th</sup>, 1973
- **Born in:** Wittmund, Germany

## *Education*

- **1980 – 1984** Elementary School in Wittmund, Germany
- **1984 – 1986** Orientierungsstufe der Alexander-von-Humboldt-Schule, Wittmund, Germany
- **1986 - 1993** Gymnasium der Alexander-von-Humboldt-Schule Wittmund, Germany
- **1993 - 1994** Military service
- **1994 - 1999** Studies of Food Chemistry at the University of Münster, Germany; Intermediate exam in April 1997; Graduation (1<sup>st</sup> exam) in April 1999
- **7/2000** Training period as food chemist in industry and food quality control
- **8/2000** Graduation (2<sup>nd</sup> exam) in food chemistry
- **10/2000** Begin of the Dissertation in Analytical Chemistry at the University of Münster, Germany with Prof. Dr. U. Karst
- **10/2001** Continuation of the Dissertation at the University of Twente, Enschede, The Netherlands with Prof. Dr. U. Karst
- **2001-2003** Fellowship of the Fonds der Chemischen Industrie, Frankfurt/Main, Germany



# List of Publications

## *Original papers*

1. H. Hayen, N. Jachmann, M. Vogel, U. Karst, *Analyst* 127 (2002) 1027.  
*LC-Electron Capture APCI-MS for the determination of nitroaromatic compounds*
2. J. Meyer, A. Liesener, S. Götz, H. Hayen, U. Karst, *Anal. Chem.* 75 (2003) 922.  
*Liquid Chromatography with On-Line Electrochemical Derivatization and Fluorescence Detection for the Determination of Phenols*
3. H. Hayen, U. Karst, *J. Chromatogr. A* 1000 (2003) 549.  
*Strategies for the liquid chromatographic-mass spectrometric analysis of non-polar compounds*
4. A. A. Dechamps, A. A. van Appeldorn, H. Hayen, J. D. de Bruijn, U. Karst, D.W. Grijpma, J. Feijen, *Biopolymers*, in press  
*In Vivo and In Vitro Degradation of Poly(ether ester) Block Copolymers Based on Poly(ethylene glycol) and poly(butylene terephthalate)*
5. H. Hayen, U. Karst, *Anal. Chem.*, in press  
*LC/Electrochemistry/MS and LC/Electrochemistry/Fluorescence Studies on Phenothiazine and its Derivatives*
6. S. M. van Leeuwen, H. Hayen, U. Karst, *Anal. Bioanal. Chem.*, in press  
*Liquid Chromatography/Electrochemistry/Mass Spectrometry of Polycyclic Aromatic Hydrocarbons*

7. H. Hayen, N. Jachmann, M. Vogel, U. Karst, *Analyst*, submitted for publication  
*LC-Electron Capture-APCI(-)-MS Determination of Nitrobenzoxadiazole Derivatives*
8. H. Hayen, A. A. Deschamps, D. W. Grijpma, J. Feijen, U. Karst, *J. Chromatogr. A*, submitted for publication  
*LC/MS Studies on the In Vitro Degradation of Poly(ether ester) Block Copolymers*
9. H. Hayen, M. M. Álvarez-Grima, S. C. Debnath, J. W. M. Noordermeer, U. Karst, *Anal. Chem.*, submitted for publication  
*Liquid Chromatography/Coordination Ion Spray-Mass Spectrometry (LC/CIS-MS) for the Analysis of Rubber Vulcanization Products*

*Other papers*

1. H. Hayen, S. M. van Leuwen, G. Zurek, U. Karst, *GIT Laboratory Journal Europe* 5 (2002) 216.  
*HPLC/MS for the Analysis of Non-Polar Compounds*